Molecular & cytological aspects of seed development in sexual & apomictic *Hieracium*

by

Matthew Robert Tucker
B. Biotech (Hons)

A thesis submitted for the degree of

Doctor of Philosophy

at

The University of Adelaide,
Department of Agricultural Science

in collaboration with

CSIRO Plant Industry,
Horticulture Unit

Urrbrae, Adelaide
April 20th 2003

CONTENTS

Abstract

Sexual reproduction in angiosperms is a highly regulated process that begins with the formation of a flower and ends with the formation of seeds. The ovule is the progenitor of the seed and during the course of reproduction it is the site of embryo sac formation, double fertilisation and embryo and endosperm development. Asexual seed reproduction in *Hieracium*, referred to as apomixis, is characterised by the formation of an embryo sac(s) without meiosis, and an embryo and endosperm without fertilisation. The molecular processes controlling apomixis are unknown.

In this study, molecular and cytological aspects of fertilisation-independent (autonomous) endosperm development were investigated in *Hieracium*. Early autonomous endosperm divisions were irregular in the apomict when compared to fertilisation-dependent endosperm divisions in the sexual plant. However, the general morphology of dividing syncytial nuclei and endosperm cells, and the expression patterns of the *AtMEA:GUS*, *AtFIS2:GUS* and *AtFIE:GUS* chimeric genes were strikingly similar in sexual and apomictic plants throughout endosperm development. Flow cytometry analyses showed that seeds arising from apomictic *Hieracium* displayed a higher level of heterogeneity compared to those from the sexual plant. These findings emphasised the presence of overlaps between sexual and apomictic processes in facultative apomictic *Hieracium*.

Hypotheses suggest that in apomictic plants, altered expression or function of the *FERTILISATION INDEPENDENT SEED (FIS)* genes, *MEA*, *FIS2* and *FIE*, which regulate endosperm initiation in sexual plants, may result in the formation of autonomous endosperm. A full-length *FIE* homologue was identified from sexual

and apomictic *Hieracium* plants, and function of the apomict equivalent of *FIE* was verified by genetic complementation of the *Arabidopsis fie-2* mutant. Further genomic characterisation and RNAi silencing studies suggested that the *HFIE* gene from apomictic *Hieracium* was required for viable autonomous seed development. Mutations in *HFIE* are unlikely to be the cause of autonomous endosperm development in apomictic *Hieracium*.

The cytological and molecular data obtained from this thesis provide evidence that apomictic and sexual pathways share common regulatory elements to produce a seed. The findings support models that suggest apomixis is caused by mutations in a key regulatory sexual gene(s) or by changes in gene expression induced by epigenetic factors[1].

[1] Findings from this thesis were combined with data from other *Hieracium* developmental marker studies in a paper published in The Plant Cell.

Tucker M.R., Araujo A.C.G., Paech N.A., Hecht V., Schmidt E.D.L., Rossel J.B., de Vries S.C., & Koltunow A.M.G. (2003) Sexual and apomictic reproduction in *Hieracium* sub genus Pilosella are closely interrelated developmental pathways. **The Plant Cell, 15**: 1524-1537.

Declaration

This work contains no material that has been accepted for the award of any other degree or diploma in any University or any other tertiary institution. To the best of my knowledge and belief this thesis is original and contains no material previously written or published by another person, except where due reference has been made in the text.

I give consent to this copy of my thesis, when deposited in the University library, being available for loan and photocopying.

Matthew Tucker

April 2003

Acknowledgements

I wish to thank my primary supervisor, Anna Koltunow, for giving me the opportunity to study in her lab, and for her invaluable intelligence, support and friendship throughout my PhD studies. Her work ethic and thirst for scientific understanding are an inspiration for me in the pursuit of my scientific career.

I also thank my co-supervisor, Geoff Fincher, for his interest in my project, and for giving me the opportunity to study my PhD through the University of Adelaide. I also thank the University of Adelaide for providing me with a Premier's Scholarship for Biotechnology to support my studies.

I am also most grateful to Susan Johnson, who is ever willing to answer my continual questions, for teaching me the skills of microscopy, and for cutting the sections presented in this study.

I also thank Ana Claudia Araujo, my crazy Brazilian friend, who brought carnival flair to the laboratory. Ana also contributed significantly towards helping me complete this thesis, by performing in situ hybridisations and helping me to harvest tissues and set up GUS stains. Saúde Ana!

Thanks also to the Canberra CSIRO Plant Industry Lab, especially Ming Luo and Abed Chaudhury, for the *FIS:GUS* constructs, *fis* mutants and their interest in the project.

Thanks to Anne Tassie for her artistic flair and ability to subculture and transform *Hieracium* plants, and Sandra Protopsaltis for tales of culinary delights and for lab orders(!). I also thank Miva Splawinski, Melissa Pickering, Georgina Smith, Carol Horsman and Adrienne Greig for their support in the lab.

I especially wish to thank Nick Paech, whose life ended prematurely in September 2002, for his love of Aussie rules footy, for his educated questions, and for his motivational view of life.

Thanks to the administration staff, especially Margaret Minter, Julie Powell and Maria Piscioneri, for all of their excellent support.

Past and present members of CSIRO Plant Industry also need to be thanked, especially Paul Boss, Chris Davies, Ian Dry, Mandy Walker, John Harvey, Adam Vivian-Smith, Matt Lynch and Jenny Guerin. Thanks also to my office mates, Marc Goetz and Thomas Payne, for putting up with me while writing this thesis!

Thanks to the Flinders University Biotechnology graduates for their ability to mix science with beer, and the Adelaide Cricket Club and Flagstaff Hill Golf Club for providing me with an escape!

To all of my extended family and friends, thanks for your support, and maybe one day I'll be able to clone that gene you want while you sort out my legal affairs, organise my finances, provide me with therapy, write my prescriptions and massage my injuries!

To my parents and sister, Sue, Brenton and Melissa, thanks for being the best family I could ever have hoped for. Without your love, support, generosity and sacrifice, it would not have been possible to achieve any of my goals.

Finally to Elise, my wonderful wife, thanks for everything. Without your eternal understanding and love of science, of companionship and of me, life wouldn't be half as much fun.

Abbreviations

AES	-	aposporous embryo sac
AI	-	aposporous initial
At	-	*Arabidopsis thaliana*
Ac	-	accession number
BAC	-	bacterial artificial chromosome
BLAST	-	basic local alignment search tool
bp	-	base pairs
β-*tub*	-	beta tubulin
(CaMV) 35S	-	cauliflower mosaic virus 35S promoter
CAPS	-	cleaved amplified polymorphic sequence
Col-4	-	*Arabidopsis* Columbia-4 ecotype
cDNA	-	complementary DNA
CSIRO	-	Commonwealth Scientific and Industrial Research Organisation
°C	-	degrees Celsius
DAPI	-	4',6-diamidino-2-phenylindole
DIG	-	dixoxygenin
DPD	-	days post decapitation
DPE	-	days post emasculation
DNA	-	deoxyribonucleic acid
dNTP's	-	2'-deoxynucleotide triphosphates
EDTA	-	ethylene-diamine-tetra-acetic acid
ET	-	enhancer trap
FAA	-	formaldehyde acetic acid
FIE	-	*FERTILIZATION-INDEPENDENT ENDOSPERM*
FIS	-	*FERTILIZATION-INDEPENDENT SEED*
FAO	-	Food and Agricultural Organisation of the United Nations
GUS	-	β-D-glucoronidase
GFP	-	green fluorescent protein
h/hr	-	hour(s)
HAP	-	hours after pollination
HOS	-	*Hieracium* Ovary Sequence
kb	-	kilobase pairs
L	-	litres

L.*er*	-	*Arabidopsis* Landsberg *erecta* ecotype
M	-	molar
MEA	-	*MEDEA*
MET	-	methyltransferase
MMC	-	megaspore mother cell
mRNA	-	messenger RNA
NCBI	-	National Centre for Biotechnology Information
No-0	-	*Arabidopsis* Nossen-0 ecotype
PcG	-	*Polycomb* group
PCR	-	polymerase chain reaction
pers. comm.	-	personal communication
RACE	-	rapid amplification of cDNA ends
RNA	-	ribonucleic acid
RNAi	-	RNA interference
RT	-	reverse transcription
s	-	seconds
SDS	-	sodium dodecyl sulphate
SSC	-	standard saline citrate
TAE	-	tris-acetate-EDTA
TAIL-PCR	-	thermal asymmetric interlaced PCR
Tris	-	tris[hydroxymethyl]aminomethane
µm	-	micrometer
UTR	-	untranslated region
WT	-	wild type

Publications

Sections of this thesis have been published in the following articles:

Chaudhury A.M., Koltunow A., Payne T, Luo M., **Tucker M.R.**, Dennis E.S., & Peacock W.J. (2001). Control of early seed development. **Ann. Rev. Cell Dev. Biol.** 17, 677-699.

Koltunow A.M., Vivian-Smith A., **Tucker M.R.**, & Paech N.P. (2002). The central role of the ovule in apomixis and parthenocarpy. In **Plant Reproduction**, S.D. O'Neill and J.A. Roberts, eds. (Sheffield UK: Sheffield Academic Press) pp. 221-256.

Koltunow A.M., & **Tucker M.R**. (2003). Advances in apomixis research: Can we fix Heterosis? In **Plant biotechnology and beyond**, I.K. Vasil, ed. (The Netherlands, Kluwer Dordrecht) pp. 39-46.

Tucker M.R., Araujo A.C.G., Paech N.A., Hecht V., Schmidt E.D.L., Rossel J.B., de Vries S.C., & Koltunow A.M.G. (2003) Sexual and apomictic reproduction in *Hieracium* sub genus *Pilosella* are closely interrelated developmental pathways. **Plant Cell, 15: 1524-1537**.

Chapter 1: Molecular and cytological aspects of early seed development

A. Preliminary Comments

The main focus of apomixis research in the Koltunow laboratory is to determine how apomictic seeds form in *Hieracium*. A considerable amount of research has characterised the cytological initiation and progression of apomixis within *Hieracium* ovules, and several molecular analyses have characterised gene expression patterns at early stages of ovule development. However, the molecular basis of autonomous apomixis and the cues regulating the development of autonomous endosperm in *Hieracium* seeds are currently unknown. This thesis presents the results of a study aimed at characterising the formation of endosperm in apomictic *Hieracium* to further determine the molecular relationships between sexual and apomictic reproduction.

In order to familiarise the reader with aspects of ovule and seed development, this review of the current literature summarises the events of sexual and apomictic reproduction from developmental and molecular perspectives. The formation of endosperm in sexual and apomictic plants is also discussed, along with the molecular controls associated with endosperm formation. Finally, the aims of the thesis are provided to focus the reader on the questions addressed during this study.

1.1 Introduction

Within developing countries, the most important food crops are cereals such as rice, wheat, maize, barley, sorghum and millets (FAO, 1996). Globally, rice is the most important crop in terms of its contribution to diet and its value of production. Over 90 percent of the world's rice is produced and consumed in the Asian region, where studies predict that rice consumption by the year 2025 will increase by more than fifty percent compared to 1995 (Papademetriou, 2000). It is uncertain how the current annual production of 538 million tonnes of rice can be increased to over 700 million tonnes by the year 2025, using less land, labour, water and pesticides (Duwayri et al., 2000). Superior conventionally bred varieties, hybrid rice and biotechnologically engineered rice all point to increased yield potentials (Papademetriou, 2000). With the aim of understanding seed development for humanitarian, commercial and scientific gain, a large amount research has been directed into the field of plant reproductive biology.

Sexual reproduction in flowering plants results in genetically diverse progeny carrying traits from both male and female parents. This genetic diversity is of great value for improving agricultural crops and has been utilised in traditional breeding programs for hundreds of years. Hybrid vigour, or heterosis, is a significant agricultural benefit derived through sexual reproduction and is defined as the increased size, growth rate or productivity of the offspring resulting from a cross involving parents of different inbred lines of a species or occasionally from two different species (Koltunow and Tucker, 2003). However, once suitable cultivars of

new agricultural crops have been developed that show characteristics of hybrid vigour, it is difficult to maintain uniformity and consistency of crop quality. Inbred lines can be developed to overcome these problems, but time is required to develop these lines and their advantageous traits also diminish through subsequent generations. The genetic diversity caused by sexual reproduction causes unwanted variability, and is disadvantageous when a fixed genotype would be preferred.

Apomixis is defined as asexual reproduction through seeds (Nogler, 1984) and, thus, leads to the production of clonal progeny whose genotype is identical to that of the mother plant (Koltunow, 1993). The apomictic mode of reproduction omits critical events observed in the sexual pathway. Meiosis is avoided prior to embryo sac formation (apomeiosis), embryo development is autonomous (parthenogenesis), and endosperm formation sometimes occurs independently of fertilisation. These three features are often referred to as the "components of apomixis". If this reproductive process could be conferred to currently sexual crop species and appropriately controlled, problems of genetic variation such as loss of hybrid vigour could be overcome. The potential economic value of apomixis technology for hybrid rice production was estimated to exceed US$2.5 billion per annum (McMeniman and Lubulwa, 1997). More importantly, by understanding apomixis, a significant contribution may be made toward ensuring that the developing world has the capacity to feed itself into the next century (Grossniklaus et al., 1998a).

Apomixis appears to be genetically controlled by a few dominant loci (Bicknell et al., 2000; Noyes and Rieseberg, 2000; Barcaccia et al., 1998; Nogler, 1984; Savidan, 1982), but the molecular factors that control apomixis have not been identified. The molecular relationships between sexual and apomictic reproduction remain unclear. Genes that control endosperm initiation have been identified in

sexual plants by mutagenesis studies (Luo et al., 1999), and mutational lesions in individual members of the *Arabidopsis FERTILISATION INDEPENDENT SEED* (*FIS*) class genes lead to the autonomous initiation of endosperm formation. *FIS*-class genes are similar to the *Polycomb* group (PcG) genes from *Drosophila* and are implicated in chromatin remodelling (Luo et al., 2000; Grossniklaus et al., 1998b). Few studies have characterised the formation of autonomous endosperm development in naturally apomictic plants (Ernst and Bernard, 1912; Stebbins and Jenkins, 1939; Cooper and Brink, 1949; Rutishauser, 1948), and the molecular cues controlling autonomous seed development are uncertain. The identification of the *Arabidopsis FIS* genes provides an opportunity to examine the role of their homologues during endosperm development in apomictic plants.

The aims of this project were to characterise early seed initiation in sexual and apomictic *Hieracium* from molecular and cytological perspectives. A member of the Asteraceae, *Hieracium* is a genus containing both sexual and apomictic species, of which the latter is capable of producing endosperm without fertilisation during apomictic seed formation.

1.2 Ontogeny of seed development in sexually reproducing plants

In flowering plants, the reproductive lifecycle initiates with a change in meristem growth from an indeterminate vegetative mode to a determinate flowering mode that ends with the production of seed and fruit. Once the flower opens and growth of the floral organs has diminished, further information is necessary to enable the initiation of fruit and seed development. Pollination and subsequent double

fertilisation provide cues that enable this transition, and the development of fruit and seed is coordinated as the fruit facilitates seed dispersal.

Chronologically, the ovule is the last organ to form during flower development. Since it is the progenitor of the seed, an understanding of ovule development is central to understanding seed formation. Key events in angiosperm reproduction take place within the ovule, including meiotic reduction (megasporogenesis), female gamete formation (megagametogenesis) and double fertilisation, which involves the fusion of male sperm cells with two specific cells of the reduced female gametophyte; the egg cell and the central cell. The products of these two fertilised cells give rise to the embryo, thus returning the ploidy to that of the sporophyte, and the endosperm respectively. The stages of ovule and seed development are described further in the subsequent sections of this chapter.

1.2.1 Early ovule development

Ovules originate subdermally through periclinal divisions within the L2 or L3 layers of the ovary wall placenta and anticlinal divisions within the epidermis (Bouman, 1984). Ovules vary in shape, which is governed in part by the extent of their curvature and the elaboration of their epidermal cells, but share three basic structures: a nucellus that is derived from the apical portion of the ovule primordium and produces the megasporocyte, a funiculus which is a stalk-like structure that connects the ovule to the placental region of the gynoecium, and one or two integuments (Figure 1.1). The most common type of ovule is termed "anatropous", because it undergoes a curvature of 180° so that it becomes completely inverted and the micropyle comes to lie close to the place of attachment

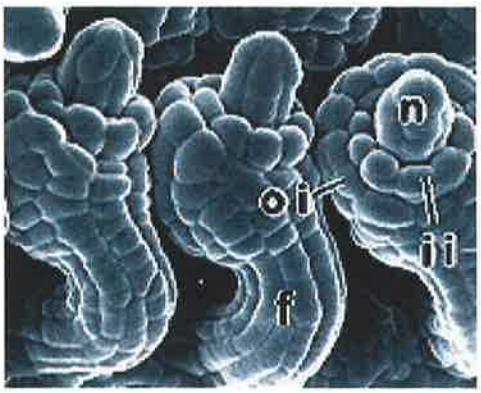

Figure 1.1 Electron micrograph of *Arabidopsis thaliana* ovule primordia showing the funiculus (f), nucellar lobe (n), inner integument (ii) and outer integument (oi) (adapted from Chaudhury et al., 1997)

of the ovule (Figure 1.2). Genetic and molecular analyses in *Arabidopsis* and other plant species have identified a range of genes involved in early ovule specification and pattern formation and these are reviewed in Chevalier et al., (2002), Gasser et al., (1998) and Schneitz et al., (1997).

1.2.2 Embryo sac development - megasporogenesis

Embryo sac development can be divided into two stages: megasporogenesis and megagametogenesis. During the early stages of ovule growth, megasporogenesis begins with the differentiation of a subdermal cell within the nucellus into an enlarged archesporial cell with a prominent nucleus (Reiser and Fischer, 1993). A megaspore mother cell (MMC; megasporocyte) will differentiate directly from this cell or from a mitotic product of this cell, and will undergo meiotic reduction to produce four megaspores (Figure 1.2). During Polygonum-type embryo sac development (Maheshwari, 1950), which is observed in approximately 70% of angiosperms, one megaspore is selected to give rise to the megagametophyte, and the other three degenerate.

Mutational studies in sexual plants have identified genetic controls that regulate aspects of megasporogenesis during early ovule development. The *multiple archesporial cells* (*mac-1*) mutant from maize (Sheridan et al., 1996) highlights the presence of a mechanism that restricts reproductive potential in the nucellus to a single cell. In *mac-1* mutant ovules, several hypodermal cells develop into archesporial cells, and the resulting megasporocytes undergo a normal meiosis. More than one megaspore survives in the tetrad and more than one embryo sac is formed in each ovule.

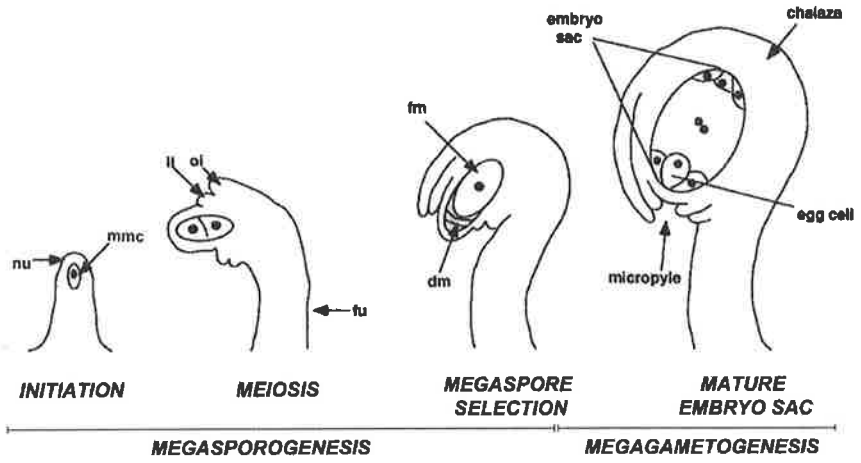

Figure 1.2 Stages of ovule growth and development in *Arabidopsis*. nu - nucellar lobe, mmc - megaspore mother cell, ii - inner integument, oi - outer integument, fu - funiculus, dm - degenerating megaspores, fm - functional megaspore (adapted from Reiser and Fischer, 1993).

Other mutants have also been described that display alterations during specific stages of female meiosis. In *Arabidopsis sporocyteless (spl)* mutants, sporocyte formation is blocked in both male and female reproductive tissues (Yang et al., 1999). A different allele of the *spl* mutation was identified as *nozzle (nzz)* in which the nucellus and the pollen sac fail to form, indicating that *NZZ* plays an early and central role in the development of both types of sporangia, and that the mechanisms controlling these processes share a crucial factor (Schiefthaler et al., 1999). The molecular cues controlling the fate of the three non-selected megaspores are not completely clear, but the *ANTIKEVORKIAN* (*AKV*) gene from *Arabidopsis* appears to regulate death of the three non-selected megaspores (Yang and Sundaresan, 2000). In *akv* mutant ovules, all four megaspores survive and are capable of producing embryo sac structures. These mutants suggest that there is a genetic framework regulating specific stages of female meiosis, and that development of the nucellus is critical for the formation of a viable archesporial cell and for the subsequent steps of reproduction.

1.2.3 Embryo sac development - megagametogenesis and maturity

During Polygonum-type megagametogenesis, mitotic divisions of the functional megaspore give rise to the two-nucleate, four-nucleate and subsequently the eight nucleate stages of embryo sac development. Nuclear migration and cytokinesis subsequently produce the seven-celled megagametophyte, which consists of two synergids, each with a filiform apparatus at its micropylar end, the egg cell and a polyploid central cell (Figure 1.3). Three antipodal cells are found at the chalazal end of the mature embryo sac.

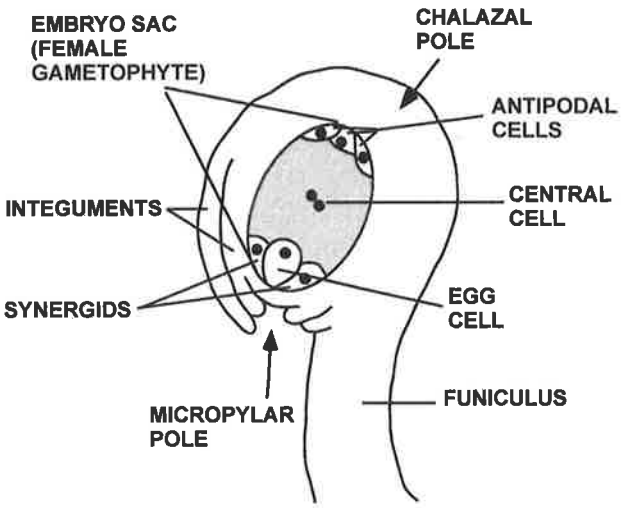

Figure 1.3 Anatropous ovule containing a Polygonum-type embryo sac (adapted from Ohad et al., 1996).

The precise mechanisms of embryo sac growth and differentiation from the functional megaspore are not well understood, but genetic data demonstrate that sporophytic as well as female gametophytic factors are involved in the process (Grossniklaus and Schneitz, 1998). All of the cells that make up the Polygonum-type embryo sac originate from a single spore and the lineage of each nucleus can be traced during the mitotic divisions. However, as outlined by Koltunow and Grossniklaus (2003), it is not clear whether the differentiation events that specify their eventual function are influenced by changes in chromatin that follow each mitotic division, or whether differentiation occurs once mitosis and cellularisation are complete.

A series of mutants affecting Polygonum-type embryo sac development have been described (Moore et al., 1997; Grini et al., 2002; Christensen et al., 1997; 2002) and enhancer-trap (ET) lines marking particular cells during embryo sac formation in *Arabidopsis* have been isolated (Vielle-Calzada et al., 2000; Grossniklaus, 2001). These ET lines are useful tools for the analysis of molecular events that control Polygonum-type embryo sac formation.

1.2.4 Post-fertilisation seed development

After megagametogenesis is complete, the unique process of double fertilisation initiates the subsequent events of seed development (reviewed in Lord and Russell, 2002). In this process, two sperm cells resulting from division of the single generative cell of the pollen grain unite with cells of the megagametophyte; one sperm nucleus fusing with the nucleus of the egg cell, forming a zygote, and the other with the two fused nuclei of the central cell, forming the primary endosperm

nucleus. The embryo develops from the zygote and the endosperm arises by divisions of the central cell. In most plant species, the embryo arises after initiation of endosperm development. Even though the zygote and the primary endosperm nucleus have similar genomes, they develop along totally different pathways to give rise to the embryo and the accompanying nutritive endosperm. This is likely due to differences in the ploidy of these cells – during Polygonum-type development the zygote is diploid and the primary endosperm nucleus is triploid. In the absence of fusion with a sperm cell, the egg and central cell remain in a quiescent state and will eventually degrade as the flower undergoes senescence. The mechanisms that prevent the egg cell in plants from initiating embryogenesis in the absence of fertilisation are not known.

1.2.5 Embryo development

The process of embryogenesis has been studied in detail, and the cellular pattern of differentiation from the single cell zygote of the fertilised ovule to the multicellular structures found in the mature dry seed has been documented for many plants (Johri and Ambegoakar, 1984). For brevity, a detailed characterisation of plant embryogenesis has been omitted from this introduction, and recent progress in relation to the molecular controls of embryogenesis is reviewed by Chaudhury et al., (2001) and Koltunow and Grossniklaus (2003). Mutational dissection and/or expression analyses have identified a number of genes that play specific roles in the induction and maintenance of embryogenesis in plants. These include *LEAFY COTYLEDON 1* and *2* (*LEC1*; Lotan et al., 1998; *LEC2*; Stone et al., 2001), *PICKLE* (*PKL*; Ogas et al., 1997; 1999)), *BABY BOOM* (*BBM*; Boutilier et al.,

2002), *SOMATIC EMBRYO RECEPTOR KINASE 1* (Hecht et al., 2001) and *WUSCHEL* (*WUS*; Zuo et al., 2002).

1.2.6 Endosperm development

Endosperm is thought to act as a necessary mediator between the sporophytic tissues of the mother plant and the embryo, especially if the absorption of nutrients from the nucellus or embryo sac is unsuitable. Studies suggest that an inter-relationship between the embryo, endosperm and maternal tissues is essential for correct seed formation (Colombo et al., 1997).

The importance of cereal grains as renewable resources has led to significant research being directed towards basic endosperm biology. Most research has been directed to crops such as maize, barley, rice and wheat, all of which employ similar mechanisms of nuclear endosperm development. Despite the fact that in *Arabidopsis* seeds, unlike cereals, the endosperm does not persist and most of the storage reserves are deposited in the embryo cotyledons, recent studies have demonstrated that early endosperm development in *Arabidopsis* follows the same general pattern observed in cereals (Brown et al., 1999).

1.2.6.1 Types of endosperm development

Endosperm tissue in angiosperm seeds develops along one of three characterised pathways designated as nuclear, cellular or helobial (Figure 1.4). In the nuclear-type, the primary endosperm nucleus divides to form a syncytium; a multinucleate mass of protoplasm that is not divided into separate cells (Figure 1.4). Later, during

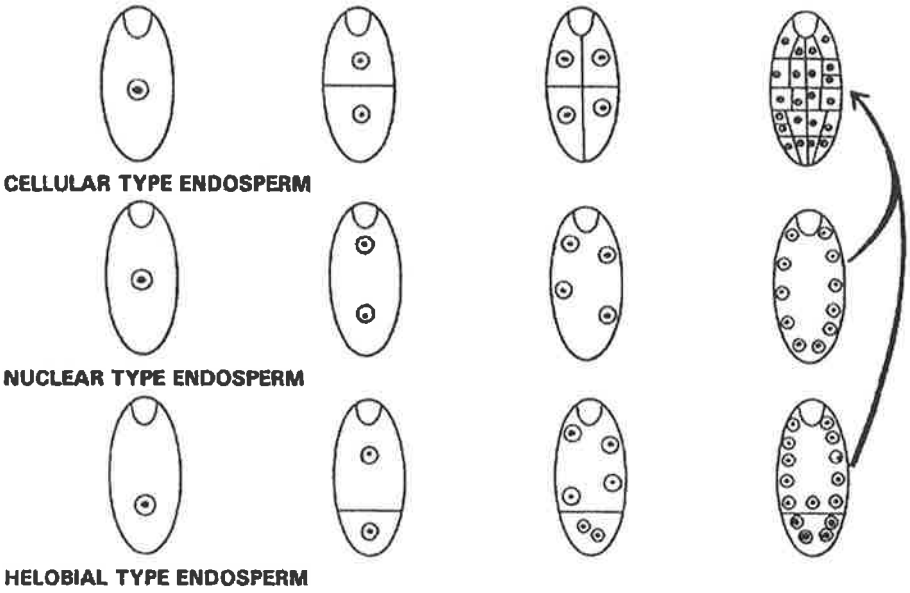

Figure 1.4 Types of endosperm development in angiosperms (adapted from Herr, 1999).

cellularisation, each nucleus becomes isolated by the development of cell walls in a gradual process that does not affect all nuclei in species such as *Arabidopsis*. Most cereals, including wheat and barley and maize follow the nuclear endosperm pathway, and further aspects of nuclear endosperm development are considered in the following sections. In the cellular-type of endosperm, such as that observed in tobacco, each nuclear division of the endosperm is directly followed by cytokinesis (Figure 1.4). The helobial-type is initiated by nuclear division of the primary endosperm nucleus, followed by cytokinesis to produce two cells (Figure 1.4). Divisions thereafter are free nuclear in both cells but more frequent in the larger micropylar cell or chamber. The multinucleate micropylar chamber becomes cellular while the chalazal chamber remains small and free nuclear. Some studies suggest that the entire ontogenic gamut of the helobial endosperm is not duplicated in any dicotyledon, thus making it almost exclusive to monocots (Swamy and Parameswaran, 1963).

1.2.6.2 Nuclear endosperm development

In model plants such as *Arabidopsis* (Figure 1.5), maize, rice and barley, endosperm development is initiated after fertilisation by successive divisions of the primary endosperm nucleus without cytokinesis (Herr, 1999, Schneitz et al., 1995; Olsen et al., 1995; Brown et al., 1996). After fertilisation in maize, the first nuclear endosperm division occurs in a plane perpendicular to the longitudinal axis of the embryo sac, and the next two at alternate planes (Olsen, 2001). In *Arabidopsis*, primary nuclear endosperm divisions are reported to be essentially the same as those observed in meristematic cells, but whereas the phragmoplast facilitates the

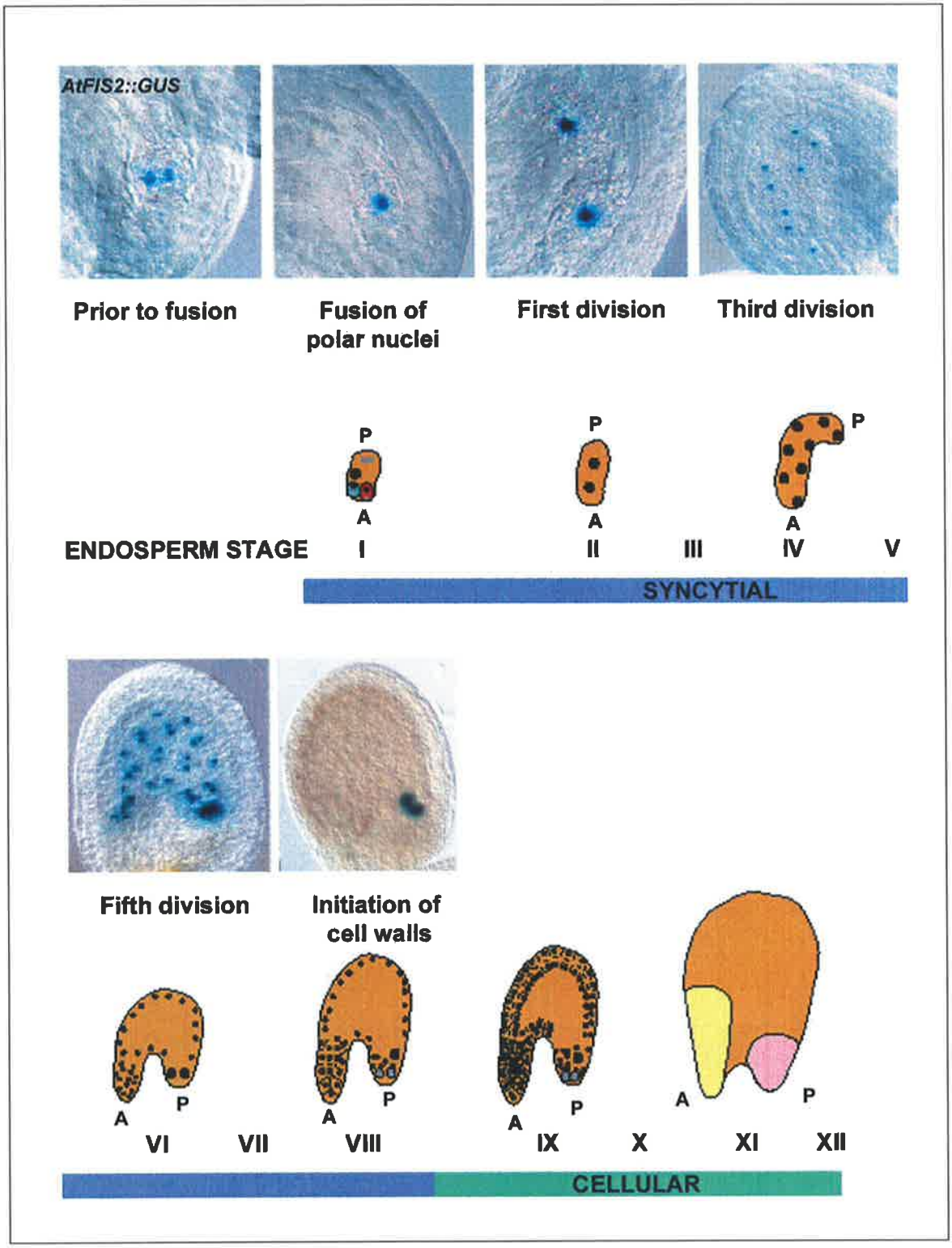

Figure 1.5 Stages of nuclear endosperm development in *Arabidopsis*. Divisions of the endosperm nuclei (from stage I - VII) are marked by the *AtFIS2::GUS* gene fusion A - anterior, P - posterior. Three domains are defined from the anterior pole to the posterior pole. The domains are micropylar endosperm (yellow), peripheral endosperm (orange) and chalazal endosperm (pink). Adapted from Luo et al., 2000 and Berger, 2003.

assembly of the cell wall in the interzone between its two parallel microtubule discs during meristematic divisions, no cell plate forms during nuclear endosperm coenocyte mitosis (Brown et al., 1999; Olsen, 2001; Otegui et al., 2002; Faure et al., 2002). At the eight-nuclear stage in maize, the nuclei form a ring in the proximal cytoplasm around the embryo before migrating to discrete and separate longitudinal sectors of the peripheral cytoplasm of the central cell. In *Arabidopsis*, nuclear migration occurs in the direction from the micropylar to the chalazal chambers (Brown et al., 1999), in the same plane to which the nuclei divide, and the nuclei move to the periphery of the embryo sac. These nuclear divisions form a syncytial coenocyte, and are clearly marked by the *Arabidopsis FIS2:GUS* chimeric gene (Figure 1.5; Luo et al., 2000). The presence of free nuclei organised at the periphery of the central cell is characteristic of the nuclear-type (Figure 1.5).

The number of nuclei that form prior to cellularisation differs between species, but cellularisation occurs after the eighth mitotic division and coincides with initiation of cotyledons in the embryo in *Arabidopsis* (Figure 1.5) and occurs approximately 100 hours after pollination in maize (Berger, 2003). Cellularisation is initiated by the formation of cell walls between sister and non-sister nuclei, which are perpendicular (i.e. anticlinal) to the syncytial cell wall. In *Arabidopsis*, the endosperm is completely cellular by the time that storage deposition begins in the embryo (Figure 1.5; Brown et al., 1999).

1.2.6.3 Endosperm cell differentiation

Following cellularisation, endosperm cells differentiate into tissue types along anterior-posterior and radial axes. Studies in *Arabidopsis* indicate that three regions

of endosperm are organised along the anterior-posterior axis during development (Figure 1.5; Mansfield and Briarty, 1990; Schneitz et al., 1995; Herr, 1999; Egnell, 1989; Berger, 2003). These are conserved in maize and most angiosperm species (Floyd and Friedman, 2000). In *Arabidopsis*, nuclei resulting from the first division migrate to opposite poles of the embryo sac; one nucleus of the binucleate endosperm migrates into the chalazal region, and the other towards the micropyle. The posterior chalazal endosperm, referred to as the cyst in *Arabidopsis* and the Basal Endosperm Transfer Layer (BETL) in maize, contains a pocket of between 2-8 nuclei and becomes enclosed in a dense pocket of cytoplasm before division of the one-celled embryo begins (Herr, 1999; Olsen et al., 1999; Gomez et al., 2002). The nuclei of the anterior region, referred to as the micropylar endosperm in *Arabidopsis* and the embryo-surrounding region in maize, are single-file in peripheral cytoplasm and situated close to the embryo. The anterior and posterior regions are separated by the central largest portion of the endosperm, referred to as the peripheral endosperm in *Arabidopsis* and the starchy endosperm in maize.

Radial symmetry is present in *Arabidopsis*, but has been more intensively studied in the cereals. This symmetry distinguishes the aleurone layer(s) from the inner mass of starchy endosperm (Becraft and Asuncion-Crabb, 2000). In maize and wheat there is one cell layer (Becraft and Asuncion-Crabb, 2000; Buttrose, 1963), in rice one to several layers (Hoshikawa, 1993) and in barley, three layers within the aleurone (Jones, 1969). In *Arabidopsis* seeds a single aleurone layer is all that remains of the endosperm at maturity. The anterior, central and posterior regions of the endosperm appear to be structurally distinct (Mansfield and Briarty, 1990; Webb and Gunning, 1991; Robinson-Beers et al., 1992; Schneitz et al., 1995) and express different genes during development (Sorensen et al., 2001; Strangeland et al., 2003;

see Olsen, 2001 for review). These regions are thought to have different roles in seed development (Olsen et al., 1999; Gomez et al., 2002).

Although *Arabidopsis* and cereals show similarity in terms of defined regions of endosperm within the seed, the cell contents of these regions differ markedly. For example, the persistent peripheral aleurone cell layer of the *Arabidopsis* endosperm and the cereal aleurone are clearly made up of different cell types (Olsen et al., 2001). Also, the contents of the non-persistent inner cell mass of *Arabidopsis* are different from the persistent cereal starchy endosperm. However, based on the high degree of conservation of the cellularisation process between *Arabidopsis* and the cereal endosperm, as well as the similarity in the ontogeny of the two main endosperm cell types, similar molecular mechanisms are likely to be employed during endosperm development.

1.2.7 The role of the endosperm in seed development

Two main views on the origin of endosperm have been advanced. In one, the endosperm is hypothesized to originate as an altruistic twin embryo, which evolved into a nourishing endosperm for the surviving embryo, whereas in the second, the endosperm is viewed as a continued development of the megagametophyte triggered by fertilisation (Friedman, 1994). Irrespective of the tissue's origin, the endosperm has classically been assigned the function of nourishing the embryo (Brink and Cooper, 1947). In cereals, the endosperm is a major site of storage reserves and provides hormones thought to regulate embryo growth (Olsen, 1998). Other roles for the endosperm include the maintenance of high osmotic potential around the embryo, mechanical support during early embryo growth, and storage of reserves,

nutrients, and hormones to facilitate and support seed germination (Lopes and Larkins, 1993). In a eudicot such as *Arabidopsis*, where the endosperm does not persist and the cotyledons form the primary storage organ, the endosperm has traditionally been thought to promote early growth of the embryo until sufficient reserves are stored in the cotyledons. Recent studies have shown that in *Arabidopsis* seeds, the endosperm plays a crucial role in the control of nutrient delivery to the embryo (Hirner et al., 1998). In Orchid species, the life of the endosperm is particularly transient because only two to eight endosperm nuclei are formed prior to endosperm degeneration (Nagashima, 1989; Ye and Guo, 1995). However, growth of the orchid embryo is likely to be associated with mycorhizzal fungi, which provide nutrients (Manning and van Staden, 1987), thus removing the need for a permanent endosperm.

Endosperm plays a role beyond simple nutrient delivery to the embryo. Studies in the eudicot carrot strongly suggest that the endosperm is a source of signals involved in embryogenesis (van Hengel et al., 1998) and that there are interactions between the embryo and the endosperm; similar conclusions were drawn from studies in maize (Opsahl-Ferstad et al., 1997). Genetic analyses suggest that maternal and endosperm tissues regulate the development of each other (Lopes and Larkins, 1993, Felker et al., 1985). In maize kernels, the endosperm acts as a sink for sucrose that enters the basal endosperm through maternal-transporting tissues. In the maize *miniature-1* mutant (Miller and Chourey, 1992), invertase activity is lost in maternal transport tissues, which leads to aborted embryo development and the failure of endosperm to accumulate starch and protein. Rice mutants, including *endospermless, giant embryo*, and *reduced embryo* specifically affect endosperm development but also display altered embryo size, suggesting that the endosperm regulates embryo development (Hong et al., 1996).

1.2.8 Molecular controls of endosperm formation - the *Arabidopsis FIS* genes

Studies have identified genes that function during stages of endosperm development, including the early syncytial divisions, later cell specification and differentiation events, and storage compound deposition and utilisation (Grini et al., 2002; Choi et al., 2002; Ingram et al., 1998; McElver et al., 2000; Becraft et al., 1996; Cheng et al., 1996; Miller and Chourey, 1992; Springer et al., 2000; Opsahl-Ferstad et al., 1997; Gomez et al., 2002). Recent studies in *Arabidopsis* have led to the identification of several key mutants that regulate early endosperm development and function. Mutations in any one of the three *FERTILIZATION INDEPENDENT SEED (FIS)* genes - *MEDEA (MEA; FIS1)*, *FIS2*, and *FERTILIZATION INDEPENDENT ENDOSPERM (FIE; FIS3)* - result in the fertilisation-independent initiation of endosperm development, indicating that endosperm development is suppressed by the wild-type function of these genes (Peacock et al., 1995; Ohad et al., 1996; Chaudhury et al., 1997; Grossniklaus and Vielle-Calzada, 1998). Autonomous endosperm in *Arabidopsis fie* ovules initiates with nuclear divisions but does not progress beyond the nuclear phase, whereas endosperm in *mea* and *fis-2* ovules proceeds to cell wall formation before seed abortion.

MEA and FIE have protein domains similar to ENHANCER OF ZESTE (E(z); a SET domain protein) and EXTRA SEX COMBS (Esc; a WD-40 repeat protein) respectively, that belong to the *Drosophila Polycomb* group (PcG) of proteins. PcG proteins form multimeric complexes that modulate gene expression by altering higher order chromatin structure. In animals, PcG complexes regulate homeotic genes and genes responsible for cell proliferation. Evidence that the FIS

proteins might form a complex has been obtained from yeast two-hybrid studies, biochemical assays, the similarity of their mutant phenotypes and comparison to *Drosophila* PcG models. MEA and FIE interact directly with each other but no interaction has been shown with FIS2, which encodes a novel protein with a zinc finger motif (Luo et al., 1999; 2000; Spillane et al., 2000; Yadegari et al., 2000). Although FIS2 does not appear to interact directly with MEA and FIE, a role for FIS2 in chromatin condensation may be inferred from its homology to the *Drosophila* protein Suppressor of zeste 12 (Su(z)12; Birve et al., 2001). The Su(z)12 protein does not interact directly with Esc or E(z) in biochemical assays, but has recently been shown to associate with the *Drosophila* Esc-E(z) complex (Muller et al., 2002; Kuzmichev et al., 2002).

Two regions of homology have been noted between FIS2, Su(z)12 and several other *Arabidopsis* proteins. One region corresponds to the amino-terminal zinc finger region of FIS2, the other to a carboxy-terminal motif of unknown significance, which is referred to as the ACE domain or VEFS-box (Chaudhury et al., 2001; Birve et al., 2001). *Arabidopsis* FIS2-like proteins EMBRYONIC FLOWER 2 (EMF2), a regulator of floral transition (Yang et al., 1995, Yoshida et al., 2001), and VERNALIZATION 2 (VRN2) (Chandler et al., 1996; Gendall et al., 2001), a mediator of flowering response to long periods of low temperature, each contain a zinc finger as well as the carboxy-terminal homology. *FIS2*-homologous sequences have also been identified in the genomes of monocots such as barley, maize, and rice (A. Chaudhury, pers. comm.).

Combined with the similarity of their mutant phenotypes, the most compelling evidence that the FIS products act together comes from their similar expression in the female gametophyte and endosperm cells. The *Arabidopsis* *MEA:GUS*, *FIS2:GUS* and *FIE:GUS* protein fusions are expressed in the female

gametophyte before fertilisation and in the developing endosperm after fertilisation (Luo et al., 2000; Figure 1.5 for example). MEA and FIE co-localize to the nucleus, and FIS2 also has a nuclear localization signal (Luo et al., 1999, Spillane et al., 2000).

Apart from their role in repressing endosperm cell division in the absence of fertilisation, the *FIS* genes are also thought to be involved in controlling pattern formation along the anterior-posterior axis of the developing seed. When *fis* ovules are fertilised, endosperm structures resembling chalazal cysts develop not only in the chalazal region but also in other regions of the seed; markers that are normally specific to chalazal endosperm in wild-type plants are also expressed in other endosperm domains. This result has been interpreted to mean that the *FIS* genes act as potent regulators of the anterior-posterior polar axis in the endosperm (Sorensen et al., 2001).

1.2.8.1 Models of FIS *Polycomb* group function during seed development

The *Arabidopsis MEA*, *FIS2* and *FIE* products can be linked in models of function with a role in seed development (Figure 1.6; Chaudhury et al., 1997; Grossniklaus and Vielle-Calzada, 1998; Ohad et al., 1999; Luo et al., 1999). In this model, the FIS proteins form in a multimeric protein complex that remodels chromatin and blocks the expression of seed development genes until after fertilisation (Figure 1.6). Once fertilisation has occurred, the FIS proteins are released from their repressive role to function in other processes related to seed development such as endosperm patterning or embryo cell proliferation. When any of the three *FIS* genes are mutated, the repressive complex does not form correctly, downstream seed

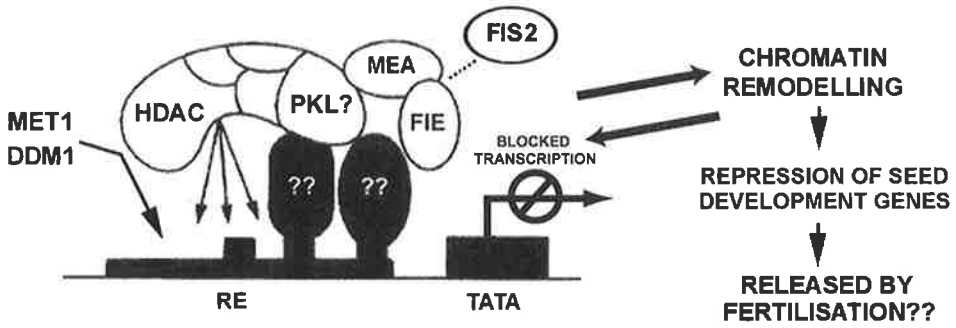

Figure 1.6 A putative model of plant *Polycomb* group (PcG) proteins and interactors functioning during seed development. The model is based on predicted FIS models (Luo et al., 1999; Ohad et al., 1999), mutant phenotypes and associations with *Drosophila* PcG models (van Louhizen, 1999). RE - response element.

development genes are expressed without fertilisation and abnormal autonomous endosperm develops. Other putative components of this FIS "complex" can by proposed based on associations with *Drosophila* models (van Louhizen, 1999), their similarity to gene products, and their reproductive tissue phenotypes.

In animal systems, PcG complexes regulate gene expression by modifying chromatin structure (Jacobs and van Louhizen, 1999). Co-purification studies have identified histone deacetylase (HDAC) proteins as part of the repressive PcG complexes (Tie et al., 2001), and shown that histone deacetylation is required for correct PcG activity (reviewed in Jacobs and van Louhizen, 2002). Three classes of histone deacetylases have been identified in plants (Reyes et al., 2002) and some play a role in seed development (Wu et al., 2000a). The role of *RPD3*-type (Class I) *HDAC* genes during ovule and seed development is not completely clear, but in *Drosophila* and mammals, the ENHANCER OF ZESTE (E(z)) and EXTRA SEX COMBS (Esc) proteins, homologues of MEA and FIE respectively, interact in repressive protein complexes with the RPD3 histone deacetylase to control gene expression (Tie et al., 2001). Whether the products of plant *HDAC* genes are involved in repressive protein complexes has yet to be determined.

Methylation plays a key role in genomic imprinting and epigenetic regulation of gene expression. In mouse, the PcG EMBRYONIC ECTODERM DEVELOPMENT (EED) protein that shows high homology to FIE is required for genomic imprinting (Mager et al., 2002). Methylation of specific histone residues is also required for the correct establishment of PcG mediated repression in *Drosophila* (Muller et al., 2002; Cao et al., 2002). The *DECREASED DNA METHYLATION 1 (DDM1)* gene from *Arabidopsis* shares homology to the SNF2/SWI2 family of DNA-dependent ATPases that have transcriptional co-repression activities (Jeddeloh et al., 1999). Interestingly, loss of *DDM1* function

decreases genome-wide cytosine methylation of heavily methylated repetitive DNA and heterochromic regions in particular (Vongs et al., 1993). The *Arabidopsis METHYLTRANSFERASE 1* (*MET1*) gene has also been implicated in genome-wide methylation, and possibly interacts with *DDM1* during chromatin remodelling (Finnegan et al., 2000). Both *MET1* and *DDM1* have been examined in relation to the *FIS* members of the plant PcG complex. In *ddm1* mutant or *MET1* antisense plants, alterations are seen in the mutant *mea*, *fis2*, and *fie* phenotypes, suggesting that the *FIS* genes or associated modifiers may be influenced by methylation (Vielle-Calzada et al., 1999; Luo et al., 2000).

The close similarity of the *Arabidopsis* PICKLE/GYMNOS (PKL; Ogas et al., 1999; GYM; Eshed et al., 1999) gene product to the *Drosophila* CHD3 protein dMi-2, and its role in embryogenesis suggest that PKL may play a similar role in recruiting PcG proteins to a repression complex (Figure 1.6). In *Drosophila*, dMi-2 binds to a domain in the gap protein Hunchback that is specifically required for the repression of homeobox (HOX) genes. Genetic analyses also show that dMi-2 participates in *Polycomb* group repression in vivo (Kehle et al., 1998). However, there are at least three dMi-2 homologues within the *Arabidopsis* genome that may play a similar role.

Despite rapid developments in understanding transcriptional gene silencing within plants, no direct interaction has been shown between dMi-2 homologues, PcG proteins, histone deacetylases or methyltransferase gene products. Protein complexes containing the *FIS* gene products and/or other interacting protein members have not been purified from plant tissues. These models are based on associations according to gene identity and not biochemical function (Figure 1.6), and more research is required to identify members of the plant PcG complex.

1.3 Apomixis: asexual reproduction through seed

The previous sections describe how sexual angiosperms utilise a structured pathway to generate fertile and genetically unique seed (Section 1.2.2 to 1.2.6). The central components of this pathway involve generation of male and female gametes by meiosis, and double fertilisation of the embryo sac to generate seeds that possess genetic characters derived from both the maternal and paternal plants. The absence or disruption of any one of these steps usually results in a cessation of the developmental program and a viable seed is not produced (Koltunow, 1993). Variations in features of megasporogenesis and megagametogenesis have been described in flowering plants (Russell, 1993), which include the number of megaspores surviving after meiosis, the number of mitotic divisions, the position of the resulting nuclei, the patterns of cellularisation and the organisation of the mature embryo sac (Battaglia, 1989).

However, in more than 400 species of plants belonging to 40 families, fertile seeds are produced despite the omission of key steps critical for progression in the sexual pathway. These plants reproduce by apomixis; an asexual reproductive process in flowering plants that results in seeds that are of the same genotype as that of the female parent. The most common apomicts arise from the families Poaceae, Asteraceae, Rosaceae and Rutaceae (Hanna and Bashaw, 1987). In general, apomictic reproduction deviates from sexuality in three main ways: through (i) avoidance of meiosis, (ii) avoidance of egg cell fertilisation by the spontaneous development of the embryo, and in some apomicts, (iii) modification of endosperm development (Koltunow et al., 1998). Most apomicts do not totally exclude the sexual process and produce a low percentage of sexually derived seeds, and are thus

termed facultative. Few apomicts appear to be truly obligate and fully penetrant for the apomictic trait (Koltunow et al., 1998).

1.3.1 Types of apomixis

Apomictic processes have been grouped broadly under two headings; gametophytic apomixis (apospory and diplospory) and adventitious embryony (Table 1.1; Nogler, 1984; Hanna and Bashaw, 1987). Gametophytic apomixis is defined by the mitotic formation of an unreduced embryo sac, in which embryogenesis occurs autonomously and endosperm develops with or without fertilisation of the central cell. Adventitious embryony is defined by the direct formation of an embryo inside the ovule but external to an embryo sac structure.

The two forms of gametophytic apomixis differ by the origin of the cell that initiates unreduced embryo sac formation (Figure 1.7). In diplosporous apomicts, unreduced embryo sacs appear to arise directly from MMCs and meiosis is circumvented in one of two ways. In *Taraxacum*-type meiotic diplospory the MMC begins meiosis, but there is no recombination as chiasmata fail to form (Nogler, 1984; van Dijk et al., 1999). A restitution nucleus forms and the second meiotic division produces a dyad of unreduced cells, of which one divides three times to produce the embryo sac. In *Antennaria*-type mitotic diplospory the MMC bypasses meiosis and divides mitotically three times to produce an unreduced 8-nucleate embryo sac (Chimielewski, 1994). Diplospory has been reported in several genera including *Tripsacum*, *Rubus* and *Parthenium* (Asker and Jerling, 1992; Leblanc et al., 1995).

During apospory, unreduced embryo sacs develop from cells within the ovule other than the MMC (Figure 1.7; Nogler, 1984; Koltunow, et al., 1998). These somatic cells are termed aposporous initials (AIs) and, in any one ovule, their numbers can range from a solitary cell through to many (Koltunow et al., 1998). AIs are cytologically similar to in appearance to differentiating sexual MMCs in that they possess large nuclei and a dense cytoplasm (Koltunow, 1993). Aposporous embryo sac (AES) development appears to occur independently of sexual meiosis, although both processes can occur simultaneously in the same ovule. Many aposporous species display concomitant existence of sexual and apomictic development (Koltunow et al., 1998; Nogler, 1984), and the timing of AI cell formation may regulate the ability of sexual and aposporous embryo sacs to co-exist (Nogler, 1984; Tucker et al., 2001).

Adventitious embryony differs from gametophytic apomixis because it usually occurs outside of the gametophytic structure and is dependent on the formation of a sexual embryo sac (Figure 1.7). Adventitious embryos can arise from individual cells within two different somatic tissues of the mature ovule, the most common tissue being the nucellus and less frequently the integument (Lakshmanan and Ambegaokar, 1984; Naumova, 1993). Polyembryony is a characteristic of adventitious embryony, and fertilisation of the embryo sac central cell is often necessary for the formation of endosperm and viable seed. In *Citrus*, adventitious embryos grow towards the expanding sexual embryo sac, and derive nutrient from the endosperm. If the sexual embryo sac is not fertilised, adventitious embryos still initiate but do not reach maturity (Koltunow et al., 1995b). Observations suggest that the nucellar cells destined to become adventitious embryos have a morphology closely related to that of aposporous initial and megaspore mother cells, with large nuclei and a dense cytoplasm (Wilms et al., 1983; Bruck and Walker, 1985). This

type of apomixis has been observed in species such as *Citrus*, mango (*Mangifera indica)* and sugarbeet (*Beta vulgaris*).

Despite their varying characteristics, the main difference between apomixis and sexuality is conserved in both types of apomixis; the cell which gives rise to the embryo develops parthenogenetically and does not require fertilisation, whether it is an un-reduced egg cell (apospory and diplospory) or a somatic nucellar cell (adventitious embryony). The different apomictic mechanisms are thought to have evolved independently multiple times from sexual ancestors (Marshall and Brown, 1981; Chapman and Darlington, 1992).

Table 1.1 The three main types of apomixis are compared to sexual reproduction.

Reproductive Process	**Sexual**	**Apomictic**		
Type	Polygonum-type *e.g. Cenchrus*	Apospory *e.g. Hieracium*	Diplospory *e.g. Tripsacum*	Adventitious embryony *e.g. Citrus*
Embryo develops from	fertilised egg cell	un-reduced egg cell	un-reduced egg cell	(i) somatic cells and/or (ii) fertilised egg cell (sexual)
Endosperm develops	from fertilised polar nuclei	(i) autonomously (*Hieracium*) (ii) pseudogamy (*Panicum*)	(i) autonomously (*Antennaria*) (ii) pseudogamy (*Tripsacum*)	from fertilised polar nuclei (sexually derived)

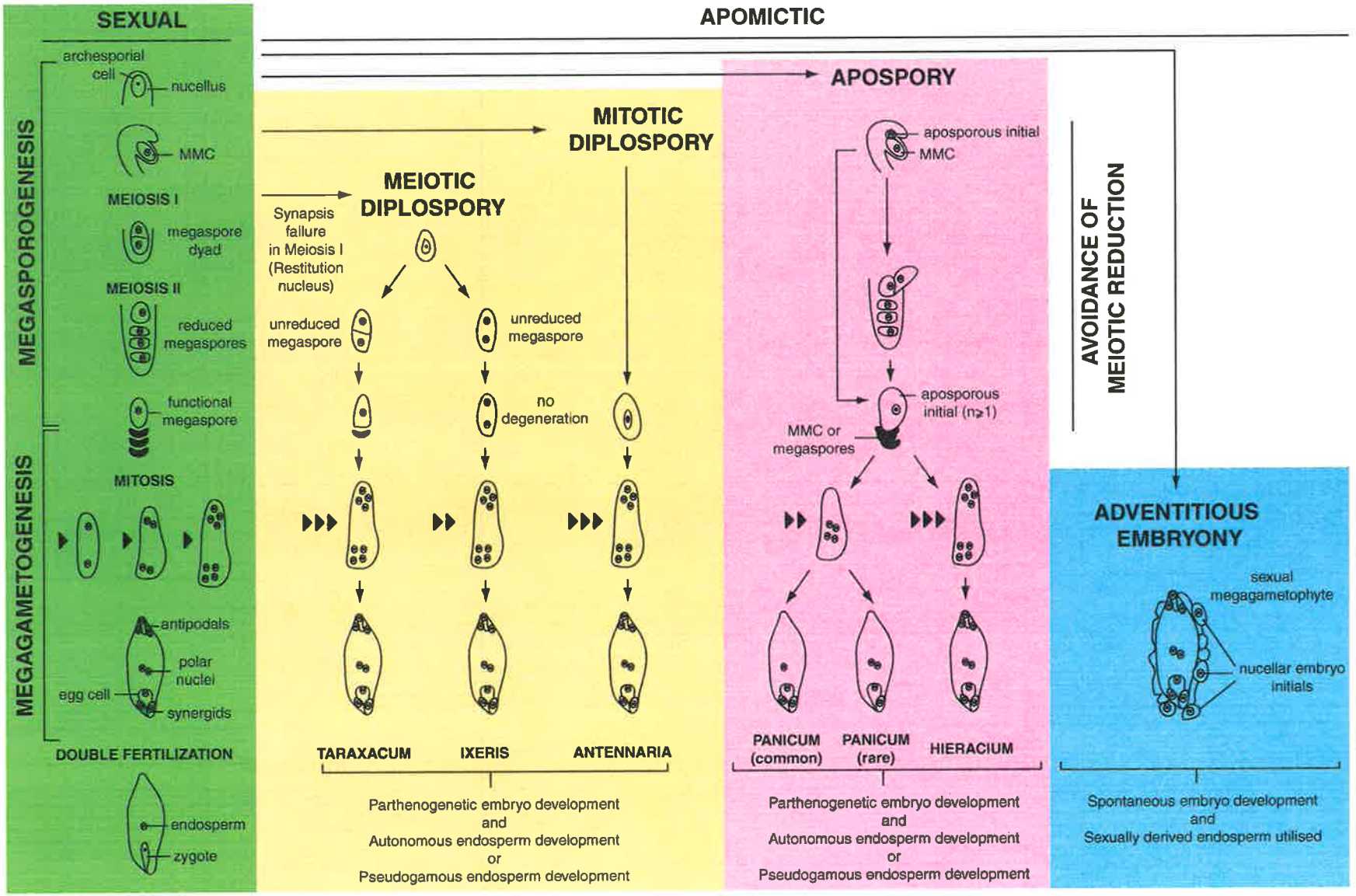
SEXUAL
APOMICTIC
MEGASPOROGENESIS
MEGAGAMETOGENESIS
archesporial cell
nucellus
MMC
MEIOSIS I
megaspore dyad
MEIOSIS II
reduced megaspores
functional megaspore
MITOSIS
antipodals
polar nuclei
egg cell
synergids
DOUBLE FERTILIZATION
endosperm
zygote
MITOTIC DIPLOSPORY
MEIOTIC DIPLOSPORY
Synapsis failure in Meiosis I (Restitution nucleus)
unreduced megaspore
unreduced megaspore
no degeneration
TARAXACUM
IXERIS
ANTENNARIA
Parthenogenetic embryo development and Autonomous endosperm development or Pseudogamous endosperm development
APOSPORY
aposporous initial
MMC
aposporous initial (n≥1)
MMC or megaspores
PANICUM (common)
PANICUM (rare)
HIERACIUM
Parthenogenetic embryo development and Autonomous endosperm development or Pseudogamous endosperm development
AVOIDANCE OF MEIOTIC REDUCTION
ADVENTITIOUS EMBRYONY
sexual megagametophyte
nucellar embryo initials
Spontaneous embryo development and Sexually derived endosperm utilised

1.4 *Hieracium* is a model apomictic plant

One taxon that has been developed as a system for the molecular study of apomixis is *Hieracium*, a member of the Asteraceae. The composite genus is comprised of over 60 apomictic biotypes native to Eurasia and North America (Bicknell, 1994). Apomictic members of the *Hieracium* subgenus *Pilosella* are often polyploid (Tutin et al., 1976) and facultative (Figure 1.8), and exhibit apospory in combination with autonomous embryo and endosperm formation (Koltunow et al., 1998). Inter-specific crosses between sexual and apomictic *Hieracium* plants show that apomixis is inherited as a monogenic dominant trait that can be transferred by both haploid and diploid gametes (Bicknell et al., 2000).

Hieracium is a small herbaceous perennial, easily propagated and maintained in the greenhouse, and flowers in response to extended photoperiod (Yeung and Peterson, 1971). The capitulum of *Hieracium* is a compound inflorescence, containing 40 - 120 individual florets, and seed is set within 3 to 4 months of germination allowing three to four generations per year (Bicknell, 1994). A number of sexual and apomictic *Hieracium* species of different ploidy have been developmentally characterised, including apomictic aneuploid *Hieracium aurantiacum* (A3.4), apomictic triploid *Hieracium piloselloides* (D3), apomictic diploid *Hieracium piloselloides* (D2) and sexual tetraploid *Hieracium pilosella* (P4) (Koltunow et al., 1998; 2000).

A range of tissue-culture methods have been described for *Hieracium*, including methods of vegetative propagation, shoot regeneration and *Agrobacterium* mediated transformation of leaf tissue (Bicknell and Borst, 1994). Constructs containing genes conferring spectinomycin, kanamycin and hygromycin resistance,

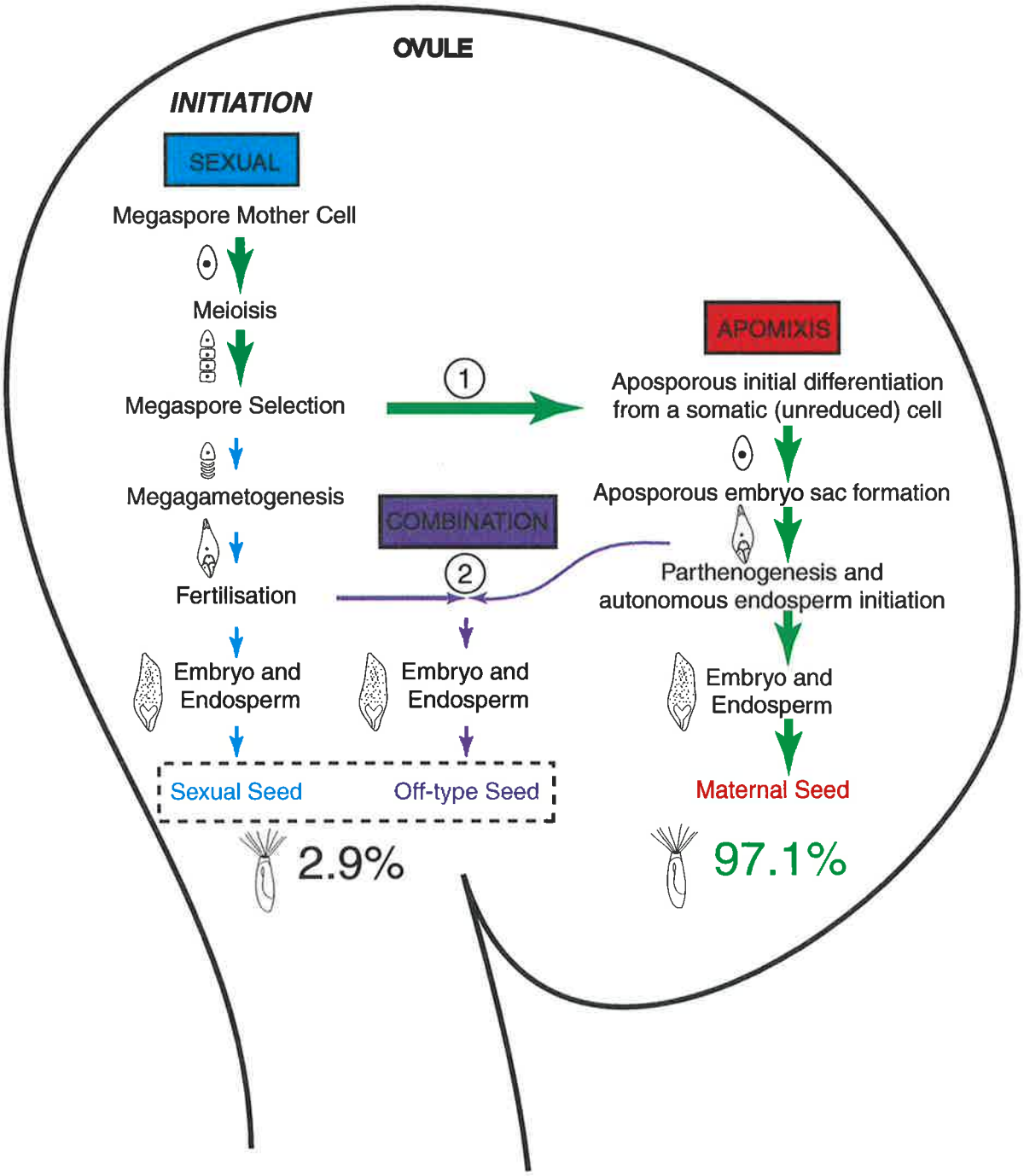

Figure 1.8 Facultative apomixis in *Hieracium piloselloides* D3. Ovules initiate reproduction with sexual events (light blue) and most initiate apomixis (red) at point 1. The majority of viable seeds produced during facultative reproduction are replicates of the maternal plant. "Off-type" seed can be generated at point 2 by various combinations (purple) of apomixis and sexuality, for example when unreduced aposporous embryo sacs are fertilised, or reduced sexual embryo sacs develop autonomously (data from Koltunow et al., (1998)).

as well as β-D-glucoronidase (GUS) and Green Fluorescent Protein (GFP) activity have been demonstrated to function in mature plants (Bicknell and Borst, 1994; Koltunow et al., 2001; M. Lynch and A. Koltunow, unpublished). *In situ* hybridisation technologies have also been developed and used to characterise spatial and temporal gene expression patterns (Guerin et al., 2000; Tucker et al., 2001).

1.4.1 Initiation of apospory in *Hieracium*

Cytological studies of apomixis in *Hieracium* ovules indicate that AI cells form in a stochastic manner (Koltunow et al., 1998). In characterised apomictic *Hieracium* plants the sexual process initiates, then depending on the species, AIs appear either before or after MMC meiosis and undergo mitosis (Koltunow et al., 1998). In triploid D3 a single AI was present in 50% of ovules examined while other ovules contained two initials and rarely three or four. Similarly, in aneuploid A3.4 AI cell number varied from one to eight. Another significant feature of AI differentiation is its close association with sexual development; AIs only ever arise in ovules that have initiated sexual development. This is also true for ectopic ovule-like structures experimentally generated by constitutive expression of the meristem-inducing gene, *rolB* (Koltunow et al., 2001.). What is the nature of this association between sexual and apomictic development? One explanation is that an ovule developmental program is required for AI differentiation and that the MMC is a marker for this program; the presence of sexual development indicates a competency of the ovule to initiate apomixis. Similarly, it seems feasible that the molecular cues specifying MMCs or functional megaspores are altered in apomictic *Hieracium*, leading to the differentiation of multiple like cells. AI cells contain an enlarged nucleus and dense

cytoplasm, and share similar morphology with MMCs. The cellular identity of AIs and the cues controlling AI differentiation are unknown, mainly due to a lack of available markers.

1.4.2 Aposporous embryo sac development in *Hieracium*

Sexual reproduction ceases soon after AI cell formation in apomictic *Hieracium* (Koltunow et al., 1998) similar to that observed in *Ranunculus* (Nogler, 1984), *Pennisetum squamulatum* (Wen et al., 1998) and *Panicum maximum* (Naumova and Willemse, 1995) but this is not the case in *Brachiaria brizantha cv. Marandu* (Araujo et al., 2000). It is uncertain if the cessation of sexual development after AI differentiation in *Hieracium* and some of the above-mentioned species is caused by targeted cell death, or is the outcome of a competitive displacement related to faster aposporous embryo sac growth (Tucker et al., 2001).

Aposporous embryo sacs (AESs) in apomictic *Hieracium* form by mitosis and contain egg-like and central cell-like structures that resemble cells in sexual embryo sacs at maturity (Koltunow et al., 1998). AESs are often highly convoluted structures, but occupy a similar position to the female gametophyte in ovules from sexual plants. It seems likely that similar molecular mechanisms are involved in the division and specification of cells within embryo sacs from sexual and apomictic *Hieracium* plants, but this has not been shown by a molecular study.

Embryos form without fertilisation (parthenogenesis) and endosperm formation in apomictic *Hieracium* is autonomous (Koltunow et al., 1998; 2000) but has not been studied in any great detail. Endosperm initiation can be either nuclear or cellular, but the final cellular product is dissipated during embryogenesis. The

ploidy of autonomous endosperm in *Hieracium* has not been determined, and the molecular cues regulating autonomous endosperm development are also unknown.

1.5 Endosperm formation in facultative apomicts

The formation of mature endosperm in plants appears to be essential for the success of seed development, whether it be apomictic or sexual. Despite studies of somatic embryogenesis and recent characterisation of genes such as *LEC1*, *LEC2*, *BBM* and *PKL* (see Section 1.2.5) that regulate aspects of embryo development, parthenogenetic embryo development does not proceed to maturity in the absence of endosperm formation in seeds. Even *citrus* species that produce embryos from somatic nucellar cells through the process of adventitious embryony still require the presence of endosperm in the seed to reach maturity (Koltunow, 1993; Asker and Jerling, 1992; Wakana and Uemoto, 1988). The endosperm is likely to play an essential nutritive function for the embryo during its early development. As stressed by Nogler (1984) and Quarin (1999), in apomictic plants, the mechanisms of endosperm development have not been well characterised. However, studies have shown that in apomictic plants, endosperm can develop in the absence of fertilisation (autonomously) or after fertilisation of the polar nuclei (pseudogamy).

1.5.1 Formation of pseudogamous endosperm

Pseudogamy is by far the most common mode of endosperm development in the characterised apomictic plants. It is typical for most apomicts, i.e., those that are members of the Rosaceae and particularly the Gramineae families (Nogler, 1984),

which form persistent endosperm. Despite the requirement for fertilisation of the central cell for endosperm development, the egg cell in an unreduced embryo sac develops autonomously. This does not mean that the egg cell cannot be fertilised, because cases of progeny with aberrant ploidy have been described where this event is the likely cause. Asker and Jerling (1992) suggest that pseudogamy is most common among aposporous species and autonomous apomixis mainly occurs in connection to diplospory.

Two types of pseudogamy have been described. In the first, pollination and fertilisation of the central cell act as a trigger for parthenogenetic egg development, otherwise the embryo will not form (Focke, 1881). In the second type, the initiation of embryo formation is precocious and independent of pollination and central cell fertilisation, but fertilisation-induced endosperm development is required for seed viability (Asker and Jerling, 1992).

1.5.1.1 Parental gene dosage in pseudogamous apomicts

In maize, the ratio of the maternal (m) to the paternal (p) genome contribution in the endosperm is maintained at 2:1, and any deviation from this ratio results in seed sterility (Lin, 1984). The maternal genome content of pseudogamous endosperm depends on the number of unreduced central cell nuclei fusing with the reduced sperm cell nucleus. Pseudogamous apomicts that produce an unreduced embryo sac with one central cell nucleus, commonly referred to as the Panicum-type (Figure 1.7), maintain a 2m:1p ratio in their endosperm (Savidan, 2000). In those pseudogamous species that form an embryo sac containing two unreduced nuclei in the central cell, the endosperm ploidy is dependent on whether these nuclei fuse

before fertilisation. If they do, as frequently appears to be the case in a number of pseudogamous apomicts with this type of unreduced embryo sac, then the endosperm in the seed will have a genome contribution ratio of 4m:1p. If the central cell nuclei do not fuse, then the ratio will be 2m:1p. However, in pseudogamous *Tripsacum*, which also has two unreduced polar nuclei in the central cell, the ratio of maternal to paternal genomes in the endosperm varies. Ratios of 4m:1p, 4m:2p, 8m:1p and 8m:2p have been observed, and all result in viable seed (Grimanelli et al., 1997). These maternal and paternal endosperm ratios in the monocot *Tripsacum* contrast with the strict conservation of the 2m:1p genome ratio required for seed fertility in maize and other plants (Johnston et al., 1980). This demonstrates that a tolerance for unbalanced endosperm is intimately related to apomictic reproduction.

1.5.2 Formation of fertilisation-independent (autonomous) endosperm

Autonomous endosperm production is rare in apomicts and is most common in the Asteraceae. Other families such as the Poaceae and Rosaceae display autonomous endosperm development only sporadically e.g. *Burmannia coelestis* (Burmanniaceae) (Ernst and Bernard, 1912), *Calamagrostis* (Poaceae) (Nygren, 1946), *Cortaderia jubata* (Poaceae) (Philipson, 1978; Costas-Lippmann, 1979) and *Alchemilla* (Rosaceae) (Izmailow, 1994). The ability of some apomictic plants to form endosperm without fertilisation may relate to altered regulation of the *FIS* genes (see Section 1.2.8).

Cytological analyses of endosperm in autonomous apomicts, although limited, show that ploidy levels are rather variable, due mainly to the variability in number and extent of fusion of polar nuclei (Matzk et al., 2000). Stebbins and

Jenkins (1939) observed diploid as well as tetraploid endosperm in diploid *Crepis* (Asteraceae), arising from free or fused polar nuclei respectively. This suggests that fusion of polar nuclei is not a prerequisite for mitotic activity in the endosperm (Nogler, 1984). Seed abnormalities that correlate with different doses of maternally or paternally expressed imprinted loci affecting endosperm development in sexual plants (Scott et al., 1998) are obviously irrelevant to autonomous apomicts. In species such as *Taraxacum* and *Hieracium*, endosperm develops in the absence of paternal genomes, suggesting perhaps a modification in imprinting of these loci.

1.6 Genetic control of apomixis

Genetic studies to determine how many genes control apomictic processes have proved difficult for a number of reasons. Apomicts are usually polyploid, pollen recipients must be sexual plants, progeny often differ dramatically in their genotypes and phenotypes and embryological assessments are required to determine the mode of inheritance. Despite such difficulties, it has been established that apomixis in some plants is conferred by no more than one or two loci per genome (Grimanelli et al., 1998; Ozias-Akins et al., 1998; Bicknell et al., 2000; reviewed in Savidan, 2000; Grossniklaus et al., 2001a). A single dominant locus confers both apospory and parthenogenetic embryo development in pseudogamous *Panicum maximum* (Savidan, 1990) and *Ranunculus auricomus* (Nogler, 1995), and diplospory and autonomous embryo formation are conferred by different loci in *Taraxacum* (van Baarlen et al., 1999; reviewed in Grossniklaus et al., 2001b; Grimanelli et al., 2001). In apomictic *Hieracium* species the dominant locus controlling apospory co-segregates with parthenogenesis and autonomous

endosperm formation suggesting that a single locus, either simple or complex, controls apomixis (Bicknell et al., 2000). Thus, in different species, multiple loci are possibly involved in apomixis. Moreover, the genetic control of each apomixis component may be complex and involve more than one gene.

An embryological study of a range of genetically related *Hieracium* plants highlighted that any alteration to genetic background resulted in significant changes in the apomictic process relative to the original apomictic parents (Koltunow et al., 2000, Bicknell et al., 2000). Alterations affected the frequency, location and timing of aposporous initial cell formation, the mode of embryo sac formation, co-ordination of embryo and endosperm development and the penetrance of each component of apomixis in the plant (Koltunow et al., 2000). This lack of developmental conservation of apomixis following alterations to the genetic background demonstrates that genetic factors in addition to the apomixis locus play a critical role as modifiers in modulating the progression of apomixis in *Hieracium* (Koltunow et al., 2000).

1.7 Models for the control of apomixis

Many models and hypotheses have been put forward that address the developmental alterations observed in apomictic plants. Given the range of apomictic processes, and that apomicts have been reported in close to 40 plant families, the routes that led to the evolution of apomixis may be as diverse as the cytological mechanisms. It is likely that different concepts may play predominant roles in different apomicts, they may not be mutually exclusive and they may occur in combination to create the

developmental diversity observed in apomictic species. Updated models for the control of apomixis are described by Koltunow and Grossniklaus (2003).

1.7.1 Hybridisation of related species

Taking into account that virtually all natural apomicts are polyploid and highly heterozygous, Ernst (1918) postulated that apomixis might result from the hybridisation of related species. The recovery of diploid apomicts in a variety of species (Nogler, 1982; Dujardin and Hanna, 1986; Leblanc et al., 1996; Visser and Spiess, 1994; Roy, 1995; Kojima and Nagato, 1997; Bicknell, 1997) has shown that polyploidy is not a pre-requisite for apomictic reproduction, but may be a consequence of asexual reproduction. The hybridisation theory for the evolution of apomixis has been extended more recently by Carman (1997; 2001), and suggests that apomixis may result from hybridisation of two ecotypes or related species with differences in reproductive characters. The hybrids are postulated to contain two sets of genes involved in female reproduction derived from the two genomes, whose asynchronous expression may lead to precocious embryo sac initiation and embryogenesis. Support for this hypothesis comes from hybrids of two sexual parents that display apomictic traits and the occurrence of reproductive anomalies in allo-polyploids or paleo-polyploids (see Carman, 2001). Importantly, the hybridisation model relies only on the additive effect of native gene expression, rather than mutations in genes involved in sexual reproduction.

1.7.2 Mutation of a key regulatory gene(s)

Genetic analyses showing that apomixis is under the control of a few loci have led to the model that apomixis results from mutations at one or a few loci (Peacock et al., 1995). For many years, researchers viewed apomixis and sexuality as two distinct and unrelated processes. However, developmental studies have stressed the inter-relatedness of the two processes and the genes conferring apomixis are now viewed as mutated alleles of genes controlling sexuality. In this context, genes conferring apomixis may not actually code for novel or aberrant functions, but rather provide wild-type activity, albeit in the wrong cell type or at the wrong time (Koltunow and Grossniklaus, 2003). For instance, a wild-type gene promoting embryo sac initiation that is expressed in a nucellar cell could cause apospory (Koltunow, 1993). Despite the strong support for this theory, most studies highlighting the inter-relatedness of apomixis and sexuality have relied upon cytological descriptions and little molecular evidence is available.

1.7.3 Epigenetic regulation of gene expression

The genes controlling apomixis may not represent mutant alleles but could be a consequence of epigenetic changes in gene regulation (Grossniklaus, 2001; Spillane et al., 2001). Stable and heritable "epialleles" can arise, for instance, through changes in DNA methylation (Kakutani, 2002; Kakutani et al., 1996; Jacobsen and Meyerowitz, 1997; Soppe et al., 2000) or chromatin structure (Stam et al., 2002). This epigenetic model is appealing for several reasons. Firstly, it unites the mutation and hybridisation theories, because epialleles behave genetically like mutations, and

epigenetic changes in gene expression have indeed been documented upon hybridisation (Lee and Chen, 2001). Secondly, the epigenetic control model provides a solution to the enigma that several traits, for example, apomeiosis, parthenogenesis and autonomous endosperm formation, which each on their own are disadvantageous, had to evolve co-ordinately to produce a functional apomict (Mogie, 1992).

Unlike mutations, epigenetic changes can occur rapidly and may be particularly frequent as a result of hybridisation and polyploidization providing the epigenetic basis for the formation of an apomict. Strong support for this view comes from the fact that a simple chromosome doubling, not involving inter-specific hybridisation or mutation, can produce functional apomicts in *Paspalum* spp. (Quarin and Hanna, 1980; Quarin et al., 2001).

1.7.4 Apomixis-specific factors - "alien" DNA

The three concepts described above are all based on genes that play a key role in sexual development and are asynchronously expressed, mutated, or mis-regulated through a genetic or epigenetic change in gene expression. Recent findings in *Pennisetum* in contrast, show that molecular makers, which are tightly linked to apospory do not hybridise to DNA from sexual plants (Ozias-Akins et al., 1998; Roche et al., 1999). Thus, these sequences are either absent from sexual plants or highly divergent (Grossniklaus et al., 2001a), suggesting a possible role of supernumerary, apomixis-specific chromatin in the control of apomixis (Roche et al., 2001). In all apomicts analysed to date, the apomeiosis locus is located in a region of the genome where recombination is suppressed (reviewed in Grossniklaus

et al., 2001a). The recombinational isolation of the apomeiosis locus may provide an explanation for the divergence from the corresponding region in sexual species, where recombination is not suppressed. While the general region may be highly divergent, an ancestral sexual gene whose activity has been altered in the apomict may still reside in this region or be linked to the region, such that the inserted or highly rearranged region affects its activity (Grossniklaus and Koltunow, 2003).

1.8 Addressing questions of apomixis in *Hieracium*

Despite the large amount of study focused on understanding apomixis for transfer into agricultural crops, there are many fundamental questions that remain unanswered. The means by which apomixis is able to avoid meiosis and produce embryos and endosperm without fertilisation is unknown, even though apomixis appears to be controlled by just a few dominant genes (Savidan, 2000). These genes have yet to be identified. It may be that sexual and apomictic reproduction share regulatory components, and differ only through modified levels or sites of expression, thus agreeing with the dominant nature of the apomictic trait. Key downstream regulatory genes of apomixis may have already been isolated, but without appropriate modifiers or the initial "switch", mutants of such genes may not confer a complete apomictic phenotype.

A detailed molecular and cytological characterisation of autonomous endosperm development has not been reported in any of the few apomictic families that produce autonomous endosperm. The isolation of putative members of a repressive plant PcG complex, such as *FIS2* and *FIE*, and examination of their expression and function during seed development in sexual and apomictic plants

will address some fundamental questions of apomixis. Do PcG genes exist in apomictic plants? Is their function modified between sexual and apomictic plants, and do these genes play a role during seed development and autonomous endosperm formation? *Hieracium* will be used as a model plant to answer these questions. By using a system that is amenable to molecular developmental analysis, the aims of this thesis were to characterise early autonomous seed formation using molecular markers, specific gene constructs, expression analyses and ploidy determinations.

1.9 Specific thesis aims

(1) To cytologically characterise and compare the formation of endosperm in apomictic and sexual *Hieracium* using

(i) Haematoxylin stains (Chapter 2)

(ii) Chimeric *FIS:GUS* gene fusions from *Arabidopsis* (Chapter 3)

(2) To determine the origin of mature seeds in apomictic and sexual *Hieracium* using a flow cytometric ploidy analysis (Chapter 2).

(3) To generate embryo sac cell-specific marker genes from *Arabidopsis* enhancer trap lines for use in addressing cell identity in apomictic *Hieracium* (Chapter 4).

(4) To identify and characterise the role of putative members of a *FIS Polycomb* group complex from *Hieracium* during the initiation of autonomous endosperm development (Chapter's 5, 6 and 7).

Chapter 2: Cytological characterisation of early seed development in sexual and apomictic *Hieracium*

2.1 Introduction

Plants that reproduce by autonomous apomixis do not depend on pollination for reproduction because neither the unreduced egg cell nor the polar nuclei require fertilisation for development. Fertilisation-independent (autonomous) endosperm development has been documented in few apomictic species, but is most frequent in genera from the Asteraceae, such as *Crepis, Hieracium* (Figure 2.1) and *Taraxacum*. Cytological studies of autonomous endosperm development are limited. Cooper and Brink (1949) studied the relationship between the embryo and endosperm in autonomous *Taraxacum officianale*, and showed that the two tissues can initiate development independently of one another. Stebbins and Jenkins (1939) observed 2n and 4n endosperm in diploid *Crepis*, arising from free or fused polar nuclei respectively. This suggests that polar nuclei fusion is not a prerequisite for autonomous endosperm initiation. In autonomous *Taraxacum scanicum*, Malecka (1973) showed that fertilisation of the polar nuclei was possible, suggesting that the central cell retains functional identity similar to the corresponding structure in sexual plants. These studies highlight the variable ploidy levels and nature of endosperm development in autonomous apomictic plants, but it is uncertain how this variation affects seed viability. It is similarly uncertain how autonomous endosperm develops without any paternal contribution of genetic information and

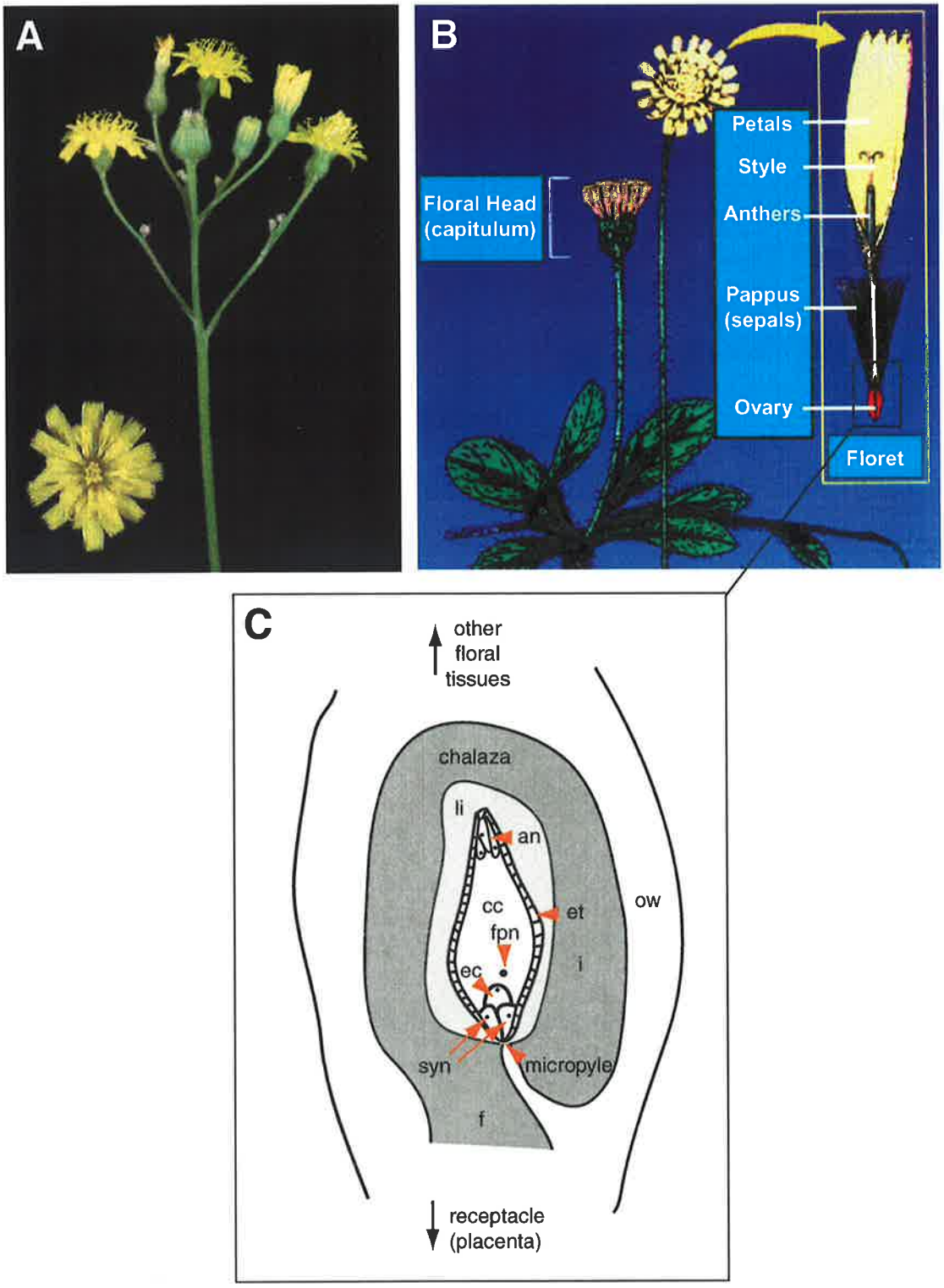

Figure 2.1 Floral morphology of *Hieracium*. **A** Floral meristem from *H. piloselloides* D3 showing capitula at different stages, and a transverse view of a stage 8 flower (inset). **B** Schematic diagram of a *Hieracium* floret. **C** Schematic diagram of a typical *Hieracium* ovary at anthesis. The ovule (shaded in dark grey) is located within the ovary wall (ow) and contains a single integument (i) and a funiculus (f). The mature embryo sac is surrounded by the endothelium (et) and a layer of liquefied integument (li; shaded light grey), and contains three antipodals (an), an egg cell (ec), tyo synergids (syn) and a central cell (cc) that contains the fused polar nucleus (fpn). The ovary is shown in chalazal (top) to micropylar (bottom) orientation.

manages to sustain embryo growth to maturity. Given the importance of the endosperm to the development of a viable seed (see Section 1.5.4), further cytological and molecular studies of this fertilisation-independent process are required.

To date, a wholemount cytological study of autonomous endosperm initiation and development in *Hieracium* has not been undertaken. Preliminary sectioning studies have shown that in sexual *Hieracium pilosella* (P4), a Polygonum-type embryo sac forms (Figure 2.1C) and endosperm development initiates with nuclear divisions before producing cellular endosperm (Koltunow et al., 1998). In autonomous apomictic *H. piloselloides* (D3) and *H. aurantiacum* (A3.4) plants, endosperm appears to initiate with nuclear divisions, and infrequently with cellular divisions, from cells within the embryo sac (Koltunow et al., 1998). The origin of endosperm in autonomous apomictic D3 is not completely clear, and it is uncertain whether the ploidy levels of endosperm vary between ovules from the same plant, similar to other species in the Asteraceae (Stebbins and Jenkins, 1939). A detailed analysis of early seed formation in apomictic *Hieracium* will address these questions and provide the basis for further molecular studies of autonomous endosperm development.

In this study a wholemount staining method was utilised to observe and compare stages of early endosperm development in sexual and apomictic *Hieracium* by differential interference contrast (DIC) microscopy. This cytological investigation was carried out in conjunction with a flow cytometry study of mature seeds in collaboration with Dr Fritz Matzk (IPK, Gatersleben), to determine the ploidy variability in mature seeds from sexual and apomictic *Hieracium* plants. The flow cytometry methodology developed by Dr Matzk also enabled some predictions of the reproductive origin of the seeds. The results extend the information

concerning the early events of endosperm development in sexual and apomictic *Hieracium* and form the fundamental background for studies assessing the effects of introduced genes on seed initiation and development.

2.2 Materials and Methods

2.2.1 Plant material and growth conditions

A triploid accession of apomictic *Hieracium piloselloides* Vill. (D3; 3x=2n=27) was used to analyse early autonomous seed development. D3 is a natural facultative apomict that was obtained from a wild population in Steiermark, Austria, and produces >93% viable apomictic seeds per capitulum. The self-incompatible sexual biotype designated P4 was obtained from Caen, France and is a tetraploid (4x=2n=36) accession of *H. pilosella* L. Both biotypes are propagated vegetatively and are maintained in culture as stocks from individual characterised source plants (Koltunow et al., 1998). Plants were grown in a glasshouse with average day and night temperatures of 26°C and 16°C respectively. Overhead mercury vapour lamps were used to supplement light quality and to provide an average continuous day length of 17 hours.

2.2.2 Haematoxylin staining of *Hieracium* ovaries

Unpollinated ovaries from stages 5-12 of floral development were collected from sexual P4 and apomictic D3 plants, and were staged as per Koltunow et al., (1998; see Appendix 1). Stage 7 (anthesis) P4 floral buds were brushed with pollen from apomictic D3 stamens, and collected 12, 24, 36, 54 and 70 hours after pollination

(HAP). After collection, florets were dissected to leave only the ovaries, which were fixed in formalin : acetic acid : alcohol (FAA) overnight as per Young et al., (1979). Ovary samples were re-hydrated and stained for 4 hours in 0.01% haematoxylin prepared in 0.08 M aluminium potassium sulphate ($AlK(SO_4)_2.12H_2O$) and 0.001 M sodium iodate ($NaIO_3$) essentially as per Stelly et al., (1984). Ovaries were rinsed in 1% acetic acid and then destained in the same solution for 5-12 hours until they became pale purple-pink in appearance. After destaining, the ovaries were rinsed in 20 mM Tris Base solution, and washed in the same solution for 2-8 hours until the tissue turned blue/grey in colour. Upon completion of staining, samples were dehydrated through a graded ethanol series, and cleared in methyl salicylate. Wholemount tissue samples were mounted on concave slides (ProSciTech) in methyl salicylate and viewed by Nomarski differential interference contrast microscopy (DIC). Images were captured using a Spot II camera (Diagnostic Instruments) in colour, but are shown in black and white to aid examination of the nuclei. A total of 735 ovaries were analysed from apomictic D3, and 1362 were analysed from sexual P4.

2.2.3 Flow cytometry analysis of *Hieracium* seed ploidy

Seed samples from apomictic D3, and cross-pollinated sexual P4 plants were collected and separated into three classes based on their morphology; fat black (FB), skinny black (SB) or brown (B). Approximately fifty seeds from each class were sent to Dr Fritz Matzk (IPK, Gatersleben) where individual and bulked samples were analysed by flow cytometry to determine their DNA content. Seed samples, comprising of one to ten seeds, were chopped with a razor blade in DAPI (4',6-diamidino-2-phenylindole) staining buffer (DNA staining solution from Partec,

Münster, Germany). The extracts were filtered (30 μm) and stored on ice until measurement. Samples were analysed by a Facstar PLUS (Becton-Dickinson) flow cytometer, as described in Matzk et al., (2000).

2.3 Results

2.3.1 Early seed development in sexual P4 *Hieracium*

Seed development in sexual P4 was characterised from stage 5 (megagametogenesis) to 12 (early torpedo stage embryogenesis) of floral development (see Appendix 1) using haematoxylin stains and methyl-salicylate clearing. To obtain seeds from self-incompatible P4 and characterise fertilised development, stage 7 (anthesis) floral heads were cross-pollinated with pollen from *Hieracium* D3 and seeds were collected at 12 (stage 8), 24 (stage 9), 36 (stage 9/10), 54 (stage 10/11) and 70 (stage 11/12) hours after pollination (HAP). Only the outer whorl of florets was collected for each pre-fertilisation stage to avoid maturity differences across the capitulum.

2.3.1.1 Pre-fertilisation embryo sac development in sexual P4

In ovaries from stage 5 flowers the ovule integument cells showed strong staining, as their nuclei made up a large proportion of the cellular volume. Embryo sac structures were small, linear and difficult to observe through the dense integument cells, but usually contained four to eight intensely stained nuclei (Figure 2.2A). By stage 6 of floral development, the majority of ovaries contained cellularised embryo

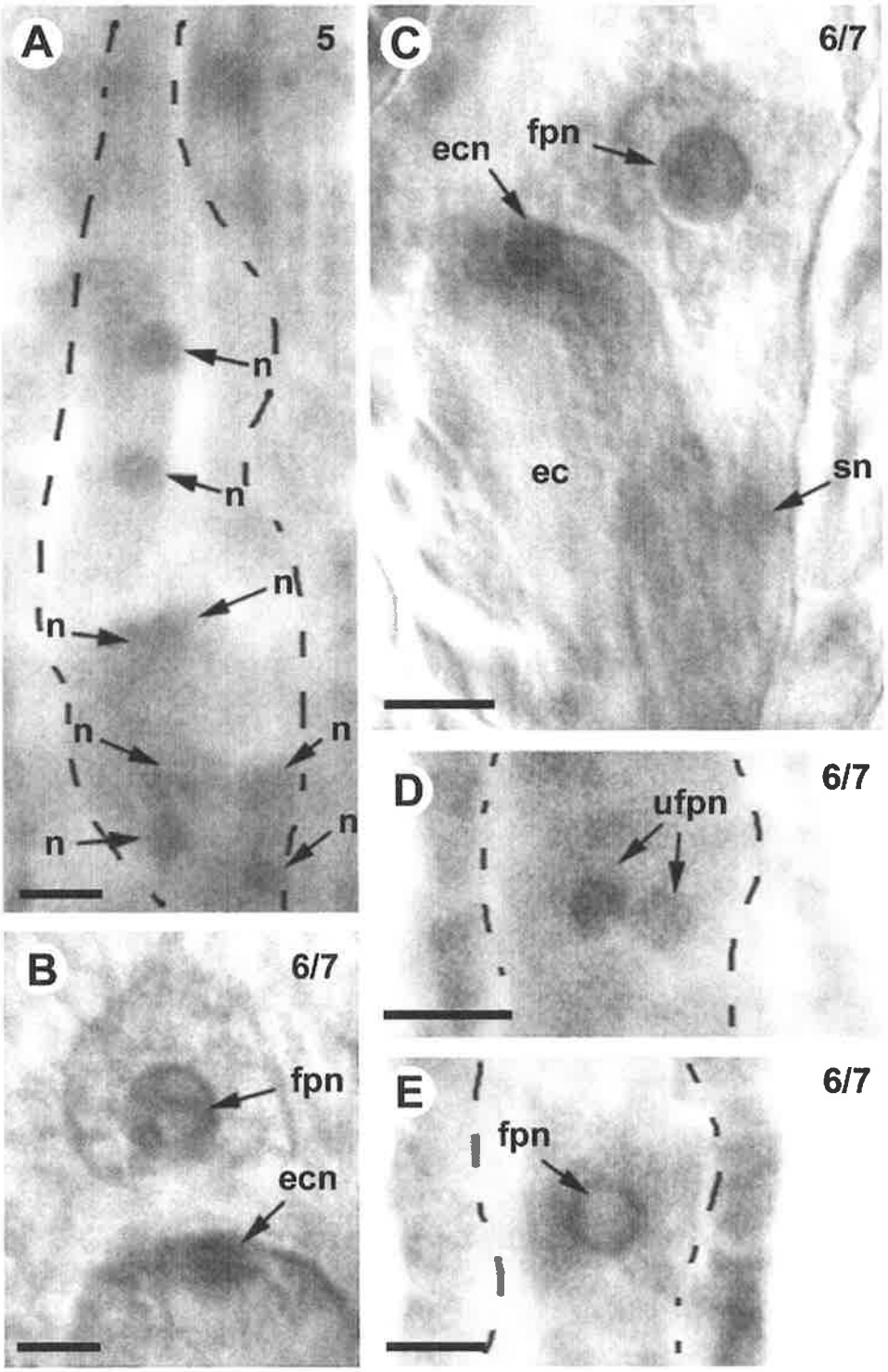

Figure 2.2 Embryo sac formation in sexual P4 *Hieracium*. In *panels* **A**, **D** and **E** the dashed line marks the inner wall of the embryo sac. **A** Embryo sac containing unidentified mitotic nuclei (n). **B** The egg cell nucleus (ecn) and fused polar nucleus (fpn) in a mature embryo sac. **C** Embryo sac containing an egg cell (ec) and a fused polar nucleus. One synergid nucleus (sn) is visible. **D** Unfused polar nuclei (ufpn) **E** fused polar nucleus with distinctive ring-like staining. All panels are in chalazal (top) to micropylar (bottom) orientation. The number in the top right corner of each panel indicates the floral stage of development. Bar = 10 μm in all panels.

sacs with specific cell types and predominant nuclei. A dense nucleus was located at the curved chalazal pole of the egg cell, a single large polar nucleus (about twice the size of the egg nucleus) was present in the central cell just above (Figure 2.2B) or to one side of the egg cell (Figure 2.2C), and two small nuclei were observed in synergid cells to either side of the egg cell (Figure 2.2C). Unfused polar nuclei were infrequently observed (Figure 2.2D), and most ovaries contained a single fused polar nucleus that was either stained throughout or only in a ring around the edge of the nucleolus (Figure 2.2E). Although there were slight variations detected between ovaries, it was difficult to observe when polar nuclei fusion occurred in the sexual plant. Differentiation of the eight embryo sac nuclei into different cell types proceeded rapidly, and polar nuclei fusion must occur concomitant to this process.

In ovaries from stage 7 flowers, the vast majority of embryo sacs had reached maximum expansion and contained a mature egg apparatus (egg cell and two synergids), a fused central nucleus, and antipodals at the chalazal pole (data not shown). The number of antipodal cells was difficult to determine because their nuclei showed only weak staining, but they were rarely detected in maturing embryo sacs after stage 7 of floral development. In unfertilised ovaries from stage 8, 9 and 10 florets, the egg cell and central cells remained present in the embryo sac, and began to display signs of nuclear degeneration.

2.3.1.2 Post-fertilisation embryo sac development in sexual P4

Sexual P4 florets were pollinated and ovaries were collected at different stages along a time course from embryo sac maturity to late embryo and endosperm development. Because P4 is a self-incompatible plant, flowers were cross-pollinated

with pollen from apomictic D3, and to increase the chance of identifying fertilised embryo sacs, all open floral whorls were collected and analysed.

Most of the ovaries collected from florets 12 HAP contained an open embryo sac that enclosed a quiescent egg cell and a single fused polar nucleus (as per Figure 2.2B and 2.2C). It was uncertain whether these ovaries had yet to be fertilised, or whether they had not been pollinated during manual pollination. The remaining embryo sacs contained an egg apparatus and two endosperm nuclei derived from a single division of the fertilised primary endosperm nucleus. The two large and dense sister endosperm nuclei were positioned close together above the egg cell, and each shared similar morphology to the fused polar nucleus (Figure 2.3A). The fertilised egg cell divided after the initiation of endosperm development, and at 24 HAP most embryo sacs contained either a two or four-celled embryo and four to eight endosperm nuclei (Figure 2.3B and 2.3C). During the second and third endosperm divisions, the syncytial nuclei migrated to the periphery of the enlarging embryo sac and the micropylar and chalazal poles (Figure 2.3B-D). In ovaries collected 36 HAP, endosperm nuclei were proceeding through the third and fourth mitotic divisions and embryo sacs contained eight to twenty evenly distributed endosperm nuclei. During the fourth mitotic division the endosperm nuclei began to condense slightly and display multiple nucleoli (Figure 2.3E). Embryos ranged in size from four to sixteen cells, and by 54 HAP were at mid-late globular stage (see Figure 2.4).

In ovaries collected 54 HAP, embryo sacs contained many endosperm nuclei each with multiple small nucleoli (Figure 2.4B), and in a few cases cell walls had initiated between the nuclei closest to the embryo (Figure 2.4C). Endosperm cellularisation began at the micropylar end of the embryo sac, around the peripheral nuclei and near the embryo, and continued towards the centre of the embryo sac.

Figure 2.3 Early endosperm and embryo development after fertilisation in sexual P4 *Hieracium*. **A** First division of the polar nucleus showing two sister nuclei (n) after fertilisation. One of the synergids has degenerated (ds). **B** Third division of the endosperm nuclei (en) and a dividing embryo (em). **C** Four celled embryo (em) and migration of the endosperm nuclei to the embryo sac periphery during the third endosperm division. **D** Dividing endosperm nuclei showing similar morphology to the polar nucleus. **E** Early globular embryo (em) and the fourth division of the endosperm nuclei. The endosperm nuclei contain multiple nucleoli. All panels are in chalazal (top) to micropylar (bottom) orientation. The stage is indicated in the top right corner of each panel in terms of hours after pollination (HAP). Bar = 10 μm in all panels.

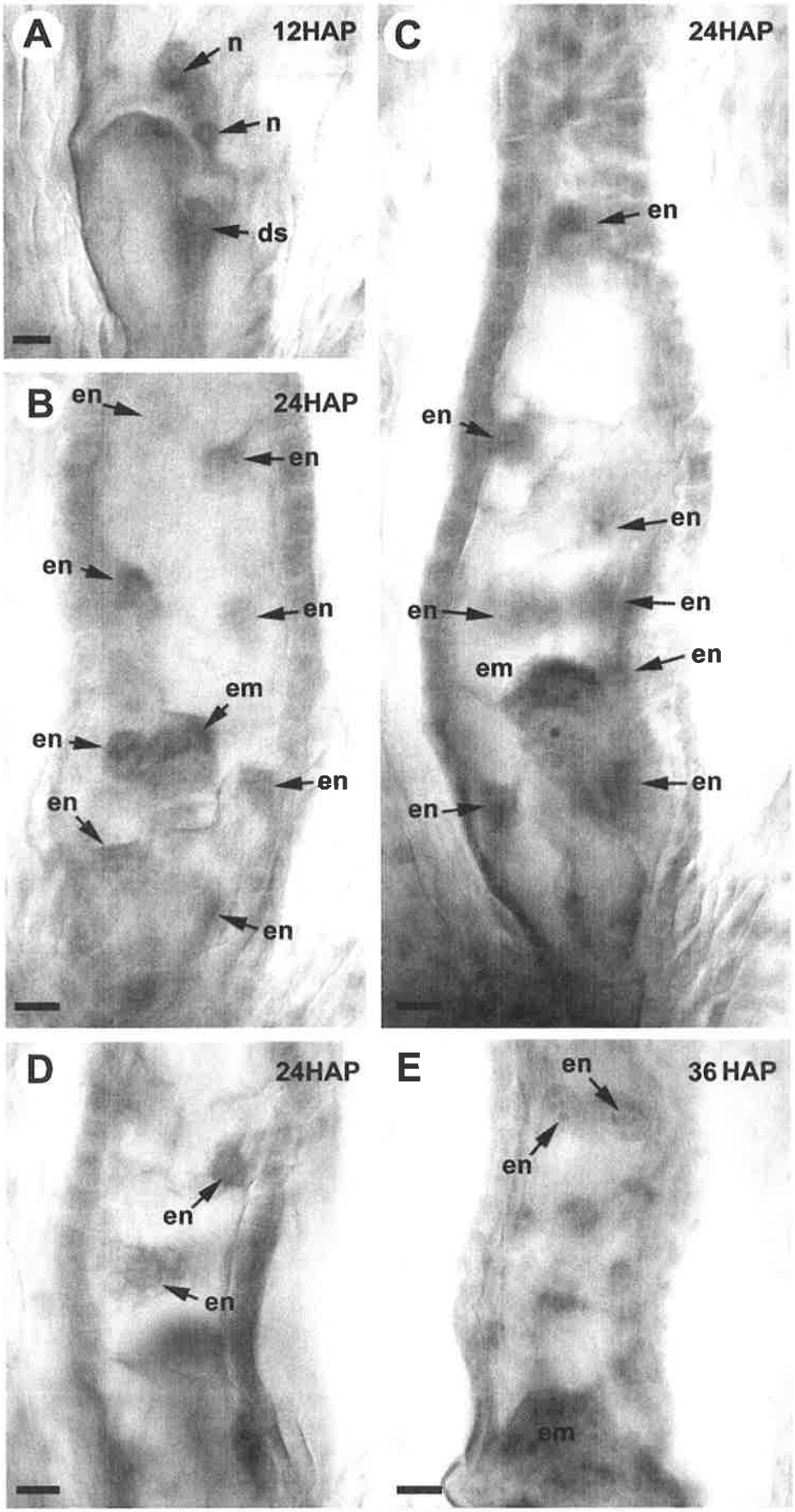
A
12HAP
n
n
ds
B
24HAP
en
en
en
en
em
en
en
en
en
C
24HAP
en
en
en
en
en
em
en
en
en
D
24HAP
en
en
E
36 HAP
en
en
em

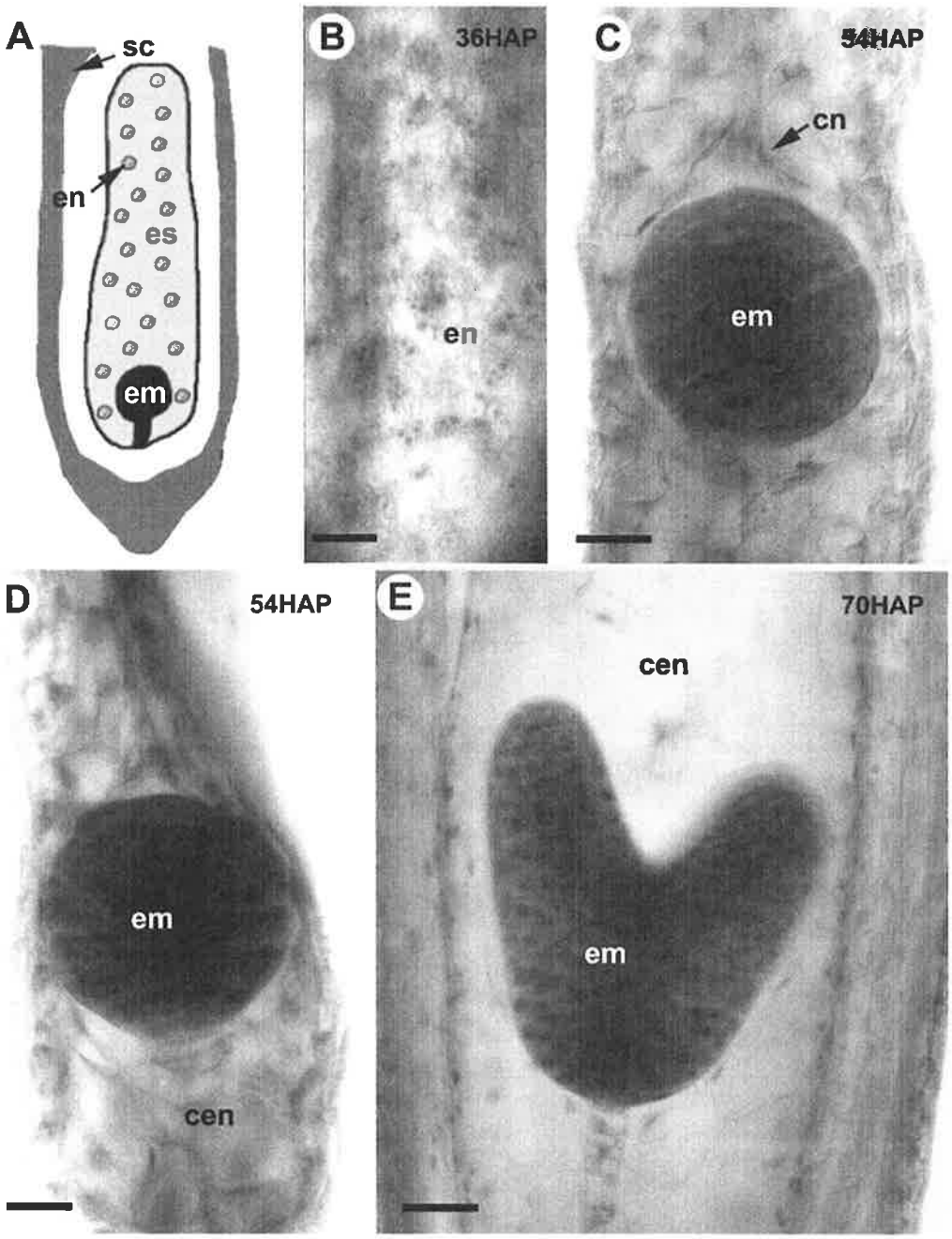

Figure 2.4 Late endosperm and embryo development after fertilisation in sexual P4 *Hieracium*. **A** Schematic diagram of a maturing *Hieracium* seed, showing the seed coat (sc; shaded in dark grey), the ovule (shaded in white) and the embryo sac (es; shaded in light grey) containing endosperm nuclei (en) and an embryo (em). **B** Endosperm nuclei (en) containing multiple nucleoli prior to cell wall formation. **C** Endosperm cells containing compressed nuclei (cn) around a globular embryo (em). **D** Globular embryo (em) and cellular endosperm (cen). **E** Heart stage embryo (em) surrounded by cellular endosperm (cen). All panels are in chalazal (top) to micropylar (bottom) orientation. The stage is indicated in the top right corner of each panel in terms of hours after pollination (HAP). Bar = 25 µm in all panels.

During this process the large rounded endosperm nuclei became positioned flat against the walls of the forming cells as vacuoles developed (Figure 2.4C and 2.4D). Cell walls had formed around all of the nuclei by 70 HAP, and a lattice of large cubic endosperm cells filled the embryo sac (Figure 2.4E). Most embryos were at heart to torpedo stage (Figure 2.4E) and had begun to consume the proximal endosperm cells.

This staged wholemount description of early seed development provides an outline of fertilised embryo and endosperm development in sexual P4 *Hieracium*, and represents a standard to compare with embryo sac development in apomictic D3 *Hieracium*.

2.3.2 Early seed development in apomictic D3 *Hieracium*

The same stages of flower and seed development examined in sexual P4 were investigated in apomictic D3 by wholemount stains. Only the outer whorl of florets was collected for each stage in an attempt to avoid maturity differences across the capitulum, because the outer whorl of florets generally opens first. The content of the *Hieracium* D3 ovaries was scored and is tabulated in Appendix 2.

In ovaries from stage 5 D3 florets, the majority of embryo sac structures were small, convoluted and linear, and contained between two and eight unidentified nuclei (Figure 2.5A and 2.5B). The identity of the individual nuclei was difficult to determine because they were intensely stained, clustered close together in the embryo sac structure (Figure 2.5B), and were generally more disorganised than the nuclei observed in embryo sacs from stage 5 sexual P4 florets. However, by stage 6 of floral development most embryo sacs were comparable in

Figure 2.5 Embryo sac formation in apomictic D3 *Hieracium*. In *panel* **C** the dotted line marks the synergid wall and in *panels* **D** to **F** the dotted line marks the egg cell wall. **A** Schematic diagram of a typical D3 ovary from a stage 6 floret, showing the ovary wall (ow), funiculus (f), integument (i), liquefied integument (li) and embryo sac (es). The chalazal (ch) and micropylar (mp) poles are shown to aid orientation. **B** Embryo sac containing unidentified mitotic nuclei (n). **C** Egg cell nucleus (ecn), a synergid (sy) and the unfused polar nuclei (ufpn) in a mature embryo sac. **D** Unfused polar nuclei displaying ring-like staining above an egg cell. **E** Unfused polar nuclei and a small secondary nucleolus (nu) above an egg cell. **F** Fused polar nucleus (fpn) above a misshapen egg cell and a synergid. **G** and **H** unidentified nuclei in the micropylar region of an aposporous embryo sac. **I** Early autonomous divisions of the endosperm nuclei (en) with similar morphology to the polar nucleus. **J** Dividing endosperm nuclei and a small embryo (em). All panels are in chalazal (top) to micropylar (bottom) orientation. The number in the top right corner of each panel indicates the floral stage of development. Bar = 10 μm in all panels.

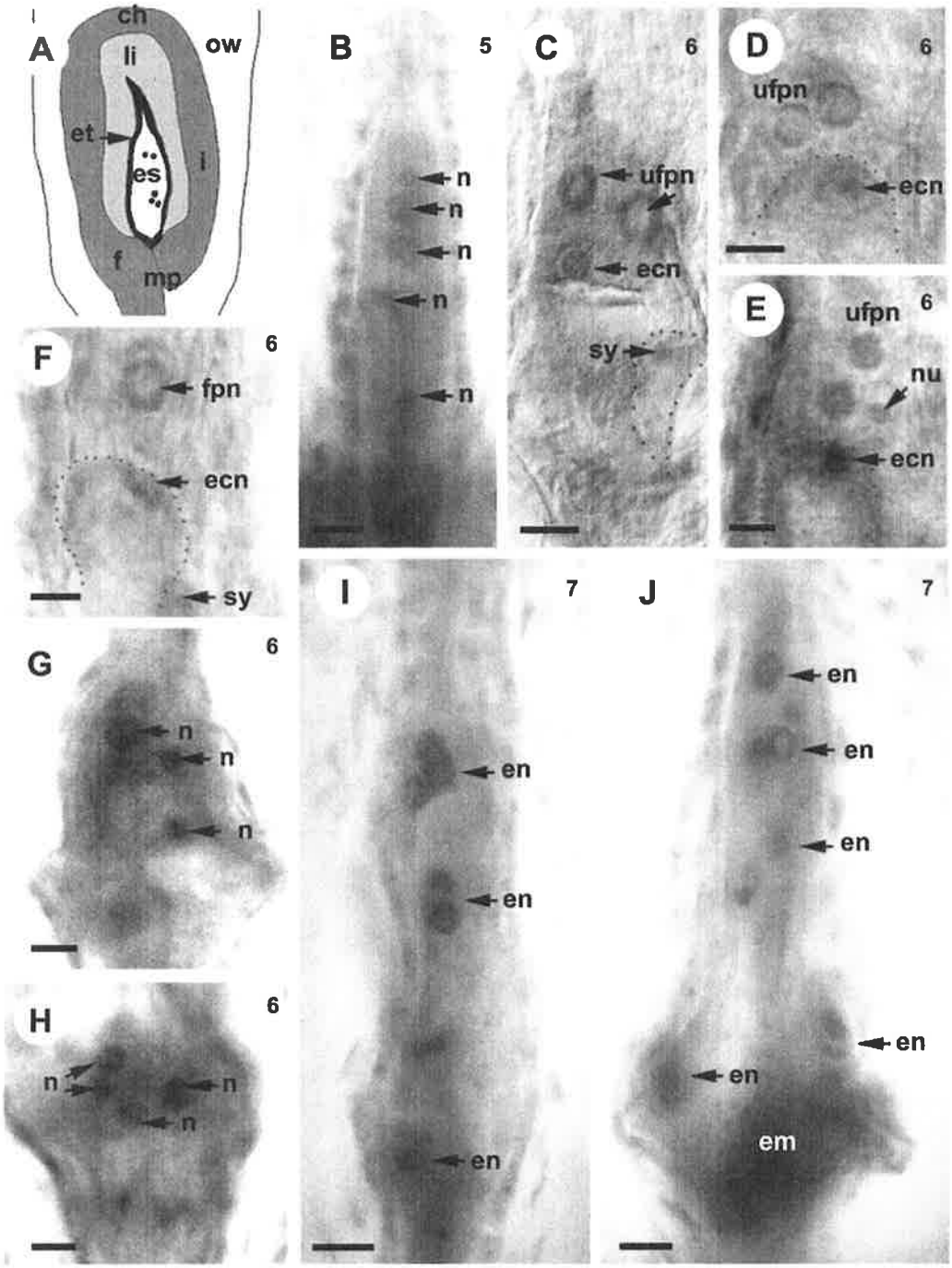
A
ch
li
ow
et
es
i
f
mp
B
5
n
n
n
n
n
C
6
ufpn
ecn
sy
D
6
ufpn
ecn
E
ufpn
6
nu
ecn
F
6
fpn
ecn
sy
G
6
n
n
n
H
6
n
n
n
I
7
en
en
en
J
7
en
en
en
en
en
em

terms of their linear shape to embryo sacs from stage 6 sexual P4 florets, and contained three to five clearly visible nuclei. The nuclei were sometimes separated by cell walls that defined an egg-like cell with a small dense nucleus and polar nuclei (Figure 2.5C-F). More frequently the identity of the nuclei was difficult to clarify, because they lacked defined cell walls and were clustered close together near the micropylar pole of the embryo sac (Figure 2.5G and 2.5H).

In contrast to sexual P4, most embryo sac structures in apomictic D3 at stage 6 of floral development contained two unfused polar nuclei that were slightly separated (Figure 2.5C) or close together (Figure 2.5D), and a small secondary nucleolus was sometimes observed near one of the polar nuclei (Figure 2.5E). A single polar nucleus was infrequently observed (Figure 2.5F) at any stage of embryo sac development in apomictic D3, and the unfused polar nuclei often displayed ring-like staining around the edge of the nucleoli (Figure 2.5C, 2.5D and 2.5F). Cells containing small dense nuclei that resembled the synergids from embryo sacs in sexual P4 were commonly observed below the egg-like cell in aposporous embryo sacs (Figure 2.5C and 2.5F), but antipodal cells were observed infrequently (data not shown).

In most ovaries from stage 6 and 7 D3 florets, embryo sacs were distorted and appeared to be suffering from torsional stress, similar to that reported by Koltunow et al., (1998). Not all embryo sacs in stage 7 florets contained an obvious egg cell, but the majority (at least 50%) displayed between four and sixteen dividing endosperm nuclei similar in appearance to the polar nuclei (Figure 2.5I and 2.5J), and these appeared to be derived from divisions of the fused polar nucleus. Early nuclear divisions of the endosperm were rapid and irregular, and the nuclei tended to remain in clusters that were predominantly chalazal to the egg cell or small embryo, if present (Figure 2.5I and 2.5J). This differed from the specific patterning

of the endosperm nuclei around the periphery of the embryo sac in sexual P4 (compare Figures 2.5I and 2.3B). In 25% of embryo sacs at stage 7, the embryo had already reached early globular stage, and in 12% the endosperm nuclei had begun to condense slightly and accumulate multiple nucleoli.

The abnormalities observed during the early endosperm divisions appeared to have been overcome by stage 8, because in the majority (44%) of ovaries, single open embryo sacs contained endosperm nuclei that had condensed and were dividing throughout the embryo sac (Figure 2.6A). However, it was clear that the endosperm developed more rapidly in apomictic D3 in relation to the floral stage of development, because nuclear condensation and nucleoli accumulation occurred at stages 7 to 8 of floral development compared to stages 9 to 10 in sexual P4. This was possibly a consequence of embryo sacs in P4 having to wait for fertilisation to occur prior to the initiation of endosperm divisions. In 10% of the ovaries from stage 8 D3 florets, multiple embryo sacs were observed, and chalazal embryo sac structures contained either nuclear (Figure 2.6B) or cellular-like (Figure 2.6C) endosperm. The endosperm-like cells present in chalazal embryo sacs differed in structure and appearance to the large cubic endosperm cells observed in late seeds from sexual P4 (compare Figure 2.6C and 2.4D).

Various stages of embryo development were observed in embryo sacs from stage 8 D3 florets, including dividing egg-like cells (9%; Figure 2.6D and 2.6E), small globular embryos (16%; Figure 2.6F) and large globular embryos (39%; 2.7A). This variability highlighted the asynchronous nature of embryo development in apomictic D3 compared to sexual P4.

The majority of seeds containing open embryo sacs at stage 9 of floral development (53%) also contained a globular embryo. In 66% of these seeds, the endosperm was still nuclear and contained many small, condensed nuclei with

Figure 2.6 Early endosperm and embryo development in apomictic D3 *Hieracium*. In *panels* **D** and **F** the dotted line outlines the embryo. **A** Embryo sac with condensed dividing endosperm nuclei (en) and a small embryo (em). The chalazal (ch) and micropylar (mp) poles are indicated to aid orientation. **B** Chalazal embryo sac (ces) and micropylar embryo sac (mes) in the same ovule. The micropylar embryo sac contains condensed dividing endosperm nuclei. **C** Chalazal embryo sac containing endosperm-like cells (ec) above a collapsed micropylar embryo sac containing endosperm nuclei (en) and an egg cell (ec). **D** Two celled embryo (em) and a synergid nucleus (sy). **E** Four to eight-celled embryo. **F** Small misshapen embryo. All panels are in chalazal (top) to micropylar (bottom) orientation. The number in the top right corner of each panel indicates the floral stage of development. Bar = 20 μm in all panels.

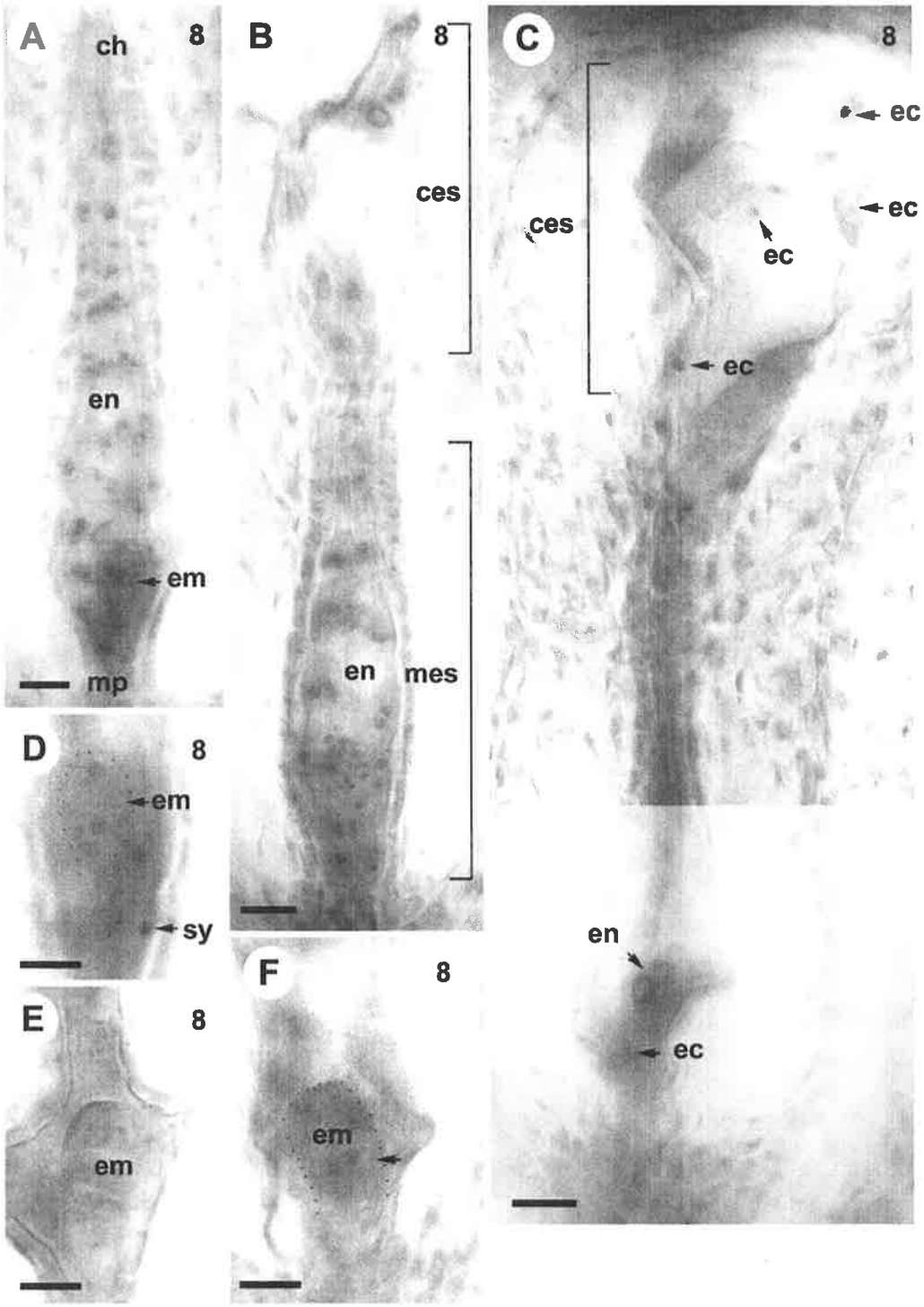
A
ch
8
en
em
mp
B
8
ces
en
mes
C
8
ec
ec
ces
ec
ec
en
ec
D
8
em
sy
E
8
em
F
8
em

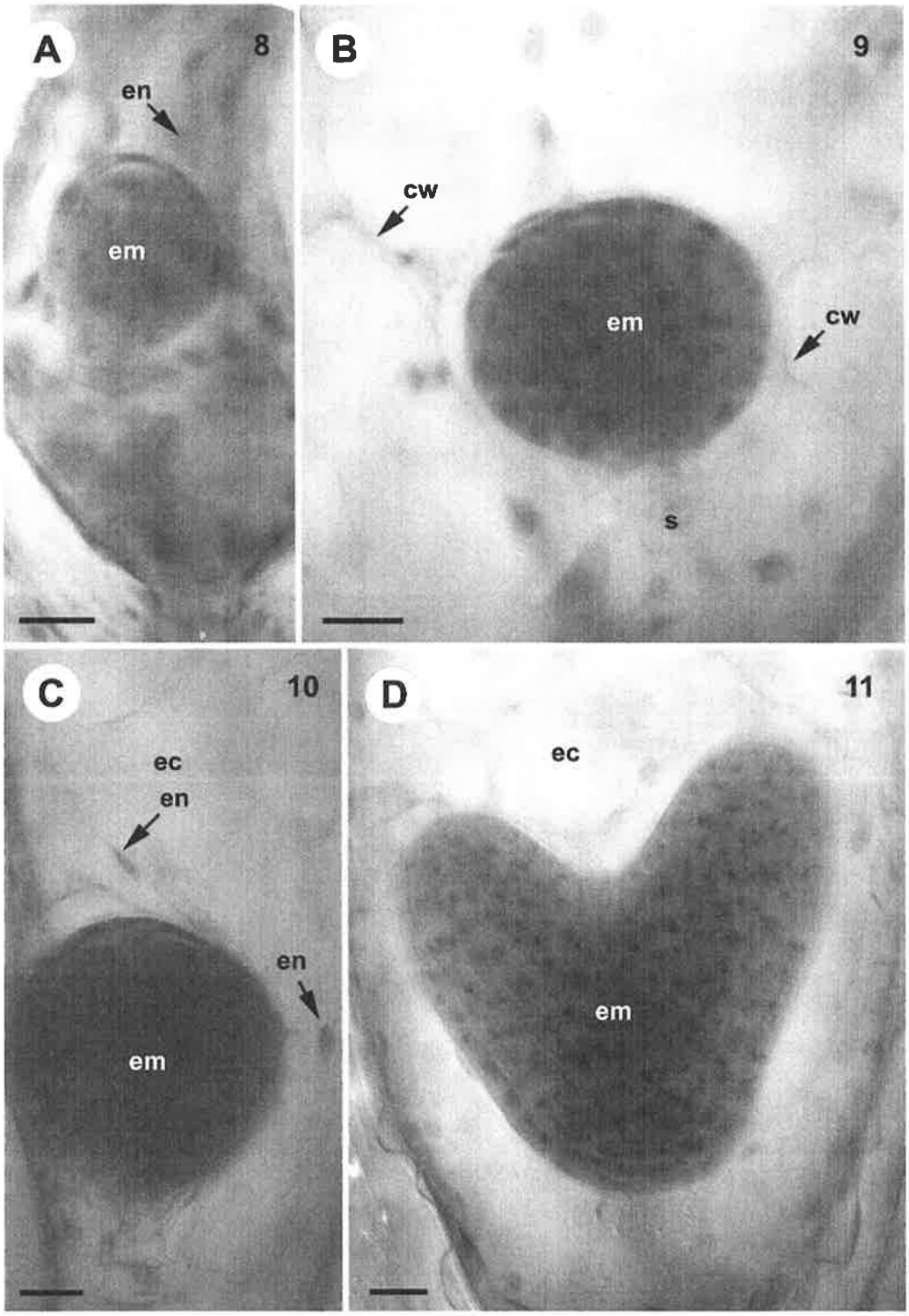

Figure 2.7 Late endosperm and embryo development in apomictic D3 *Hieracium*. **A** Small globular embryo (em) surrounded by endosperm nuclei (en). **B** Globular embryo and suspensor (s) surrounded by endosperm cell walls (cw). **C** Late globular embryo and endosperm cells (ec) with compressed endosperm nuclei (en). **D** Heart stage embryo (em) and endosperm cells. All panels are in chalazal (top) to micropylar (bottom) orientation. The number in the top right corner of each panel indicates the floral stage of development. Bar = 25 μm in all panels.

multiple nucleoli. The endosperm nuclei were evenly spread throughout the embryo sac structure, and between three and eight small nucleoli were observed in the vicinity of each endosperm nucleus (see Figure 2.8B). The morphology and organisation of these endosperm nuclei was remarkably similar to those observed in fertilised P4 embryo sacs 36 HAP. In 19% of the stage 9 embryo sacs containing an embryo, cell walls had begun to form between endosperm nuclei in the vicinity of the globular embryo (Figure 2.7B), and by stage 10, embryos were either at late globular (15%; Figure 2.7C) or heart-torpedo stage (21%; Figure 2.7D) and 44% of the seeds contained cellular endosperm. The endosperm cells were large and cubic in shape, and each contained a small, flattened nucleus close to the cell wall. These cells were essentially identical to those observed following cell wall formation in sexual P4 during fertilised endosperm development.

The morphology of the endosperm nuclei during seed development was strikingly similar in fertilised sexual and autonomous apomictic *Hieracium* plants. Although the early endosperm migration patterns were disorganised in apomictic D3 compared to sexual P4, primary endosperm divisions in both plants produced nuclei with similar morphology to the polar nuclei(us) (Figure 2.8A). Interestingly, after the initial problems during early nuclear divisions, endosperm development appeared to correct itself in apomictic D3. During subsequent endosperm divisions in embryo sacs from both plants the nuclei migrated throughout the sac, condensed slightly and accumulated three to eight nucleoli (Figure 2.8B), before becoming almost granular in appearance prior to cellularisation (Figure 2.8C). After cell walls had formed, the nuclei were squashed flat against the walls (Figure 2.8D).

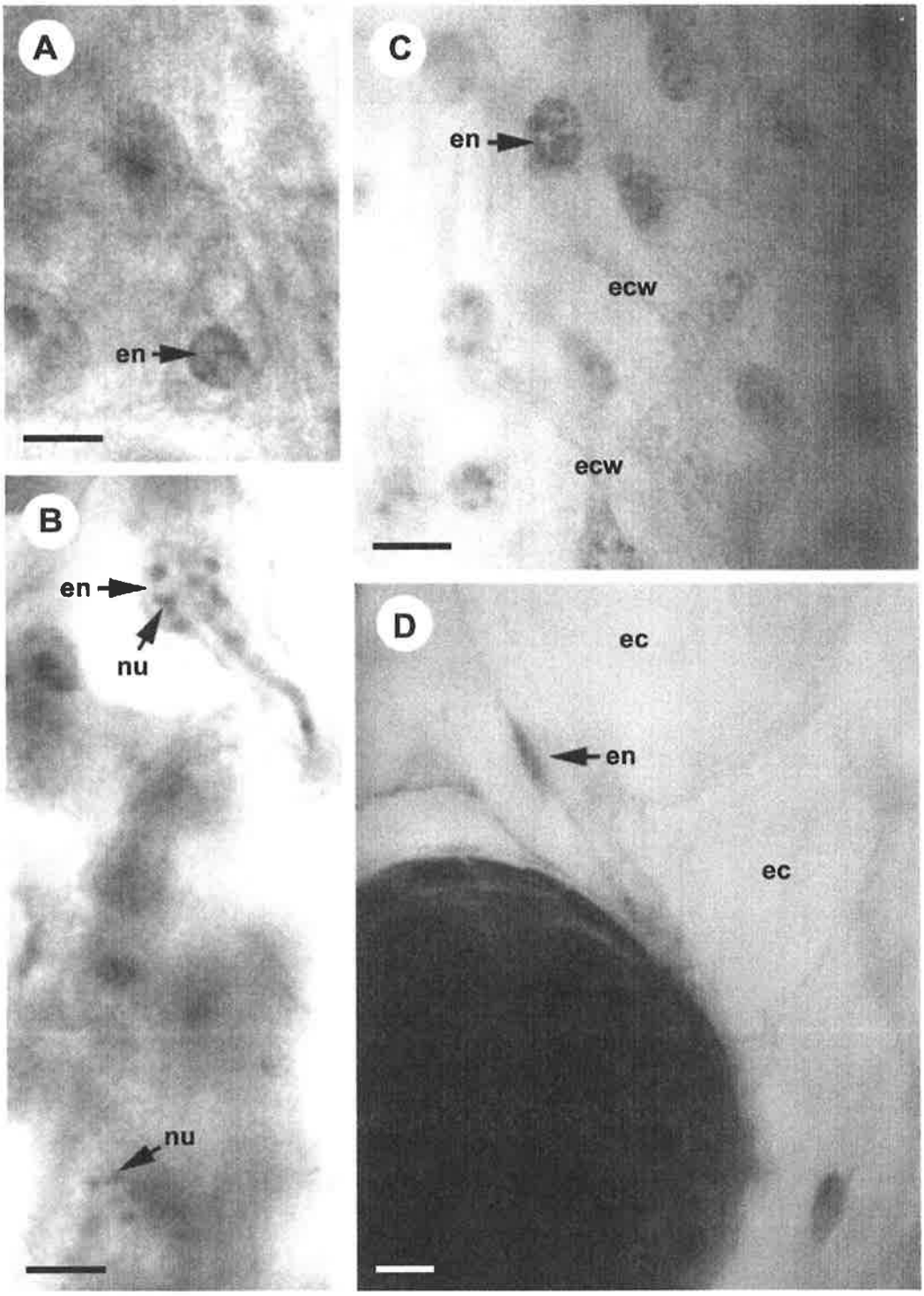

Figure 2.8 Morphology of endosperm cells in *Hieracium* seeds. **A** Early endosperm nuclei (en) with similar morphology to the polar nucleus. **B** Dividing endosperm nuclei displaying multiple nucleoli (nu). **C** Endosperm nuclei during endosperm cell wall (ecw) formation. **D** Compressed endosperm nuclei after the formation of endosperm cells (ec). All panels are in chalazal (top) to micropylar (bottom) orientation. Bar = 20 μm in all panels.

2.3.3 Abnormalities during seed development in apomictic D3

Embryo sac abnormalities became apparent during later stages of floral growth in apomictic D3, when endosperm and embryo development were highly asynchronous. At floral stages 8, 9 and 10, between 11% and 18% of embryo sacs contained many small endosperm nuclei (Figure 2.9A) or completely cellular endosperm in the absence of an embryo. In several seeds, a single embryo sac contained dividing nuclear endosperm above a quiescent egg cell and a single polar nucleus (Figure 2.9B and 2.9C), suggesting that polar nuclei-fusion is not a prerequisite for endosperm development. Multiple embryo sac structures were obvious in 6% to 10% of D3 ovaries, and these often contained different cell types. In several ovaries (2%), a chalazal embryo sac enclosed an embryo and embryo-like cells above a micropylar embryo sac that contained a single polar nucleus and an apparently quiescent egg cell (Figure 2.9D-F). In 2% of the ovaries from stage 8 to 10 florets a second chalazal embryo sac structure was observed that contained nuclear (Figure 2.9A) or cellular-like (Figure 2.9G) endosperm and/or an embryo above a collapsed micropylar embryo sac (Figure 2.9G). In other ovaries (2%), a secondary chalazal sac contained cellular endosperm above an open micropylar embryo sac that enclosed syncytial endosperm nuclei, and the two structures appeared to be developing independently of one another.

In 40% of the open embryo sacs from stage 10 D3 florets, similar to sexual P4, a single late globular or early heart stage embryo was observed at the micropylar end of the embryo sac, and the endosperm was completely cellular (see Figure 2.7C and 2.7D). In contrast to sexual P4, a smaller secondary embryo was observed in 12% of the ovaries from stage 10 D3 florets, usually at the chalazal end of the embryo sac structure (Figure 2.10A-C). Multiple embryos formed either

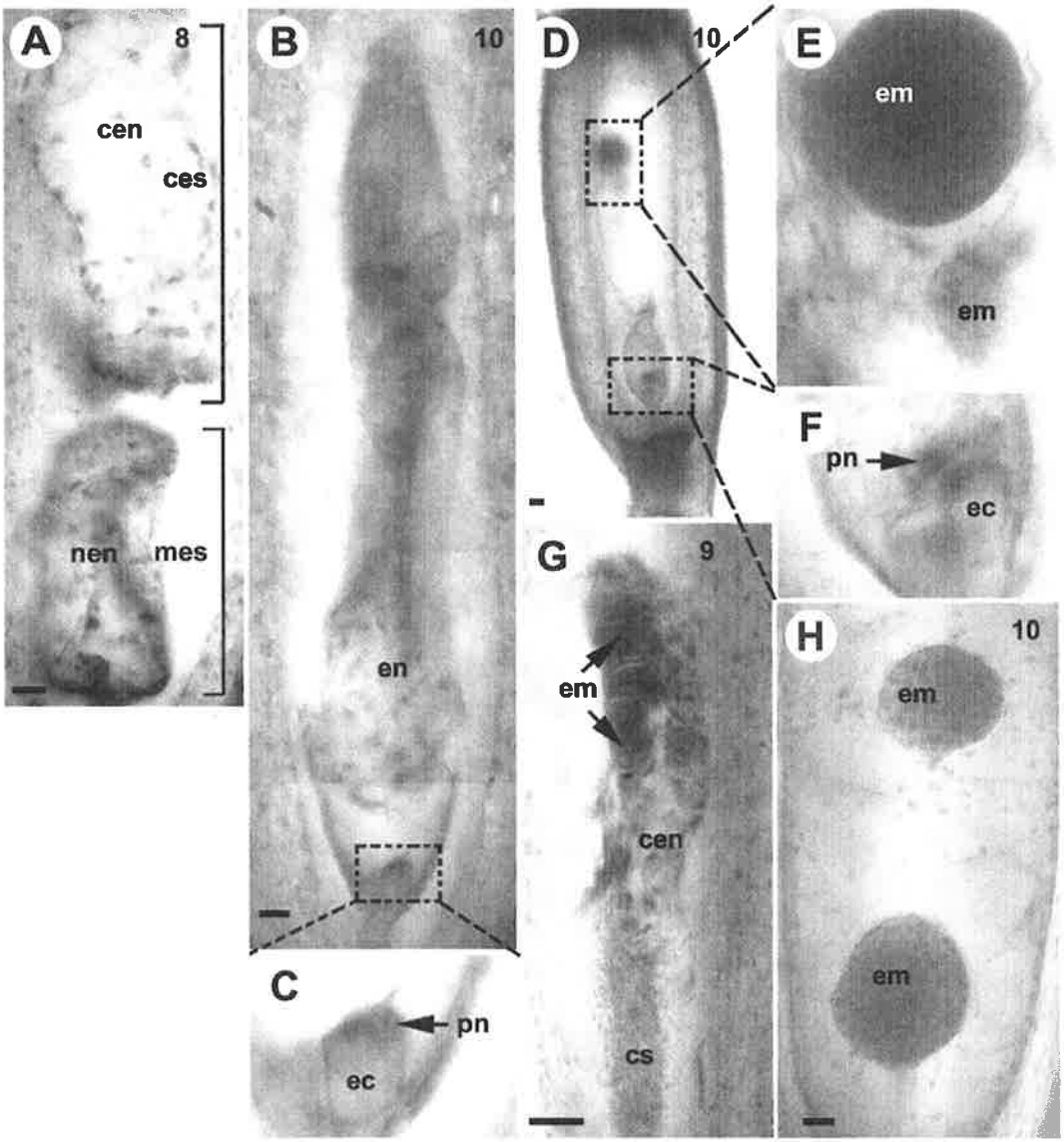

Figure 2.9 Abnormalities during seed development in apomictic D3 *Hieracium*. **A** Chalazal embryo sac (ces) containing cellular endosperm (cen) and micropylar embryo sac (mes) containing nuclear endosperm (nen). **B** Embryo sac containing endosperm nuclei and **C** an egg cell (ec) with a polar nucleus (pn). **D** Seed containing two embryo sacs, one **E** with no obvious endosperm and two external embryos (em) and one **F** with an egg cell and polar nucleus. **G** Embryo sac containing cellular endosperm (cen) and embryo-like structures, above a collapsed micropylar embryo sac (cs). **H** Two embryos in the same embryo sac surrounded by cellular endosperm. All panels are in chalazal (top) to micropylar (bottom) orientation. The number in the top right corner of each panel indicates the floral stage of development. Bar = 20 μm in all panels.

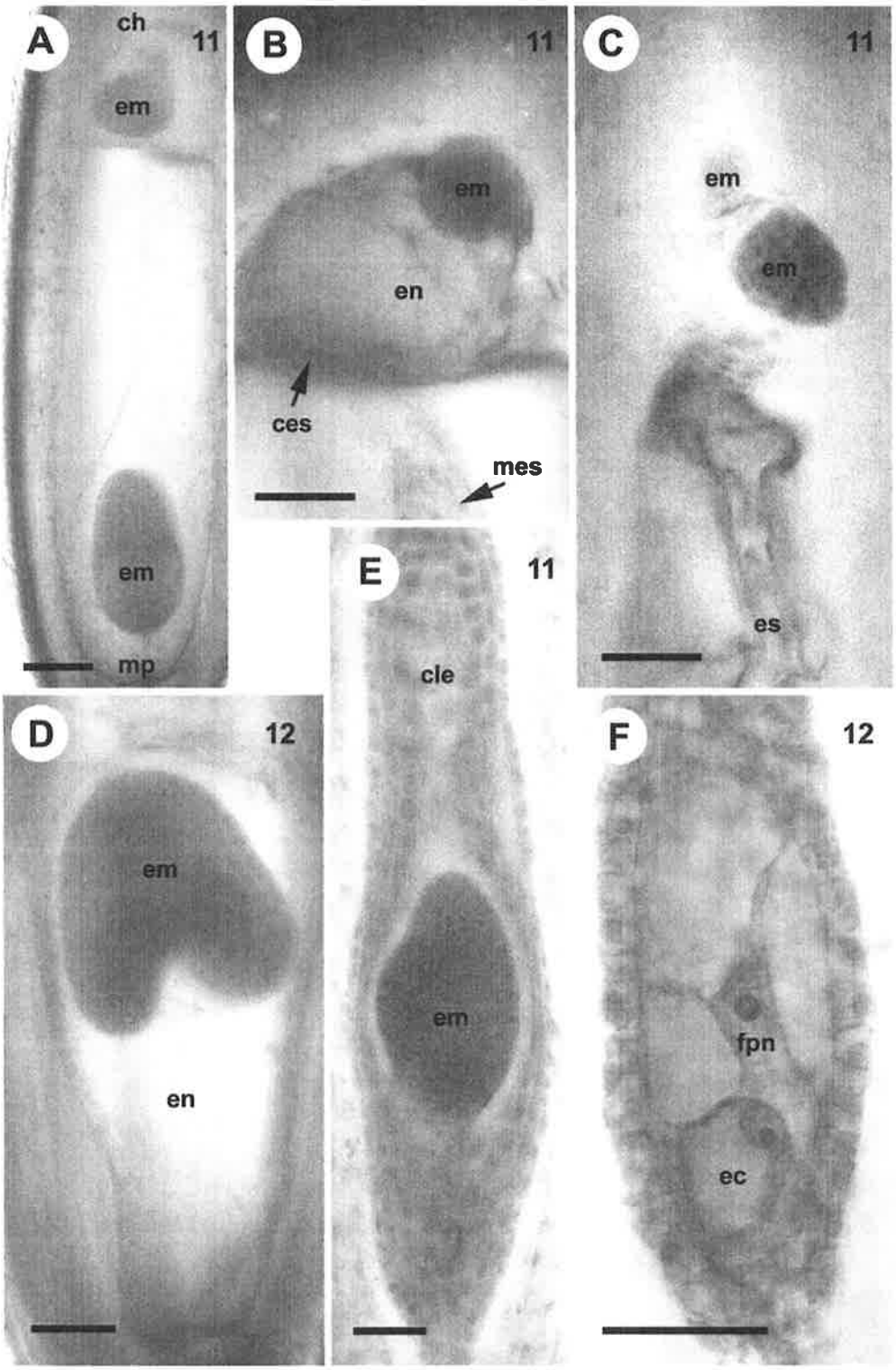

Figure 2.10 Abnormalities during late seed development in apomictic D3 *Hieracium*. **A** Seed containing two embryos (em) in different embryo sacs. **B** Small embryo in a chalazal embryo sac structure (ces) containing cellular endosperm (en), above a micropylar embryo sac (mes). **C** Two small embryos forming outside of an embryo sac (es) structure. **D** Heart stage embryo elongating towards the micropylar pole of the embryo sac. **E** Abnormal embryo (em) surrounded by cellular-like endosperm (cle). **F** Embryo sac from a stage 12 seed containing a fused polar nucleus (fpn) and an egg cell (ec). All panels are in chalazal (top) to micropylar (bottom) orientation. The number in the top right corner of each panel indicates the floral stage of development. Bar = 50 μm in all panels.

within the same embryo sac, in a small secondary chalazal sac (Figure 2.10A and 2.10B) or infrequently outside of the embryo sac structures (Figure 2.10C). The formation of these secondary embryos corresponded closely with the formation of cell walls between the endosperm nuclei.

By stage 12 of floral development in apomictic D3, most (60%) of the seeds contained a single late stage embryo, and the cellular endosperm was dissipating due to embryo growth. In a few seeds the embryo had developed upside down, with the cotyledons elongating towards the micropylar end of the embryo sac (Figure 2.10D). Other seeds contained misshapen embryos surrounded by cells that differed in appearance to normal cubic endosperm cells (Figure 2.10E). Interestingly, some stage 12 seeds displayed an embryo sac that contained a fused polar nucleus and a quiescent egg cell (Figure 2.10F). These two structures had not degenerated completely, and possibly retained the potential to initiate endosperm and embryo development. Similarly, egg cells and polar nuclei were observed in late unfertilised seeds (stage 10) from sexual P4, but these commonly displayed signs of nuclear degeneration and embryo sac wall collapse.

2.3.4 Tracking seed variability during development in apomictic D3

Despite attempts to avoid maturity differences in D3 seeds by collecting only the outer whorl of florets, a large amount of variation was observed within ovules and seeds from the same developmental stage. This was likely to be caused by differences in development between ovaries from within the same or different capitula. To gain an indication of the spectrum of different developmental events occurring (in terms of endosperm and embryo growth) at each floral stage in

apomictic D3, the embryo sac contents of each ovule from stage 5-12 of floral development was scored and plotted as a percentage of the total number of embryo sacs analysed (Figure 2.11).

The aposporous embryo sac structure in terms of nuclei/cell content was less variable during the early stages of embryo sac development and the late stages of seed development (Figure 2.11A and 2.11B). For example, most embryo sacs (72%) in ovaries from stage 5/6 florets contained an egg cell and unfused polar nuclei, while only a few (5% to 10%) contained dividing endosperm nuclei. Similarly, most seeds (60%) from stage 11 florets contained a late globular or early heart stage embryo and completely cellular endosperm.

In contrast, endosperm divisions initiated anywhere between stages 5/6 and 9 of floral development (Figure 2.11A). Accumulation of multiple nucleoli in the nuclei typically coincided with stages 7 to 8 of floral development, and cell wall formation coincided predominantly with stages 9 to 11 (Figure 2.11A). However, exceptions to these rules were found in every case. Most seeds contained an embryo by stage 8 (Figure 2.11B), but micropylar embryos were observed to initiate as late as stage 10, possibly from egg-like cells. Embryos retained the capacity to form in mature seeds already containing nuclear or cellular endosperm, as the proportion of seeds containing only endosperm decreased throughout development (Figure 2.11A). Multiple embryos only became apparent during later seed development (~stage 10-12), and their formation coincided closely with cell wall formation in the endosperm. Further aspects of variation in mature *Hieracium* seeds were addressed in the flow cytometry study.

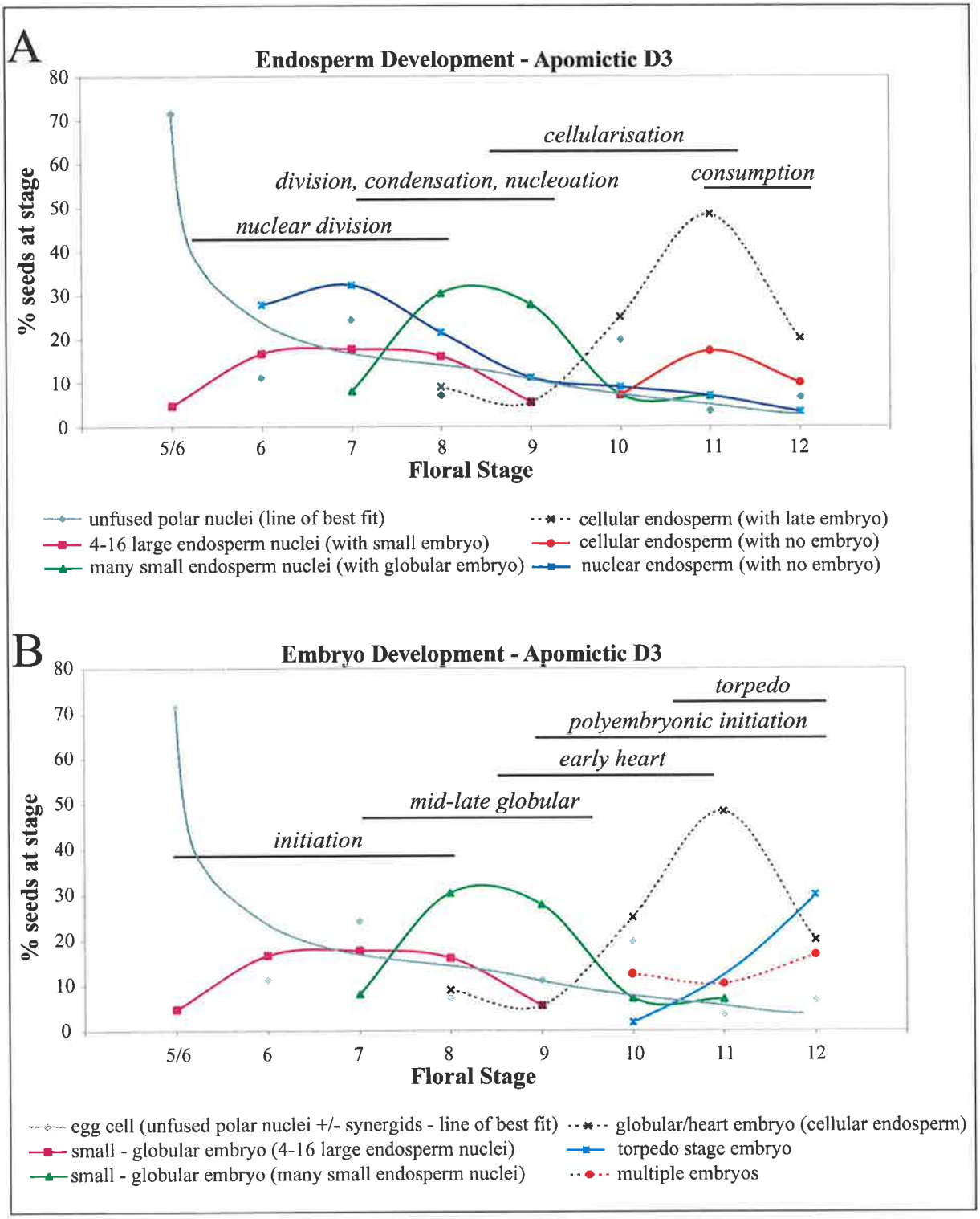

Figure 2.11 Growth trends of the endosperm and embryo in apomictic D3 *Hieracium*. **A** Endosperm development in apomictic D3 *Hieracium*. The graph displays the percentage of seeds containing particular types of endosperm (see legend) at floral stages 5/6 to 12. The generalised stages of endosperm growth are indicated above the growth curves. **B** Embryo development in apomictic D3 *Hieracium*. The graph displays the percentage of seeds containing particular types of embryo growth (see legend) at floral stages 5/6 to 12. The generalised stages of embryo development are indicated above the growth curves.

2.3.5 Ploidy analysis of mature *Hieracium* seeds

In most apomictic plants, the majority of seeds are maternal in origin. However, variation in the reproductive origin of seeds from the same apomictic plant has been noted previously in apomictic species (Rutishauser, 1948; Nogler, 1982; Davis, 1968). Similarly, studies in facultative apomictic *Hieracium* have shown that only 90-96% of seeds derived from D3 or A3.4 are apomictic (Koltunow et al., 1998), and that progeny can arise from combinations of sexual and apomictic events (Koltunow et al., 2000). To gain further insight into the variability amongst apomictic *Hieracium* seeds and the reproductive processes that give rise to them, the ploidy of the endosperm and embryo in seeds from apomictic D3 and sexual P4 *Hieracium* was analysed by a flow cytometry approach called a "seed screen" (Matzk et al., 2000).

The contents of mature capitula were analysed and divided into seed classes based on their morphology; fat black (FB; Figure 2.12C), skinny black (SB; Figure 2.12D) and brown (B; Figure 2.12E). The FB class make up the majority of the material collected and usually correspond to fertile seeds that contain a mature embryo, whereas the B class generally represent unfertilised ovules. However, to remain consistent throughout the study, and to verify their "unfertilised" origin, the B structures were referred to as "seeds". Seven stage 7 floral capitula from sexual self-incompatible P4 were cross-pollinated with pollen from apomictic D3 plants, and 529 seeds were recovered, at an average of 76 seeds per capitulum (Figure 2.12A). Floral heads from apomictic D3 were not decapitated to remove anthers and stigmas to prevent pollination, as this would limit the identification of any seeds

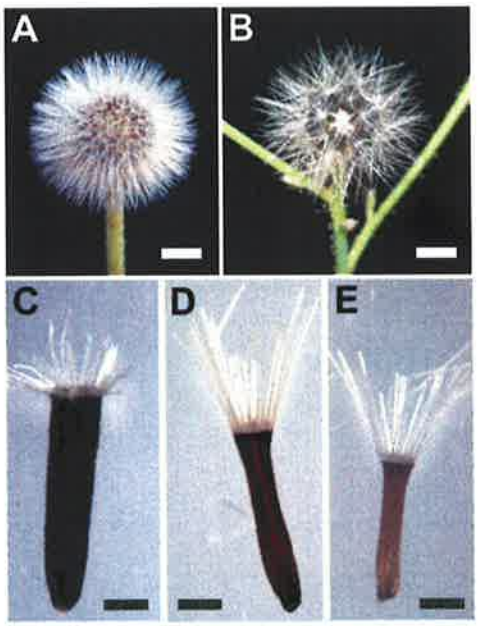

Figure 2.12 Seed morphology in sexual P4 and apomictic D3 *Hieracium*. **A** P4 seed head. **B** D3 seed head. **C** Fat black (FB) seed. **D** Skinny black (SB) seed. **E** Brown (B) seed. Bar = 3 mm in **A** and **B** and 1 mm in **C** to **E**.

obtained through sexual processes. A total of 349 seeds were collected from 12 D3 capitula (Figure 2.12B), and this corresponded to an average of 29 seeds per capitulum. In the sexual P4 seed samples, each individual capitulum comprised on average 47 FB, 20 SB and 7 B seeds, whereas individual D3 floral heads contained 20 FB, 6 SB and 3 B seeds. In total, 178 seeds (89 FB, 48 SB, 41B) from sexual P4 *Hieracium* and 136 seeds (77FB, 32SB, 27B) from apomictic D3 *Hieracium* were analysed by flow cytometry. The data were considered in two ways, (i) by comparing the ploidy of seeds present in each seed morphology class (Figure 2.13A and 2.14A), and (ii) by determining the proportion of seeds with a particular ploidy per individual capitulum (Figure 2.13B and 2.14B).

Five ploidy classes of seeds were identified in sexual P4. The DNA content of nuclei (C value) was adjusted and compared against a peak position representing the 2C nuclear DNA content of fertilised diploid embryo cells. The bulk of the FB seeds obtained from sexual P4 contained a 4C embryo and a 6C endosperm (Figure 2.13A), and this class made up the majority of seeds in each capitulum (Figure 2.13B). In tetraploid P4 this was the expected ploidy level of the embryo and endosperm tissues, and suggests that the majority of functional male gametes derived from D3 pollen were reduced and diploid. A small percentage of P4 FB seeds contained a 4C embryo and 8C endosperm (Figure 2.13A), and this small proportion (<1%) of seeds were probably fertilised with unreduced male gametes from D3. The remaining three classes of seeds were unlikely to be viable. Most SB and B seeds contained no nuclei (Figure 2.13A), probably as a result of female sterility or lack of fertilisation. A small proportion (3%) of seeds per capitulum contained an aborted 4C embryo but no endosperm, and others (2.8%) contained no embryo with a few 6C endosperm nuclei (Figure 2.13B). These sterile seeds correspond to those in which only one cell in the reduced embryo sac has been

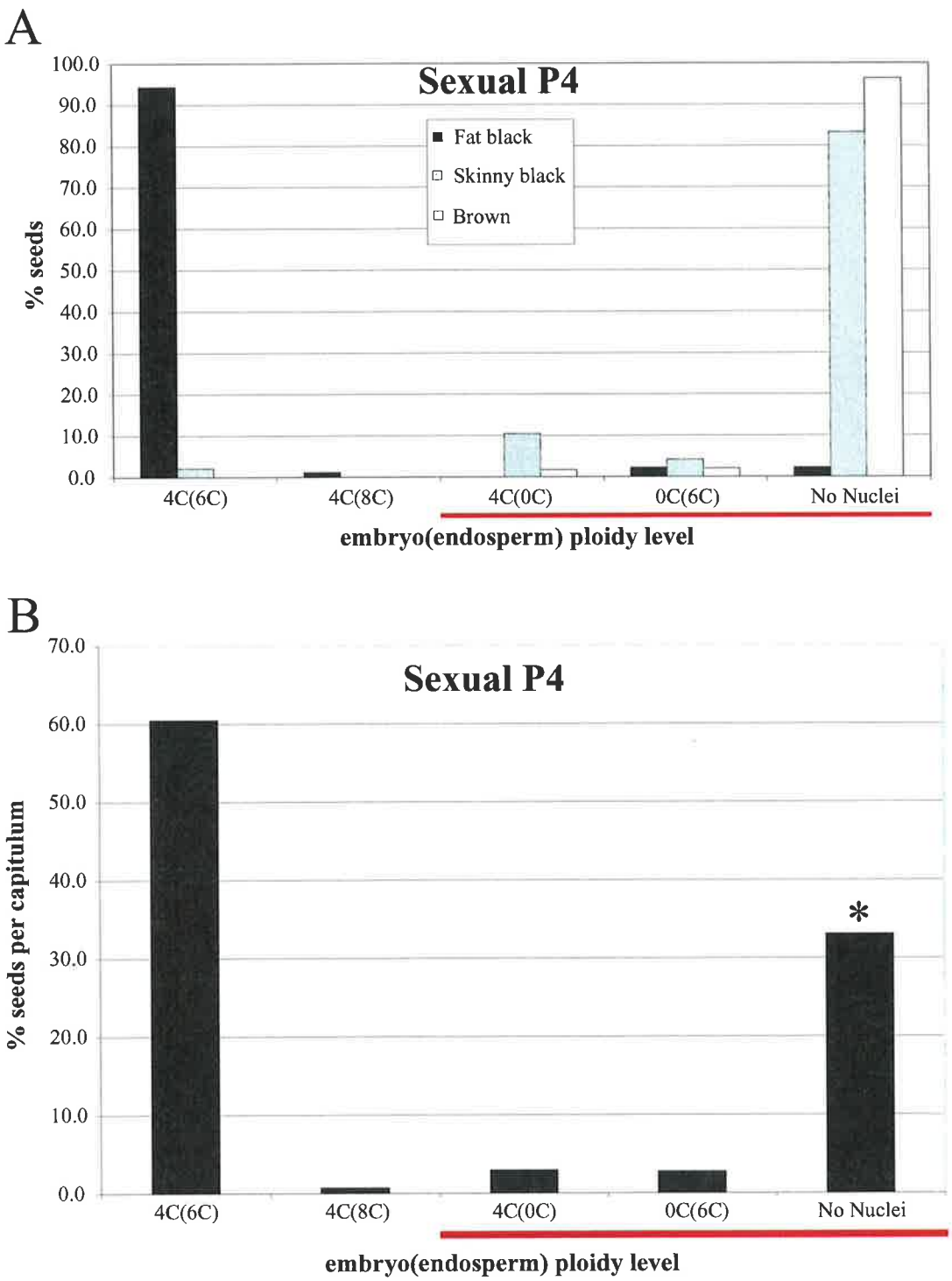

Figure 2.13 Ploidy analysis of mature seeds from sexual P4 *Hieracium* cross-pollinated with D3 pollen. The red bar indicates seed types unlikely to be viable. **A** Embryo and endosperm ploidy levels in the Fat Black, Skinny Black, and Brown seed types. **B** Embryo and endosperm ploidy levels of seeds in a typical P4 capitulum. The percentage of "seeds" containing no nuclei, indicated by an asterisk, may represent unfertilised ovules and be biased by manual pollination.

successfully fertilised i.e. the egg cell or the central cell, and may result from early abortion of the egg cell or zygote, or failed development of the endosperm.

2.3.6 Variable ploidy levels in mature seeds from apomictic D3 *Hieracium*

In contrast to sexual P4, nine different seed ploidy classes were identified in facultative apomictic D3. The majority of FB seeds contained a 4C embryo and 8C endosperm (Figure 2.14A), and this was the most common seed ploidy level observed in each capitulum (Figure 2.14B). *H. piloselloides* D3 is a triploid plant, as verified by chromosome analysis (Bicknell et al., 2000) and unreduced autonomous seeds were expected to contain a 3C embryo and a 6C endosperm. It is uncertain why the flow cytometry approach detected the presence of 4 genomes in the embryo and 8 in the endosperm, but a similar phenomenon has been identified in apomictic *Hypericum*, where the DNA content per chromosome in apomictic plants was found to be measurably higher than that in sexual plants (F. Matzk, pers. comm.). Therefore, the 4C(8C) ploidy level observed in the majority of D3 seeds was most likely derived from autonomous development of the unreduced egg and central cells.

Three variations of the 4C embryo ploidy level were observed in mature D3 seeds. A small proportion of FB seeds (1.3%) contained a 4C embryo with a 6C endosperm (Figure 2.14A), and this ploidy level was representative of reduced female gametes being fertilised with reduced male gametes via sexual reproduction. A higher percentage of FB seeds (6.5%) contained a 4C embryo and 12C endosperm with an extra 8C peak (Figure 2.14B), and these were possibly derived from fertilisation of unreduced female gametes with unreduced sperm cells, along with concurrent development of a secondary maternal embryo i.e. 4C maternal

A

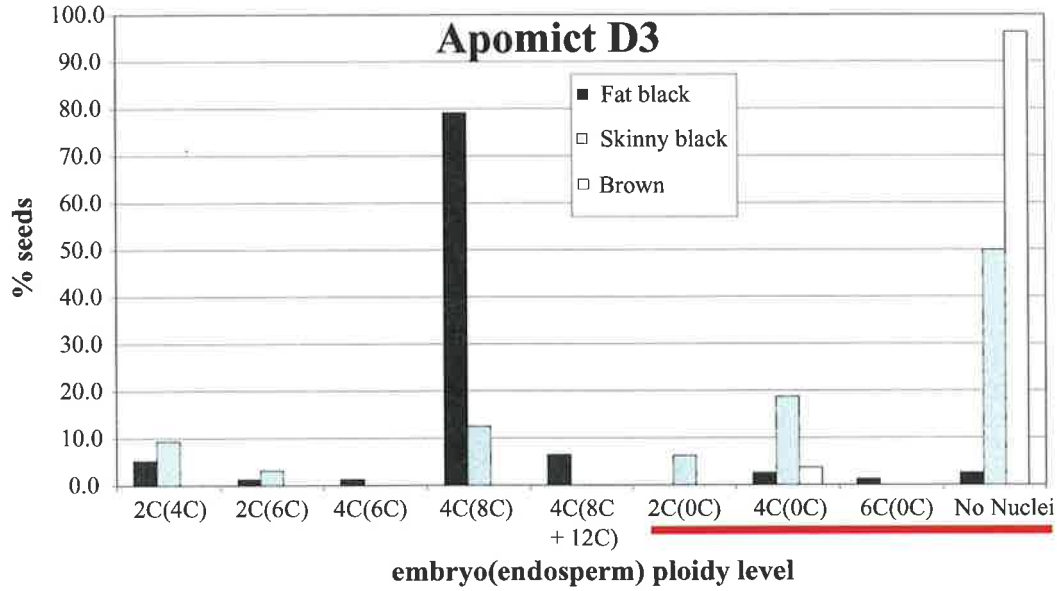

B

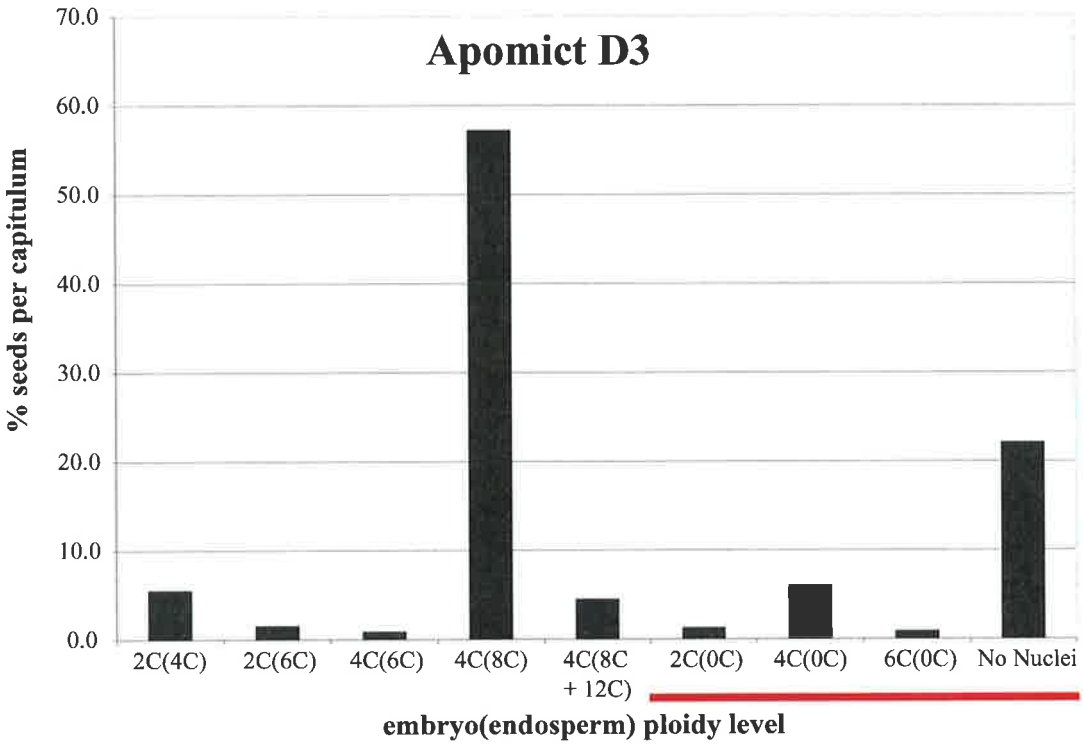

Figure 2.14 Ploidy analysis of mature seeds from apomictic D3 *Hieracium*. The red bar indicates seed types unlikely to be viable. **A** Embryo and endosperm ploidy levels in the Fat Black, Skinny Black, and Brown seed types. **B** Embryo and endosperm ploidy levels of seeds in a typical D3 capitulum.

embryo, 8C embryo ($4C_{egg}$ + $4C_{sperm}$), and 12C endosperm ($4C_{polar\ nucleus}$ + $4C_{polar\ nucleus}$ + $4C_{sperm}$). Some FB seeds (2.6%) contained a 4C embryo and no apparent endosperm. The 4C(0C) seeds may have arisen from reduced fertilised development of the egg ($2C_{egg}$ + $2C_{sperm}$) or autonomous development of the unreduced egg ($4C_{egg}$), with concurrent abortion of the endosperm or autonomous development of a single unreduced polar nucleus ($4C_{polar\ nucleus}$) indistinguishable from the embryo ploidy.

Three different mature D3 seed classes were identified that contained a 2C embryo (Figure 2.14A), derived from parthenogenetic development of a reduced egg cell. These seeds also contained either a 4C endosperm (5.5% per capitulum) resulting from autonomous development of a reduced central cell ($2C_{polar\ nucleus}$ + $2C_{polar\ nucleus}$), a 6C endosperm (1.5% per capitulum) resulting from fertilisation of a reduced central cell with reduced male gametes ($2C_{polar\ nucleus}$ + $2C_{polar\ nucleus}$ + $2C_{sperm}$), or no endosperm nuclei (1.3% per capitulum) as a result of endosperm abortion. A small proportion (1.3%) of FB seeds contained a 6C embryo with no apparent endosperm, and this ploidy probably arose from fertilisation of an unreduced egg cell with reduced male gametes ($4C_{egg}$ + $2C_{sperm}$) with coincident endosperm abortion. Alternatively, the endosperm in this class may also have been 6C (derived from fertilisation of a single unreduced polar nucleus with a reduced male gamete; $4C_{polar\ nucleus}$ + $2C_{sperm}$) and hence indistinguishable from the embryo. Similar to P4, the majority of D3 B seeds contained no nuclei, and the bulk of D3 SB seeds were unlikely to be viable (Figure 2.14B).

Most of the variable seed types in apomictic D3, which make up the minority of total seeds, are likely to be infertile. The majority of fertile seeds per capitulum (Figure 2.14B) contained a parthenogenetic embryo that was the same ploidy as the maternal plant. Of the "potentially" viable seeds, 82% were 4C(8C), 1.3% were 4C(6C), 6.5% were 4C(8C + 12C), 2.1% were 2C(6C) and 7.9% were

2C(4C). This showed that although overlaps occur between the apomictic and sexual processes in apomictic D3 plants, the majority of fertile seeds are produced through apomixis and the maternal nature of apomictic plants is maintained without meiosis and recombination in successive seed generations.

2.4 Discussion

Embryologically, the Asteraceae is the most variable family of angiosperms in terms of reproductive modes and contains the majority of autonomous apomictic plants. Murbeck (1904) and Ostenfeld and Raunkiaer (1903) first described the ability of central cells to divide without fertilisation in composite *Hieracium* early in the last century, but there are few cytological analyses of endosperm in autonomous apomicts. Some studies in *Crepis* (Stebbins and Jenkins, 1939), *Calotis* (Davis, 1968) and *Taraxacum* (Malecka, 1971; van Baarlen et al., 2002) have briefly described features of autonomous endosperm development, and these highlight the variable nature of endosperm formation in autonomous apomictic plants. However, a detailed wholemount cytological examination of autonomous endosperm development in apomictic *Hieracium*, in comparison to fertilised endosperm development in a closely related sexual plant, has not been described.

2.4.1 Early divisions of the embryo sac and endosperm are altered in apomictic D3 *Hieracium*

In this study, embryo sac formation and seed initiation in apomictic D3 and sexual P4 *Hieracium* was compared using a wholemount staining procedure that enabled

observation of embryo sac and endosperm nuclei in three dimensions. Mitotic divisions of the embryo sac and cellularisation events were generally similar in apomictic D3 and sexual P4, and both plants typically produced an eight nucleate Polygonum-type embryo sac. However, variations were often observed in apomictic D3. The position of the mitotic embryo sac nuclei in aposporous embryo sacs was disorganised compared to sexual P4, and after cellularisation the egg cell was often distorted. In some embryo sacs, the identity of the egg and polar nuclei could not be clearly discerned. Antipodal cells were infrequently observed in embryo sacs from either plant, but were more commonly observed in embryo sacs from sexual P4. Notably, the position of the polar nuclei(us) close to the egg cell was conserved in both aposporous and sexual embryo sacs. The general similarity of embryo sacs derived from apomixis and sexuality has been noted in many diplosporous and aposporous apomictic species (see Savidan, 2000 for review).

Apart from the structural distortion commonly observed in aposporous embryo sacs from D3, the main differences in mature embryo sac morphology between D3 and P4 *Hieracium* related to the timing of polar nuclei fusion within the central cell, and the position of endosperm nuclei within the embryo sac during the primary autonomous divisions. Early fusion of the polar nuclei in sexual P4 possibly prevents fertilisation and formation of endosperm from a single polar nucleus, and delayed fusion in apomictic D3 possibly increases the chance of this occurring. While this augments the possible origins of endosperm in seeds from apomictic *Hieracium*, as observed in the flow cytometric analysis, the temporal difference in polar nuclei fusion between D3 and P4 is likely to relate to a species or ploidy variation between the plants, rather than an adaptation of autonomous apomixis.

In contrast, the differences in spatial patterning of the nuclei during early endosperm divisions in sexual and apomictic plants suggest that positional regulators are modified in autonomous apomictic D3. Studies of the maize *indeterminate gametophyte-1* (*ig-1*) mutant suggest that cytoskeletal activity most likely controls the polarization and nuclear migration underlying the formation and fate of the cells of the normal embryo sac (Huang and Sheridan, 1996). *ig*-1 female gametophytes display irregular positioning of the nuclei, asynchronous microtubular patterns in different pairs of nuclei, and abnormal phragmoplasts after the third mitotic division (Huang and Sheridan, 1996). Somewhat similarly, in the *titan1* mutant of *Arabidopsis* cytoskeletal organisation in the endosperm is disrupted because endosperm nuclei fail to migrate to the chalazal end of the seed (Liu and Meinke, 1998). It is possible that aspects of the cytoskeletal framework are altered during the early autonomous divisions of endosperm in D3 *Hieracium*, leading to abnormal migration patterns of the dividing nuclei.

2.4.2 Endosperm growth and differentiation occurs independently of embryogenesis in some D3 *Hieracium* seeds

Endosperm development was predominantly of the free-nuclear type and preceded embryogenesis in both sexual P4 and apomictic D3 *Hieracium* plants. The order in which the endosperm and embryo initiate tends to vary between species, and sometimes between the ovules of a single plant. Nogler (1984) suggested that in the majority of autonomous apomicts, including species such as *H. aurantiacum* (Skalinska, 1973) and *Taraxacum officianale* (Cooper and Brink, 1949) precocious embryony prevails. However, in autonomous *Crepis* (Stebbins and Jenkins, 1939) and *Cortaderia jubata* (Costas-Lippman, 1979), division of the egg cell only takes

place after endosperm divisions have initiated. Precocious embryony is potentially an advantage for apomictic plants, as division of the egg cell before anthesis makes fertilisation impossible, and prevents the formation of hybrid plants. Hybrid embryos were detected in seeds from apomictic D3 *Hieracium*, highlighting the capacity of reduced and unreduced egg cells to be fertilised and indicating overlaps between sexual and apomictic processes.

Although endosperm development characteristically initiated earlier in apomictic D3 than in sexual P4 and proceeded more rapidly in relation to the floral stage, the differentiation of endosperm cell types coincided with similar developmental events in sexual and apomictic plants. For example, in most seeds from D3 and P4, endosperm cellularisation typically coincided with the late globular-stage of embryogenesis. The temporal sequence of events that occurred during endosperm development in apomictic D3 was actually very similar to that in sexual P4, but appeared faster because the divisions initiated earlier.

In contrast to sexual P4, a late globular-stage embryo was not a prerequisite for cell wall formation in the endosperm, because some D3 seeds contained mature cellular endosperm in the absence of embryo growth. This phenotype is similar to that observed in a hybrid *Taraxacum* line described by van Baarlen et al., (manuscript in preparation; http://www.dpw.wau.nl/genetics/apomixis/) and is reminiscent of the *Arabidopsis mea, fis2* and hypo-methylated *fie* mutants that develop endosperm to maturity in the absence of embryo growth and fertilisation (Chaudhury et al., 1997; Vinkenoog et al., 2000). However, not all seeds spontaneously developed endosperm in the absence of fertilisation in apomictic *Hieracium*. Quiescent polar nuclei were observed in D3 seeds as late as stage 12, suggesting that the molecular control of autonomous endosperm development in *Hieracium* may not be as simple as a direct mutation in one of the three *FIS* genes.

2.4.3 Cellular endosperm is required for embryo growth to maturity in apomictic D3 *Hieracium*

The presence of cellular endosperm correlated with mature embryo development suggesting it is required for viable embryo growth in apomictic D3 seeds. Few seeds from apomictic D3 were observed at any stage of development that contained an embryo in the absence of nuclear, cellular or cellular-like endosperm. In the diploid apomict *Hieracium* D2, Koltunow et al., (2000) observed the formation of globular and irregular embryos in the chalazal region of the ovule external to an embryo sac structure. These embryos only progressed to maturity if endosperm cells were present in the nearby embryo sac. Haematoxylin stains in this study revealed a small percentage of D3 seeds contained similar "adventitious" embryos. Koltunow et al., (2000) also noted that in some progeny plants derived from crosses between sexual and apomictic *Hieracium*, embryos initiated in seeds and progressed to globular stage without initiation of endosperm. During later development however, embryo sac collapse was noted around these aborted globular embryos. These observations verify that similar to most angiosperms, the endosperm is required to sustain parthenogenetic embryo growth in apomictic *Hieracium*.

This conclusion contrasts with a study in apomictic *Taraxacum officianale* that proposed the endosperm is rendered a superfluous tissue by protein-rich nutrient material in the ovule integument capable of supporting embryo growth (Cooper and Brink, 1949). This material was observed in ovules from apomictic *Taraxacum officianale* but was absent from those in sexual *T. kok-saghz* (Cooper and Brink, 1949). Degradation of integument cells concomitant with embryo growth

has also been observed during seed development in apomictic D3 and sexual P4 *Hieracium*, and is described as integument liquefaction (Koltunow et al., 1998). The relevance of this tissue to parthenogenetic embryo growth in *Hieracium* is uncertain, given that it is detected in both sexual and apomictic plants. It is possible that the embryo(s) can draw nutrients from this tissue, but this substance is not capable of supporting parthenogenetic embryo growth to maturity in the absence of endosperm development in apomictic D3.

2.4.4 Multiple origins of the endosperm and embryo in apomictic D3 *Hieracium*

The flow cytometry analysis of mature seeds revealed that the DNA content of chromosomes from apomictic D3 *Hieracium* was higher than those from sexual P4 *Hieracium*. A similar observation has been made in *Hypericum* (F. Matzk, pers. comm.), and may relate to the accumulation of large amounts of repetitive DNA in the genomes of some apomictic plants (see Chapter 6). Despite the discrepancy in expected ploidy levels, the majority of seeds from apomictic D3 contained 8C endosperm derived from autonomous division of the fused unreduced polar nuclei (see Figure 2.15A). Although some endosperm ploidy levels may not have been detected by the flow cytometry method due to the DNA content being indistinguishable from that of the embryo, the cytological and flow cytometry data combined suggested that endosperm formed along a variety of pathways from unreduced (Figure 2.15A) and reduced polar nuclei (Figure 2.15B) in apomictic *Hieracium*.

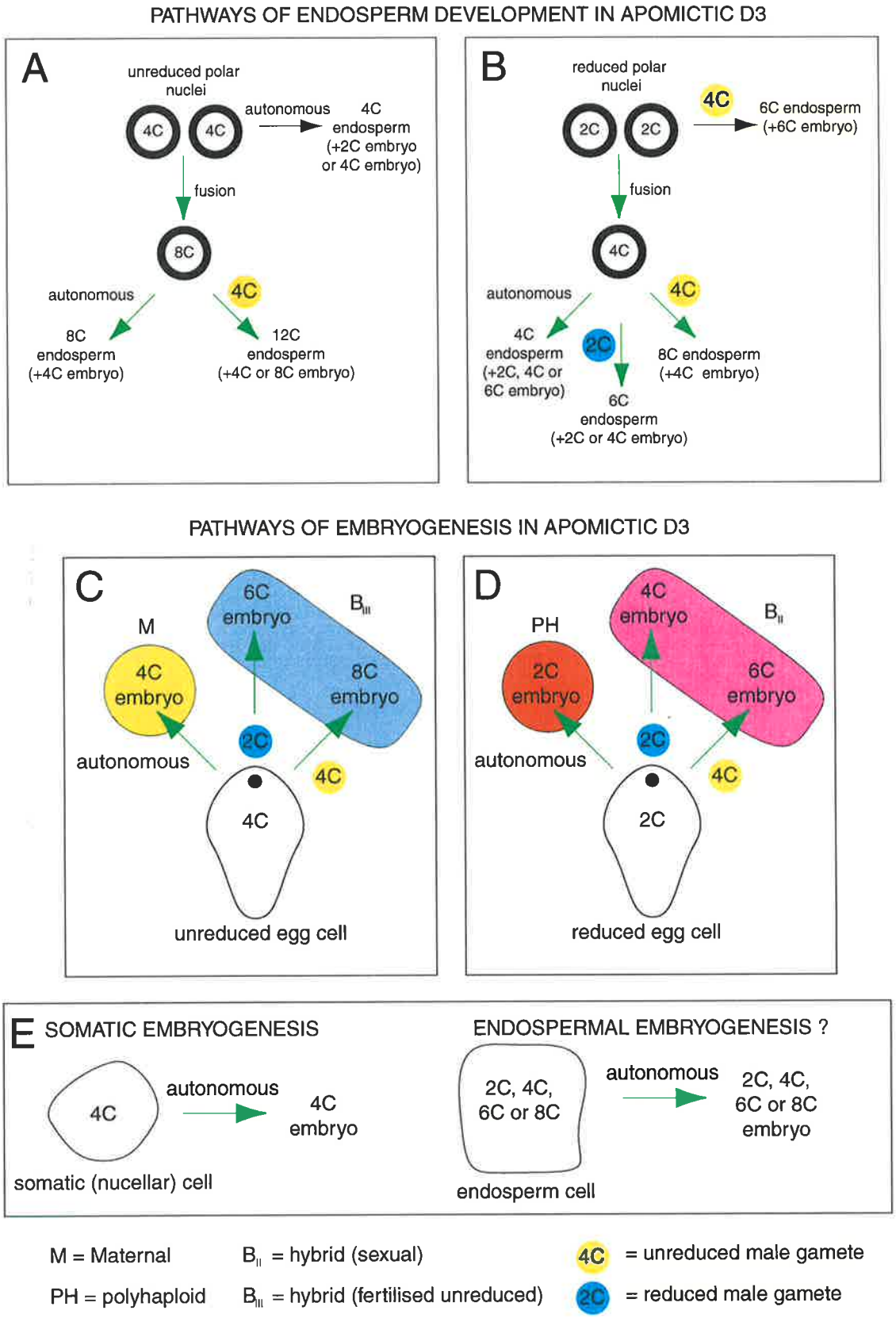

Figure 2.15 Pathways of embryo and endosperm development in facultative apomictic D3 *Hieracium*. **A** Unreduced endosperm development. **B** Reduced endosperm development. **C** Unreduced embryo development. **D** Reduced embryo development. **E** Somatic and endospermal embryo development.

The flow cytometry data also showed that reproductive variations in apomictic D3 *Hieracium* give rise to seeds containing an embryo(s) and endosperm through different combinations of apomictic and sexual processes. Such anomalies that yield progeny of different ploidy are not specific to *H. piloselloides*, and similar observations have been described in other apomictic species including *Potentilla*, (Ruthisauser, 1943), *Ranunculus* (Nogler, 1982), *Calotis* (Davis, 1968), *H. aurantiacum* (Skalinska, 1971; 1973; 1976) and *Chondrilla* (Koscinska-Pajak, 1996; 1998). The formation of heterogeneous seeds in apomictic plants emphasises the presence of overlaps between sexual and apomictic processes. Rutishauser (1948) first described the different types of progeny that can be obtained from apomictic plants. Embryos formed from unreduced cells during apomixis retain a maternal genotype, and are referred to as maternals (M). However, seeds containing embryos derived from sexual reproduction (B_{II} hybrids), fertilisation of unreduced egg cells (B_{III} hybrids) and autonomous development of reduced egg cells (polyhaploids) also form in apomictic species. The capacity to form B_{III} hybrids suggests that unreduced egg cells formed during apomictic processes are comparable to eggs derived through meiotic reduction, because they have the ability to attract the pollen tube and complete fertilisation. Furthermore, the formation of polyhaploids through autonomous development of reduced egg cells suggests that structures derived through meiotic reduction retain the capacity to develop autonomously through apomictic processes. The formation of these two "off-type" progeny in apomictic plants supports the concept of shared regulation of reproductive pathways and patterning during apomictic and sexual reproduction (Koltunow et al., 2002).

Analysis of the flow cytometry data for 136 D3 seeds confirmed the presence of embryos from maternal (4C - 82%; Figure 2.15C and 2.15E), B_{II} hybrid

(4C - 1.3%; Figure 2.15 D), B_{III} hybrid (8C - 6.5%; Figure 2.15C) and polyhaploid (2C - 10%; Figure 2.15D) classes. A recent study in *Hieracium* D3 investigated the frequency of off-type embryos in seeds by using molecular markers (Kanamycin and cod-A) to distinguish between maternal and hybrid progeny (R. Bicknell, S. Lambie, R. Butler, manuscript submitted). Bicknell et al., (submitted) showed that 97.1% of the D3 progeny were derived from maternal embryos, 0.94% from polyhaploid embryos, 1.9% from B_{II} hybrid (sexual) embryos and 0.1% from B_{III} hybrid embryos. The discrepancy in frequencies of embryo types between the flow cytometry and germination study is informative. The percentage of B_{III} embryos observed in the flow cytometry study may have been skewed, because the origin of the 4C + 8C + 12C seeds was uncertain. This class of seed may have contained an embryo of maternal origin (4C) along with an altered ploidy combination in the endosperm (8C + 12C), rather than a fertilised unreduced embryo (8C) and endosperm (12C) along with a secondary maternal (4C) embryo.

The frequency of polyhaploids also differed between the two studies. The flow cytometry data clearly identified 10% of the "potentially" viable seeds (5.5% of the total seeds) to contain polyhaploid embryos, whereas the molecular marker data only detected 0.94% viable polyhaploids in progeny. This discrepancy is possibly caused by the inability of all polyhaploid embryos to germinate. This would suggest that while only 0.94% of the polyhaploid embryos are viable, the proportion of polyhaploid events in D3 *Hieracium* seeds is likely to be significantly higher.

2.4.5 Molecular identity of endosperm cells in apomictic and sexual *Hieracium*

In apomictic D3 *Hieracium*, variations in seed content and ploidy stem from the asynchronous development of embryo sacs between stages 6 and 10 of floral development and overlaps between sexual and apomictic reproductive pathways. Particular developmental events are not confined to occur only at specific points in time, and this is exemplified by the initiation of embryogenesis. Embryo sacs containing only endosperm (either nuclear or cellular) were observed from stage 6 onwards, but their frequency decreased between stages 6 and 12 highlighting the capacity for parthenogenetic embryos to initiate at many different stages of seed development. In sexual plants, this window for embryo initiation remains restricted to anthesis and a short time thereafter, because egg cells show obvious signs of degradation and collapse if they are not fertilised promptly.

Despite the asynchronous nature of seed development in apomictic D3 *Hieracium*, endosperm and general seed development was morphologically similar to that observed in sexual P4. However, variations were observed between the plants in terms of the positional organisation of the endosperm and embryo sac nuclei, the presence of antipodals, the distorted shape of the egg cell, and the reproductive origin of the endosperm and embryo. It remains uncertain from this study whether endosperm cells in apomictic D3 and sexual P4 share similar molecular identity and whether they form along similar pathways. Sorenson et al., (2001) used molecular markers to show that endosperm cell identity is not maintained correctly in the fertilisation-independent endosperm of the *Arabidopsis fis* mutants, due to alterations in anterior-posterior cell specification. Do fertilised and autonomous endosperm cells share similar molecular identity and express the

same genes in *Hieracium*? To date, studies of autonomous endosperm cell identity have been limited, due to a lack of specific markers. However, the recent identification of the *Arabidopsis FIS* genes and the generation of *FIS:GUS* protein fusions provides new tools for the comparison of sexual and apomictic processes.

Chapter 3: *AtMEA:GUS*, *AtFIS2:GUS* and *AtFIE:GUS* expression during seed development in sexual and apomictic *Hieracium*[2]

3.1 Introduction

The events of sexual seed formation are characterised by spatial and temporal changes in the nuclear DNA content of cells both in terms of chromosome ploidy and the DNA contributed from maternal and paternal genomes. The gametophyte cell nuclei are reduced in DNA content distinguishing them from the surrounding sporophyte. Fertilisation restores the nuclear DNA content in the egg cell to that of the sporophytic generation and each subsequent embryo cell contains maternal and paternal genomes present in equal ratio. By contrast, primary endosperm nuclei contain an unequal maternal to paternal genome ratio of 2:1 respectively, which is essential for seed viability in many species (Johnston et al., 1980; Lin, 1984; Chaudhury et al., 2001).

In plants that reproduce by apomixis meiosis is avoided during embryo sac formation, embryo development is fertilisation-independent and endosperm formation may or may not require fertilisation (Nogler, 1984; Koltunow, 1993). These features result in unreduced embryo sac formation, embryos retaining the maternal genotype of the sporophyte and endosperm that either retains the 2:1

[2] Data from this chapter are included in the publication: **Tucker M.R.**, Araujo A.C.G., Paech N.A., Hecht V., Schmidt E.D.L., Rossel J.B., de Vries S.C., & Koltunow A.M.G. (2003) Sexual and apomictic reproduction in *Hieracium* sub genus Pilosella are closely interrelated developmental pathways. **The Plant Cell, 15: 1524-1537.**

maternal:paternal genome ratio or deviates significantly from it to the extent of completely lacking a paternal genome equivalent (see Chapter 2; Savidan, 2000, Grimanelli et al., 2001, Spillane et al., 2001).

The nature of the cells initiating apomixis and the subsequent structures formed has been surmised from their position within a tissue and their morphological appearance in comparison to sexual reproduction. Structures formed during apomixis can be similar to or vary significantly in form and position relative to the surmised sexual counterpart (see Chapter 2; Willemse and van Went, 1984; Nogler, 1984; Naumova and Willemse, 1995; Koltunow et al., 1998; Araujo et al., 2000; Koltunow et al., 1993). In apomictic *Beta* (Jassem, 1990), *Hieracium* (see Chapter 2; Koltunow et al., 1998), Rosaceae (Nybom, 1998; Izmailow, 1994) and *Hypericum* (Brutovska et al., 1998), variation in embryo sac, embryo and endosperm development is evident amongst the ovules and seeds of an individual plant.

Plants that reproduce by apomixis also retain the capacity to reproduce sexually to varying degrees (see Chapter 2). The two reproductive processes appear independent but they are not mutually exclusive. For example, in some apomicts such as *Hieracium* (Figure 3.1), the sexual process ceases if apomixis initiates in the ovule while in others both processes occur side by side in a competitive manner. Models proposed to explain the manifestation of apomixis suggest that it may be a novel pathway distinct from sexual reproduction (Roche et al., 1999), or an aberrant form of sexual reproduction generated by hybridisation, mutation or epigenetic change (Carman, 1997; Peacock, 1992; Grossniklaus, 2001).

There is, however, a complete absence of data concerning the identity of cells initiating apomixis and autonomous endosperm development, the molecular processes regulating apomixis and the relationship between sexual and apomictic

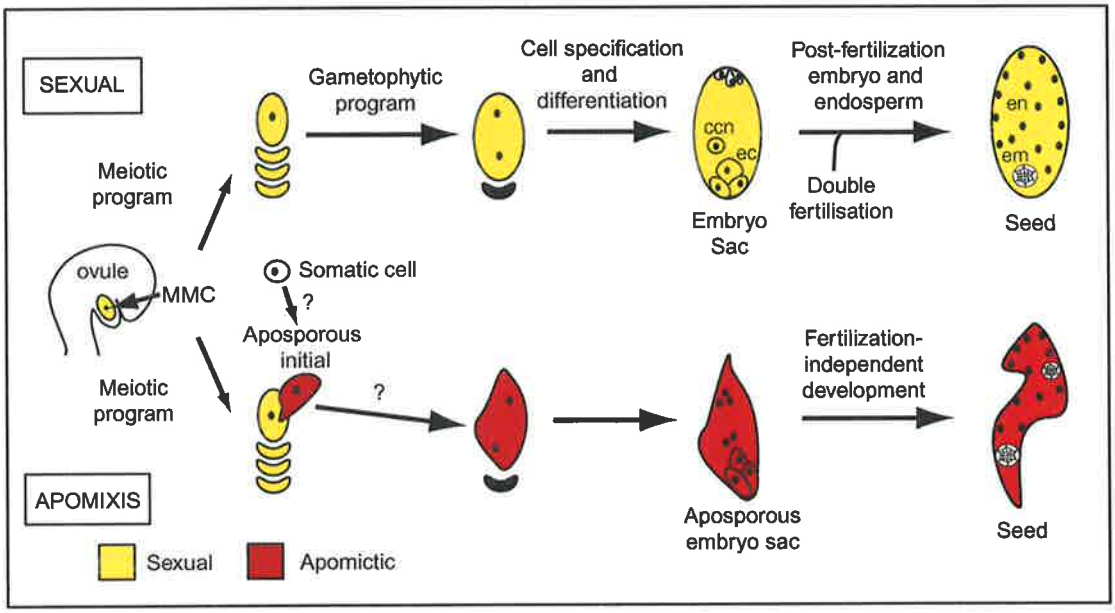

Figure 3.1 Mechanisms of sexual and apomictic reproduction in *Hieracium*. MMC - megaspore mother cell, ccn - central cell nucleus, ec - egg cell, en - endosperm, em - embryo.

pathways. Relatively few apomicts are studied at the molecular level. Genes involved in, and known to regulate gametophyte, endosperm and embryo development have now been identified in sexually reproducing plant species providing tools for the comparative analysis of gene expression programs during sexual and apomictic reproduction (see Christensen et al., 2002; Grini et al., 2002; Chaudhury et al., 1997 for examples).

In this study, the molecular identity of fertilisation-dependent and fertilisation-independent endosperm cells and relationships between sexual and apomictic pathways were examined in *Hieracium*. The *MEA:GUS, FIS2:GUS*, and *FIE:GUS* developmental markers from *Arabidopsis thaliana* (*At*), which have characterised and informative expression patterns during sexual reproduction, were introduced into sexual and apomictic plants. Comparative analyses of gene expression patterns suggested that autonomous endosperm is derived from central cell nuclei in *Hieracium*. These data together with that from other reproductive marker studies carried out by colleagues and visitors to the Koltunow laboratory suggest that in *Hieracium*, sexual and apomictic reproduction are molecularly related pathways that share regulatory programs.

3.2 Materials and Methods

3.2.1 Plant Material

Three different genetically characterised *Hieracium* plants were utilized in this study that have been described previously (Koltunow et al., 1998; 2000; Tucker et al., 2001); sexual *Hieracium* P4, apomictic D3 (see Section 2.2.1) and apomictic A3.4, a natural apomictic aneuploid (3x+4=2n=31) accession of *H. aurantiacum*

that was obtained from Central Otago, New Zealand. In the apomictic plants >93% of the viable seed is apomictic (Koltunow et al., 1998; 2000). Tissues for GUS staining, histology and in situ hybridisation were staged and collected as described by Koltunow et al., (1998).

Arabidopsis Landsberg *erecta* seeds homozygous for *AtFIS2:GUS* were provided by Abed Chaudhury (CSIRO, Canberra), and grown at 20°C with a 16h day-length under fluorescent lighting. Ovules and early seeds were staged as per Schneitz et al., (1995).

3.2.2 *Arabidopsis MEA, FIS2, FIE:GUS chimeric genes* and *Hieracium* transformants

The chimeric genes utilized in this study were provided by Abed Chaudhury (CSIRO, Canberra). The *AtMEA:GUS* fusion contains 2,070 bp of nucleotide sequence upstream of the predicted translation site, exons 1, 2 and 305 bp of exon 3 in the vector pBI101-3 (CLONTECH). The *AtFIS2:GUS* and *AtFIE:GUS* fusions are identical to those used by Luo et al., (2000). All binary constructs were mobilized in *Agrobacterium tumefaciens* AGL1, and the T-DNA was transformed into *Hieracium* leaf pieces as per Bicknell and Borst (1994). Kanamycin resistant progeny were screened for the presence of the desired construct using GUS primers (see Appendix 3) that produce a 515 bp product after PCR. The number of independent, kanamycin resistant and GUS PCR positive transformants obtained for *AtFIS2:GUS* was 24 (7 P4, 11 D3, 6 A3.4), for *AtMEA:GUS* was 28 (11 P4, 17 D3) and for *AtFIE:GUS* was 19 (5 P4, 14 D3).

To determine transgene copy number, genomic DNA was isolated from the leaves of transformed plants as described in Tucker et al., (2001) and DNA samples

were digested with *HindIII* and *EcoRV*. Digested DNA was transferred to Hybond-N (Amersham) membrane and hybridised with α-[32P]dCTP labelled GUS probe (515 bp PCR fragment - see above). Hybridisation solutions and washes were carried out as described in Tucker et al., (2001).

3.2.3 *In situ* localization of *GUS* mRNA

In situ hybridisation was performed as described by Guerin et al., (2000) with modifications. To verify ovule staging, capitula collected for in situ analysis were cut in two, one half was submitted to GUS stain analysis (see below) and the other was fixed in 4% paraformaldehyde and 0.25% glutaraldehyde for *in situ* analysis. Fixed tissues were embedded in BMM and sectioned to 2 μM. Sections and hybridisation experiments were carried out by Ana Claudia Araujo (CSIRO, Adelaide).

A 515 bp fragment of GUS (for primers see Appendix 3) was amplified by PCR from pBI101-3 and cloned into pGEM T-easy (Promega). The clone was linearised with *SalI* (sense) and *NcoI* (Antisense), and digoxygenin (DIG)-labelled RNA probe was produced using the DIG-RNA labelling kit (Boehringer Mannheim) and SP6 or T7 RNA polymerase to generate sense and antisense probes respectively.

3.2.4 Microscopy and GUS staining

Histological analysis of GUS enzyme activity in *Hieracium* tissues was carried out as described by Koltunow et al., (2001). Stained tissues were fixed in FAA overnight and cleared in methyl salicylate as described by Stelly et al., (1984).

Arabidopsis AtFIS2:GUS ovule tissues were stained for GUS activity as per Koltunow et al., (2001). Ovules were cleared in a solution of 20% lactic acid, 20% glycerol in 1× PBS. Wholemount tissue samples were placed on concave slides (ProSciTech) in clearing solution and viewed by Nomarski differential interference contrast microscopy (DIC) or by dark field microscopy with a Zeiss Axioplan Microscope. Selected GUS-stained samples were embedded in butyl-methyl methacrylate (BMM), sectioned to 2 μM and counterstained with Fuschin Red. Digital images were captured using a Spot II camera (Diagnostic Instruments Inc.).

3.3 Results

Previous studies in *Hieracium* have utilized *Arabidopsis* gene fusions to determine the identity of reproductive cells during seed development. For example, expression of the *Arabidopsis SPOROCYTELESS:GUS* (*SPL:GUS*) gene (Yang et al., 1999) was detected in megaspore mother cells from apomictic D3 and sexual P4 *Hieracium*, but was absent from aposporous initial cells, suggesting that AIs do not share homology with the MMC (Figure 3.2A; N. Paech and A. Koltunow, unpublished). Likewise, the expression of the *Arabidopsis SOMATIC EMBRYOGENESIS RECEPTOR KINASE1:GUS* (*SERK1:GUS*) gene (Hecht et al., 2001) was detected in young embryos at the same stage of development in sexual and apomictic *Hieracium* plants, suggesting that they share similar identity (Figure 3.2B; J-B. Rossel and A. Koltunow, unpublished). These studies show that chimeric genes from *Arabidopsis* can be used in *Hieracium* to determine cell identity, and similar conclusions were drawn from the analysis of the *AtFIS:GUS* genes in *Hieracium* during this study.

A *AtSPL:GUS* expression (N. Paech and A. Koltunow, unpublished)

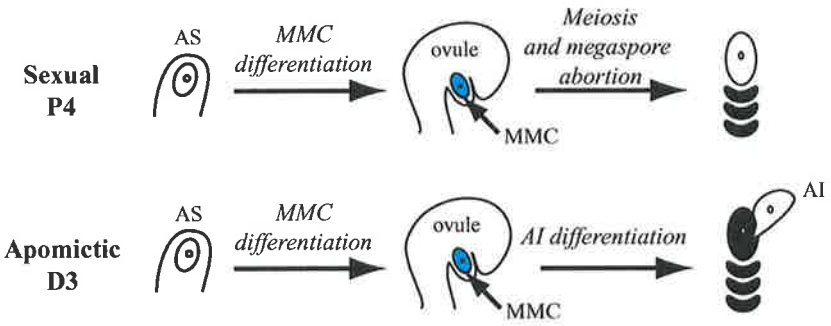

B *AtSERK1:GUS* expression (J.B. Rossel and A. Koltunow, unpublished)

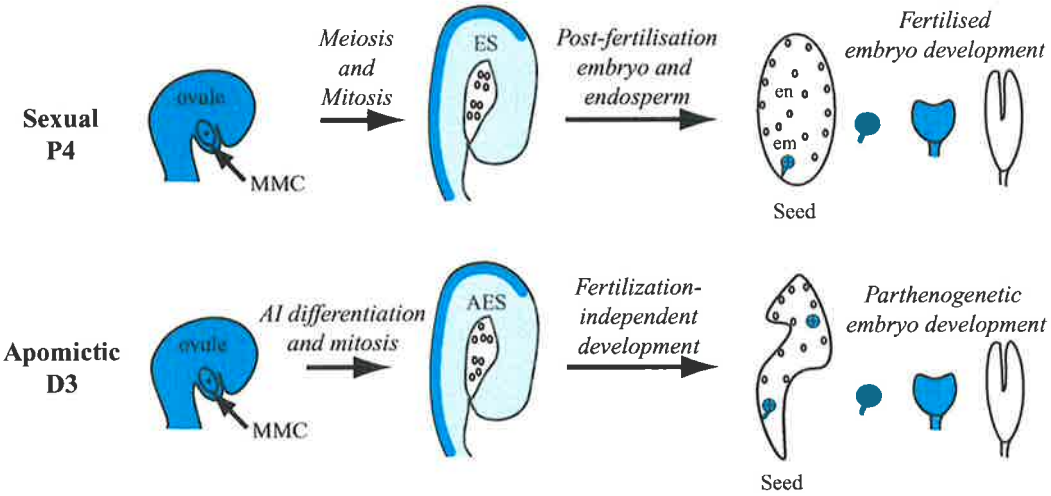

Figure 3.2 Expression of the chimeric *Arabidopsis SPL:GUS* (**A**) and *SERK1:GUS* (**B**) genes in sexual and apomictic *Hieracium*. AS - archesporial cell, MMC - megaspore mother cell, AI - aposporous initial, ES - embryo sac, AES - aposporous embryo sac, en - endosperm, em - embryo.

3.3.1 At*FIS*:*GUS* gene expression marks mature embryo sacs and initiating seed structures in sexual *Hieracium*

Fertilisation-independent (autonomous) endosperm development is one component of apomixis in *Hieracium*. In *Arabidopsis thaliana* (*At*), mutations in either one of the three *FERTILISATION INDEPENDENT SEED* (*FIS*) class genes *MEDEA* (*FIS1*), *FIS2* and *FERTILISATION INDEPENDENT ENDOSPERM (FIE; FIS3*) result in the fertilisation-independent initiation of endosperm development (Ohad et al., 1996; Chaudhury et al., 1997; Grossniklaus and Vielle-Calzada, 1998). Chimeric *AtMEA:GUS*, *AtFIS2:GUS* and *AtFIE:GUS* protein fusion gene constructions are co-expressed in comparable amounts during the late events of gametophyte development and early endosperm formation in transgenic *Arabidopsis* (Luo et al., 2000; Yadegari et al., 2000). However, the spatial expression patterns of the three chimeric genes vary slightly in developing seeds; *AtFIS2:GUS* activity is specific to the endosperm nuclei, *AtMEA:GUS* activity is restricted to the nuclear endosperm domains and *AtFIE:GUS* activity is detected in both the endosperm nuclear domains and the embryo. The expression of *AtFIS2:GUS* is first detected around the two central cell nuclei prior to their fusion (Figure 3.3A) and continues in the dividing endosperm nuclei until the fifth or sixth nuclear division (Figure 3.3B), and thereafter only in the endosperm cyst (Figure 3.3C). *AtFIE:GUS* expression is also detected during pollen and embryo development (Luo et al., 2000; Yadegari et al., 2000).

The three chimeric *AtFIS:GUS* genes were introduced into *Hieracium* to compare their expression during fertilisation-dependent and fertilisation-

Figure 3.3. *AtFIS2:GUS* expression during early seed development in *Hieracium*. Ovules from *Arabidopsis* L.*er AtFIS2:GUS* (**A** to **C**), sexual *Hieracium* P4 (**D** to **F**) apomictic *Hieracium* D3 (**G** to **I**) and apomictic A3.4 (**J** to **L**) were GUS stained and viewed whole-mount using Nomarski DIC microscopy. Bar = 50μm in all panels. **A** Anthesis ovule containing unfused polar nuclei (upn) within the mature embryo sac. **B** Post-fertilization ovule containing dividing endosperm nuclei (en). **C** Post-fertilization ovule after the sixth mitotic division of endosperm development, with GUS staining in the endosperm cyst (c). **D** Mature embryo sac in chalazal (ch) to micropylar orientation (mp) surrounded by the endothelium (et), containing a fused polar nucleus (pn) and egg cell (ec). **E** Post-fertilization embryo sac containing dividing endosperm nuclei and a dividing pro-embryo (pe). **F** Developing fertilized seed containing an early heart stage embryo (em) and cellular endosperm (cen). **G** Mature aposporous D3 embryo sac (aes) containing central cell-like nuclei (n). **H** Aposporous D3 embryo sac showing dividing autonomous endosperm nuclei (aen) and two globular embryos. **I** Developing D3 seed showing a heart stage embryo and autonomous cellular endosperm. **J** Multiple aposporous embryo sac structures developing within a single A3.4 ovule. **K** Aposporous embryo sacs containing dividing nuclei and a small globular embryo. **L** Developing A3.4 seed containing endosperm and an embryo.

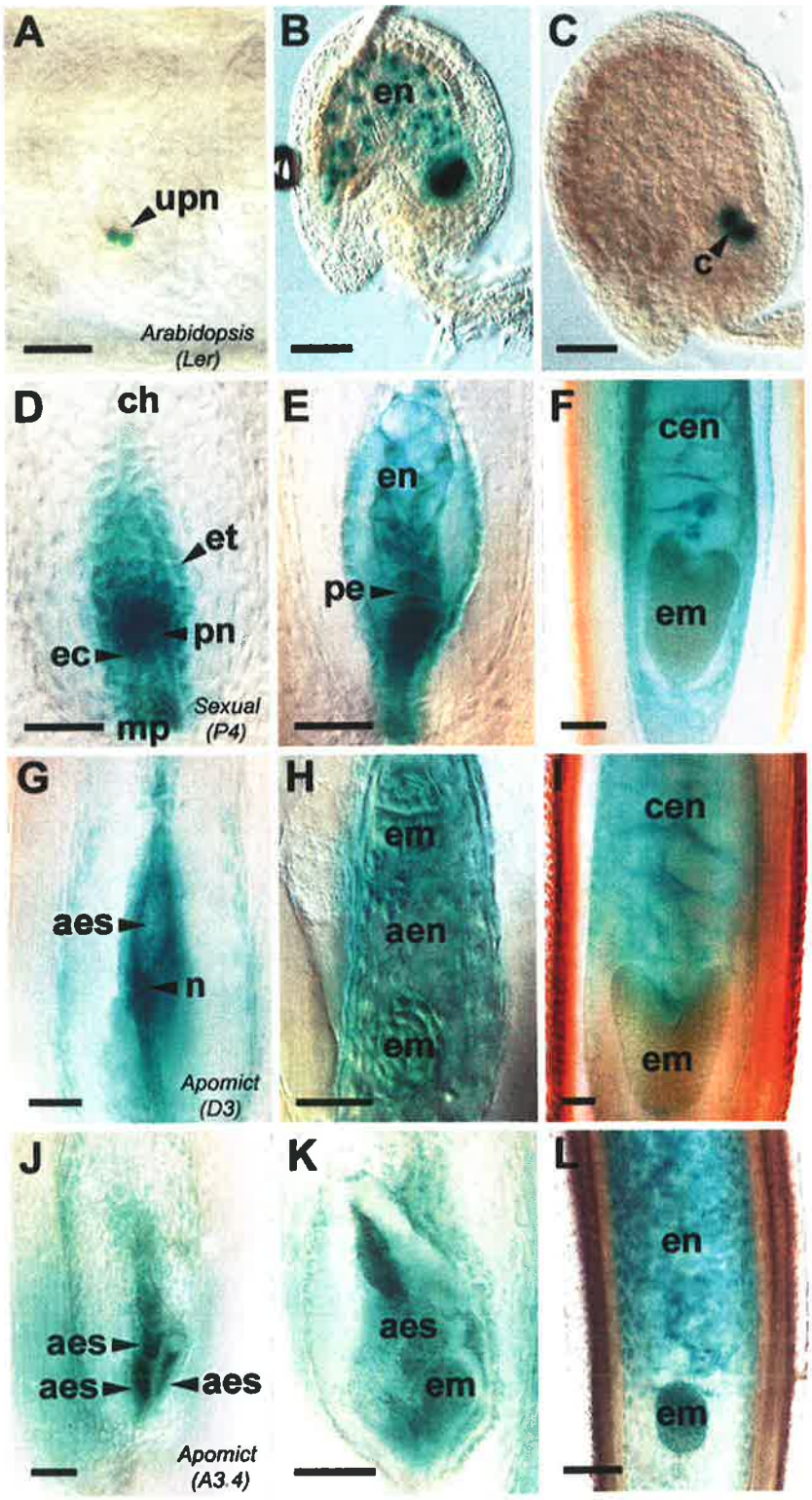
A
upn
Arabidopsis
(Ler)
B
en
C
c
D
ch
et
pn
ec
mp
Sexual
(P4)
E
en
pe
F
cen
em
G
aes
n
Apomict
(D3)
H
em
aen
em
I
cen
em
J
aes
aes
aes
Apomict
(A3.4)
K
aes
em
L
en
em

independent seed development. The expression patterns of *AtFIS2:GUS* (Figure 3.3D to 3.3F) and *AtMEA:GUS* (Figure 3.4A to 3.4C) were identical at embryo sac maturity and during early seed development in sexual *Hieracium* P4. High levels of GUS activity were detected around the polar nuclei within the embryo sac, and at a lower level throughout the central cell, the egg apparatus and endothelium (Figure 3.3D and 3.4A). After fertilisation, *AtFIS2:GUS* and *AtMEA:GUS* expression in sexual *Hieracium* resembled that observed in *Arabidopsis* for *AtMEA:GUS*, and was associated predominantly with the primary endosperm nucleus and the nuclear domains of the dividing endosperm nuclei (Figure 3.3E and 3.3B). *AtFIS2:GUS* expression was not tightly localized to endosperm nuclei as observed in *Arabidopsis* (compare Figure 3.3E and 3.3B). *AtFIS2:GUS* and *AtMEA:GUS* genes continued to be expressed in sexual P4 fertilised endosperm after the formation of cell walls (Figure 3.3F and 3.4C), and this also differed from the pattern observed in *Arabidopsis* seeds. During embryogenesis, *AtFIS2:GUS* expression was detected in the dividing zygote and persisted until the heart stage of embryo development (Figure 3.3E and 3.3F). The same expression was observed for *AtMEA:GUS* in fertilised *Hieracium* embryos (Figure 3.4B and 3.4C), and this has not been observed in *Arabidopsis*.

Expression of *AtFIE:GUS* at embryo sac maturity and during early endosperm and early embryo development was barely detectable in all transgenic plants examined compared to plants containing the *AtMEA:GUS* and *AtFIS2:GUS* genes. However, the intensity of *AtFIE:GUS* expression increased during later stages of embryo development in sexual *Hieracium* (Figure 3.4G) attaining a level comparable to that observed from the other two genes (Figure 3.4H).

Taken together, the expression patterns of the three *AtFIS:GUS* genes at embryo sac maturity and seed initiation in sexual *Hieracium* were similar but not

Figure 3.4 *AtMEA:GUS* and *AtFIE:GUS* expression during early seed development in *Hieracium*. *Panels* **A** to **F** show *AtMEA:GUS* expression and **G** to **I** show *AtFIE:GUS* expression. Ovules from sexual *Hieracium* P4 (**A** to **C, G** and **H**) and apomictic *Hieracium* D3 (**D** to **F** and **I**) were GUS stained and viewed whole-mount using Nomarski DIC microscopy. Bar = 50μm in all panels. **A** Mature embryo sac in chalazal (ch) to micropylar orientation (mp) surrounded by the endothelium (et), containing a fused polar nucleus (pn) and egg cell (ec). **B** Post-fertilization embryo sac containing dividing endosperm nuclei and a dividing pro-embryo (em; inset). **C** Developing fertilized seed containing a heart stage embryo (em) and cellular endosperm (cen). **D** Mature aposporous D3 embryo sac (aes) containing central cell-like nuclei (n). **E** Aposporous D3 embryo sac containing dividing endosperm and a small globular embryo. **F** Developing D3 seed showing a triangle stage embryo and cellular endosperm. **G** Sexual P4 embryo sac containing a globular embryo and dividing endosperm nuclei. **H** Developing P4 seed containing an early heart-stage embryo. **I** Developing D3 seed containing an early heart stage embryo.

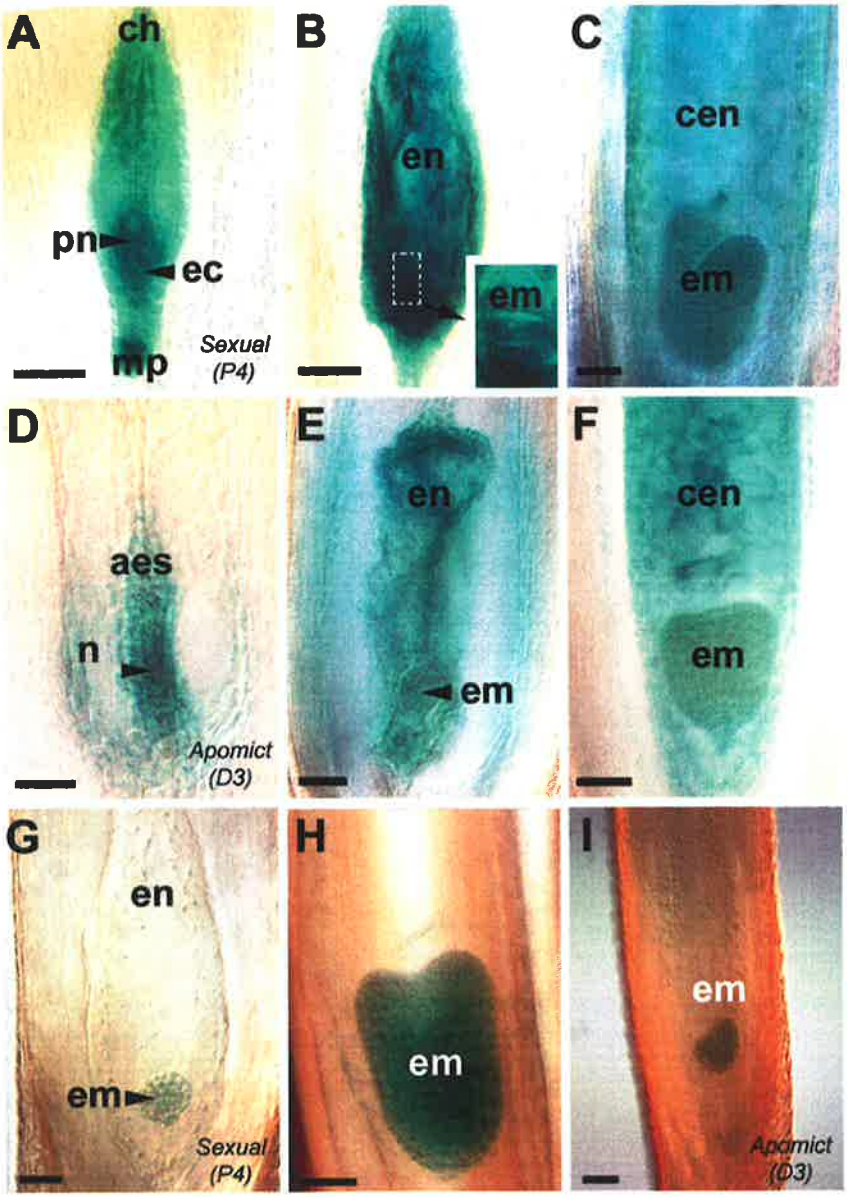
A
ch
pn
ec
mp
Sexual
(P4)
B
en
em
C
cen
em
D
aes
n
Apomict
(D3)
E
en
em
F
cen
em
G
en
em
Sexual
(P4)
H
em
I
em
Apomict
(D3)

identical to those observed in *Arabidopsis*. However, the coordinated expression of the three heterologous *AtFIS:GUS* genes in key structures formed during sexual reproduction underscored their suitability as markers for comparing gene expression patterns during aposporous embryo sac formation and fertilisation independent seed initiation in apomictic *Hieracium*.

3.3.2 Conservation of *AtFIS:GUS* expression in sexual and apomictic *Hieracium*

Plants from two distinct apomictic *Hieracium* species, *H. aurantiacum* A3.4 and *H. piloselloides* D3, were selected to examine the expression patterns of introduced *AtFIS:GUS* genes (Figures 3.3, 3.4 and 3.5). These plants are well characterised, vegetatively propagated and exhibit different modes of aposporous embryo sac formation (Koltunow et al., 1998). One to four aposporous initial cells differentiate in D3 of which only one usually gives rise to a mature embryo sac (see Figure 3.1). A3.4 characteristically initiates multiple aposporous embryo sacs in different locations in an ovule and these generally coalesce to form a single aposporous embryo sac of varying cellular structure with variable spatial location. Mature ovules from both apomicts tend to contain a single mature aposporous embryo sac that is situated in the micropylar region of the ovule, the conserved position of embryo sacs in ovules of sexual plants. However, both apomicts can also develop an embryo sac in the chalazal region of the ovule.

Similar to that observed in sexual P4, the expression patterns of the *AtFIS2:GUS* (Figure 3.3G to 3.3I) and *AtMEA:GUS* (Figure 3.4D to 3.4F) chimeric genes were identical during embryo sac and fertilisation-independent seed development in apomictic *Hieracium* D3. GUS activity arising from the introduced

AtFIS2:GUS and *AtMEA:GUS* genes was evident in mature aposporous embryo sacs situated in the micropylar (Figure 3.3G and 3.4D) and/or chalazal region of ovules (Figure 3.5A and 3.5B) from the transgenic apomictic *Hieracium* plants. *AtFIS2:GUS* expression was also observed in multiple coalescing embryo sacs in A3.4 (Figure 3.3J). Similar to the expression in sexual P4, *AtFIE:GUS* expression was significantly lower than the other two genes during early embryo sac development (data not shown). Just prior to the initiation of fertilisation-independent endosperm in apomictic D3, a high level of *AtFIS2:GUS* and *AtMEA:GUS* activity was detected around nuclei positioned in the centre of the aposporous embryo sac and a lower level of GUS activity was consistently observed throughout the rest of the embryo sac (Figure 3.3G and 3.4D). This increase in staining around the polar nuclei-like structures suggests that as in sexual reproduction, central cell nuclei are the likely progenitors of autonomous endosperm in apomictic *Hieracium*.

The nuclei formed during fertilisation-independent endosperm divisions, although disorganised, were also marked with *AtFIS2:GUS* (Figure 3.3H and 3.3K) and *AtMEA:GUS* (3.4E). After cell walls had formed between the syncytial nuclei, the endosperm cells continued to express the *AtFIS2:GUS* (Figure 3.3I and 3.3L) and *AtMEA:GUS* (Figure 3.4F) genes until the torpedo stage of embryo development, consistent with the expression observed in the fertilised sexual plant (see Figure 3.3F and 3.4C). GUS activity was also observed in the aleurone endosperm cells after their differentiation (Figure 3.3L). Expression of *AtFIS2:GUS* and *AtMEA:GUS* was also observed in patches of endosperm that failed to cellularise (data not shown) and in the cellularised endosperm of seeds where embryos failed to initiate (Figure 3.5C).

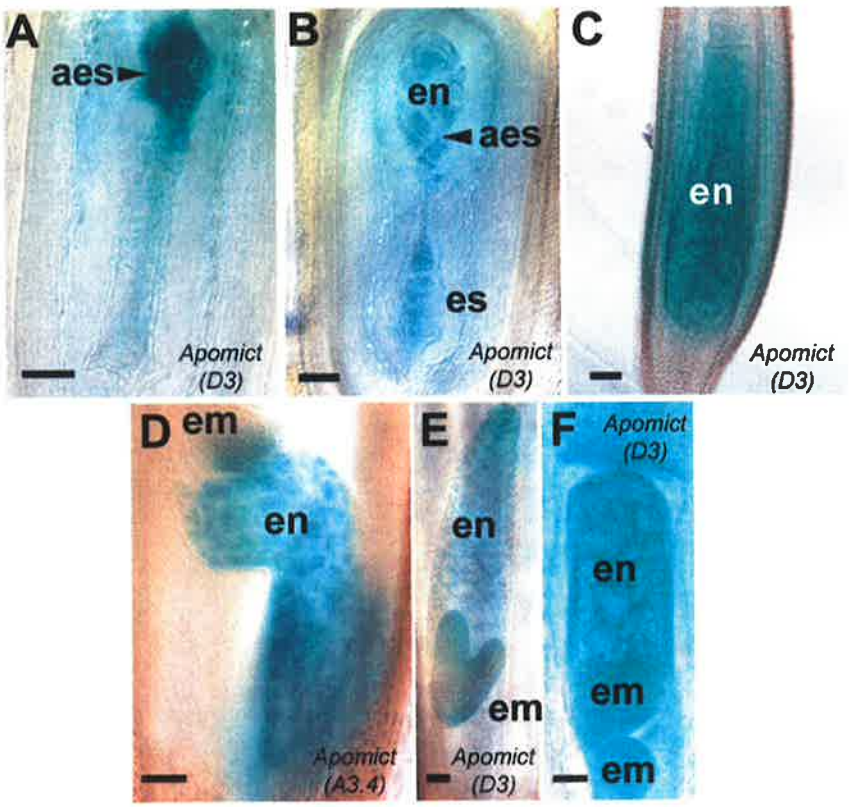

Figure 3.5 *AtFIS2:GUS* expression in abnormal structures within *Hieracium* D3 seeds. Ovules from apomictic *Hieracium* D3 (**A** to **C**, **E** and **F**) and A3.4 (**D**) were GUS stained and viewed whole-mount using Nomarski DIC microscopy. Bar = 50µm in all panels. **A** Displaced aposporous embryo sac (aes) developing in the chalazal region of a D3 ovule. **B** Two embryo sacs (es) developing in a D3 ovule. **C** Late D3 seed containing autonomous cellular endosperm (en) and no embryo. **D** Developing A3.4 seed containing endosperm and a parthenogenetic embryo (em) at the chalazal end of the embryo sac. **E** Developing D3 seed containing endosperm and a parthenogenetic embryo in the middle region of the embryo sac. **F** Developing D3 seed containing a globular embryo and a large embryo like structure in the same embryo sac.

The *AtFIS2:GUS* (Figure 3.3H to 3.3I and 3.4K to 3.4L), *AtMEA:GUS* (Figure 3.4E and 3.4F) and *AtFIE:GUS* (Figure 3.4I) genes were co-expressed during fertilisation-independent embryo formation when an embryo formed at the micropylar end of the aposporous embryo sac, and also in multiple embryos that formed in different spatial locations (Figure 3.3H and 3.5D to 3.5F). GUS activity of the three chimeric genes in apomictic seeds diminished at the mid to late heart stage of embryo development (Figure 3.3I), comparable to the expression in the sexual plant (compare with Figure 3.3F).

The *AtFIS:GUS* genes were co-expressed in maturing aposporous embryo sacs and in the early embryo and endosperm of fertilisation-independent seeds of two apomictic *Hieracium* species. The spatial and temporal expression pattern was comparable to that observed in embryo sacs, embryos and endosperm in sexual *Hieracium*. This indicates that the spatial and temporal regulation of the introduced *AtFIS:GUS* genes is common to both sexual and apomictic pathways despite the absence of meiosis and fertilisation in the apomictic pathway.

3.3.3 At*FIS2:GUS* marks megaspores and is down-regulated in the selected megaspore

Given the common spatial and temporal regulation of the *AtFIS:GUS* markers during early sexual and apomictic seed development in *Hieracium,* studies were targeted to determine the point of molecular convergence between the two reproductive processes. Few marker genes other than *AtSPL* have been identified that show specific expression patterns in the dividing megaspores or expanding functional megaspore. The expression of an *Arabidopsis* megaspore mother cell

(MMC) marker, *AtSPL:GUS*, in apomictic and sexual *Hieracium* was detected in MMCs from both plants but not in AI cells (N. Paech and A. Koltunow, unpublished). This suggested that at the time of morphologically discernable differentiation, AI cells do not share similar identity to enlarging MMCs.

Surprisingly, *AtFIS2:GUS* expression was detected early in *Hieracium* ovule development, and provided novel data as to the identity of AI cells. *AtFIS2:GUS* expression was not detected during MMC formation in the sexual P4 plant, but was observed after meiosis during megaspore selection. GUS activity was absent in the enlarging selected chalazal-most megaspore, but was present in the three micropylar spores destined to degenerate (Figure 3.6A). These expression patterns were confirmed by serial sections (data not shown) and wholemount analysis (Figure 3.6B). GUS activity remained absent in the functional selected megaspore as it expanded to fill the cavity left by the degenerating megaspores and the nucellar epidermis (Figure 3.6C). *AtFIS2:GUS* expression was then observed once the selected megaspore nucleus divided during the first division of embryo sac formation (Figure 3.6D), and expression continued during embryo sac maturation and fertilisation-dependent seed initiation as described previously (see Figure 3.3).

In situ hybridisation using a probe to detect *GUS* mRNA transcripts was carried out to examine if the megaspore expression pattern in *AtFIS2:GUS* related to selective distribution of mRNA synthesized in the MMC prior to meiosis or to regulatory events occurring during and/or after meiosis. *AtFIS2:GUS* mRNA was not detectable in the MMC of sexual plants (Figure 3.7A). Transcripts were not detected in the selected functional megaspore after meiosis, but were evident in degenerating megaspores and some of the degenerating nucellar cells (Figure 3.7B and 3.7C). Once the nucleus of the functional megaspore divided *AtFIS2:GUS* mRNA was detected in the early embryo sac (data not shown).

Figure 3.6 *AtFIS2:GUS* expression during early ovule development in *Hieracium.* Ovules from sexual *Hieracium* P4 (**A** to **D**), apomictic *Hieracium* D3 (**E** to **H**) and A3.4 (**I** to **L**) were GUS stained and viewed whole-mount using dark-field microscopy (**A**, **E** and **I**) or Nomarski DIC microscopy. Bar = 50 μm in panels (**A**), (**E**), (**I**) and (**L**) and 25 μm in panels (**B**) to (**D**), (**F**) to (**H**) and (**J**). The numbers at the top right of each panel indicate the floral stage (Koltunow et al., 1998). **A** P4 ovule in chalazal (ch) to micropylar (mp) orientation, showing GUS stain in pink. **B** Enlarging selected spore (ss) and blue GUS stained degenerating megaspores (dms) surrounded by the nucellar epidermis (ne). Indicated structures are outlined with a black line. **C** Enlarging functional megaspore (fm) with a large nucleus (n) chalazal to degenerated megaspores. The functional megaspore is outlined with an unbroken line. **D** Ovule containing an early embryo sac (es) with dividing embryo sac nuclei (esn), surrounded by the endothelium (et). **E** D3 ovule showing the corresponding stage of apomictic development to **A**. **F** Enlarging aposporous initial (ai) at the corresponding stage of apomictic development to **B.** The aposporous initial, outlined with a broken line, is forming in a slightly different plane to the other structures that are outlined with an unbroken line. **G** Enlarging aposporous initial cell above two smaller initials. **H** D3 ovule containing a dividing aposporous embryo sac (aes) with embryo sac nuclei (esn), at the corresponding stage of apomictic development to **D**. **I** A3.4 ovule showing the corresponding stage of apomictic development to **A** and **E**. **J** Enlarging aposporous initials at the corresponding stage of apomictic development to **B** and **F.** Multiple aposporous initial cells are indicated with broken lines, and some are forming in slightly different planes compared to the sexual structures that are outlined with an unbroken line. **K** Enlarging aposporous initial cells. **L** Aposporous embryo sac structures at the corresponding stage of apomictic development to **D** and **H**.

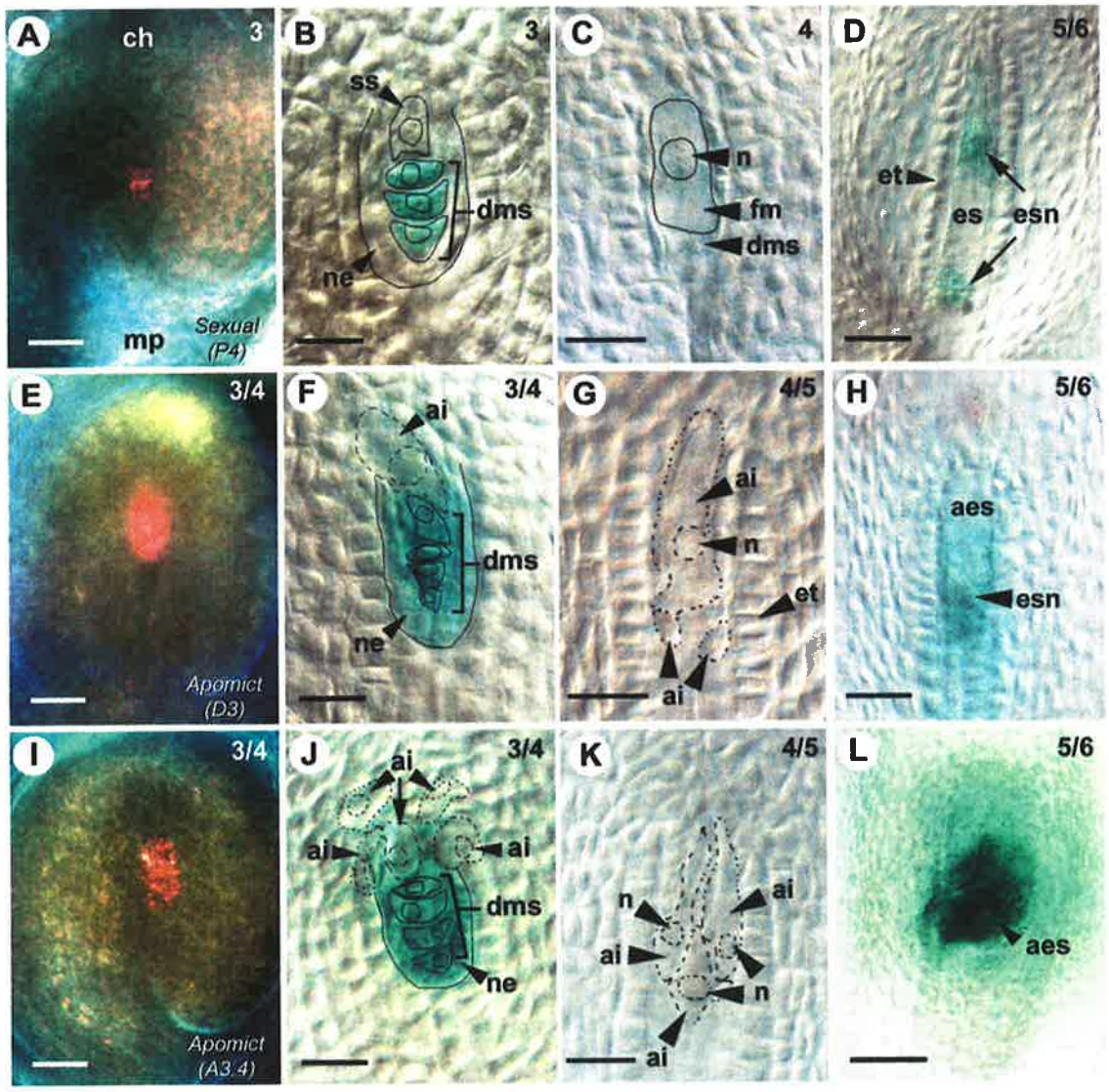
A
ch
3
mp
Sexual
(P4)
B
3
ss
dms
ne
C
4
n
fm
dms
D
5/6
et
es
esn
E
3/4
Apomict
(D3)
F
3/4
ai
dms
ne
G
4/5
ai
n
et
ai
H
5/6
aes
esn
I
3/4
Apomict
(A3.4)
J
3/4
ai
ai
ai
dms
ne
K
4/5
n
ai
ai
n
ai
L
5/6
aes

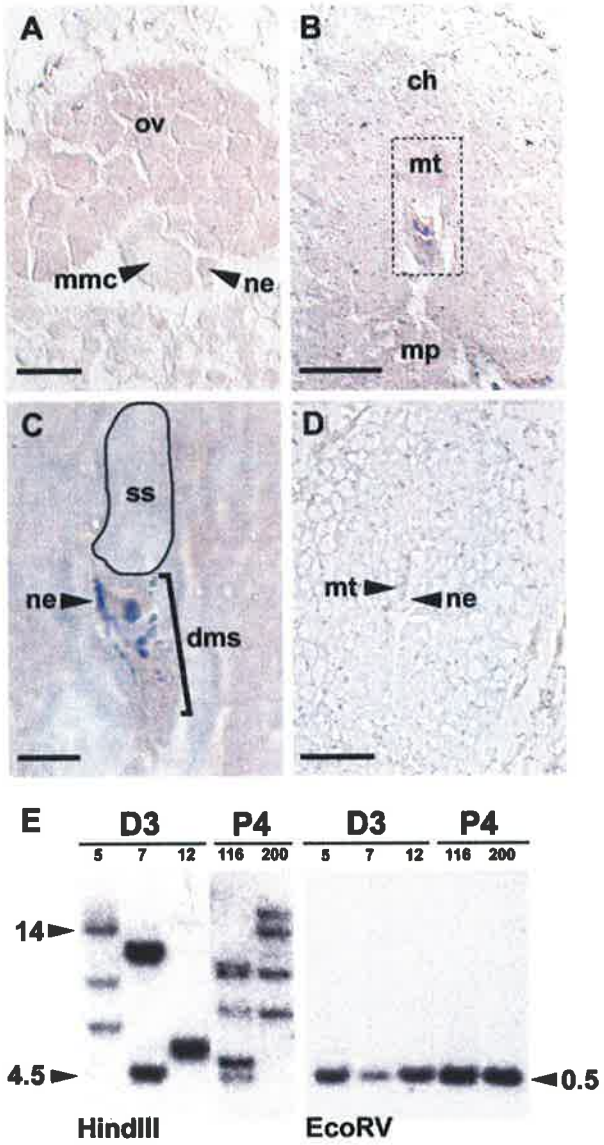

Figure 3.7 In situ hybridization (A.C. Araujo, CSIRO, Adelaide) and genomic analysis of *AtFIS2:GUS* in *Hieracium*. *Panels* show thin sections of *AtFIS2:GUS* sexual P4 ovules hybridised with antisense (**A**) to (**C**), or sense (**D**) labelled GUS RNA. **A** Megaspore mother cell (mmc) surrounded by the nucellar epidermis (ne). Bar = 15 µm. **B** Ovule in chalazal (ch) to micropylar (mp) orientation showing the megaspore tetrad (mt) outlined with a dashed line. Bar = 50 µm. **C** Magnified outlined region from B, showing staining in the degenerating megaspores (dms) and some nucellar epidermal (ne) cells. No staining is evident in the selected spore (ss). Bar = 12.5 µm. **D** Ovule at a similar stage to **B**, hybridised with sense GUS RNA. Bar = 50 µm. **E** DNA gel blot analysis of the *AtFIS2:GUS* transgene in apomictic D3 (independent lines 5, 7 and 12), and sexual P4 (independent lines 116 and 200) *Hieracium*. Genomic DNA (15 µg each) was digested with *HindIII*, which only cuts the transgene 5' of the probed sequence, or *EcoRV*, which cuts the transgene either side of the probed sequence. The expected size of the *EcoRV* fragment is 575 bp. The lengths of the DNA fragments (kilobases) are indicated for each blot.

The absence of both *AtFIS2:GUS* mRNA and protein activity in the enlarged functional megaspore was not a consequence of the absence of the *AtFIS2:GUS* gene from that cell as a result of meiotic segregation. Seven independent sexual *AtFIS2:GUS* transgenic lines were generated and the copy number of the gene in these hemizygous plants varied from 3-5 insertions (Figure 3.7E). In *AtFIS2:GUS* plants containing a single copy of the transgene, 50% of the megaspores should contain the gene after meiosis, while all megaspores are likely to contain the transgene in plants with multiple unlinked copies of the gene.

Examination of 657 ovules from sexual P4 plants with different numbers of transgene insertions showed that the temporal and spatial patterns of *AtFIS2:GUS* expression were surprisingly conserved between MMC differentiation and meiosis. GUS activity was never evident in the MMC, but in ovules that contained early megaspores soon after meiosis (n=148), *GUS* activity was detected in all four spores with the activity in the selected chalazal-most spore weaker than that of the other megaspores. Ovules containing an enlarged functional megaspore displayed GUS activity only in the three degenerating megaspores (n=509). This suggests that in plants containing multiple copies of the transgene where all meiotic products should inherit a copy, processes associated with functional megaspore specification are also involved in switching off *AtFIS2:GUS* expression in that cell.

3.3.4 At*FIS2:GUS* is differentially expressed at meiosis in apomictic *Hieracium*

The *AtFIS2:GUS* gene was considered a suitable marker to further investigate AI cell identity. A differential expression of the *AtFIS2:GUS* gene was observed in two

apomictic *Hieracium* species (D3 and A3.4), possessing different modes of aposporous embryo sac formation, soon after meiosis by dark field microscopy (Figure 3.6E and 3.6I) and the pattern was confirmed by serial sections (data not shown). In contrast to the pattern observed in sexual plants, *AtFIS2:GUS* was detected in all four megaspores soon after their formation and during their subsequent degeneration. *AtFIS2:GUS* was also expressed in the surrounding cells of the nucellar epidermis enveloping the tetrad of megaspores (Figure 3.6F and 3.6J), which degrades in both sexual and apomictic plants.

In both apomictic *Hieracium* species, *AtFIS2:GUS* expression was completely absent from aposporous initial cells as they enlarged and expanded towards the tetrad and nucellar epidermal cells expressing GUS (Figure 3.6F and 3.6J), just as it was absent from the enlarging selected megaspore in sexual plants. In the apomict D3, a single aposporous initial usually expanded into the position vacated by the degenerating megaspores and nucellar epidermis (Figure 3.6F). GUS activity was absent from the aposporous initial cell as it expanded into the position vacated by the degenerated megaspores (Figure 3.6G), but was detected in the aposporous structure as soon as the nucleus divided and aposporous embryo sac formation began (Figure 3.6H). In the apomict A3.4, multiple aposporous initials differentiated and none of these initials expressed *AtFIS2:GUS* (Figure 3.6K) until each nucleus divided to initiate aposporous embryo sac development (Figure 3.6L). As in D3, expression of *AtFIS2:GUS* in A3.4 ovules was also evident in the nucellar epidermis and in all four megaspores until these cells had degenerated.

Reasons for the expression of GUS in all four meiotic products of apomictic plants containing only a single insert of the *AtFIS2:GUS* transgene (Figure 3.7E) are not clear. Repeated transformation experiments have failed to identify a single-copy sexual P4 *AtFIS2:GUS* line to enable comparison. We speculate that post-meiotic

movement of either the mRNA or protein may occur during megaspore and/or nucellar epidermal cell degeneration.

The observation that *AtFIS2:GUS* expression is first observed in AI cells when the nucleus undergoes mitosis during early embryo sac formation suggests that the AI cell may acquire functional identity resembling that of a selected megaspore soon after differentiation. Alternatively, the AI cell may switch to an embryo sac program at the initiation of nuclear mitosis. This requires further clarification with appropriate markers as they become available.

3.4 Discussion

3.4.1 Apomixis reflects a deregulated sexual program

In the past, apomixis and sexual reproduction were viewed as two distinct processes that had little in common. Ernst (1918) postulated that apomixis might result from the hybridisation of related species to take into account the observation that the apomicts examined at that time were polyploid and highly heterozygous. The pioneering studies of Nogler (1984) and Savidan (1982) proved that apomixis was under genetic control although genetic modifiers or environmental conditions (Nogler, 1984; Savidan, 2001) may affect its expressivity. The subsequent confirmation that relatively few loci control different modes of apomixis and that mutagenesis can induce apparent components of apomixis in sexual plants has lent further support to the hypothesis that apomixis and sexual reproduction might share common elements.

Previous studies in *Hieracium* showed that expression of the *AtSPL:GUS* and *AtSERK:GUS* genes were similar during early ovule development and embryogenesis respectively in apomictic and sexual plants (J.B. Rossel, N. Paech

and A. Koltunow, unpublished). The expression of these reproductive markers, combined with the expression patterns of the various *AtFIS:GUS* chimeric constructs in sexual and apomictic *Hieracium* described here, have directly confirmed that apospory and the components of autonomous embryo and endosperm development share gene expression and regulatory components with sexual reproduction. This is despite the comparative structural differences in embryo sac, embryo and endosperm development (see Chapter 2) and also temporal and spatial changes in cell and tissue ploidy status in the two reproductive pathways.

3.4.2 A simple model for the regulation of apomixis in *Hieracium*

Data obtained from the spatial and temporal expression of the *AtFIS:GUS*, *AtSPL:GUS* and *AtSERK1:GUS* marker genes in sexual and apomictic *Hieracium* were considered, and a model for the control of apomixis in *Hieracium* D3 was devised (Figure 3.8). The results of the *AtFIS:GUS* marker analyses indicate that aspects of meiosis are avoided during aposporous embryo sac formation in *Hieracium*, because the AI cell that differentiates from the nucellus (or nucellar epidermis) is directed onto a mitotic embryo sac formation pathway combined with fertilisation-independent embryo and endosperm development. This finding, coupled with the shared nature of gene expression programs in sexual and apomictic pathways, suggests apomixis is manifested by the induction of a sexual developmental program deregulated in both time and space that leads to cell fate changes and the omission of critical steps in the sexual process (Figure 3.8). Novel

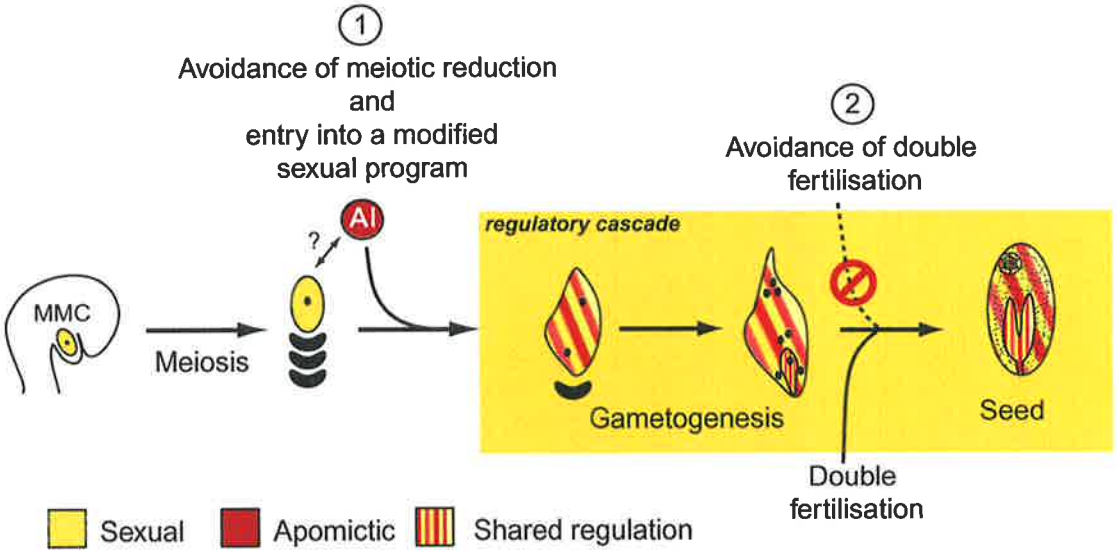

Figure 3.8 A model for apomixis in *Hieracium*. Numbers **1** and **2** indicate the checkpoints where the sexual process is modified in apomictic *Hieracium*. MMC - megaspore mother cell, AI - aposporous initial(s).

reproductive markers from *Hieracium* and *Arabidopsis* could test this model further as they become available.

The identity of the genetic factor that controls the initiation of apomixis remains uncertain, but this model suggests that it may be a key regulator of gene expression that has the ability to induce a modified sexual program. It is possible that mutations in a key regulator of a signal cascade directly lead to the manifestation of apomixis, or indirectly through an epigenetic alteration to chromatin structure. The variable nature of apomixis in terms of the frequency and timing of initiation, as well as the multiple components, favours a model that incorporates epigenetic regulation.

3.4.3 Interactions between sporophytic tissues, sexual and apomictic pathways

Genetic analyses in sexual plants have shown that the events leading to female gametophyte formation and seed development are both independent of and interdependent on the events and signals from surrounding sporophytic ovule tissues (Gasser et al., 1998). The importance of sporophytic ovule signals in governing the progression of the apomictic process is not entirely clear. Earlier studies in *Hieracium* spp with apospory show that induced alterations in ovule development correlate with changes in the apomictic process in terms of the frequency of initiating cells (Koltunow, 2000; Koltunow et al., 2001). Continuation of these studies targeting different ovule cell types in *Hieracium* and similar examinations in other apomicts should further clarify the dependence of sporophytic ovule signals in apomictic development. However, further studies targeting specific ovule cell types,

both sporophytic and gametophytic, rely upon the identification of genes expressed in specific cell types during reproduction. The limited availability of such genes was further addressed in this study by utilising *Arabidopsis* enhancer trap technology to identify putative cell specific marker genes (Chapter 4), and differential library screens and degenerate PCR to identify putative regulators of ovule and embryo sac development (Chapter 5).

Differentiation of the AI cell in apomictic *Hieracium* coincides with the demise of the sexual process in the ovule. Previous studies have shown that this does not always occur by simple physical displacement (Tucker et al., 2001). The demise of the sexual pathway in *Hieracium* was shown to correlate with a change in the spatial pattern of *AtFIS2:GUS* marker expression. A shift in GUS activity from the three non-selected megaspores in the sexual plant to all four megaspores and also surrounding nucellar epidermal cells in two apomictic species suggested that the presence of the AI might directly influence the demise of the sexual program by altering gene expression programs.

Molecular studies in *Arabidopsis* have suggested that positional signals involving the functional megaspore control cell fate and degeneration and result in the death of the three non-selected megaspores during megaspore selection in sexual plants (Yang and Sundaresan, 2000; Wu and Cheung, 2000). These mechanisms ensure that only a single cell is specified to initiate megagametogenesis and form an embryo sac. Utilization of such signals by the AI might influence the demise of all four sexual megaspores in *Hieracium* and this could be tested with the appropriate markers as they become available.

Other aposporous species form initials at different times of ovule development in comparison to *Hieracium* spp and in some of these, such as *Brachiaria* spp (Araujo et al., 2000), the demise of the sexual pathway does not

occur. Marker studies examining cell fate in other aposporous species should determine whether there are differences in the identity of cells initiating apospory. They should also lead to clarification of the interrelationships between sexual and aposporous embryo sac development and to an understanding of the factors favouring the development of one type at the expense of the other or enabling their coexistence.

3.4.4 Roles of *FIS*-class genes in apomictic reproduction

The early expression of *AtFIS2:GUS* in *Hieracium* and the conservation of synchronized expression of the *AtMEA:GUS*, *AtFIS2:GUS* and *AtFIE:GUS* genes during the late events of embryo sac formation and early seed development raises questions concerning the role of *Hieracium FIS*-class genes during sexual and apomictic reproduction. The *FIS*-class genes are postulated to form complexes that alter chromatin structure to inhibit or promote the expression of seed development genes and to regulate endosperm polarity in *Arabidopsis* (Chaudhury et al., 2001; Sorenson et al., 2001). Recently, homologues of the *MEA* and *FIE* genes were cloned from maize but the functional role of these genes during maize ovule and seed development has not been ascertained (Springer et al., 2002; Danilevskaya et al., 2003). A plausible hypothesis is that altered regulation of *Hieracium FIS* genes may enable autonomous seed development in apomictic plants. The isolation and characterisation of *Arabidopsis FIS* gene homologues from sexual and apomictic *Hieracium* should elucidate the role of these genes during autonomous endosperm development (see Chapters 5, 6 and 7).

Chapter 4: Isolation of *Arabidopsis* enhancer trap tagged promoters and characterisation of their expression during megagametogenesis and seed development

4.1 Introduction

The advent of enhancer and gene trap technology in plants has aided the identification of novel genes and markers for developmental studies. Enhancer trap (ET) technology relies upon a mobile genetic element (e.g. activator transposon) carrying a reporter gene (e.g. GUS) under the control of a weak, constitutive promoter interacting with genomic *cis*-acting elements that direct specific temporal and spatial expression. The pattern of reporter gene expression is proposed to reflect the expression of a nearby gene controlled by the same regulatory elements (Bellen et al., 1989, Bier et al., 1989, Grossniklaus et al., 1989). Such studies in *Arabidopsis* (Sundaresan et al., 1995; Springer et al., 1995; Campisi et al., 1999) have enabled the identification of genes involved in cell signalling, polarity and lineage within the *Arabidopsis* female gametophyte based on their pattern of expression (Grossniklaus and Schneitz, 1998). This technology also provides a potential tool for the identification and generation of cell-specific marker genes, capable of use as reproductive markers in apomictic plants such as *Hieracium*.

In this study the genomic position of five *Arabidopsis* ETs that direct expression of the GUS reporter gene to specific cells within the mature *Arabidopsis* embryo sac was determined. The 5' flanking sequences (promoter fragments) from

proximal genes were cloned, and these were fused to GUS and transformed into *Arabidopsis* to evaluate their capacity in directing cell-type specific expression of the linked *GUS* gene. Concomitant transformation into apomictic *Hieracium* examined their utility as developmental markers during aposporous embryo sac formation.

4.2 Materials and Methods

4.2.1 Identification of enhancer trap insertion sites

DNA sequences from TAIL-PCR reactions on selected enhancer trap lines, generated at Cold Spring Harbour Laboratories, were provided by Professor Ueli Grossniklaus (University of Zurich, Switzerland) and obtained as per Liu et al., (1995) using ET specific primers. Sequences were submitted to BLAST alignment programs (Altschul et al., 1990) and localised to *Arabidopsis* genomic BAC fragments. The site of insertion was used to determine which gene promoters might contain enhancer elements contributing to the described expression patterns.

4.2.2 Generation of promoter:GUS marker genes

Promoter fragments were PCR amplified from *Arabidopsis* Col-4 genomic DNA using standard *Taq* polymerase (Gibco) and appropriate primers (see Appendix 3 for primers). Purified DNA fragments were either digested directly, or cloned into pGEM T-easy vector (Promega) and digested to release the desired promoter fragment for ligation to HK Thermolabile phosphatase (Epicentre Technologies) treated pCAMBIA 1391z vector (CAMBIA). Clones containing the promoter

fragment in the desired orientation were identified by PCR and verified by sequencing with the 1391zREV1 primer (see Appendix 3).

The *At1041:GUS* construct contained 1281 bp of nucleotide sequence upstream from the ATG start codon of the *PROLIFERA* (*PRL*) gene (Springer et al., 1995). The promoter fragment was amplified with 1041AvrIIFWD and 1041AvrIIREV primers that contained *AvrII* restriction endonuclease adapters (see Appendix 3).

The *At1811:GUS* construct contained 632 bp of nucleotide sequence upstream from the ATG start codon of the 14-3-3 transcription factor GF14mu (Rosenquist et al., 2001), and was amplified using 1811SalIFWD and 1811NcoIREV primers that contained *SalI* and *NcoI* restriction endonuclease adapters respectively (see Appendix 3).

The *At2209-1:GUS* construct contained 1513 bp of nucleotide sequence upstream from the ATG start codon of a RNA-recognition motif (RRM) RNA-binding protein, designated UBA2b (Lorkovic and Barta, 2002). The *At2209-2:GUS* construct contained essentially the same sequence in the reverse orientation, and incorporated 1508 bp of nucleotide sequence upstream from the ATG start codon of a hypothetical protein. Promoter fragments were amplified using 2209.1FwdBam and 2209.1RevNco primers containing *BamHI* and *NcoI* restriction endonuclease adapters respectively, or the 2209.2FwdBam and 2209.2RevNco primers (see Appendix 3).

The *At2567:GUS* construct contained 693 bp of nucleotide sequence upstream from the ATG start codon of a hypothetical protein, and was amplified with 2567Fwd and 2567NcoIRev primers. The 2567NcoIRev primer contained an *NcoI* restriction endonuclease adapter (see Appendix 3).

The *At3536:GUS* construct contained 1996 bp of nucleotide sequence upstream from the ATG start codon of a putative DNA-binding protein, and was amplified using 3536Fwd and 3536NcoIRev primers. The 3536NcoIRev primer contained an *NcoI* restriction endonuclease adapter (see Appendix 3).

4.2.3 Transformation of *Arabidopsis* and identification of transgenic progeny

The promoter:GUS marker genes were transformed into *Agrobacterium tumefaciens* strain LBA4404. *Arabidopsis* No.0, L.*er* and Col-4 plants were transformed with the desired constructs by the floral dipping method (Clough and Bent, 1998). Seeds were harvested and hygromycin resistant plants (25-35 μg L^{-1}) were assayed for the presence of the T-DNA insert using PCR primers designed to detect the GUS gene (see Appendix 3). Homozygous lines were identified in the F2 generation by germinating seeds on 1% MS plates containing Hygromycin and scoring for 100% resistance.

4.2.4 Transformation of apomictic *Hieracium* and identification of transgenic progeny

The *At2209-1:GUS* and *At1811:GUS* marker genes were transformed into apomictic D3 *Hieracium* as described in Section 3.2.2. Plantlets were regenerated on 2.5 μg. L^{-1} Hygromycin B (Boehringer Mannheim) selection media, and positive transgenic plant lines were identified by PCR with Hygromycin and GUS primers (see Appendix 3).

4.2.5 GUS staining and microscopic analysis

Histological analysis of GUS enzyme activity in *Arabidopsis* tissues was carried out as per Section 3.2.4.

4.3 Results

4.3.1 Insertion sites of five ETs in the Arabidopsis genome and their expression characteristics

The *Arabidopsis* ET lines examined in this study were chosen because of their specific expression pattern within the developing female gametophyte and endosperm (U. Grossniklaus, R. Baskar and J.P-Calzada, unpublished). Figure 4.1 shows the general expression patterns of the ET lines at anthesis and during early seed development. ET 1041 displayed GUS expression within all cell nuclei of the embryo sac throughout mitotic development, and also in the embryo and endosperm throughout cell proliferation (Vielle-calzada et al., 2000; Figure 4.1A). ET 1811 showed GUS expression within the antipodals, egg cell and synergids, and also in the embryo and endosperm after fertilisation (Figure 4.1B). ET 2209 displayed weak GUS expression in the central cell prior to fertilisation, and then comparatively strong expression in the endosperm after fertilisation (Figure 4.1C). ET 2567 displayed strong expression in the egg apparatus and weak expression in the other cells of the gametophyte, and also in the developing endosperm (Figure 4.1D). ET 3536 expression was not analysed in the gametophyte, but was detected during endosperm development (Figure 4.1E).

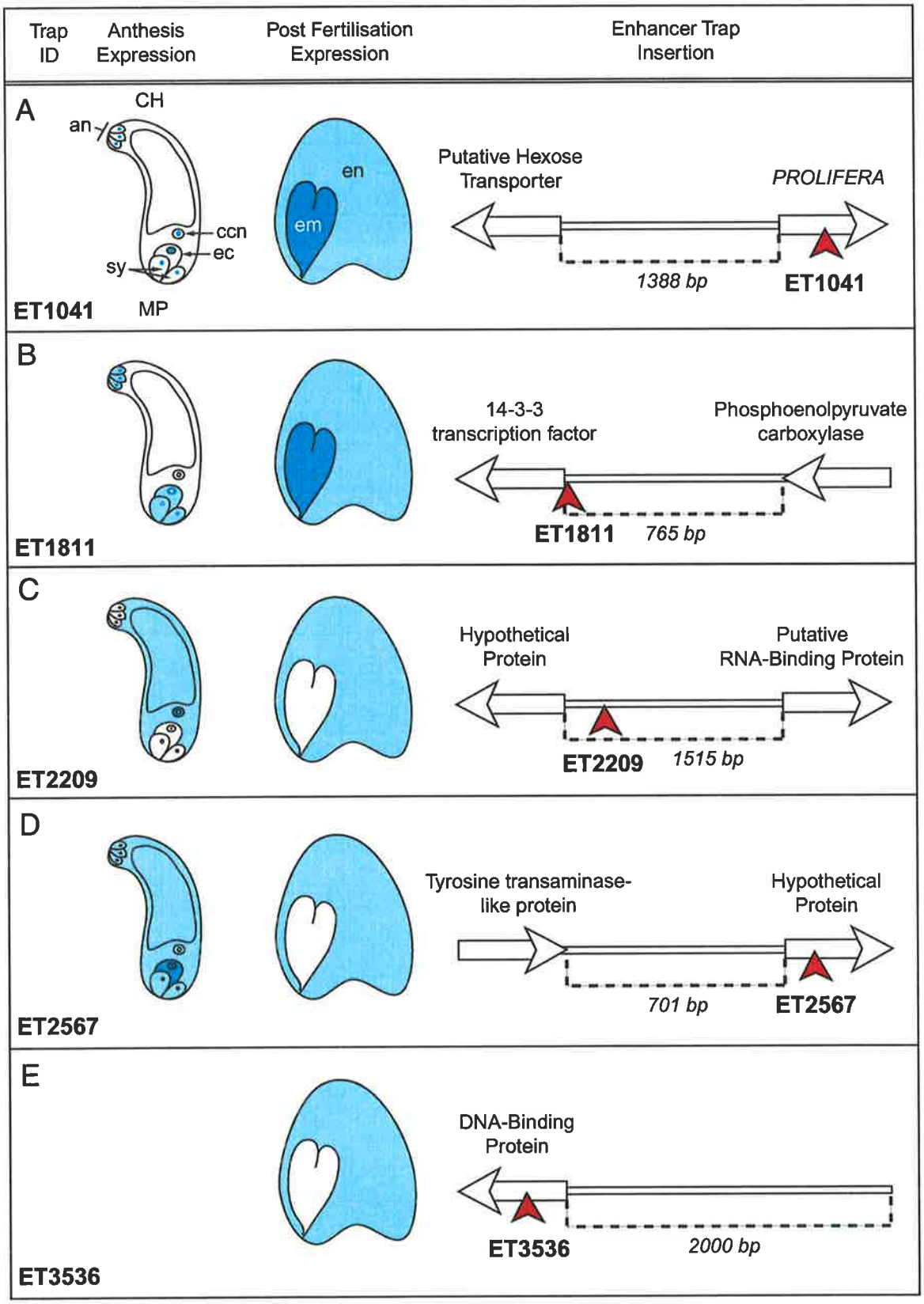

Figure 4.1 GUS expression patterns during ovule development in enhancer trap (ET) lines and positional location of ETs in the *Arabidopsis* genome as determined by TAIL-PCR and BLAST analysis. **A** ET1041. **B** ET1811. **C** ET2209. **D** ET2567. **E** ET3536. an - antipodals, ccn - central cell nucleus, CH - chalazal pole, ec - egg cell, MP - micropylar pole, sy - synergids

The five ET insertions were mapped to positions in the *Arabidopsis* genome based on their TAIL-PCR sequence (Table 4.1). Three of the five insertions were found within the coding regions of putative genes, and two in non-coding DNA 5' of putative genes (Figure 4.1). ET 1041 was located in the last exon of the *PRL* gene, which was previously identified in a general gene trap screen (Springer et al., 1995; Figure 4.1A), ET 2567 was positioned within the first exon of a hypothetical protein (Figure 4.1D), and ET 3536 was located in the last exon of a putative AT-hook DNA-binding protein (Figure 4.1E). ET 1811 was located in non-coding DNA upstream of the 14-3-3 transcription factor GF14mu (Rosenquist et al., 2001; Figure 4.1B). ET 2209 was positioned in non-coding DNA between a hypothetical transmembrane-protein homolog and a putative RRM RNA-binding protein (Figure 4.1C).

Table 4.1 Genome location and identity of putative enhancer trapped genes from *Arabidopsis* thaliana. ID - identity, Chr - chromosome.

Trap ID	Chr	BAC/Clone	Gene ID	Gene Type/Name
1041	4	T10M13	At4g02060	MCM2-3-5-like (PROLIFERA; Springer et al., 2000)
1811	2	F14N22	At2g42590	14-3-3 transcription factor (GF14mu [grf9]; Rosenquist et al., 2001)
2209-1	2	T3K9	At2g41060	RRM RNA-Binding protein (UBA2b; Lorkovic and Barta, 2002)
2209-2	2	T3K9	At2g41050	Probable membrane protein (hypothetical)
2567	4	F20O9	At4g28430	Hypothetical protein
3536	4	T12H17	At4g22770	DNA-Binding protein (Similar to PD1 from *P. sativum*)

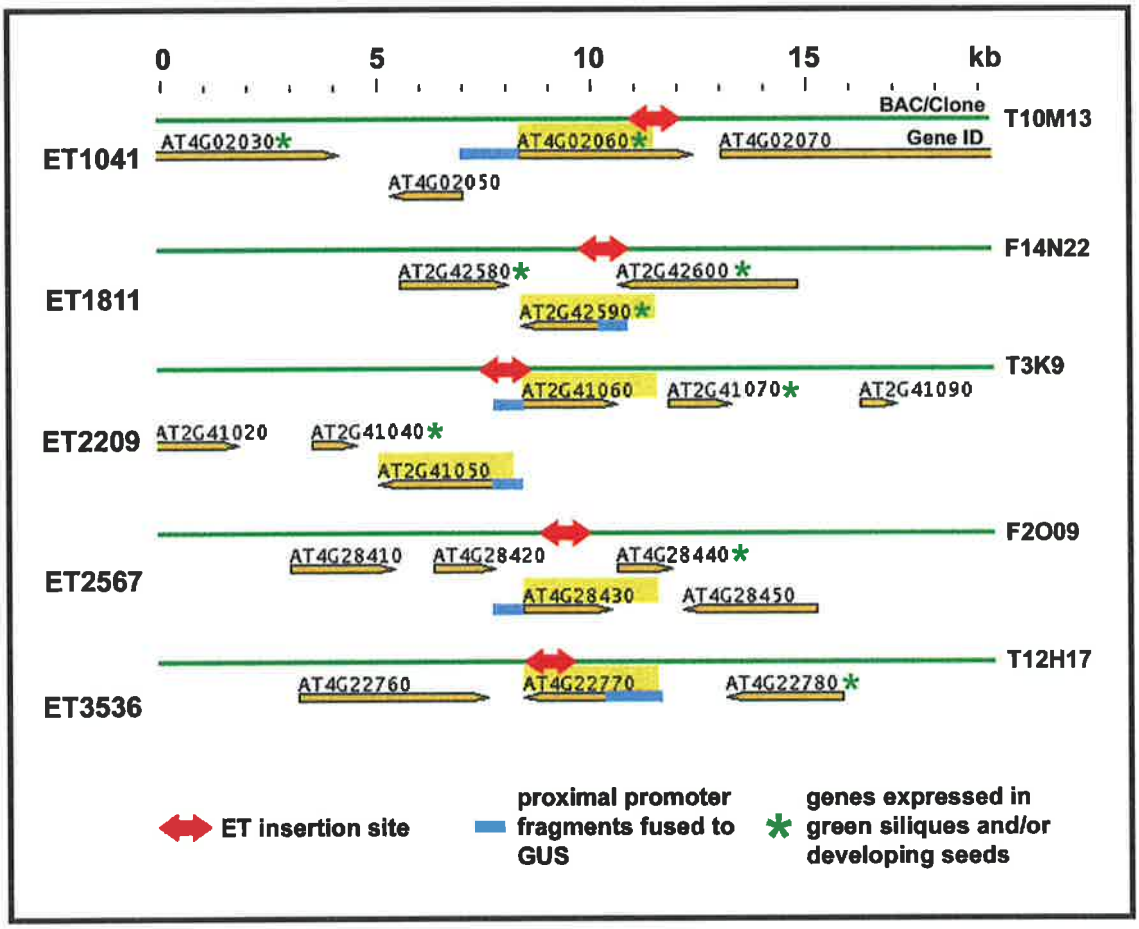

Figure 4.2 Position and identity of *Arabidopsis* genes within 5-10 kb of the enhancer trap insertions. The gene and BAC clone nomenclature was obtained from TAIR (The *Arabidopsis* Information Resource) and the NCBI database. Gene names shaded in yellow were targeted in this study.

The position of the ETs relative to other genes in the genome is shown in Figure 4.2. BLAST searches identified EST and/or cDNA sequences for all of the genes within a 10 kb radius of the ET insertions (Table 4.2). The most proximal genes to ET1041 (AT4G02060), ET1811 (AT2G42950), ET2209 (AT2G41060 or AT2G41050) and ET3536 (AT4G22770) matched *Arabidopsis* ESTs from seed, silique or mixed whole plant tissue libraries. This was not the case for ET2567 (AT4G28430), which only matched ESTs from leaf libraries. Some genes distal to the ET insertions also showed ESTs in seed libraries (Figure 4.2 and Table 4.2). The EST data suggested that in chimeric constructs, most of the selected promoter fragments might contain *cis*-elements capable of directing GUS expression to specific cells during ovule and early seed development.

To test whether the enhancer elements located within the 5' promoter region of the trapped or proximal gene regulated GUS expression, DNA fragments corresponding to these regions were fused to GUS and transformed into *Arabidopsis* plants. In the case of ET2209, it was hypothesised that the elements controlling GUS expression were located in the genomic region separating the hypothetical trans-membrane protein and the putative RRM RNA-binding protein. This region was fused to GUS in both forward (*At2209-1:GUS*) and reverse (*At2209-2:GUS*) orientations to determine which promoter fragment was regulating expression.

Table 4.2 (next page) EST matches of genes within 5-10 kb of inserted enhancer traps in the *Arabidopsis* genome. The most proximal genes targeted in this study are highlighted in bold. TAIR - The *Arabidopsis* Information Resource

Trap ID	Proximal genes	Proximal Gene Identity	TAIR EST hits	Arabidopsis EST Sequences
1041	**At4g02060**	**Prolifera**	1	green siliques
	At4g02070	G/T DNA mismatch repair enzyme	2	above-ground organs
	At4g02050	putative hexose transporter	1	inflorescences
	At4g02030	hypothetical protein	4	developing seeds, green siliques, various mixed tissues
1811	**At2g42590**	**14-3-3 transcription factor**	32	leaves, inflorescences, roots, green siliques, above-ground organs
	At2g42580	unknown protein	5	developing seeds, various mixed tissues
	At2g42600	phosphoenolpyruvate carboxylase	28	green siliques, developing seeds, flower buds, above-ground organs, seedling hypocotyls, roots
2209	**At2g41060**	**RNA-binding protein**	2	various mixed tissues
	At2g41050	hypothetical membrane protein	1	above ground organs
	At2g41040	hypothetical	2	green siliques, roots
	At2g41070	bZIP family transcription factor	14	green siliques, developing seeds, siliques and flowers
	At2g41090	calcium-binding protein	3	rosettes, leaves, seedlings
2567	**At4g28430**	**Hypothetical protein**	1	leaves
	At4g28420	tyrosine transaminase-like protein	0	
	At4g28440	putative protein	3	various mixed tissues, green siliques
	At4g28450	G-protein beta family	0	
	At4g28410	hypothetical protein	1	roots
3536	**At4g22770**	**DNA-binding protein**	1	various mixed tissues
	At4g22760	similar to selenium-binding protein	1	various mixed tissues
	At4g22780	Translation factor EF-1 alpha-like protein	4	green siliques, developing seeds

4.3.2 Four of the six tested chimeric marker genes were not expressed in floral tissues

The chimeric gene test constructs were introduced into three *Arabidopsis* ecotypes, Columbia-4 (Col-4), Landsberg *erecta* (L.*er*) and Nossen-0 (No-0). The number of hygromycin resistant and *GUS* PCR positive transformants obtained for *At1041:GUS* was 13 (11 Col-4, 2 L.er), for *At1811:GUS* was 9 (4 Col-4, 5 L.*er*), for *At2209-1:GUS* was 7 (3 Col-4, 4 No0), for *At2209-2:GUS* was 5 (5 No0), for *At2567:GUS* was 6 (5 Col-4, 1 L.er) and for *At3536:GUS* was 5 (5 No0).

In the case of the *At1041:GUS*, *At2209-2:GUS*, *At2567:GUS* and *At3536:GUS* transgenics, GUS expression was not detected in ovules or floral tissues after staining in hemizygous or homozygous plants. This contrasted with the expression observed in the original ET lines. GUS expression was detected in young leaves growing from around the shoot apex in seedlings of *At1041:GUS* plants (data not shown), and this pattern was very similar to that observed in *PRL::GUS* seedlings (Springer et al., 1995), suggesting that the *At1041:GUS* gene is functional.

4.3.3 Expression of *At1811:GUS* was detected in vascular tissues

The *At1811:GUS* chimeric gene was highly expressed in the vascular tissues of most organs examined. In germinating seedlings, *At1811:GUS* was detected in the shoot apical meristem and vascular tissue within the elongated cotyledons and developing roots (Figure 4.3A). In mature plants *At1811:GUS* was detected within the flower (Figure 4.3B), specifically in the vascular tissues of the sepals (Figure 4.3C and 4.3D), the anther filaments within the stamens (Figure 4.3E) and in the

Figure 4.3 *At1811:GUS* expression in *Arabidopsis*. Bars in **A** and **B** = 1 mm, in **D**, **E**, **G**, **H** and **K** = 50 μm, in **F** = 250 μm, in **H** = 500 μm and in **J** = 25 μm. **A** Germinated seedling showing two cotyledons (c), a shoot apical meristem (sam) and developing roots (r). **B** Schematic diagram of an *Arabidopsis* flower, reproduced with permission from Vivian-Smith et al., (2001). **C** Flowers at different developmental stages. The anthers (a), petals (p), sepals (s) and stamens (st) are indicated. **D** Vascular tissue (v) within a sepal. **E** The anther filament (af) within a post-anthesis stamen. **F** Pollen grains within anthers after anthesis. **G** Developing seed connected to the placenta by the funiculus (f). **H** Receptacle tissue at the boundary of the carpel and stem. **I** Silique wall 4 days post-pollination. **J** Fertilised ovule containing an embryo (em), nuclear endosperm (en) and a chalazal cyst (cc). **K** Mature seed containing a late embryo with the hypocotyls (h) and cotyledons indicated (c).

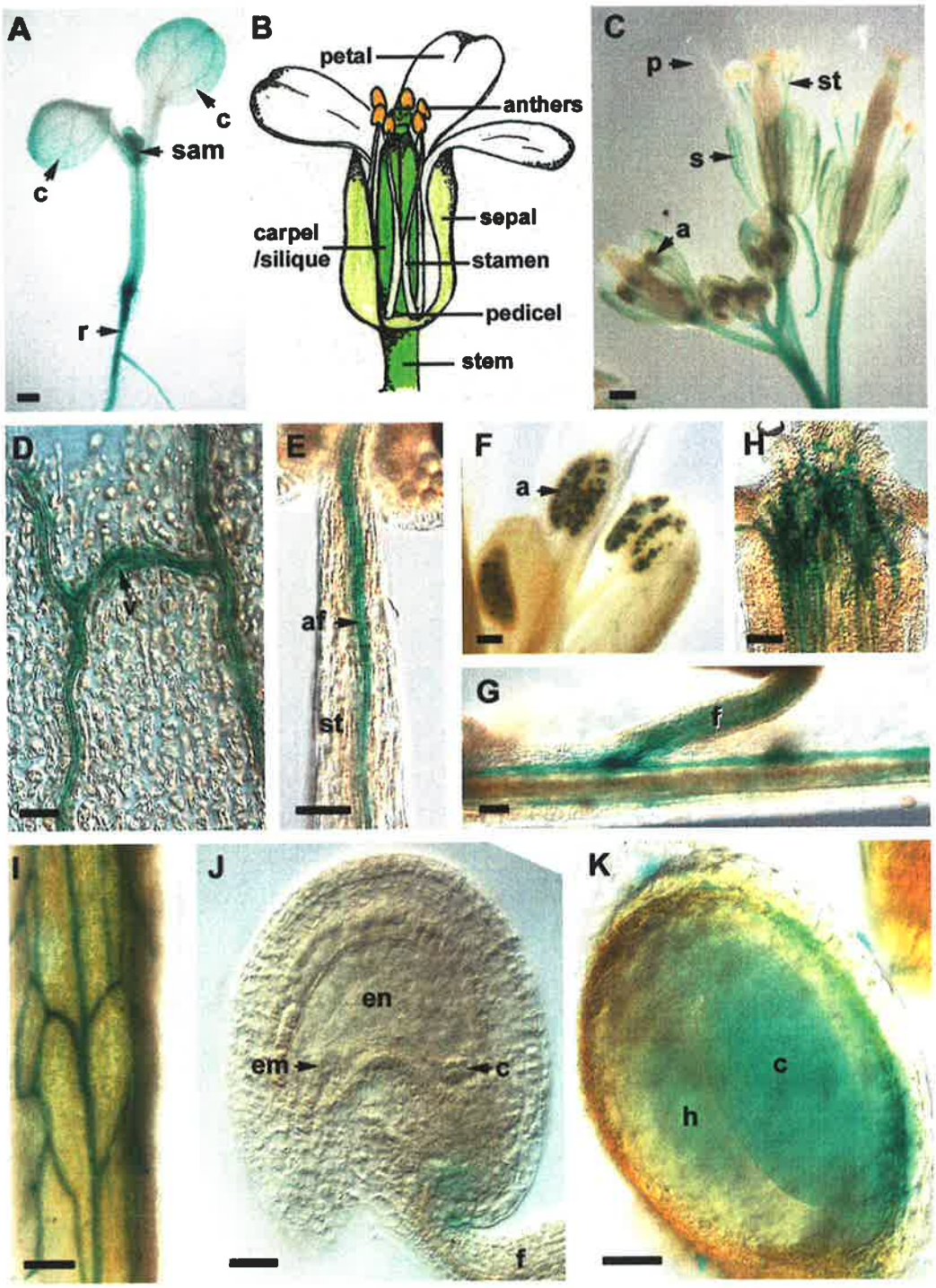
A
c
sam
c
r
B
petal
anthers
sepal
carpel
/silique
stamen
pedicel
stem
C
p
st
s
a
D
E
af
st
F
a
H
G
f
I
J
en
em
c
f
K
c
h

connective tissue below the stigma (Figure 4.3C), but not the petals (Figure 4.3C). GUS activity was also high in developing pollen grains (Figure 4.3F), and vascular tissue within the placenta (Figure 4.3G), receptacle (Figure 4.3H), and stem (Figure 4.3C). Expression was not evident in the carpel wall, but was apparent in vascular tissues within the maturing silique wall (Figure 4.3I). In ovules at anthesis and after fertilisation, GUS expression was weak in some cells at the base of the ovule adjoining the funiculus (Figure 4.3J).

GUS expression driven by the selected 5' proximal sequences was not detected in any cells within the female gametophyte during mitosis or at anthesis, unlike the original ET1811 line that showed expression in the egg apparatus and antipodals. However, GUS activity was detected in the seed during late development and was localised predominantly in the developing cotyledons of the embryo (Figure 4.3K). The pattern of *At1811:GUS* expression in apomictic D3 *Hieracium* plants was similar to that observed in *Arabidopsis* (data not shown).

4.3.4 Expression of *At2209-1:GUS* was detected in synergids and antipodal cells in *Arabidopsis* ovules

In transgenic *Arabidopsis* plants, expression of the test *At2209-1:GUS* chimeric construct was detected in ovules and anthers. The expression in anthers was localised mainly to the developing pollen grains, but was also detected in the connective tissue of the anther (data not shown). Within the ovule (Figure 4.4A), GUS expression was first detected in the female gametophyte just prior to anthesis in a bi-polar pattern (Figure 4.4B). It was spatially expressed at the chalazal end of the developing gametophyte in the vicinity of the degenerating antipodals, and also

Figure 4.4 *At2209-1:GUS* expression in *Arabidopsis* No-0 ovules. *Panels* **B-D** and **F-K** show whole-mount GUS stained specimens viewed under Nomarski optics. *Panel* **E** shows a 2μm section of a wild type *Arabidopsis* ovule stained with toluidine blue, courtesy of S. Johnson (CSIRO, Adelaide). Bar = 20 μm in all panels except **G**, where bar = 50 μm. **A** Schematic diagram of an *Arabidopsis* ovule at anthesis, with the female gametophyte in the centre and the sporophytic integument cell layers surrounding it, modified from Mansfield et al., (1991). **B** Ovule at anthesis showing the position of the synergids (sy) at the micropylar end, the central cell (cc), and the antipodals (an) at the chalazal end of the embryo sac. The funiculus (f) is also indicated. **C** Side-on view of the synergids and their position relative to the egg cell (ec) and polar nucleus (pn) at anthesis. **D** Front-on view of an anthesis ovule showing the two synergids below the egg cell. **E** section of an anthesis wild-type ovule, showing the synergids, egg cell, fused polar nucleus (fpn) and central cell. **F** Fertilised ovule containing one intact synergid, and showing the vascular strand (v) within the funiculus. **G** Multiple squashed ovules showing GUS expression in the vascular strands within the funiculi. **H** Fertilised ovule containing one intact synergid. **I** and **J** Ovules from emasculated siliques 3 days after emasculation, showing GUS staining within the intact synergids. **K** Fertilised ovule containing an embryo (em), endosperm (en) and a chalazal cyst (c). The funiculus is indicated.

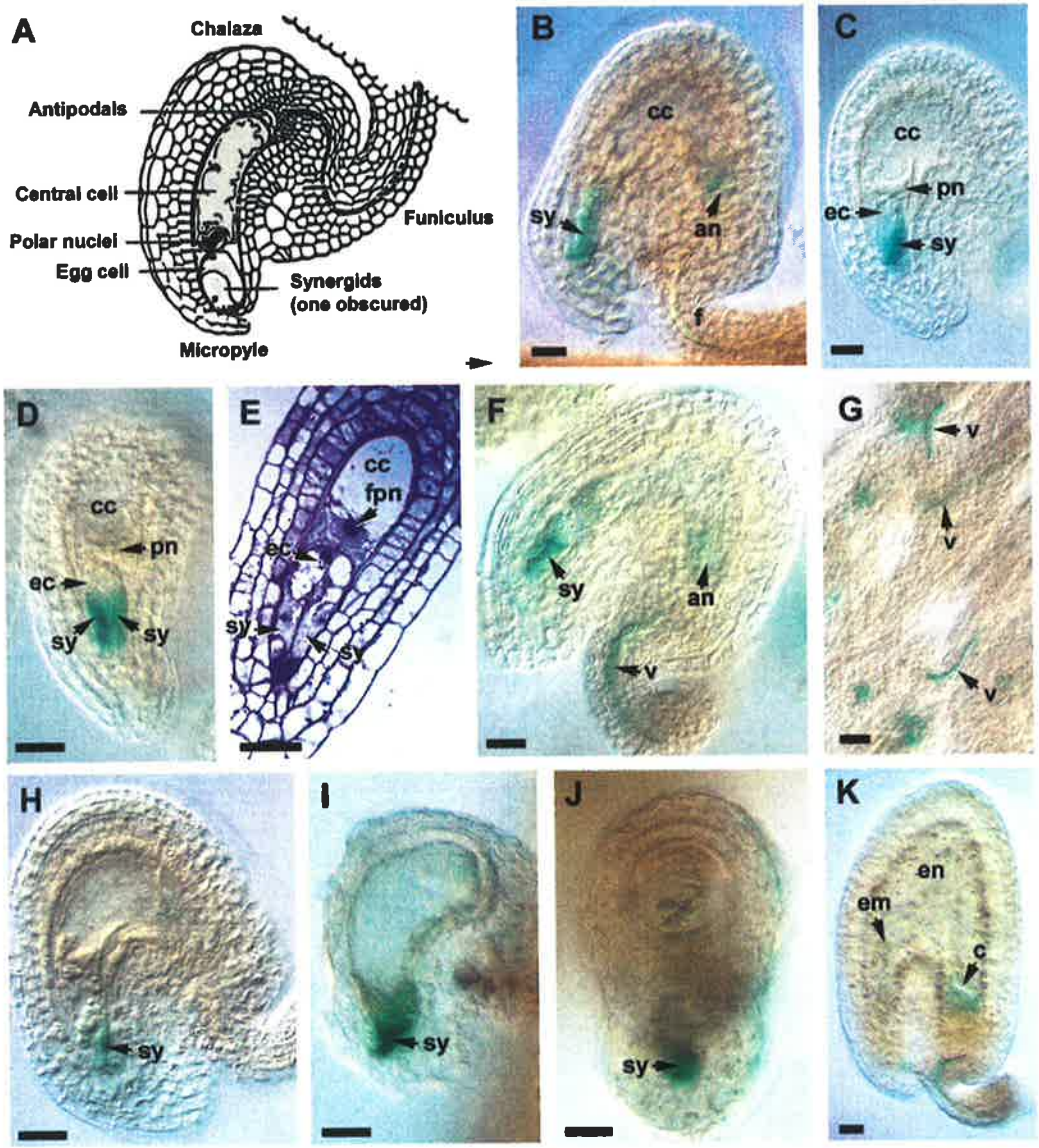
A
Chalaza
Antipodals
Central cell
Funiculus
Polar nuclei
Egg cell
Synergids
(one obscured)
Micropyle
B
cc
sy
an
f
C
cc
pn
ec
sy
D
cc
pn
ec
sy
sy
E
cc
fpn
ec
sy
sy
F
sy
an
v
G
v
v
v
H
sy
I
sy
J
sy
K
en
em
c

at the micropylar end within the two synergids that, with the egg cell, comprise the egg apparatus. GUS activity was not detected in the egg cell, and was also absent from the central cell (Figure 4.4C) where expression was detected in the primary ET2209 line.

Immediately prior to anthesis, GUS activity was clearly detected throughout both synergid cells (Figure 4.4D). Figure 4.4E shows the location of these two cells micropylar to the egg cell in the *Arabidopsis* ovule. Expression was also clearly detected in the vascular strand within the funiculus (Figure 4.4F and 4.4G). After pollination, GUS activity in one of the synergids rapidly diminished (Figure 5.4H), possibly corresponding to degeneration of that cell just prior to pollen tube penetration. GUS activity remained present in the vicinity of the persistent synergid cell (Figure 4.4H), but eventually disappeared from the micropylar end of the ovule as that cell degraded. In ovules from emasculated siliques, GUS activity continued to mark the synergids up to 3 days post-emasculation (Figure 4.4I and 4.4J). Both synergids remained intact in the micropylar region of the ovule in the absence of pollination. After fertilisation, GUS activity was not detected in the developing embryo or micropylar endosperm, but was faintly detected in the chalazal endosperm cyst (Figure 4.4K). *At2209-1:GUS* activity also remained present in the vascular strand within the ovule funiculus until the later stages of seed development.

4.3.5 Expression of *At2209-1:GUS* was not detected in apomictic D3 *Hieracium*

Cytological studies of *Hieracium* embryo sacs suggest that synergid-like cells are present in both sexual and apomictic plants. The two synergid cells flank the egg

and contain small dense centrally located nuclei (Koltunow et al., 1998). Although the egg apparatus is often structurally irregular in apomictic D3 *Hieracium*, synergid-like cells occupy a similar position and share similar morphology to synergids from sexual P4. Synergids are involved in the attraction of the pollen tube towards the egg cell prior to fertilisation in sexual plants, and hence their role in autonomous apomictic plants is uncertain. The *At2209-1:GUS* chimeric gene was transformed into apomictic D3 *Hieracium* to determine whether synergid-like cells in aposporous embryo sacs expressed the synergid marker, allowing their fate to be tracked during development.

Five D3 *Hieracium* plants containing the *At2209-1:GUS* marker gene were generated via transformation experiments. Stage 5 to 9 floral buds (see Appendix 1) were collected from these plants, dissected to expose the ovaries and stained for GUS activity. After 3 days of staining, no GUS activity was detected in ovules, developing seeds, anthers or any other floral tissues. It was uncertain whether the construct was functional in D3 *Hieracium*. The lack of expression may be due to limited numbers of transgenic lines, gene rearrangements, or altered identity of synergid cells in aposporous embryo sacs. Unfortunately, sexual transgenic *Hieracium* plants/lines containing the gene construct were not obtained even after multiple transformation experiments. Transformation of sexual *Hieracium* P4 with the *At2209:1:GUS* gene will determine if the construction is a relevant synergid marker in *Hieracium,* and will also clarify if the lack of expression in synergid like cells in aposporous embryo sacs reflects their altered cell identity.

4.4 Discussion

4.4.1 Proximal promoter sequences do not regulate the ovule expression of five *Arabidopsis* enhancer trap lines

Genes that identify specific cell types during plant development are particularly useful for determining cell identity. However, a lack of useful gametophytic markers in general makes it difficult to address questions of cell identity during apomixis in *Hieracium.* In this study, five ET lines that showed specific GUS expression in *Arabidopsis* embryo sac cells were selected to isolate promoter elements proximal to the ET and test their efficiency as cell-specific molecular marker constructs when fused to GUS. Multiple transgenic lines (>5) were analysed for each promoter:*GUS* construct, and none of the regenerated *Arabidopsis* plants showed expression patterns in the ovule that resembled those observed in the original ET lines. This suggested that the enhancer elements controlling expression of the original ETs are unlikely to be present in the selected promoter sequences.

Most ET studies suggest that integration of the ET minimal reporter adjacent to an enhancer element or proximal promoter element is the main requirement for reporter gene expression (Campisi et al., 1999; Ramachandran and Sundaresan, 2001; Sundaresan et al., 1995). This assumption is supported by a recent limited study in *Arabidopsis* that showed conservation of expression patterns for two ETs and their corresponding proximal promoter:GUS marker genes (Estrada-Luna et al., 2002). By contrast, the data presented here and other studies suggest that there are limitations to enhancer trap screens for identifying marker promoter fragments (Springer, 2000). Elements within proximal promoter (5') regions as well as gene introns and 3' gene/UTRs (Belitsky and Sonenshein, 1999) many kilobases away

can influence gene expression in prokaryotes and eukaryotes (Reitzer and Magasanik, 1986; Martin et al., 2001). One example is the *FLOWERING LOCUS C* (*FLC*) gene from *Arabidopsis* that requires specific promoter and intragenic sequences for correct spatial and temporal expression (Sheldon et al., 2002). The five ETs investigated in this study were positioned in gene rich regions of genomic DNA (see Figure 4.2), possibly under the influence of multiple or distant enhancer elements.

Analysis of genes within 5-10 kb of the ET insertions showed that at least one gene (sometimes many) in each region was expressed in developing seeds, inflorescences or green siliques (see Table 5.2). It is possible that sequences controlling the expression of the ETs, absent from the most proximal sequences analysed in this study, are present in these distal genes. Two techniques could be used in further studies of these ETs to generate markers for embryo sac cell-specific expression. A large DNA fragment (10-20 kb) of WT genomic DNA spanning the ET insertion site fused to GUS might reflect the expression patterns of the original ET line. Alternatively, the same region of DNA could be amplified from the original ET line, thus including the enhancer trap transposon and surrounding sequences, and transformed back into *Arabidopsis* to test the GUS expression pattern. These methods are less specific than those used in this study, and the identity of the gene(s) and elements regulating embryo sac specific expression might be difficult to determine. However, further studies aimed at identifying the enhancer elements controlling expression in these lines could focus on the individual genes in each chimeric construct.

4.4.2 The *At1041:GUS* gene lacks ovule regulatory sequences

At1041:GUS (*PROLIFERA:GUS*) expression was detected in young leaves within the vegetative apex, in a pattern similar to that described in the gene trap of *PRL* in *Arabidopsis* (Springer et al., 2000). The *PRL* promoter fragment used to generate the *At1041:GUS* construct in this study comprised 1281 bp upstream from the ATG. *At1041:GUS* expression was not detected during ovule development however, and this contrasted with the pattern observed in the *PRL::GUS* gene trap line and plants containing a *PRL::PRL::GFP* fusion construct (P. Springer, pers. comm.), which comprised 1045 bp of *PRL* promoter and the *PRL* gene fused to GFP (Springer et al., 2000). Combined, these results suggest that the enhancers regulating *PRL* expression in the ovule are likely to be located within the coding region or introns of the *PRL* gene, and not the promoter or 5'UTR.

Expression was not detected in seedlings or various floral tissues from plants containing the *At2567*, *At2209-2* or *At3536* promoters fused to GUS. EST data suggested that the most proximal genes trapped by ET2567, ET2209 and ET3536 produce mRNA and are expressed in above ground organs, and hence the promoter elements should be capable of directing GUS expression. However, the low frequency of EST sequences detected for these genes, as compared to the ET1811 14-3-3 gene which showed 32 matches (See Table 5.2), suggests that they may not be expressed at a high level, or may be localized in specific tissues other than the ovule. Because this study was predominantly aimed at determining the expression patterns of chimeric genes during ovule development, the expression of the *At2567:GUS*, *At2209-2:GUS* or *At3536:GUS* constructs in tissues other than developing flower was not intensively investigated.

4.4.3 At*1811:GUS* is a vascular tissue marker gene

The test *At1811:GUS* chimeric gene, comprising 632 bp of the gf14mu 14-3-3 promoter fused to GUS, identified vascular structures in floral and vegetative tissues of *Arabidopsis* and *Hieracium*. The role of gf14mu in plant development has not been described, although the family of *Arabidopsis* 14-3-3 proteins has been intensively studied (Wu et al., 1997; Rosenquist et al., 2001). 14-3-3 proteins play key functional roles in many critical physiological pathways that are regulated by phosphorylation (DeLille et al., 2001). In *Arabidopsis*, like most organisms, a family of 14-3-3 proteins exists consisting of 13 members. These proteins function in many developmental processes including nitrogen and carbon assimilation, starch synthesis and control of turgor pressure (Ferl et al., 1999; Sehnke et al., 2001; Korthout and de Boer, 1994). Although the *At1811:GUS* construct is not a useful marker for determining specific ovule cell identity in *Arabidopsis* or *Hieracium*, the *1811* promoter may be useful in studies of vascular development and the role of 14-3-3 proteins in that process.

4.4.4 At*2209-1:GUS* is a synergid and antipodal cell marker gene

The only reconstituted marker gene found to be expressed in the female gametophyte was *At2209-1:GUS*, which contained the promoter region of an RNA Recognition Motif (RRM) RNA-binding protein from *Arabidopsis* fused to GUS. The *At2209-2:GUS* chimeric gene, which contained the same promoter fragment in the reverse orientation, was not expressed in the ovule suggesting that some elements in the *2209-1* promoter are direction-dependent. The expression of

At2209-1:GUS in the synergids occurred independently of fertilisation, suggesting that the GUS protein was specifically produced from expression in the synergid itself and not derived from the pollen tube after fertilisation. Furthermore, *At2209-1:GUS* was absent from the synergids after fertilisation, suggesting that it may be a useful marker for studies related to embryo sac development and fertilisation.

In the original ET screen aimed at identifying ovule specific markers, 218 lines were identified that showed expression in the synergids (U. Grossniklaus, R. Baskar and J-P Vielle-Calzada, unpublished). 209 of these ET lines showed expression only after fertilisation as a result of pollen tube-produced enzyme discharge. Eight of the lines were specific for the synergids, and only one, ET1811, showed expression in the egg apparatus and antipodals. Interestingly, the patterns of expression detected in the *At2209-1:GUS* lines were almost identical to those observed in the original ET1811 line. The possibility of sequence and ET mislabelling cannot be excluded

The *Arabidopsis* genome encodes 196 RRM RNA-binding proteins (Lorkovic and Barta, 2002). Most of these can be classified into structural and/or functional groups based on similarity with either known metazoan or *Arabidopsis* proteins. The *2209-1* RNA-binding protein UBP2b has not been characterised (Lorkovic and Barta, 2002) but shares greatest homology with UBP2a, a member of the U-binding protein (UBP) RRM protein group, from *Nicotiana plumbaginofolia* and *Arabidopsis*. UBP2a is a component of the complex recognizing U-rich sequences in plant 3'-UTRs that contributes to the stabilization of mRNAs in the nucleus (Lambermon et al., 2002). It is possible, given the expression pattern of the *2209-1* promoter, and the high similarity of the UBP2b and UBP2a amino acid sequences, that 2209-1 functions to stabilise polyA$^+$ messages in the synergids and

antipodals prior to fertilisation. This is purely speculative, however, and UBA2b has yet to be functionally characterised.

The lack of *At2209-1:GUS* expression in apomictic *Hieracium* may be explained in a number of ways. Only five hygromycin resistant lines were identified from the transformation experiment, and this number may not be sufficient to evaluate the expression of the chimeric gene. Genomic T-DNA number copy analysis was not performed, and gene rearrangements may have occurred during integration. Alternatively, it is possible that synergid cells in aposporous *Hieracium* embryo sacs have altered identity to those in sexual plants. In some plant species, embryos are observed to form from the synergids (Johri and Tiagi, 1952; Sindhe et al., 1980). It is uncertain whether these embryos always arise due to penetration of multiple pollen tubes, such as that observed in *Pennisetum squamalatum* (Sindhe et al., 1980), or because of altered cell specification in the embryo sac. In apomictic *Hieracium*, embryos can arise from synergid-like cells (S. Johnson and A. Koltunow, unpublished) and it is possible that even though the position of synergid-like cells in aposporous *Hieracium* embryo sac resembles that of sexual P4, they may not have the same identity. This will be clarified by the generation of sexual transgenic *Hieracium* plants/lines containing the *At2209-1:GUS* construct and examination of gene expression patterns.

4.4.5 Enhancer traps and cell identity in apomictic *Hieracium*

The results from this study confirmed that ET expression patterns are not always directed by elements localised 5' to the inserted trap, and are likely to be influenced by other distal genomic sequences. Future approaches aimed at identifying the

genomic fragments controlling ET expression could utilise larger genomic fragments spanning the ET insertions. These large DNA fragments would be more likely to contain the elements regulating ET expression, and when fused to GUS, or cloned from the original ET lines with the GUS trap insertion present, might prove to be useful marker genes. Alternatively, candidate genes from the vicinity of the ET insertion expressed in seeds could be analysed more closely by cDNA expression profiling. Genes that show overlapping spatial and temporal expression patterns with the GUS activity in the ET lines could be targeted for further study.

The development of an endogenous enhancer trap strategy in *Hieracium* has the potential to identify novel genes expressed in specific cells during apomictic seed development (R. Bicknell and A. Koltunow, pers. comm.). However, the implicit problems associated with apomictic plants, such as high ploidy levels, stochastic reproductive events, and the inability to cross in transposable elements complicates the generation of such a strategy. At present, the rapid detection of ET lines from *Arabidopsis*, and the subsequent analysis of genes in the vicinity of the traps provides a much more reliable tool for the generation of chimeric genes capable of marking specific cell types during seed development. The identification of such genes will aid clarification of the apomictic process and is necessary to determine the developmental stages at which apomixis deviates from sexual reproduction in different species.

Chapter 5: Identification of cDNAs from *Hieracium* encoding putative regulators of gametophyte[3] and seed development

5.1 Introduction

The previous chapters described cytological aspects of endosperm development and the use of chimeric genes from *Arabidopsis* to address questions of aposporous embryo sac cell identity in *Hieracium*. Further studies were carried out in an attempt to characterise molecular aspects of seed development in apomictic *Hieracium*, using library screens and targeted isolation approaches.

Genes expressed during the initiation of apomixis in *Hieracium* have yet to be identified, but are required to clarify the cellular identity of AI cells. Analysis of early ovule development in the model sexual species, *Arabidopsis* has identified numerous genes involved in the initiation and outgrowth of the ovule primordia and development of the integuments (Gasser et al., 1998; Schneitz, 1999). In contrast, only two *Arabidopsis* genes have been identified through mutation screens that are involved in cell specification events during megasporogenesis. *SPOROCYTELESS* (*SPL*) has been implicated in the specification of the MMC, and *ANTIKEVORKIAN* (*AKV*) regulates the degeneration of non-selected megaspores after meiosis (Yang and Sundaresan, 2000).

[3] Note: M.R. Tucker and N.A. Paech contributed equally to the screening and isolation of plaques from the early ovule cDNA library. N. A. Paech, who passed away in September 2002, performed sequencing and further characterisation of cold plaques. Subsequent BLAST searches were performed by M.R. Tucker, and the identity of the genes are included in this chapter to perpetuate their use in other studies.

Similarly, the isolation of genes expressed during the autonomous initiation of endosperm development in *Hieracium* might provide clues as to the molecular controls regulating apomixis. Analysis of early seed development in *Arabidopsis* has identified key regulators of gametophyte, endosperm and embryo development (reviewed in Drews and Yadegari, 2002). Three of these genes, *MEA*, *FIS2* and *FIE* control the initiation of endosperm development (Luo et al., 2000) and when mutated give rise to autonomous endosperm in the absence of fertilisation, a similar phenotype to that observed in apomictic *Hieracium* plants during seed formation. Based on comparisons with similar proteins in *Drosophila*, the three *FIS* gene products possibly interact in large complexes to control gene expression, via histone deacetylation and methylation (Muller et al., 2002; Cao et al., 2002; Tie et al., 2001). Although they are yet to be directly linked to a plant PcG complex, *METHYLTRANSFERASE1* (*METI*) and *HISTONE DEACETYLASE* (*HDAC*) genes have also been identified from *Arabidopsis* that play a key role during seed and flower development (Genger et al., 1999; Luo et al., 2000; Wu et al., 2000a; Wu et al., 2000b; see Section 1.2.8.1). Hypotheses suggest that the function of endogenous *FIS* genes, or other members of a putative plant PcG complex may be compromised in autonomous apomictic plants, leading to the initiation of endosperm development in the absence of fertilisation (Chaudhury et al., 2001; Vinkenoog and Scott, 2001). The isolation and characterisation of endogenous *FIS* genes and putative PcG interactors from *Hieracium* will address their function in relation to autonomous seed development.

As an approach to better understand the processes that specify fate in cells initiating sexual and apomictic events, and the cues that regulate the development of autonomous endosperm, several strategies were employed. Cold-plaque screening of an early ovule-enriched cDNA library from *H. piloselloides* D2 was used to identify regulatory genes expressed in the ovule at the time of aposporous initial formation. The

cold-plaque screening method has been verified in many studies as a tool for identifying clones from a cDNA library that are present at low or medium abundance (Hodge et al., 1992). Genes expressed at low levels are not usually identified in traditional cDNA library differential screens, and might be involved in cell-fate specification within only a few cells, such as the MMC, megaspores or aposporous initial cells. Candidate genes regulating aspects of endosperm and seed development were also targeted for isolation by degenerate PCR. Using these methods, *Hieracium* homologues of genes involved in cell-fate specification, endosperm development and global gene expression were identified and partially characterised

5.2 Materials and Methods

5.2.1 *Hieracium* tissue and RNA extraction

Various tissues including actively dividing leaves, roots, ovaries and other floral tissues were collected from apomictic D2, a diploid accession (2x=2n=18) derived from D3, D3 and sexual P4 (Section 2.2.1). D2 stage 2, 3 & 4 ovule-enriched tissue used in generating the cDNA library was collected by Susan Johnson (CSIRO, Adelaide), and the library was made as described in Tucker et al., (2001). Ovary tissues were also collected from stage 2/3, 4, 5/6, 7, 8/9, 10 and 11/12 florets (see Appendix 1) from sexual P4 and apomictic D3 *Hieracium*, and frozen in liquid nitrogen. Frozen tissue samples were ground at -80°C and RNA was extracted using the Trizol LS reagent (Gibco BRL) or an RNeasy kit with DNAse treatment (Qiagen) as per manufacturers instructions.

5.2.2 Cold-plaque screening of a *Hieracium* ovule-enriched cDNA library

Library screens were performed as described by Tucker et al., (2001), in collaboration with N.A. Paech, with the same filters used to identify differentially expressed clones up-regulated in ovule-enriched tissues. Duplicate filter lifts from the ovule-enriched cDNA library were hybridised with α-P^{32} labelled leaf cDNA or ovule cDNA probe for 16 hours. After hybridisation, filters were rinsed in 2 × SSC, 1 % SDS at 65°C, washed for 20 min in 2 × SSC, 1% SDS at 65°C and three times for 20 min in 0.1 × SSC, 1% SDS at 65°C. Filters were air dried on Whatman 3MM paper, placed in autoradiography cassettes with Kodak XOmat film and exposed at -80°C for 2 days and 7 days.

5.2.3 Identification of cold plaques and in vivo excision of pBluescript

Putative cold plaques were identified as plaques that did not hybridise to labelled leaf or ovule cDNA probe after 2-7 days exposure. Cold plaques were cored and the ExAssist (Stratagene) system was used to excise pBluescript plasmids from the λZAP II vector. Bacterial colonies containing rescued pBluescript clones were grown overnight at 37°C in LB + Ampicillin (50μg/mL), and plasmids were isolated using the Wizard Miniprep kit (Promega).

5.2.4 Detection and verification of "cold" inserts in pBluescript clones

The presence of inserts in the pBluescript clones was determined by N.A. Paech using PCR with the T7 and T3 vector primers (Stratagene) and also by digestion

with *EcoRI* restriction endonuclease. To determine if independent plaques were rescued, replicates of excised clones were digested with *RsaI* restriction endonuclease. PCR amplified and digested samples were electrophoresed on 1.0% TAE agarose gels and transferred to Hybond N membrane (Amersham). Membranes were hybridised with radiolabelled leaf or ovule-enriched cDNA as per Section 5.2.2 to verify that cold clones did not hybridise to either probe.

5.2.5 End sequencing of clones

Cold plaque clones were end sequenced with BigDye Terminator (Applied Biosystems) using appropriate vector primers and a 373A DNA sequencer (Applied Biosystems) at the Flinders Medical Centre sequencing facility (Bedford Park, South Australia), or at the Institute for Medical and Veterinary Sciences (IMVS, Adelaide, South Australia).

5.2.6 Isolation of *Hieracium* cDNAs by degenerate PCR

5.2.6.1 *FERTILISATION INDEPENDENT ENDOSPERM* (*FIE*)

The *Arabidopsis FIE* nucleotide sequence (AF129516) was compared to the NCBI EST database to identify similar sequences. ESTs were identified from cotton (AI730405), tomato (AI484570) and rice (C26788) that aligned with *Arabidopsis FIE* over WD repeats 2 and 3. Degenerate nested primers were designed to this region, and a 200 bp fragment of *Hieracium FIE* was isolated from anthesis ovary cDNA using FIS3F433 and FIS3R656 primers with a subsequent nesting step using FIS3F459 and FIS3R636 primers (see Appendix 3). 3'RACE, 5'RACE and full-length clones were obtained using *Hieracium FIE* (*HFIE*) gene specific primers and

the B26 and B25 primers, a 5'RACE kit (Invitrogen) and a One-step Omniscript RT-PCR kit (Qiagen) respectively.

5.2.6.2 *METHYLTRANSFERASE I* and *II* (*METI/METII*)

The DNA sequence for *Arabidopsis METI* was compared to the NCBI non-redundant DNA database to identify similar sequences. Full-length *METI*-like DNA sequences from tomato (AJ002140), carrot (AF007807), maize (AF229183) and pea (AF034419) were aligned with the *Arabidopsis METI* (AB016872) and *METII* (AF138283) sequences over the methyltransferase domain. Degenerate nested primers were designed and a 340 bp fragment of a *Hieracium MET* (*HMET*) gene was isolated from the early D2 ovule-enriched cDNA library using the MF3204 and MR3848 primers with a subsequent nesting step using MF3280 and MR3754 primers and a final nesting with MF3407 and MR3754 primers (see Appendix 3).

5.2.6.3 *HISTONE DEACETYLASE* (*HDAC*)

Three *Arabidopsis* putative RPD3-type *HDAC* amino acid sequences (CAB72470, CAB88531, CAB72468) were aligned with similar peptides from maize (AAD10139), mouse (CAA66870), Xenopus (AAC60346) and *Drosophila* (AAC23917). Most significant homology was observed over the histone deacetylase domain. Degenerate nested primers were designed to span part of this region, and a 360 bp *Hieracium HDAC* (*HHDAC*) fragment was isolated from D3 anthesis ovary cDNA using the HDF287 and HDR418 primers with a nested round using HDF297 and HDR416 primers (see Appendix 3).

5.2.6.4 *FERTILISATION INDEPENDENT SEED 2* (*FIS2*)-like sequences

The *Arabidopsis FIS2* mRNA (AF096096) and protein (AAD09105) sequences were compared to the NCBI protein and DNA databases to identify similar sequences. Few sequences were identified that showed homology to *FIS2*, and the closest matches were unknown sequences also from *Arabidopsis*. These sequences, one from chromosome 4 (CAB80952; *VERNALISATION 2* (*VRN2*); Gendall et al., 2001), and another from chromosome 5 (BAA97387; *EMBRYONIC FLOWER 2* (*EMF2*); Yoshida et al., 2001), were aligned with *FIS2* and showed high sequence homology over what is termed the ACE domain or VEFS Box (Chaudhury et al., 2001; Birve et al., 2001). Degenerate nested forward primers were designed to this region and used in PCR with the B26 and B25 reverse primers. A 430 bp cDNA sharing homology with *FIS2*-like genes was isolated from D3 stage 5-7 ovary cDNA after PCR with fis2fwd1630 and B26 primers, a secondary nesting step using fis2fwd1828 and B25 primers and a final PCR using fis2fwd1837 and B25 primers. Gene specific primers designed from this fragment were used with vector primers to isolate a similar cDNA from the early D2 ovule-enriched cDNA library, and in 5'RACE to isolate an almost full-length cDNA fragment from sexual P4 stage 5-8 ovary cDNA.

5.2.7 Temporal expression analysis and genomic characterisation

Total RNA was extracted from tissue samples as per Section 5.2.1. Northern blot analysis was performed as described in Tucker et al., (2001), and RT-PCR was performed using a two-step approach. Single-stranded cDNA was generated from 500 ng of total RNA template, an oligo(dT) primer and the thermoscript RT-PCR

system (Invitrogen) as per manufacturers instructions. PCR reactions were performed in a 20μl total volume containing 1 μL (~25ng) of cDNA, 0.5 μM of each gene specific primer, 1 unit of RedTaq polymerase (Sigma), 2μl of 10× PCR Buffer (containing $MgCl_2$) and 50 μM of each dNTP. Primers used for the RT-PCR reaction were BtubRTfwd and BtubRTrev, RTHFIEF3 and RTHFIER2, RTFIS2likeF1 and RTFIS2likeR1, HDSFWD and HDSREV. The β-*tubulin* (β-*tub*), *FIE* and *FIS2*-like primers span introns and the *HDAC* primers spanned an intron/exon boundary to exclude the possibility of genomic DNA contamination. Samples were equilibrated using the β-*tub* primers as a control, electrophoresed, transferred to nylon membranes and probed with corresponding radioactively labelled cDNA clones to verify PCR-product identity.

Genomic DNA was isolated from the leaves of *Hieracium* plants using the CTAB method (Doyle, 1991), and genomic characterisation of clones was performed as described in Tucker et al., (2001).

5.2.8 Phylogenetic and comparative analysis of clones

Sequences were aligned using the Pileup program from the EGCG package (Rice, 1994) or the CLUSTALW program at the Biology Workbench (http://workbench.sdsc.edu/). Alignments were submitted to phylogenetic analysis using the distances, growtree and treeview programs at GCG (Rice, 1994; Page, 1996) or the GROWTREE program at the Biology Workbench.

5.3 Results

5.3.1 Low abundance clones from an early *Hieracium* ovule cDNA library

In total, 4500 plaques were screened at low density, and 185 (4.1%) putative cold plaques were identified that did not hybridise to ovule-enriched or leaf cDNA probe after 2-7 days of membrane exposure to autoradiography film. Six of these clones were subsequently found to contain no insert after PCR with vector primers and also digestion with *EcoRI*. Seven could not be rescued by the ExAssist protocol and eight clones were contaminated with multiple phage inserts (N. A. Paech and A. Koltunow, unpublished). Of the remaining 164 clones, reverse northern analysis showed that 16 hybridised strongly and 27 hybridised weakly to leaf cDNA after 2 days of exposure, and a further 52 hybridised weakly to leaf cDNA after 7 days of membrane exposure to autoradiography film (N. A. Paech and A. Koltunow, unpublished). The remaining 69 clones did not hybridise to leaf cDNA after 7 days of exposure to autoradiography film and were classified as ***H****ieracium* **O**vary **S**equence (HOS) genes; true cold plaques from the ovule-enriched cDNA library. This number corresponded to 1.5% of the total plaques screened, and contrasted with the 50% of recombinant plaques that gave no signal when Hodge et al., (1992) cold-plaque screened an anther cDNA library. This significant reduction in cold plaques was probably due to the incorporation of the secondary differential leaf probe in the screen that eliminated cDNAs weakly expressed in ovules and up-regulated in leaves.

5.3.2 Putative identity of HOS clones

The 69 cold plaque clones were end sequenced using the SK and KS primers from pBluescript, and compared to the NCBI protein database using the BLASTX program. Eleven of the clones failed to produce a sequence. The closest matching database sequences for the remaining 58 clones at the last search date of 20th November 2002 are indicated in Table 5.1. Notably, 21% of the HOS sequences matched unknown or hypothetical proteins, mostly from *Arabidopsis*, and 19% of the sequences were *Hieracium* specific. The remaining 60% of clones could be divided into groups based on putative functions, including nucleic acid-binding proteins, protein-interacting proteins, pathogenesis and stress-related proteins, cell wall and sugar metabolism proteins, fatty acid related proteins, receptor kinases and transposon proteins (Table 5.1).

Table 5.1 (page 114) Putative sequence identity of cold plaque clones isolated from apomictic D2 *Hieracium* as determined by BLASTX searches. The expression column highlights sequences that are expressed or up-regulated (+) in either ovary tissue or **O**ther **F**loral **T**issues (OFTs) (N. A. Paech and A. Koltunow, unpublished).

Clone ID	Closest Blast X match (20/11/02)	Expression	Name
cDNAs similar to unknown proteins expressed in other organisms			
2.11	hypothetical protein (*Arabidopsis*)		
2.16	hypothetical protein (*Arabidopsis*)		
2.20	unknown protein (*Arabidopsis*)		
4.06	hypothetical protein (*Arabidopsis*)		
4.07	putative protein (*Arabidopsis*)		
5.13	hypothetical protein (*Arabidopsis*)		
7.02	hypothetical protein (*Arabidopsis*)		
9.23	unknown protein (*Arabidopsis*)		
9.41	unknown protein (*Arabidopsis*)		
24.12	unknown (*Saccharomyces*)		
25.04	unknown protein (*Arabidopsis*)		
26.04	unknown (proline-rich protein - *Arabidopsis*)		
Hieracium-specific cDNAs			
4.05	no match		
5.09	no match (Glycine-rich protein)		
5.15	no match		
9.06	no match		
9.18	no match		
9.26	no match		
9.38	no match		
9.47	no match		
26.02	no match		
26.06	no match		
27.09	no match		
Proline-rich Proteins			
4.19	small proline-rich protein		
24.03	proline-rich protein		
Protein-interacting proteins			
2.21	Su(VAR)3-9-related protein (SET domain)		
4.20	ankyrin-like protein	+ ovary	***HOS-ANK***
27.28	RING zinc finger protein	+ ovary	***HOS-ZF***
Nuclei acid-interacting proteins			
9.03	RNA-binding protein		
9.21	RRM (RNA recognition motif)-binding protein	+ OFT	***HOS-RBP***
9.34	Putative transcriptional regulatory protein		
24.14	DNA-binding protein		
PR and Stress-Related genes			
9.45	BURP domain-containing protein (dehydration responsive protein)		
25.03	S-protein homologue		
27.06	putative senescence-associated protein		

Table 5.1 continued

Clone ID	Closest Blast X match (20/11/02)	Expression	Name
House-keeping genes			
2.13	tubulin-like protein		
5.07	heat shock protein		
5.11	RNA-dependent RNA polymerase		
9.01	heat shock protein		
27.24	subtilisin-like proteinase		
Cell wall protein/Sugar metabolism cDNAs			
9.42	cinnamoyl-CoA reductase		
9.29	glycosyl hydrolase (family 1)		
24.02	polygalacturonase	+ ovary	***HOS-PG***
27.29	putative glucan synthase	ovary	***HOS-GS9***
Fatty acid related cDNAs			
9.27	acyl-CoA reductase	+ OFT	***HOS-ACR***
25.10	acetyl-CoA synthetase		
Cellular function related cDNAs			
4.15	peroxisomal copper-containing amine oxidase		
5.14	guanine nucleotide exchange factor-like protein		
5.16	ubiquitin-specific protease	ovary	***HOS-USP***
9.15	putative ABC transporter		
25.02	iron-regulated transporter		
Transposon related genes			
26.07	putative En/Spm-like transposon protein (Class II)		
27.14	putative retroelement pol polyprotein		
Hormone-related cDNAs			
9.10	cytokinin oxidase	+ OFT	***HOS-CO***
Receptor Kinases			
5.04	CLAVATA1 receptor-like kinase protein (leucine-rich)	+ ovary	***HOS-CLV***
7.01	MAP3K epsilon protein kinase		
9.02	receptor-like kinase protein (RLK)	ovary	***HOS-RLK***
Others			
9.30	endothelial nitric oxide synthase (eNOS)-like interacting protein		

5.3.3 Candidate genes regulating cell-specification and developmental processes in early *Hieracium* ovules

Ten clones were chosen based on sequence homology for further expression analysis in ovule, leaf, root and other floral tissue samples. Northern analysis showed that four clones (*HOS-ANK*, *HOS-ZF*, *HOS-CLV* and *HOS-PG*) were up-regulated in ovules relative to other tissues, three were expressed in ovules at a similar level relative to other tissues (*HOS-GS9*, *HOS-USP* and *HOS-RLK*) and three were up-regulated in other floral tissues relative to roots, leaves and ovaries (*HOS-RBP*, *HOS-ACR* and *HOS-CO*) (N. Paech and A. Koltunow, unpublished; Table 5.1). The seven clones expressed in the ovule included two different CLAVATA1-like receptor kinases, a RING zinc-finger protein, an ankyrin-repeat protein, a polygalacturonase, a putative glucan synthase (GS11) homologue, and a ubiquitin-specific protease. The 58 putative HOS clones identified in this screen provide a tool for the further characterisation of early ovule development in apomictic *Hieracium*. Further descriptions of these genes will be reported elsewhere (N. Paech and A. Koltunow, unpublished). The remainder of this study focussed on the isolation of regulatory genes and putative members of a plant PcG complex expressed during endosperm initiation and early development.

5.3.4 Isolation of early seed regulators from *Hieracium*

A degenerate PCR approach was used in an attempt to isolate four genes expressed during seed initiation in sexual and/or apomictic *Hieracium*. Two of these genes,

METI and *HDAC*, encode potential global regulators of gene expression and possibly function during PcG repression (Finnegan and Kovac, 2000; Finnegan, 2001; see Section 1.2.8.1). The *FIE* and *FIS2* genes were also targeted for isolation, as these encode putative members of a plant *Polycomb* group (PcG) complex that regulates the initiation of endosperm development in *Arabidopsis* (Luo et al., 2000; Ohad et al., 1999). cDNA clones showing significant homology to all four genes were isolated (Table 5.2) and are described in greater detail below.

5.3.4.1 *Hieracium HDAC* and *MET*-like cDNAs

Partial cDNA sequences were cloned for *MET* and *HDAC* homologues from apomictic *Hieracium* D3. The degenerate *MET* primers failed to detect a *MET*-like gene in stage 5-8 ovary cDNA, but a clone that showed significant homology to the methyltransferase domain of type 1 plant methyltransferases was isolated from the D2 ovule-enriched cDNA library (Finnegan and Kovac, 2000; Figure 5.1A). The putative amino acid sequence of *Hieracium MET* (*HMET*) showed 96% similarity to the *Arabidopsis METII* sequence (At4g14140; O23273), 90% similarity to *Arabidopsis METI* sequence (At5g49160; DNM1_ARATH), 90% similarity to *O. sativa* MET707 (AAL77415), and 88% similarity to the *Z. mays* MET101 sequence (AAM28226). The putative amino acid sequence of *HMET* was aligned with *MET* sequences from plants and animals over a portion of the methyltransferase domain (Figure 5.1B), and this highlighted the conservation between the sequences. Similarly, at the DNA level, the *HMET* cDNA fragment was most similar to the *Arabidopsis METII* gene (81% identical on the DNA level). Phylogenetic analyses clustered the *HMET* putative amino acid sequence with the plant type-1

Figure 5.1 Comparison of *HMET* to other known methyltransferases. **A** Schematic alignment of putative amino acid sequences for *HMET* and *Arabidopsis METII*. The functional domains are indicated. **B** Comparison of *MET*-like amino acid sequences over a portion of the isolated *HMET* methyltransferase domain. Black shading highlights amino acid conservation, and grey shading highlights similarity. See **C** for accession numbers. **C** An unrooted phylogenetic tree showing relationships between the putative amino acid sequences of type-1 methyltransferases and the *HMET* cDNA fragment. The species name and Genbank identity is followed by the length of the putative amino acid (AA) sequence and the protein accession number.

A

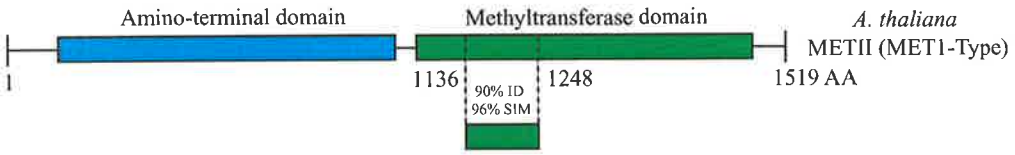

H. piloselloides MET cDNA fragment
113 AA (341 bp)

B Amino acid sequence alignment of *METI/II* like genes over a fragment of the methyltransferase domain

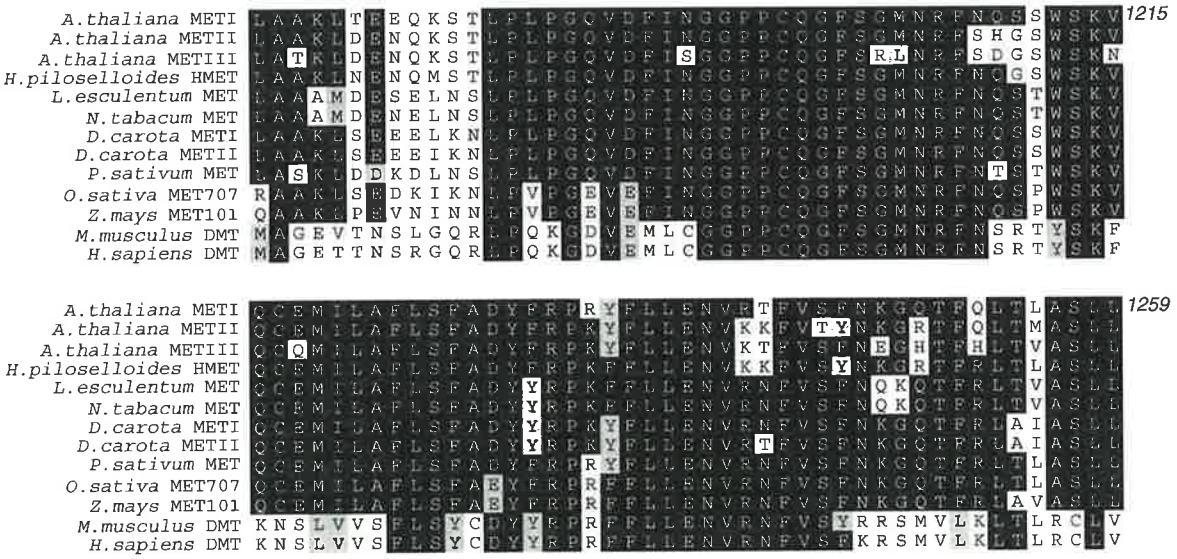

C

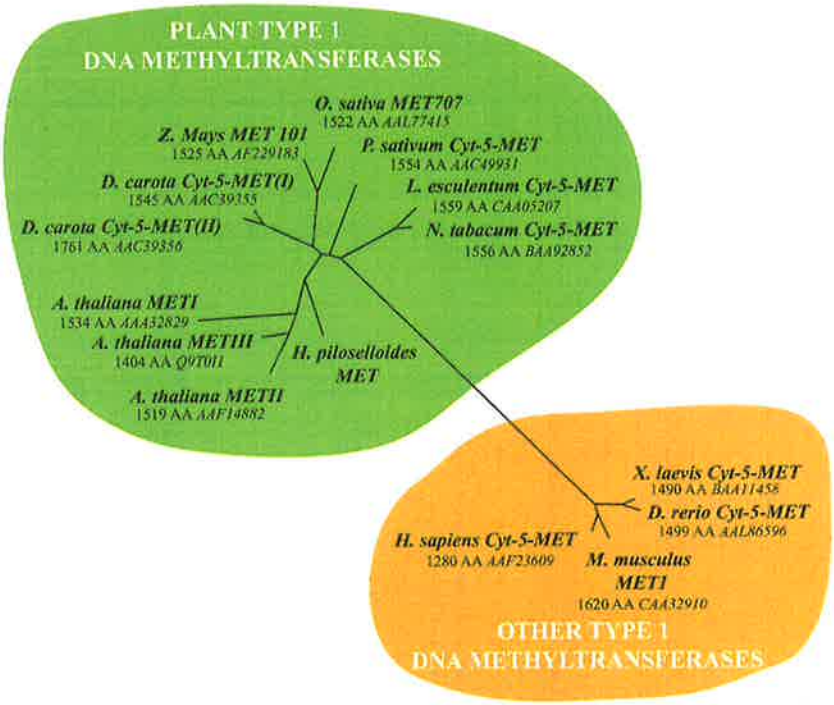

methyltransferases (Figure 5.1C). RT-PCR expression analysis failed to detect *HMET* expression in various ovule and seed RNA samples, but preliminary genomic analysis suggested that the *HMET* gene was likely to be a member of a family of methyltransferase-like sequences in *Hieracium* (data not shown). It is possible that the *HMET* cDNA was derived from a contaminating anther mRNA transcript present in the early ovule enriched library.

The *Hieracium* histone deacetylase (*HHDAC*) cDNA was isolated from D3 stage 5-7 ovary RNA and showed significant homology to plant and animal HDACs across a portion of the histone deacetylase domain (Figure 5.2A). *HHDAC* shared greatest homology with a putative *Arabidopsis HDAC*, *HDA9,* (90% on the amino acid level) and Maize *HDAC102* (88% on the amino acid level), and clustered with these sequences in a phylogenetic comparison to other *RPD3*-type *HDAC*s (Figure 5.2B). Three main classes of *HDAC*s have been identified in plants. These include the class 1 *RPD3*-type *HDAC*s named because of similarity to the yeast transcriptional repressor *RPD3* protein, the class 2 *HDA1*-type *HDAC*s named because of similarity to the yeast transcriptional co-repressor *HDA1* protein, and the plant-specific class 3 *HD2*-type *HDAC*s that are localised to the nucleolar organiser region (Pandey et al., 2002). Phylogenetic analysis of the amino acid sequences of plant HDACs from the three classes, obtained from the Plant Chromatin Database (http://www.chromdb.org/), and the *S. cerevisiae* RPD3 protein showed that the D3 *HHDAC* was likely to encode a class 1-type protein (Figure 5.2C). DNA gel blot analysis with labelled *HHDAC* probe detected four to six similar sequences in D3 and P4 genomic DNA samples (Figure 5.2D). This suggested that multiple *HHDAC*-like genes are likely to be present in the D3 and P4 genomes. RT-PCR expression analysis during ovary development in sexual P4 and apomictic D3 showed that the *HHDAC* mRNA was present at all stages, and was slightly up-

Table 5.2 Genes targeted for isolation by degenerate PCR, and the corresponding cDNA clones identified from *Hieracium*

Gene ID	Clone	Tissue of Origin	cDNA Length	Closest BLASTX protein matches
MET1 **(Methyltransferase 1)**	*H. piloselloides* D2 *HMET*	Stage 2-4 ovule-enriched cDNA library	341 bp (partial)	· METII (cytosine-5-methyltransferase [*A. thaliana* Ac AAF14882], METII-type cytosine DNA-methyltransferase-like protein [*A. thaliana* Ac CAB78023], DNA (cytosine-5-methyltransferase [*A. thaliana* Ac BAB10334]
HDAC **(RPD3-type Histone Deacetylase)**	*H. piloselloides* D3 *HHDAC*	Stage 5-8 (anthesis) ovaries	363 bp (partial)	· putative HDA9 [*A. thaliana* Ac NP_190054], histone deacetylase 102 [*Z. mays* Ac AAL33655], putative histone deacetylase [*P. polycephalum* Ac AAL83942]
FIS2 **(Fertilisation Independent Seed 2)**	*H. pilosella* P4 *EMF2*	Stage 5-7 (anthesis) ovaries	1980 bp (missing 3'UTR)	· embryonic flower 2 (EMF2) protein [*A. thaliana* Ac BAB58956], vernalization 2 (VRN2) protein [*A. thaliana* Ac AAL32135], FIS2 protein [*A. thaliana* Ac AAD09104]
	H. piloselloides D3 *ACE*	Stage 5-8 (anthesis) ovaries	414 bp (partial)	
	H. piloselloides D2 *ACE*	Stage 2-4 ovule-enriched cDNA library	252 bp (partial)	
FIE **(Fertilisation Independent Endosperm)**	*H. piloselloides* D3 *HFIE*	Stage 5-8 (anthesis) ovaries	1414 bp (full)	· FIE protein [*A. thaliana* Ac AAD23584], FIE protein 1 [*Z. mays* Ac AAL35974], FIE protein 2 [*Z. mays* Ac AAL35973]
	H. pilosella P4 *HFIE*	Stage 5-7 (anthesis) ovaries	1421 bp (full)	

regulated in ovaries from stage 4 florets during female meiosis and megaspore selection (Figure 5.2E). *HHDAC* expression was also up-regulated in stage 11/12 seeds containing heart/torpedo stage embryos from apomictic D3 compared to

Figure 5.2 Characterisation of *Hieracium HISTONE DEACETYLASE (HHDAC).* **A** Schematic alignment of the putative amino acid sequences of *HHDAC* and the *Arabidopsis RPD3A* and *HDA9* histone deacetylases. The functional deacetylase domain and the percentage identity and similarity to *HHDAC* are indicated. **B** An un-rooted phylogenetic tree showing histone deacetylase sequences in comparison to the putative amino acid sequence of the *HHDAC* fragment. The species name and Genbank identity is followed by the length of the putative amino acid (AA) sequence and the protein accession number. The gene names indicated in red refer to the Chromatin Database (www.chromdb.org) nomenclature. **C** Rooted phylogenetic tree showing *Arabidopsis*, rice and maize histone deacetylase sequences from three different classes (I, II and III) obtained from the Chromatin Database, in comparison to the *HHDAC* sequence from *Hieracium* and the *RPD3* sequence from *S. cerevisiae*. The gene names indicated refer to the Chromatin Database (www.chromdb.org) nomenclature. **D** Genomic analysis of *HDAC*-like sequences in apomictic D3 and sexual P4 *Hieracium*. DNA samples were digested with *EcoRI* (*E1*), *EcoRV* (*EV*) or *HindIII* (*H*) that cut external to the *HHDAC* fragment. The size of the DNA fragments in kilobases is indicated at left. **E** RT-PCR expression analysis of *HHDAC* during ovary development in sexual P4 and apomictic D3 *Hieracium*. Numbers indicate stages of floral development (see Appendix 1).

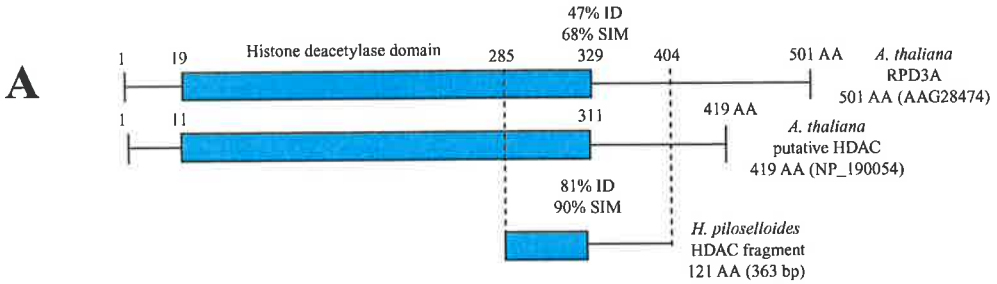
A
47% ID
68% SIM
1
19
Histone deacetylase domain
285
329
404
501 AA
A. thaliana
RPD3A
501 AA (AAG28474)
1
11
311
419 AA
A. thaliana
putative HDAC
419 AA (NP_190054)
81% ID
90% SIM
H. piloselloides
HDAC fragment
121 AA (363 bp)

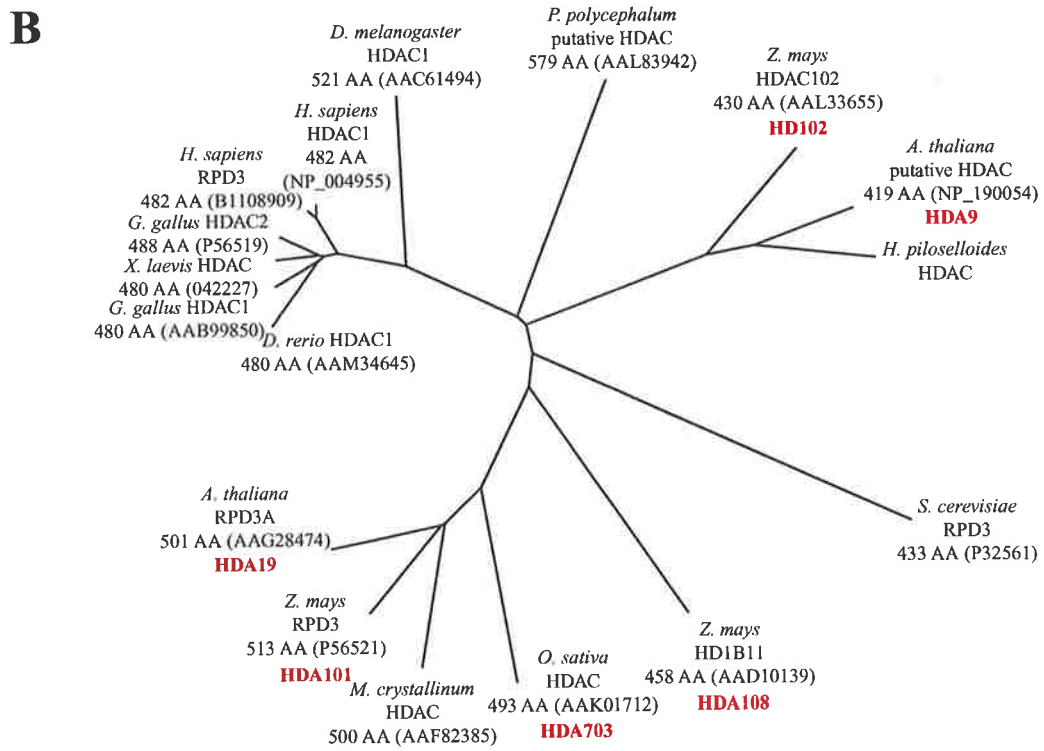
B
D. melanogaster
HDAC1
521 AA (AAC61494)
P. polycephalum
putative HDAC
579 AA (AAL83942)
Z. mays
HDAC102
430 AA (AAL33655)
HD102
H. sapiens
HDAC1
482 AA
(NP_004955)
H. sapiens
RPD3
482 AA (B1108909)
G. gallus HDAC2
488 AA (P56519)
X. laevis HDAC
480 AA (042227)
G. gallus HDAC1
480 AA (AAB99850)
A. thaliana
putative HDAC
419 AA (NP_190054)
HDA9
H. piloselloides
HDAC
D. rerio HDAC1
480 AA (AAM34645)
A. thaliana
RPD3A
501 AA (AAG28474)
HDA19
S. cerevisiae
RPD3
433 AA (P32561)
Z. mays
RPD3
513 AA (P56521)
HDA101
M. crystallinum
HDAC
500 AA (AAF82385)
O. sativa
HDAC
493 AA (AAK01712)
HDA703
Z. mays
HD1B11
458 AA (AAD10139)
HDA108

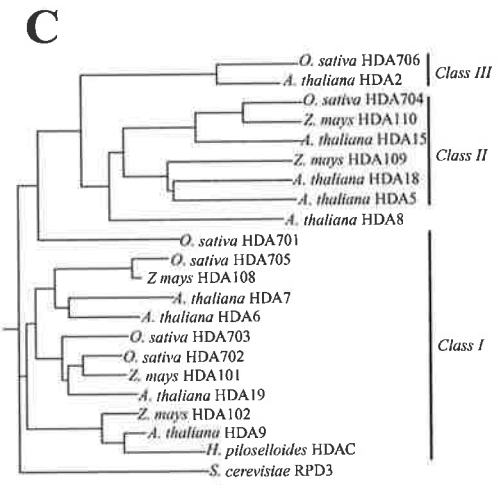
C
O. sativa HDA706
A. thaliana HDA2
Class III
O. sativa HDA704
Z. mays HDA110
A. thaliana HDA15
Z. mays HDA109
A. thaliana HDA18
A. thaliana HDA5
Class II
A. thaliana HDA8
O. sativa HDA701
O. sativa HDA705
Z mays HDA108
A. thaliana HDA7
A. thaliana HDA6
O. sativa HDA703
O. sativa HDA702
Z. mays HDA101
A. thaliana HDA19
Z. mays HDA102
A. thaliana HDA9
H. piloselloides HDAC
S. cerevisiae RPD3
Class I

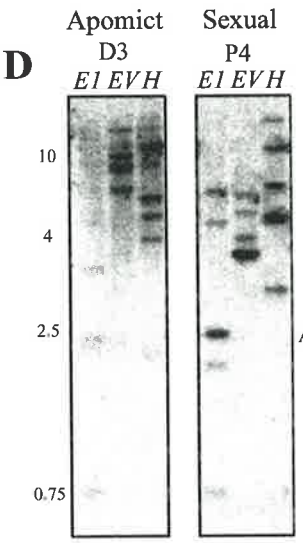
D
Apomict
D3
E1 EV H
Sexual
P4
E1 EV H
10
4
2.5
0.75

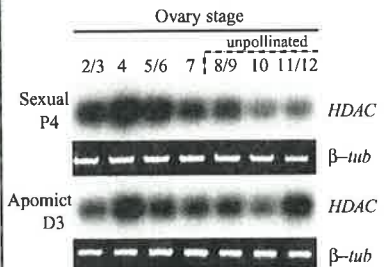
E
Ovary stage
unpollinated
2/3 4 5/6 7 8/9 10 11/12
Sexual
P4
HDAC
β–tub
Apomict
D3
HDAC
β–tub

unfertilised collapsing seeds from sexual P4. This suggested that the *HHDAC* gene might play some role in late embryogenesis.

5.3.4.2 *Hieracium FIS2*-like cDNAs

The *FIS2*-like genes of *Arabidopsis* (*FIS2*, *VRN2* and *EMF2*) display high conservation over two domains; the C2H2 Zinc Finger domain and the VEFS Box/ACE domain (Figure 5.3A; Chaudhury et al., 2001; Birve et al., 2001). Greatest homology is evident in the ACE domain, and degenerate primers were designed to this region (Figure 5.3A). cDNA clones were isolated from three *Hieracium* species (sexual P4 and apomictic D3 and D2) that showed significant homology to the *FIS2*-like genes of *Arabidopsis*. The partial 414 bp D3 *ACE* cDNA clone was isolated from stage 5-7 D3 ovary RNA by degenerate PCR, and comprised 213 bp of coding region, 190 bp 3'UTR and a poly(A)+ tail. The partial 252 bp D2 *ACE* cDNA fragment was cloned from the early D2 ovule-enriched cDNA library and comprised 252 bp of coding region. The 1980 bp P4 *EMF2* clone was originally isolated as a small cDNA fragment from stage 5-8 P4 ovary RNA, and was extended by 5'RACE to incorporate a 100 bp 5'UTR and 1880 bp of coding region. The putative amino acid sequences of all three clones were very similar and overlapped with the ACE/VEFS domain from the *Arabidopsis FIS2*-like genes (Figure 5.3A).

In BLAST searches of the Genbank and NCBI databases, the *Hieracium FIS2*-like sequences isolated from the three different species showed greatest homology to *EMF2* from *Arabidopsis* and were almost identical to each other in their 135 bp overlap (Table 5.2; Figure 5.3B). The putative amino acid sequence of

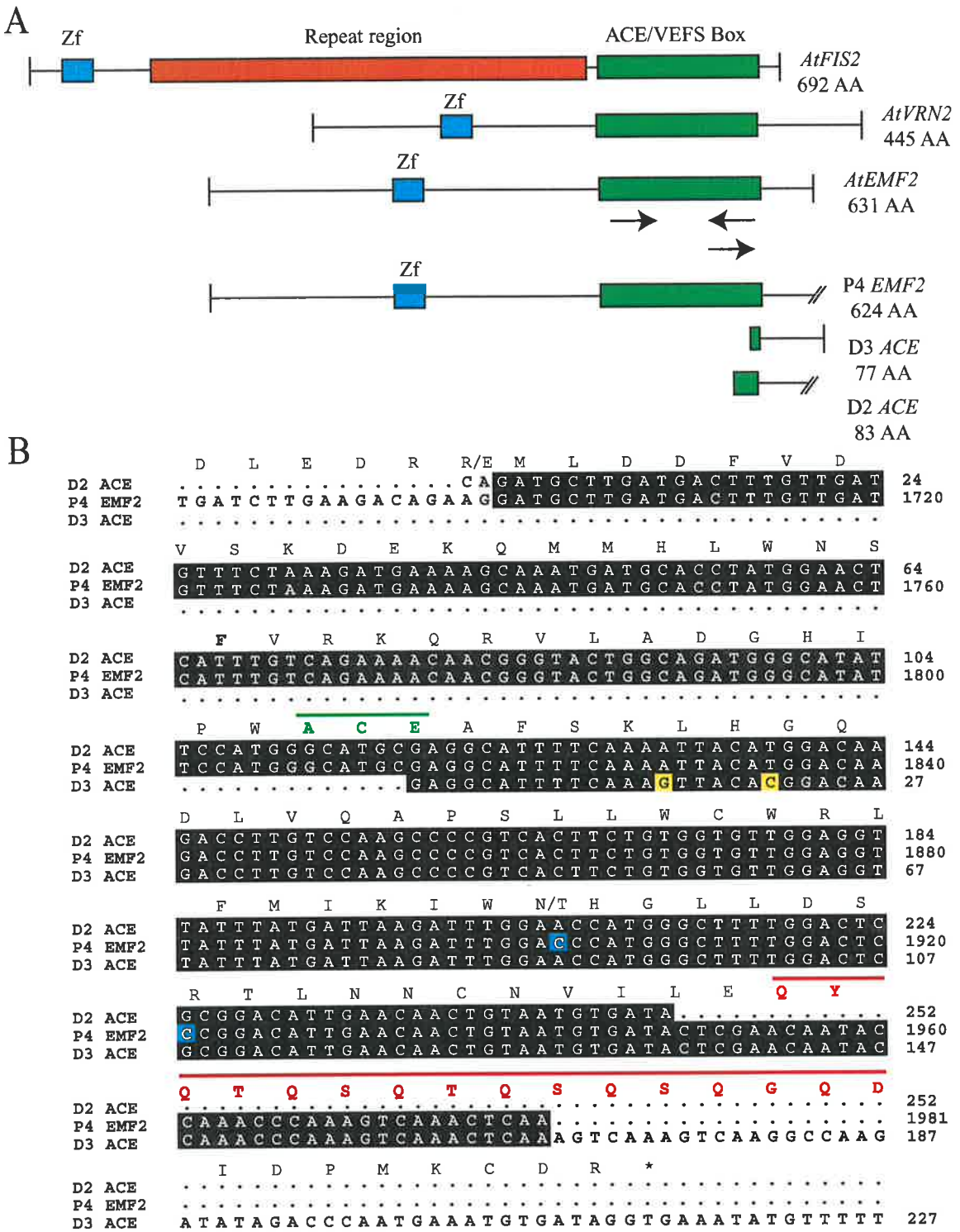

Figure 5.3 Comparison of *Arabidopsis* and *Hieracium* *FIS2*-like sequences. **A** Schematic alignment of putative amino acid sequences for *Arabidopsis* (*At*) *FIS2*, *AtVRN2* and *AtEMF2* with P4 *EMF2*, D3 *ACE* and D2 *ACE* from *Hieracium*. The arrows indicate the position of degenerate primers used to amplify the *Hieracium* sequences. The positions of the putative functional domains are indicated. **B** Alignment and consensus amino acid sequence of the three *Hieracium* *FIS2*-like cDNA clones over the ACE domain. The ACE motif is indicated in green. Base pair differences between D3 *ACE* and D2 *ACE* are indicated in yellow, and between P4 *EMF2* and the other sequences in blue. The C-terminal extension of the *Hieracium* amino acid consensus sequence is indicated in red.

P4 *EMF2* contained a putative C2H2 zinc-finger domain and ACE domain/VEFS box in similar positions to those in *AtEMF2* (Figure 5.3A and 5.3B), and showed 66% similarity over the length of the *AtEMF2* sequence. The sequence conservation between P4 *EMF2* and *AtEMF2* was highest over these putative regulatory regions (Figure 5.4A). One notable difference between the *Hieracium* and *Arabidopsis FIS2*-like sequences was a short extension of the amino acid sequence of P4 *EMF2* and D3 *ACE* at the C-terminal end of the putative proteins. The glutamine rich sequence N'-ILEQYQTQSQTQSQSQGQD-C' detected in the *Hieracium* sequences was absent from *AtEMF2* but was detected in several transcriptional repressors and activators from *Mus musculus* and *Drosophila melanogaster* including ZAC1 (XM_192663), ZESTE (z; NM_080312) and Repressor/activator protein 1 (Rbf1; D85862). Based on homology to these DNA-binding transcription factors and the putative function of glutamine-rich repeats, it is possible that this region is required for binding the P4 *EMF2* and D3 *ACE* proteins to DNA

The D2 *ACE* sequence was compared to the plant EST database to identify similar genes. Over 200 matches were identified across a wide range of species, but many corresponded to duplications of the same cDNA sequence. Independent ESTs from nine different species were translated and aligned with the P4 *EMF2*, D2 *ACE* and *Arabidopsis FIS2*-like putative amino acid sequences using CLUSTALW. A phylogenetic tree was generated from this alignment based on sequence relationships (Figure 5.4B). The tree showed no clear clusters of sequences that might have related to groups of *FIS2* and *VRN2*-like genes, but four *EMF2*-like sequences (two from *Hieracium*, one from tomato and one from potato) clustered with Arabidopsis *EMF2*. Most of the sequences clustered more closely with ESTs from the same or similar species.

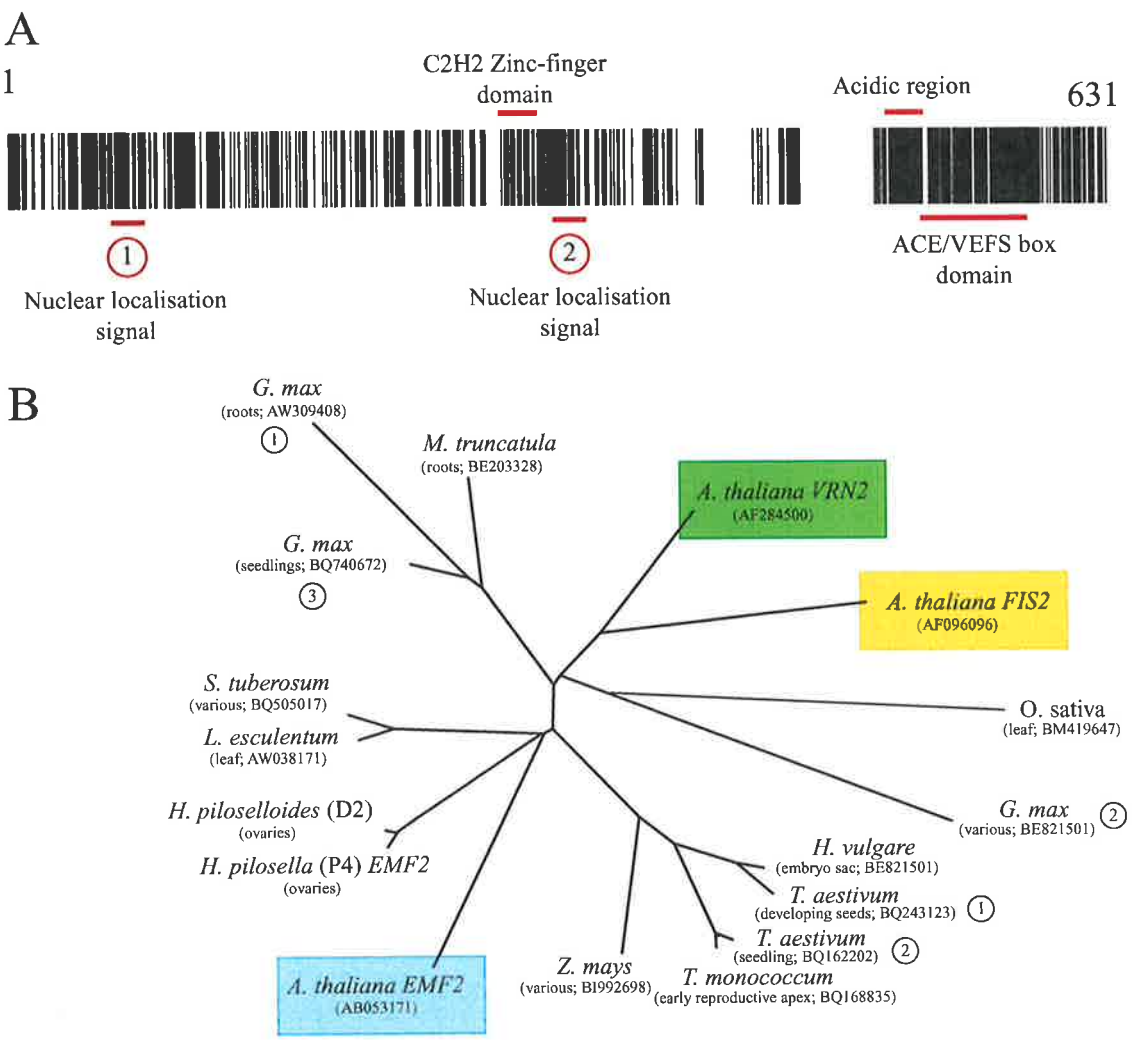

Figure 5.4 Comparison of EST sequences with the ACE domain of *FIS2*-like genes. **A** Conservation of amino acid residues over the length of the *Arabidopsis* EMF2 and P4 EMF2 sequences. Black blocks indicate complete conservation and the putative functional regions are indicated. **B** An un-rooted phylogenetic tree comparing the putative amino acid sequences of ESTs that encode ACE motifs to *Arabidopsis* and *Hieracium FIS2*-like sequences. The species name is followed by the EST tissue origin and the accession number. The numbers in circles indicate species that show multiple differing ESTs. **C** Alignment of the putative amino acid sequences shown in **B**. Black shading indicates identical residues, dark grey shading indicates highly conserved residues and light grey shading highlights similar residues.

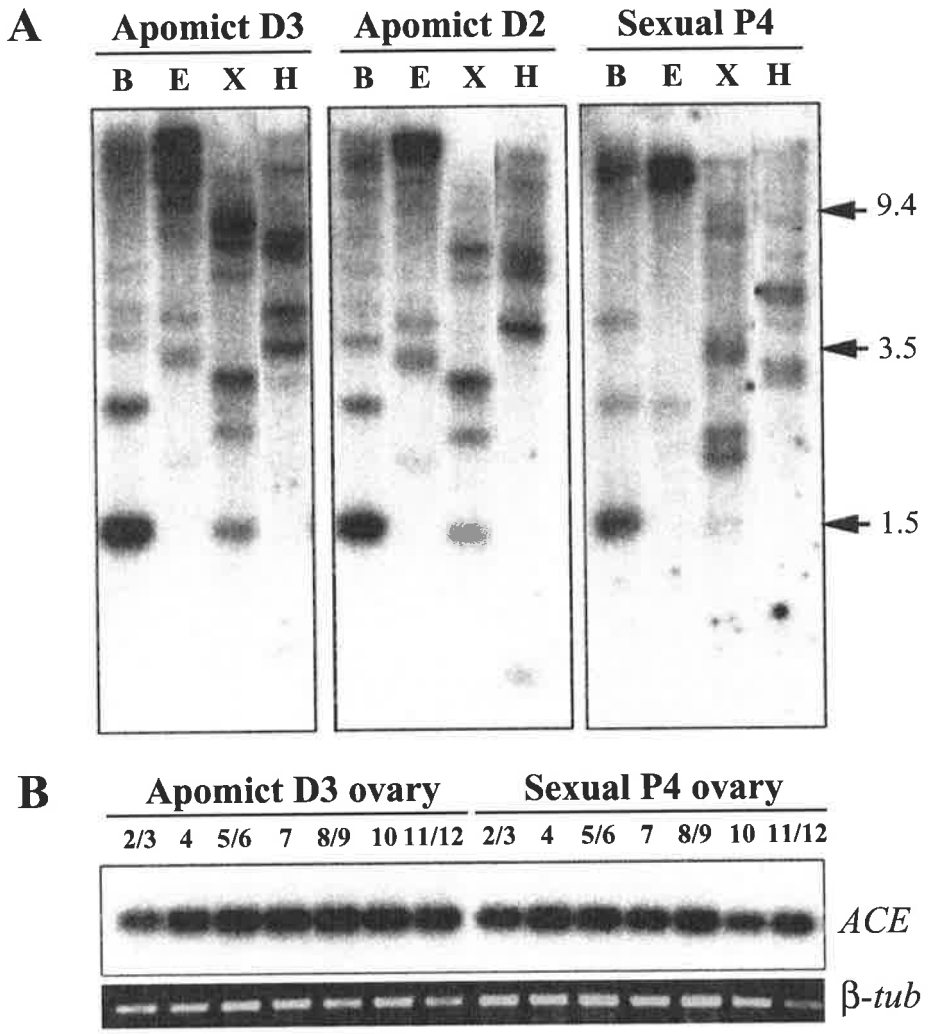

Figure 5.5 Characterisation of *ACE*-like sequences in *Hieracium*. **A** Genomic analysis of *ACE*-like sequences in sexual P4 and apomictic D3 and D2 *Hieracium*. DNA samples were digested with *BglII* (B), *EcoRV* (E), *XbaI* (X) or *HindIII* (H) and fragments were separated by electrophoresis, transferred to membranes and then hybridised to radioactively labelled D2 *ACE* probe. The size of the DNA fragments in kilobases is indicated at right. **B** RT-PCR expression analysis of *ACE*-like sequences during ovary development in sexual P4 and apomictic D3 *Hieracium*. The numbers refer to stages of floral development (see Appendix 1).

The same D2 *ACE* sequence used in database searches and phylogenetic analysis was radioactively labelled and used to probe genomic blots of *Hieracium* D3, D2 and P4 DNA. Multiple DNA fragments hybridised to the labelled D2 *ACE* clone, suggesting that four to seven similar genes are present in the genome of each plant (Figure 5.5A). RT-PCR analysis using *Hieracium* ACE domain specific primers showed that the *FIS2*-like genes were expressed at a similar level throughout ovary development in both apomictic D3 and sexual P4 plants (Figure 5.5B).

In *Arabidopsis*, the only clear difference between the *EMF2*, *VRN2* and *FIS2* putative amino acid sequences is the position of the Zinc finger and ACE domains in relation to the C and N terminal ends of the putative proteins (Figure 5.3A), and a *FIS2*-specific repeat region that showed no homology to any database EST or other sequence. It is likely, based on sequence similarity and the position of the putative activity domains, that the three *Hieracium* cDNAs isolated in this screen corresponded to *EMF2*-like genes, and not to *FIS2*.

5.3.4.3 Isolation of a *FIE* homologue from sexual and apomictic *Hieracium*

The *FIE* gene from *Arabidopsis* (*AtFIE)* encodes a protein that contains seven WD-40 repeats and is likely to form a propeller-like structure capable of binding other proteins (Ohad et al., 1999). This WD-repeat structure is highly conserved in a variety of plant and animal species, and is essential for protein function (Smith et al., 1999; Neer et al., 1994). When *AtFIE* function is blocked by mutagenesis, seed development is severely effected. Seeds inheriting a maternal copy of the mutant *fie* allele abort at the heart stage of embryogenesis if fertilised, and display autonomous

nuclear endosperm development if they are not fertilised. Given the similarity of this fertilisation-independent endosperm phenotype to the autonomous endosperm component of apomixis in *Hieracium*, we aimed to isolate *Hieracium* homologues of *AtFIE* and determine their function (see also Chapter's 6 and 7).

A cDNA showing high homology to *AtFIE* was cloned from sexual P4 and apomictic D3 *Hieracium* anthesis ovary RNA. The D3 *HFIE* and P4 *HFIE* cDNAs contained 1113 bp of coding sequence and were highly conserved on the DNA (96% identical) and putative protein (99% identical) levels (Table 5.3). Comparison of the D3 *HFIE* and P4 *HFIE* coding sequences identified 36 single base pair differences, and three amino acid differences at residues 14, 159 and 283 in the putative proteins (Figure 5.6). Only residue 14 contained amino acids with highly differing characteristics, with D3 *HFIE* displaying hydrophilic polar serine[14] and P4 *HFIE* displaying hydrophobic non-polar proline[14], but all three substitutions were outside of the predicted WD-40 domains (Figure 5.6 and 5.7). Comparison of the putative D3 and P4 *HFIE* proteins to the three-dimensional model of the yeast WD-40 transcriptional repressor Tup1 highlighted the similarity of the propeller-like WD repeats at the amino terminus of the proteins (data not shown). No obvious differences were affected by the amino acid changes, and it was uncertain whether the three amino acid substitutions would affect the three dimensional conformation of the *HFIE* proteins.

The D3 and P4 *HFIE* sequences showed high similarity to the *AtFIE* gene, as well as to the *ZmFIE1* and *ZmFIE2* genes recently cloned from maize (Table 5.3), and alignments of the putative amino acid sequences highlighted the level of conservation (Figure 5.7). *AtFIE* and the *HFIE* putative amino acid sequences differed in length by only one amino acid, and showed remarkably high conservation over the whole length of the proteins (84% similar). No large gaps

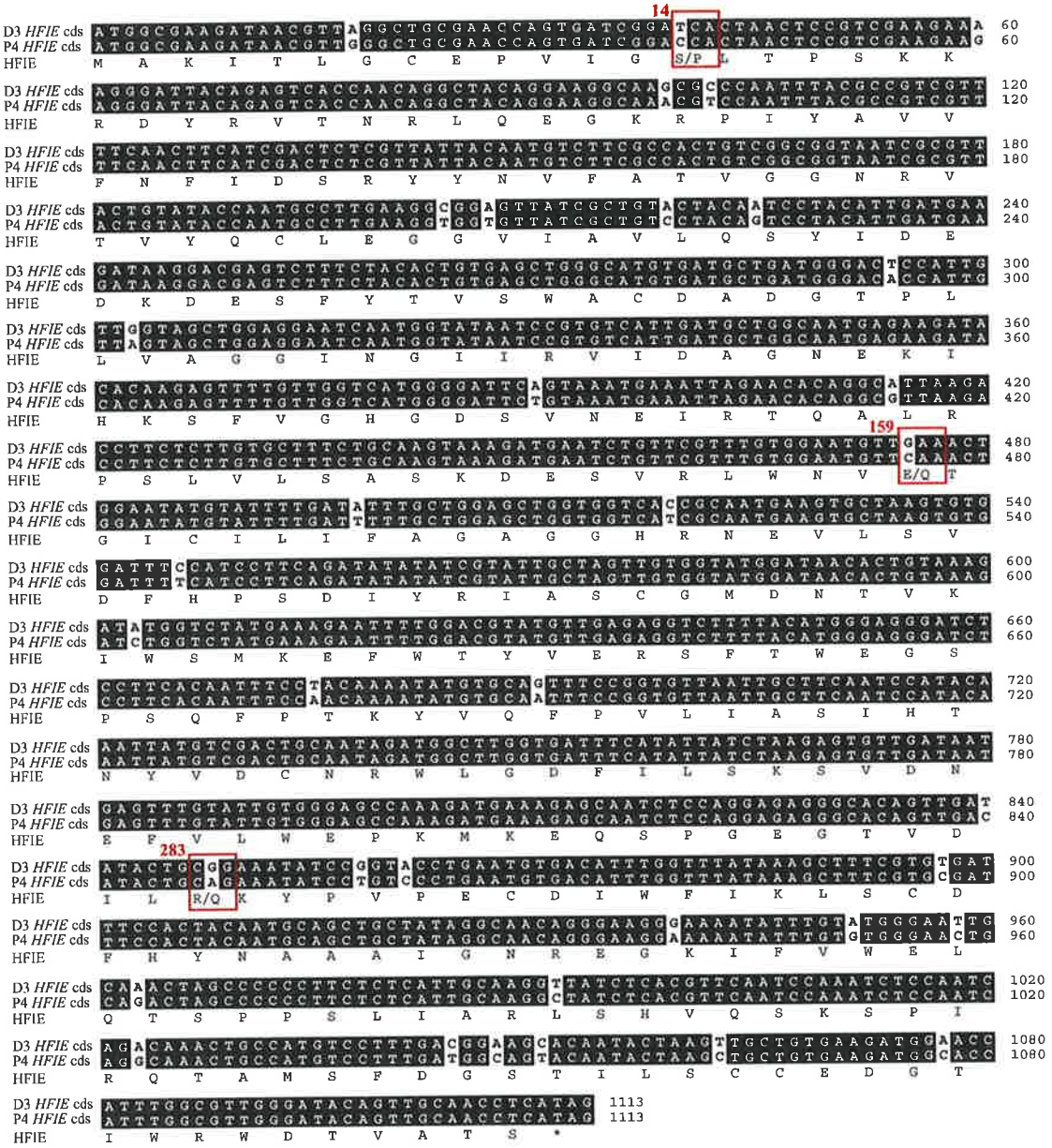

Figure 5.6 Alignment of the coding sequence of D3 and P4 *HFIE*. The putative consensus amino acid sequence is indicated, and residues outlined with a red box differ between the two sequences.

Figure 5.7 Alignment of the putative *Hieracium* D3 and P4 *HFIE* amino acid sequences with maize *ZmFIE1* (AAO26659) and *ZmFIE2* (AAO26660) and *Arabidopsis FIE* (AAD23584). Black shading indicates identical residues and grey shading indicates highly conserved residues. The putative WD-40 domains are indicated with lines and the amino acids differing between D3 and P4 *HFIE* are shaded in green.

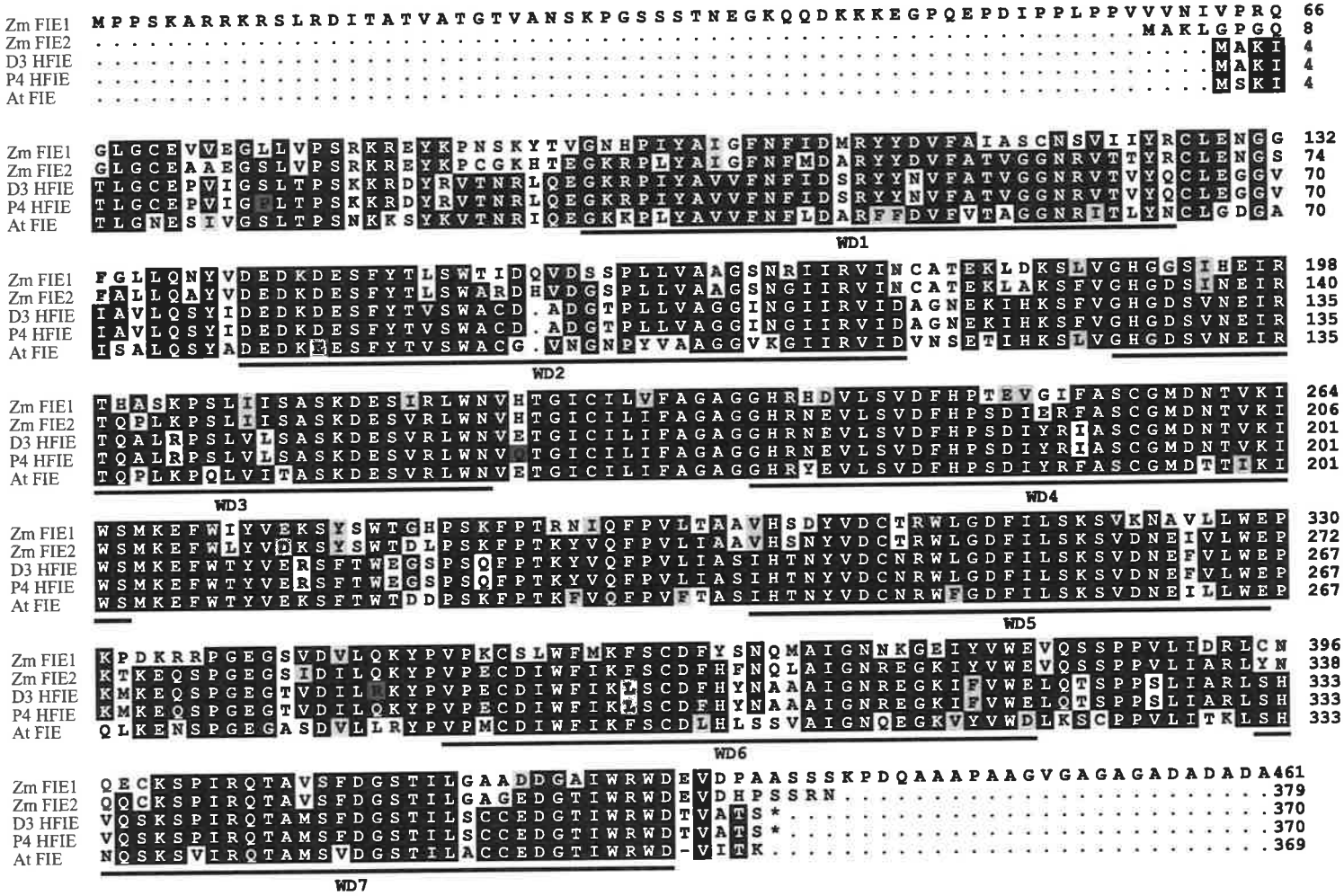
Zm FIE1 MPPSKARRKRSLRDITATVATGTVANSKPGSSSTNEGKQQDKKKEGPQEPDIPPLPPVVVNIVPRQ 66
Zm FIE2 MAKLGPGQ 8
D3 HFIE MAKI 4
P4 HFIE MAKI 4
At FIE MSKI 4
Zm FIE1 GLGCEVVEGLLVPSRKREYKPNSKYTVGNHPIYAIGFNFIDMRYYDVFAIASCNSVIIYRCLENGG 132
Zm FIE2 GLGCEAAEGSLVPSRKREYKPCGKHTEGKRPLYAIGFNFMDARYYDVFATVGGNRVTTYRCLENGS 74
D3 HFIE TLGCEPVIGSLTPSKKRDYRVTNRLQEGKRPIYAVVFNFIDSRYYNVFATVGGNRVTVYQCLEGGV 70
P4 HFIE TLGCEPVIGSLTPSKKRDYRVTNRLQEGKRPIYAVVFNFIDSRYYNVFATVGGNRVTVYQCLEGGV 70
At FIE TLGNESIVGSLTPSNKKSYKVTNRIQEGKKPLYAVVFNFLDARFFDVFVTAGGNRITLYNCLGDGA 70
WD1
Zm FIE1 FGLLQNYVDEDKDESFYTLSWTIDQVDSSPLLVAAGSNRIIRVINCATEKLDKSLVGHGGSIHEIR 198
Zm FIE2 FALLQAYVDEDKDESFYTLSWARDHVDGSPLLVAAGSNGIIRVINCATEKLAKSFVGHGDSINEIR 140
D3 HFIE IAVLQSYIDEDKDESFYTVSWACD.ADGTPLLVAGGINGIIRVIDAGNEKIHKSFVGHGDSVNEIR 135
P4 HFIE IAVLQSYIDEDKDESFYTVSWACD.ADGTPLLVAGGINGIIRVIDAGNEKIHKSFVGHGDSVNEIR 135
At FIE ISALQSYADEDKEESFYTVSWACG.VNGNPYVAAGGVKGIIRVIDVNSETIHKSLVGHGDSVNEIR 135
WD2
Zm FIE1 THASKPSLIISASKDESIRLWNVHTGICILVFAGAGGHRHDVLSVDFHPTEVGIFASCGMDNTVKI 264
Zm FIE2 TQPLKPSLIISASKDESVRLWNVHTGICILIFAGAGGHRNEVLSVDFHPSDIERFASCGMDNTVKI 206
D3 HFIE TQALRPSLVLSASKDESVRLWNVETGICILIFAGAGGHRNEVLSVDFHPSDIYRIASCGMDNTVKI 201
P4 HFIE TQALRPSLVLSASKDESVRLWNVETGICILIFAGAGGHRNEVLSVDFHPSDIYRIASCGMDNTVKI 201
At FIE TQPLKPQLVITASKDESVRLWNVETGICILIFAGAGGHRYEVLSVDFHPSDIYRFASCGMDTTIKI 201
WD3
WD4
Zm FIE1 WSMKEFWIYVEKSYSWTGHPSKFPTRNIQFPVLTAAVHSDYYVDCTRWLGDFILSKSVKNAVLLWEP 330
Zm FIE2 WSMKEFWLYVQKSYSWTDLPSKFPTKYVQFPVLIAAVHSNYVDCTRWLGDFILSKSVDNEIVLWEP 272
D3 HFIE WSMKEFWTYVERSFTWEGSPSQFPTKYVQFPVLIASIHTNYVDCNRWLGDFILSKSVDNEFVLWEP 267
P4 HFIE WSMKEFWTYVERSFTWEGSPSQFPTKYVQFPVLIASIHTNYVDCNRWLGDFILSKSVDNEFVLWEP 267
At FIE WSMKEFWTYVEKSFTWTDDPSKFPTKFVQFPVFTASIHTNYVDCNRWFGDFILSKSVDNEILLWEP 267
WD5
Zm FIE1 KPDKRRPGEGSVDVLQKYPVPKCSLWFMKFSCDFYSNQMAIGNNKGEIYVWEVQSSPPVLIDRLCN 396
Zm FIE2 KTKEQSPGEGSIDILQKYPVPECDIWFIKFSCDFHFNQLAIGNREGKIYVWEVQSSPPVLIARLYN 338
D3 HFIE KMKEQSPGEGTVDILQKYPVPECDIWFIKLSCDFHYNAAAIGNREGKIFVWELQTSPPSLIARLSH 333
P4 HFIE KMKEQSPGEGTVDILQKYPVPECDIWFIKLSCDFHYNAAAIGNREGKIFVWELQTSPPSLIARLSH 333
At FIE QLKENSPGEGASDVLLRYPVPMCDIWFIKFSCDLHLSSVAIGNQEGKVYVWDLKSCPPVLITKLSH 333
WD6
Zm FIE1 QECKSPIRQTAVSFDGSTILGAADDGAIWRWDEVDPAASSSKPDQAAAPAAGVGAGAGADADADA 461
Zm FIE2 QQCKSPIRQTAVSFDGSTILGAGEDGTIWRWDEVDHPSSRN 379
D3 HFIE VQSKSPIRQTAMSFDGSTILSCCEDGTIWRWDTVATS* 370
P4 HFIE VQSKSPIRQTAMSFDGSTILSCCEDGTIWRWDTVATS* 370
At FIE NQSKSVIRQTAMSVDGSTILACCEDGTIWRWD-VITK 369
WD7

were observed in a comparison between the P4 *HFIE* and *AtFIE* amino acid sequences (Figure 5.8A), unlike those observed for P4 *EMF2* and *AtEMF2* (compare with Figure 5.4A).

Table 5.3 Similarity of *Arabidopsis*, *Hieracium* and maize *FIE* sequences. The length of the coding region of DNA is indicated for each gene, and the DNA and amino acid percentage (%) similarity are shown where appropriate [(DNA)/AA]. Sequences were compared with the BLAST 2 Sequences program (Tatusova and Madden, 1999)

	AtFIE	D3HFIE	P4HFIE	ZmFIE1	ZmFIE2
AtFIE	1110 bp	(74)/85 %	(74)/84 %	75%	82%
D3HFIE	-	1113 bp	(96)/99 %	79%	87%
P4HFIE	-	-	1113 bp	80%	87%
ZmFIE1	-	-	-	1386 bp	85%
ZmFIE2	-	-	-	-	1140 bp

RT-PCR analysis of D3 *HFIE* and P4 *HFIE* showed that both genes were expressed at similarly constant levels throughout ovary development (Figure 5.8B). Expression was also detected in leaves, other floral tissues (comprising pollen, anthers, stigmas and petals) and roots, similarly in sexual and apomictic plants (Figure 5.8C). Northern analysis failed to detect *HFIE* transcript in total RNA samples. Genomic analysis in sexual P4 and apomictic D3 *Hieracium* suggested that *HFIE* was present as either a single, or low copy gene. DNA samples were digested with *HindIII*, which digests the known D3 *HFIE* and P4 *HFIE* cDNA sequences once, *XbaI* and *EcoRV*, which do not cut the cDNA sequence. A radioactively labelled D3 *HFIE* 3' fragment (Figure 5.8D) hybridised to two bands in *HindIII*

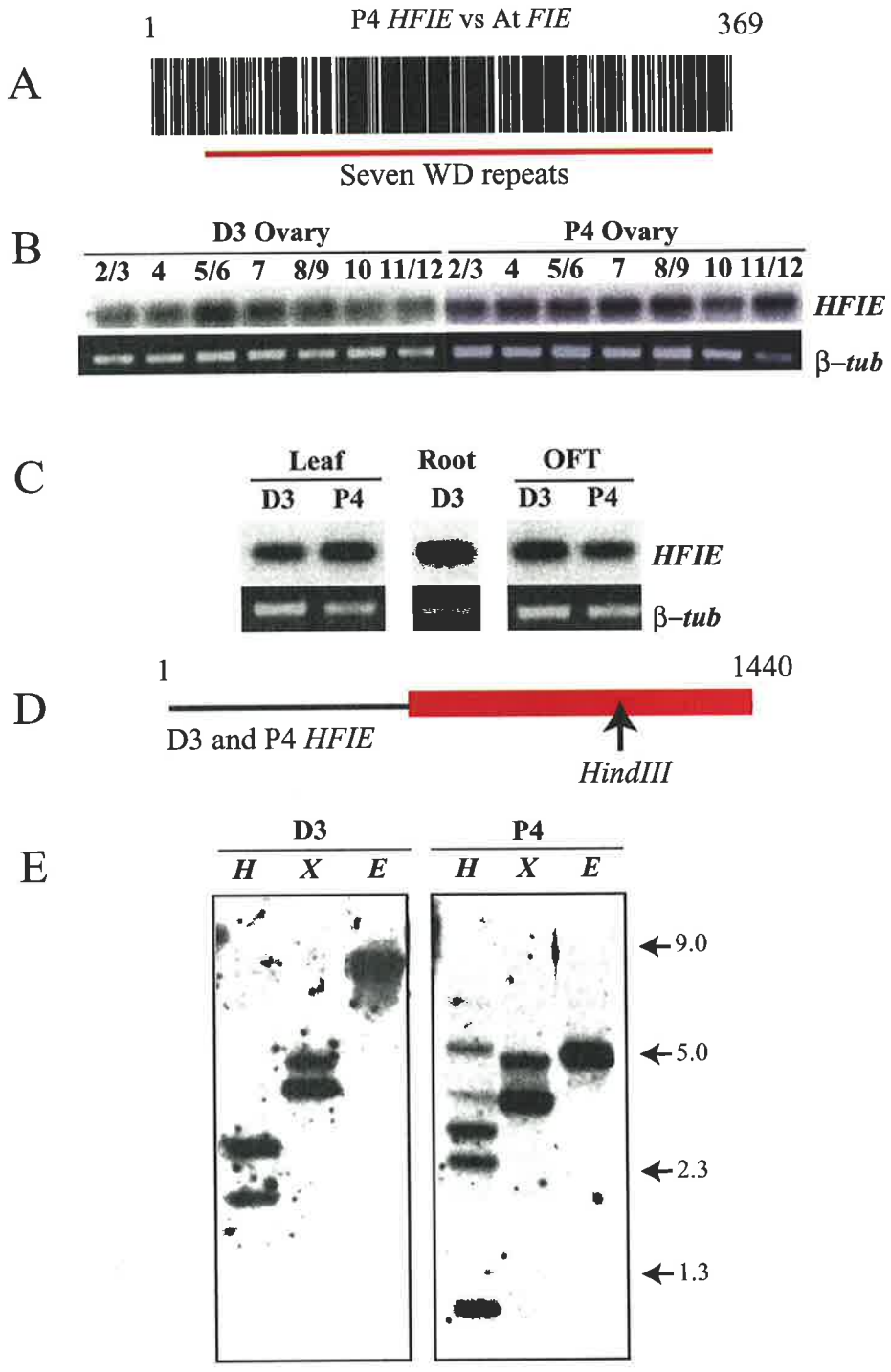

Figure 5.8 Characterisation of *Hieracium FIE* sequences. **A** Conservation of amino acid residues over the length of the *Arabidopsis FIE* and P4 *HFIE* sequences. Black blocks indicate complete conservation. **B** RT-PCR expression analysis of *HFIE* during ovary development in sexual P4 and apomictic D3 *Hieracium*. Numbers indicate stages of floral development (see Appendix 1) **C** RT-PCR expression analysis of *HFIE* in leaves, roots and other floral tissues (OFT). **D** Probe fragment used for hybridisation to genomic blots (indicated in red) and the position of the *HindIII* site. **E** Genomic analysis of *HFIE*-like sequences in sexual P4 and apomictic D3 *Hieracium*. DNA samples were digested with *HindIII* (H), *XbaI* (X) or *EcoRV* (E), and hybridised to the radioactively labelled D3 3'*HFIE* probe indicated in **D**. The size of the DNA fragments in kilobases is indicated at right.

digested D3 genomic DNA as expected (Figure 5.8E). However, at least six DNA fragments hybridised to labelled probe in *HindIII* digested P4 genomic DNA, possibly indicating the presence of multiple *HFIE*-like genes in the genome of sexual P4, or multiple *HindIII* sites within introns of a single P4 *HFIE* gene. Probe hybridised to two bands in *XbaI* digested genomic DNA from both plants, possibly indicating the presence of a conserved intron located *XbaI* site. *HFIE* probe detected only a single band in *EcoRV* digested genomic DNA from both plants (Figure 5.8E).

These data highlight the similarity of the D3 and P4 *HFIE* mRNA sequences, their genomic organisation and their temporal expression pattern in various tissues. From these analyses there appears to be no obvious lesion in the D3 *HFIE* gene that might account for a direct role in autonomous endosperm formation. However, this does not discount the possibility that *HFIE* promoter sequences or protein function may be altered in apomictic D3 to influence endosperm formation.

5.4 Discussion

5.4.1 Identification of *Hieracium* Ovule Sequence (HOS) genes

The molecular cues regulating the differentiation of AIs from somatic ovule cells are unknown. Differential screens have been used to compare the expression of genes in ovules from apomictic and sexual species during the initiation of apomixis to identify candidate genes involved in AI formation. These screens have had little success in identifying any genes, let alone key regulators, that are differentially expressed (Vielle-Calzada et al., 1996; Leblanc et al., 1997; Guerin et al., 2000; Tucker et al., 2001). Such screens assume that genes involved in the regulation of

apomixis will be up or down regulated relative to their expression in the sexual plant. One possibility is that the genes expressed during the initiation of apomixis are also expressed in cells during sexual processes. Furthermore, in the apomict, genes regulating the initiation of apomixis may only show slight spatial or temporal differences in expression, similar to that observed for the *AtFIS2:GUS* chimeric gene in *Hieracium* (see Chapter 3). Such temporal and spatial changes are not detectable by current differential screens.

In this study, a cold-plaque screening technique was utilised to obtain a subset of genes expressed at low levels in *Hieracium* ovules that by inference might represent regulatory genes expressed during the initiation of apomixis. A differential step was included in the screen, to subtract genes that were expressed in young leaves. A total of 58 putative HOS clones were identified, of which 60% showed matches to known genes or proteins, and 40% showed no matches in the NCBI database. These clones provide a pool of genes that can be used in further studies to characterise early ovule development in *Hieracium*.

The subsequent analysis of ten HOS clones by northern analysis showed that seven were expressed in ovaries and four were up-regulated in ovaries compared to other tissues (N. Paech and A. Koltunow, unpublished). The four genes up-regulated in ovary tissues showed homology to an ankyrin-like protein (*HOS-ANK*), a RING zinc-finger protein (*HOS-ZF*), a polygalacturonase (*HOS-PG*) and a CLAVATA1 receptor-like kinase (*HOS-CLV*). Ankyrin and RING-zinc finger domain proteins function in a wide variety of plant processes, and are generally involved in protein-protein interactions. In eukaryotes, ankyrin repeat structures have been found in the p53-binding protein 53BP2 (Gorina and Pavletich, 1996), cyclin-dependent kinase inhibitor p19Ink4d (Yuh et al., 1997) and transcriptional regulator GABP-beta (Batchelor et al., 1998). Similarly, many proteins containing

RING-zinc finger domains have putative involvement in aspects of transcriptional regulation (Satijn et al., 1997). In contrast, polygalacturonase (PG) genes in *Arabidopsis* function during cell wall metabolism and have been associated with fruit ripening, organ abscission and pollen grain development, and can be grouped into a large gene family that is ubiquitously expressed (Torki et al., 2000). Functional analysis of the *HOS-ANK*, *HOS-ZF* and *HOS-PG* genes was not performed in this study, and hence their role in ovule development is yet to be determined.

5.4.2 Identification of *CLAVATA1* (*CLV1*)-like genes from early *Hieracium* ovaries

In *Hieracium* D2, three to eight AIs differentiate early in ovule development and give rise to multiple embryo sacs (Koltunow et al., 2000). The early ovule-enriched cDNA library utilised in this study was generated from early *Hieracium* D2 tissues with the aim of identifying regulatory genes that might be expressed during the period of AI cell differentiation. During plant development, specification of cell fate depends to a large degree on cell position within the developing organ; hence a plant cell must interpret positional cues to differentiate correctly. The CLAVATA1 (CLV1) receptor protein kinase is a key component of the signalling processes that regulate the differentiation of stem cells in shoot meristems (see DeYoung and Clark, 2001 for review). The function of the *CLV1*-like gene, *HOS-CLV*, has not been determined, but it is tempting to speculate that it may play some role in cell differentiation during ovule development. A second receptor-like kinase (RLK)

showing homology to *CLV1*, *HOS-RLK*, was expressed in early ovule tissues as well as pollen. The recently sequenced *Arabidopsis* genome contains more than 600 RLK homologs, but few of these genes have an assigned function. RLKs control a wide range of processes, including development, disease resistance, hormone perception, and self-incompatibility (Shiu and Bleecker, 2001). Some RLK genes function during reproduction, such as the *EXTRA SPOROGENOUS CELLS (EXS)* gene from *Arabidopsis*, which plays roles in male germ-line and early ovule development (Canales et al., 2002). Further analysis of the *HOS-CLV* and *HOS-RLK* genes by silencing and expression studies would assist in determining their function during early ovule development in *Hieracium*.

5.4.3 The *HMET* and *HHDAC* clones are tools for the investigation of epigenetic gene regulation in *Hieracium*

The cues controlling the formation of endosperm without fertilisation in apomictic plants are also unknown. Candidate genes have been isolated from sexual systems that regulate the development of endosperm and these include the putative chromatin remodellers *MEA, FIS2, FIE* and the putative PcG interactors *MET* and *HDAC,* which regulate gene transcription. Changes in DNA methylation and histone modification through acetylation or deacetylation alter the structure of chromatin and the expression of endogenous genes and represent forms of epigenetic regulation (Tian and Chen, 2001).

DNA methylation and chromatin structure affect transcriptional and post-transcriptional regulation of genes in *Arabidopsis* (Morel et al., 2000). Methyltransferase (MET) genes that regulate methylation of nucleic acid residues

form a large family containing three classes in *Arabidopsis* (Finnegan and Kovac, 2000). Similarly, sixteen histone deacetylase genes have been identified within the *Arabidopsis* genome, and these are grouped into three classes based on homology to characterised HDACS in yeast and maize (Pandey et al., 2002). Inhibition and over-expression of class 1 RPD3-like histone deacetylases, such as *HDA1* from *Arabidopsis* (Tian and Chen, 2001) and *OsHDAC1* from rice (Jang et al., 2003) leads to changes in gene expression and subsequent developmental abnormalities. Decreased expression of *MET1*-type methyltransferases by antisense constructs in *Arabidopsis* result in altered methylation levels, release of transcriptional gene silencing (Steimer et al., 2000) and altered expression of some regulatory genes (Finnegan et al., 1996; Kishimoto et al., 2001).

The *HMET* and *HHDAC* genes identified in this study showed over 90% similarity on the putative amino acid level to *MET1* (Finnegan and Kovac, 2000) and *HDA9* RPD3-type sequences from *Arabidopsis* respectively. Detection of *HHDAC* transcript throughout ovary development, and its up-regulation during female meiosis and late embryo development, suggest that this gene may function to regulate gene expression during seed development in *Hieracium*. Isolation of a full-length *HHDAC* gene, and subsequent analysis of plants down-regulated for *HHDAC* in the ovule and seed will potentially elucidate the role of deacetylation during apomixis in *Hieracium*.

In contrast to the *MET1* gene of *Arabidopsis* that was highly expressed in most plant tissues during development (Genger et al., 1999), *HMET* expression was not detected during ovary or leaf development in *Hieracium*. *HMET* was closely related to *METII* in sequence comparisons and showed a similar expression pattern; *Arabidopsis METII* expression was also barely detectable during plant development. However, it is not clear if *HMET* is an orthologue of *AtMETII*.

Although the *HMET* and *HHDAC* genes were not investigated thoroughly in this study, their presence in the *Hieracium* genome suggests that similar epigenetic mechanisms may regulate gene expression during development in *Hieracium* similar to other species. Furthermore, it is possible that altered epigenetic regulation of gene expression might be linked to the manifestation of apomixis in *Hieracium*. Studies in the *Arabidopsis fis* mutants have shown that methylation plays a key role in the regulation of seed development. In plants containing a mutant *fis* allele and an antisense *METI* gene, seed development proceeds normally after fertilisation without embryo abortion during heart stage (Luo et al., 2000), and autonomous endosperm is able to cellularise in *fie* mutants rather than remaining in the nuclear phase (Vinkenoog et al., 2000). Seed rescue possibly relates to the expression of unknown downstream maternal genes that recover wild type activity irrespective of altered *fis* function. This is particularly relevant to apomixis, as it shows that changes in methylation level can induce the expression of genes that are normally inactive, allowing seeds to develop to maturity despite the presence of maternal effect mutations. However, the effect of altered methylation levels on reproduction in apomictic *Hieracium* was beyond the scope of this study, and more emphasis was placed on the characterisation of putative *Hieracium FIS* genes.

5.4.4 *FIS2*-like genes in *Hieracium*

Attempts to isolate a *FIS2* homologue from *Hieracium* were complicated by the presence of other highly expressed *FIS2*-like genes in the seed, such as *EMF2* (Yoshida et al., 2001) and possibly *VRN2* (Gendall et al., 2001). *EMF2* regulates the transition from a vegetative to a floral state in *Arabidopsis*, and is expressed at high

levels in the embryo and endosperm of developing seeds as detected by *in situ* hybridisation (Yoshida et al., 2001). In contrast, preliminary *in situ* studies suggest that *FIS2* mRNA is detected only at low levels around the polar nuclei in the central cell of *Arabidopsis* and also in the dividing endosperm, although this requires further clarification (J. Guerin, A. Koltunow, unpublished).

Various degenerate primer sets designed to the ACE domain/VEFS box (Chaudhury et al., 2001; Birve et al., 2001) preferentially amplified *EMF2*-like sequences from *Hieracium*. Primers designed to the specific middle repeat region of *FIS2* failed to identify *FIS2*-like products, and no ESTs from other plant species showing homology to this region were found in the Genbank database. The origin of this region in *Arabidopsis FIS2* is uncertain; it is potentially an *Arabidopsis*-specific sequence that forms a conserved protein structure required for DNA binding (Luo et al., 1999).

The *P4 EMF2* clone showed 66% amino acid similarity to the *Arabidopsis EMF2* sequence, and even less to *Arabidopsis FIS2*. This lower homology was due to divergent residues between the zinc finger motif and the C-terminal ACE domain that showed no homology to the repeat region in *Arabidopsis FIS2*. Although a *Hieracium FIS2* cDNA was not identified in this study, it is possible that these interdomain-regions could be used to distinguish between different *FIS2*-like genes in *Hieracium*. Similarly, the position of the zinc finger domain in FIS2, VRN2 and EMF2 differs between the three amino acid sequences (Gendall et al., 2001). Considering the high similarity shared between *Hieracium* cDNA clones over the ACE domain identified in this study, further attempts to isolate a *FIS2* gene might focus on the 5' end of the genes. Alternatively, the role of *FIS2*-like genes during embryo sac and seed development in *Hieracium* could be indirectly investigated by

generating RNAi constructs that contain the conserved D2 *ACE* domain behind a seed-specific promoter, such as *AtFIS2* or *AtMEA*.

5.4.5 Conserved *FIE*-like genes exist in sexual and apomictic *Hieracium*

Isolation and sequencing of the D3 and P4 *HFIE* cDNA clones revealed 36 different bases over the 1113 bp coding regions of the two genes, and these resulted in only three different amino acid residues. The putative amino acid sequences of D3 and P4 *HFIE* were very similar to *FIE* from *Arabidopsis* (Ohad et al., 1999) and the two *ZmFIE* genes from maize (Springer et al., 2002). Similarly, the mRNA expression patterns of the *Hieracium* and *Arabidopsis FIE* genes detected by RT-PCR were essentially the same during ovary and plant tissue development.

Studies of nine mutant *fie* alleles in *Arabidopsis* showed that eight resulted from single base changes that generated either a stop codon, an altered intron border or a frame-shift mutation and one resulted from a 27 bp deletion within the sixth WD-40 repeat (Ohad et al., 1999). These mutations are likely to alter the functional structure of FIE, preventing interaction with other members of the PcG complex such as MEDEA. Point mutations that generate amino acid changes in WD-40 domains of the human and mouse FIE homologue, EMBRYONIC ECTODERM DEVELOPMENT (EED), result in null or hypomorphic alleles that can prevent the interaction of EED and ENHANCER OF ZESTE 2 (EZH2; Schumacher et al., 1996; Denisenko et al., 1998; van der Vlag and Otte, 1999). EZH2 is the human and mouse equivalent of *Drosophila* ENHANCER OF ZESTE and *Arabidopsis* MEA (Yadegari et al., 2000). Although base changes were detected between the D3 and P4 *HFIE* sequences that generated different amino acid residues in the putative

proteins, these were not located in the putative WD-repeats and did not generate stop codons or frame-shift mutations. However, it is possible that these amino acid changes in D3 *HFIE* alter the function of the predicted protein leading to the initiation of autonomous endosperm in apomictic D3 *Hieracium*. The functional identity of the isolated D3 *HFIE* gene was further examined by complementation experiments in the *Arabidopsis fie* mutant (see Chapter 6).

Chapter 6: Characterisation of *Hieracium FIE* genes

6.1 Introduction

Apomixis in *Hieracium* is a reproductive process that has three components; the ability to mitotically produce an embryo sac from a somatic cell without prior meiosis (apospory), and the formation of embryos (parthenogenesis) and endosperm without fertilisation and thus contribution from the paternal genome. The molecular cues that lead to the manifestation of these three components are unknown, but it appears from the data presented in Chapter 3 that sexuality and apomixis share regulatory factors and are closely interrelated processes.

As described previously, the *Arabidopsis mea, fis2* and *fie* mutants display aspects of autonomous endosperm initiation in the absence of fertilisation (Ohad et al., 1996; Chaudhury et al., 1997; Grossniklaus and Vielle-Calzada, 1998). Although autonomous endosperm development occurs only in the minority of apomictic species, and is mainly restricted to the Asteraceae, elucidation of the molecular cues regulating its development are fundamentally relevant to understanding how a seed forms without fertilisation. A plausible hypothesis is that altered regulation of endogenous *FIS* genes may enable autonomous endosperm and seed development in apomictic plants.

To address this hypothesis, a *Hieracium FIE* (*HFIE*) homologue was identified from sexual and apomictic plants (see Chapter 5). The *HFIE* mRNA sequences from sexual and apomictic *Hieracium* were 99% identical at the putative amino acid level, and showed similar temporal expression patterns during ovary

development (See Chapter 5). However, temporal expression data provides limited information in relation to the conservation of *HFIE* function in apomictic and sexual plants.

To determine whether *HFIE* function was altered in apomictic D3 *Hieracium*, several approaches were utilised. A complementation strategy was designed to test the function of the D3 *HFIE* cDNA (*D3-cHFIE*) in the *Arabidopsis fie-2* mutant. *HFIE* promoter sequences were also identified from sexual and apomictic plants using a PCR-based gene walking approach, and *HFIE:GUS* marker genes were generated to test the spatial localization of *HFIE* expression in *Arabidopsis*. The results show that the D3 *HFIE* cDNA encodes a functional protein that is capable of restoring the requirement for fertilisation-dependent endosperm development in the *Arabidopsis fie-2* mutant, and is likely to be required for seed development in apomictic D3 *Hieracium*.

6.2 Materials and Methods

6.2.1 Growth and phenotype of *Arabidopsis* plants

Arabidopsis plants were grown as per Section 3.2.1. L.*er fis3-2* seeds were provided by A. Chaudhury and M. Luo (CSIRO, Canberra) and contain the same mutation as the *fie-2* allele described by Ohad et al., (1999). Germinated seedlings were transferred to soil after the four-leaf stage, and after flowering, 50% of the seeds in siliques from some plants had aborted after fertilisation.

6.2.2 Genetic complementation and design of a *fie*-2 CAPS marker

Heterozygous *fie-2/FIE*(+) plants were identified by screening segregating populations with a CAPS PCR marker designed during this study. The *fie-2* mutation causes an A → G mutation at the border of intron 3 of the *Arabidopsis FIE* gene, resulting in the loss of a *Hinf*I site (M. Luo, pers. comm.). PCR primers were designed to obtain a 241 bp product spanning this region, which incorporates three *Hinf*I sites. Digestion of the wild-type PCR product with *Hinf*I produced three bands of the expected size after electrophoresis on a 4% agarose TAE gel; 156 bp, 66 bp and 19 bp. The loss of the *Hinf*I site in the mutant *fie-2* gene results in only two bands after digestion of 156 bp and 85 bp. However, because *fie-2* plants are maintained as heterozygotes, plants containing the mutant allele are identified as those containing all four of the 156 bp, 85 bp, 66 bp and 19 bp bands.

A complementation construct was generated containing 2004 bp of the *Arabidopsis MEDEA* (*MEA*) promoter (upstream from the ATG) fused to 1308 bp (1113 coding + 191bp 3'UTR) of *D3-cHFIE* (see Chapter 5) in the pBINplus vector (van Engelen et al., 1995). The cloned MEA promoter directs specific expression of GUS to the central cell and endosperm in *Arabidopsis*. This binary plasmid was mobilised in *Agrobacterium* strain LBA4404 and was transformed by floral dip into *Arabidopsis* wild type Col-4 plants (see Section 4.2.3). Four independent lines were obtained, and lines #1 and #2 were utilised in subsequent experiments.

Heterozygous *fie-2*/+ L.*er* plants were crossed as males with female Col-4 WT plants and *MEA:D3-cHFIE* Col-4 lines #1 and #2. Plants containing both the *fie-2* mutation and the *MEA:D3-HFIE* construct were selected on kanamycin and screened for by CAPS PCR analysis. To test for complementation, flowers from F2 plants were emasculated by removing the sepals, petals and anthers prior to

anthesis. Siliques were then collected 3 days post emasculation (DPE) and fixed in FAA for 3 - 30 days at 4°C. The siliques were then stained using haematoxylin (as per Section 2.2.2) and scored for the presence of multi-nucleate central cells, essentially as per Ohad et al., (1996).

6.2.3 Isolation of *HFIE* promoter sequences from *Hieracium*

Libraries for promoter walking were constructed during this study following the method of Siebert et al., (1995). Five libraries were constructed for both P4 *H. pilosella* and D3 *H. piloselloides* from *ScaI*, *DraI*, *PvuII*, *PmlI* and *EcoRV* restriction digests of genomic DNA, and these were used to attempt the PCR amplification of DNA upstream of the *HFIE* gene. The nested adapter primers used were AP1 for the first reaction and AP2 for the second and third reactions (see Appendix 3). The nested gene specific primers for *HFIE* were PrFIE3 for the first reaction, PrFIE2 for the second reaction and PrFIE1 for the third reaction (see Appendix 3). Primary PCR reactions were conducted in 50 µL volumes containing 1 µL of the library, 200 µM dNTPs, 1 mM $MgSO_4$, 60 mM Tris-SO_4 (pH 8.9), 18 mM $(NH_4)_2SO_4$, 0.4 µM adapter primer AP1 and gene specific primer, and 0.3 µL (~1.5 units) of High Fidelity Platinum Taq DNA Polymerase enzyme mix (Invitrogen). The cycle parameters were as follows: initial denaturation step at 94°C for 1 min, followed by 35 cycles of denaturation at 94°C for 30 s and annealing/extension at 68°C for 6 min, and a final annealing/extension time of 15 min. Secondary and tertiary PCR reactions were conducted in 50 µL volumes using 1 µL of a 1/100 dilution of the first or second round reaction and the adapter specific primer AP2 with the appropriate nested gene specific primer. The cycle

parameters were slightly modified to use an extension/annealing time of only 3 minutes instead of 6, and 20 cycles instead of 35. PCR products were examined on a 1% TAE agarose gel and DNA fragments were isolated using the Qiaquick kit (Qiagen) and cloned into pGEM T-easy (Promega) as per manufacturers instructions.

6.2.4 Amplification of *HFIE* gene 5'UTR sequences

PCR primers were designed to highly conserved regions in the D3 and P4 *HFIE* 5'UTR and coding sequences to amplify genomic DNA fragments spanning the ATG start codon. PCR reactions were performed on D3 and P4 genomic DNA using two primer sets. "Span PCR" products were amplified using the D3PrF-232 and PrFIE2 (see above) primers and "sPCR" products were amplified with the P4PrF-228 and PrFIE2 primers (see Appendix 3). The cycle parameters were as follows: initial denaturation step at 94°C for 3 min, followed by 30 cycles of denaturation at 94°C for 30 s, annealing at 50°C for 1 min and extension at 72°C for 1 min, and a final extension time of 7 min. Products were examined on 1% agarose gels, all bands were excised and purified together, and cloned into pGEM T-easy. Clones were randomly selected for sequencing after purification from bacterial colonies.

6.2.5 Generation of *D3-cHFIE:GUS, P4-cHFIE:GUS, D3-EHFIE:GUS* and *P4-EHFIE:GUS* transgenic plants.

The *HFIE:GUS* marker genes used in this study were created by PCR amplification of promoter sequences from *Hieracium* genomic DNA, and transcriptional fusion to the *β-glucoronidase* (*GUS*) gene in the pCAMBIA 1391z vector. The *P4-*

EHFIE:GUS gene contained 1997 bp of DNA upstream from the putative ATG start codon of the P4 *EcoRV 3-2* (*HFIE3)* gene, and the *D3-EHFIE:GUS* contained 1990 bp of DNA upstream from the ATG of the corresponding D3 *EcoRV* 3-2 (*HFIE8*) gene. The promoter fragments were amplified from P4 and D3 genomic DNA using the PrFIEFwd primer and the PrFIERev *NcoI* adapter primer (see Appendix 3).

The *P4-codingHFIE (cHFIE):GUS* gene contained 485 bp of DNA upstream from the putative start codon of the P4 *EcoRVshort* 1-1 (*HFIE1)* gene, and the *D3-cHFIE:GUS* gene contained 2264 bp (~498 bp promoter and 5'UTR, 1766 bp transposon) of DNA upstream from the ATG of the corresponding D3 *PmlI* 2-1 (*HFIE5*) gene. The promoter fragments were amplified from P4 genomic DNA using the P4codeFwd and P4NcoIRev primers, and D3 genomic DNA using the D3code2-1Fwd and D3NcoIRev primers (see Appendix 3). The binary vectors were mobilised in *Agrobacterium* strain LBA4404, and transformed into *Arabidopsis* No-0 plants as per Section 4.2.3. The number of transgenic lines identified that contained the marker genes was four for *P4-EHFIE:GUS*, four for *D3-EHFIE:GUS*, sixteen for *D3-cHFIE:GUS* and six for *P4-cHFIE:GUS*.

6.3 Results

6.3.1 Design of a complementation strategy for the *Arabidopsis fie-2* mutant

The *HFIE* and *Arabidopsis FIE* cDNA sequences displayed high homology and similar temporal expression patterns during seed development. From the data presented in Chapter 5, there appeared to be no evidence to suggest that the function of the *D3-cHFIE* gene was compromised by significant alterations in the coding sequence. However, three amino acid residues were detected that differed between

the *D3-cHFIE* and *P4-cHFIE* putative amino acid sequences that might alter protein function. A complementation strategy was designed to test the functional identity of the putative D3-cHFIE WD-40 protein in the *Arabidopsis fie-2* mutant.

The *fie-2* allele represents a gametophytic maternal lethal mutation such that any seed inheriting the mutation will abort after embryo sac development but prior to seed maturity. A seed that inherits a paternal mutant *fie*-2 allele which already contains a maternal wild type *FIE* allele is viable and does not abort. Hence, *fie*-2 plants can be maintained in a heterozygous state. *fie-2* plants display two phenotypes depending on whether silique growth occurs in a fertilisation-dependent or -independent manner (Figure 6.1A). When a *fie-2*/+ flower is emasculated to remove the anthers and prevent fertilisation of the embryo sac, approximately 50% of the seeds will develop endosperm in the absence of fertilisation (Figure 6.1A). These seeds correspond to those that contain a maternal *fie*-2 allele. The remaining 50% of ovules that contain a wild type *FIE* allele senesce and do not show any sign of endosperm development. The *fie*-2 seeds that develop endosperm without fertilisation do not show autonomous embryo growth and abort prior to endosperm cellularisation. If carpels from *fie-2*/+ plants are pollinated and the ovules are fertilised, all of the seeds initiate endosperm and embryo development. However, irrespective of the pollen donor, seeds that inherit a maternal *fie-2* allele (~50%) abort at the heart stage of embryo development and the remainder (~50%) continue to maturity (Figure 6.1A).

The complementation strategy was designed to recover an increased proportion of wild type *FIE* activity in emasculated seeds (Figure 6.1B), which would be manifested as a reduction in the number of ovules developing autonomous endosperm. In plants containing a single copy of the endosperm specific *MEA:D3-cHFIE* construct and the mutant *fie-2* allele, 25% of the ovules should inherit

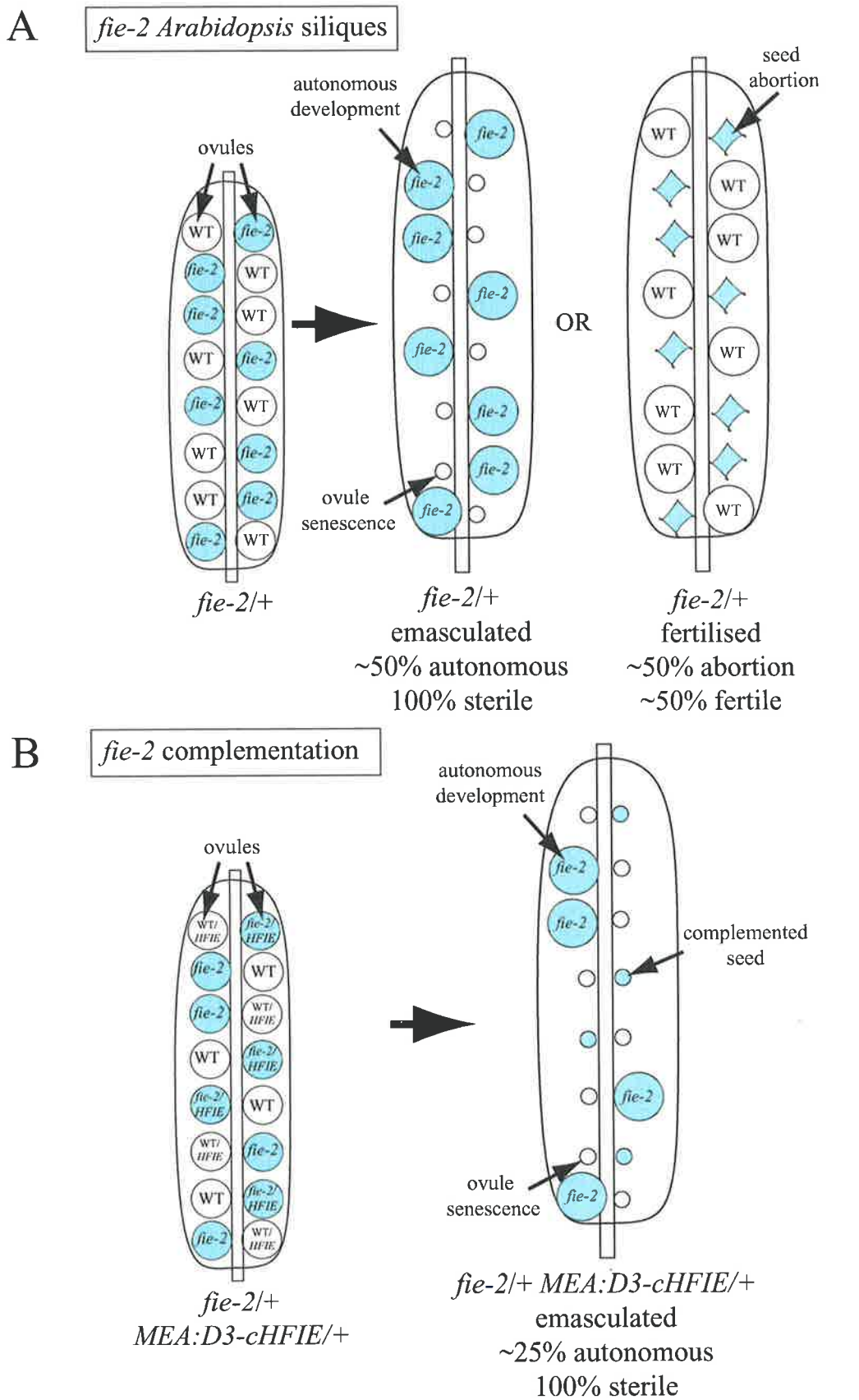

Figure 6.1 Complementation strategy for the *Arabidopsis fie-2* mutant. **A** Schematic representation of seed development in emasculated or fertilised siliques from *fie-2* heterozygous plants. Ovules shaded in blue contain a maternally inherited *fie-2* allele. **B** Predicted seed development in emasculated siliques from *fie-2/+ MEDEA:D3-cHFIE/+* plants.

maternal alleles of both genes. If complementation was successful, only 25% of the seeds would develop autonomous endosperm after emasculation, thus representing a 50% reduction in the number of *fie-2* seeds that develop autonomously (Figure 6.1B).

6.3.2 Complementation of *Arabidopsis fie*-2 with the D3 *HFIE* cDNA

Two independent Col-4 lines containing the *MEA:D3-cHFIE* construct were generated, and both expressed the *D3-cHFIE* mRNA in flowers by RT-PCR (data not shown). Pollen from L. *er fie-2*/+ plants was crossed onto Columbia-4 wild type plants and *MEA:D3-cHFIE* lines #1 and #2 (Figure 6.2). F1 progeny containing both the *fie*-2 and *MEA:D3-cHFIE* genes were identified by CAPS PCR, and approximately 50% of the seeds aborted in these plants (Table 6.1). Viable seeds from these plants were germinated, and F2 plants containing both genes were recovered. Segregation analysis suggested that the majority of F1 complementation plants contained only a single copy of the *MEA:D3-cHFIE* gene, and hence some of the analysed progeny may have been homozygous for the complementation gene (Figure 6.2). The F2 plants were analysed to determine complementation.

Between five and ten flowers were emasculated for each F2 plant (Figure 6.2), and siliques were collected 3 days post emasculation (DPE). In plants containing the *fie-2* mutation and the complementation gene, the length of the emasculated siliques after 3 or 10 DPE did not differ significantly from that detected in plants only containing the *fie-2* mutation (Table 6.1). In wild type plants, 3-7% of the ovules (4% on average) from emasculated siliques (n=10) contained multinucleate central cells 3 DPE (Figure 6.3A). These represented ovules in which

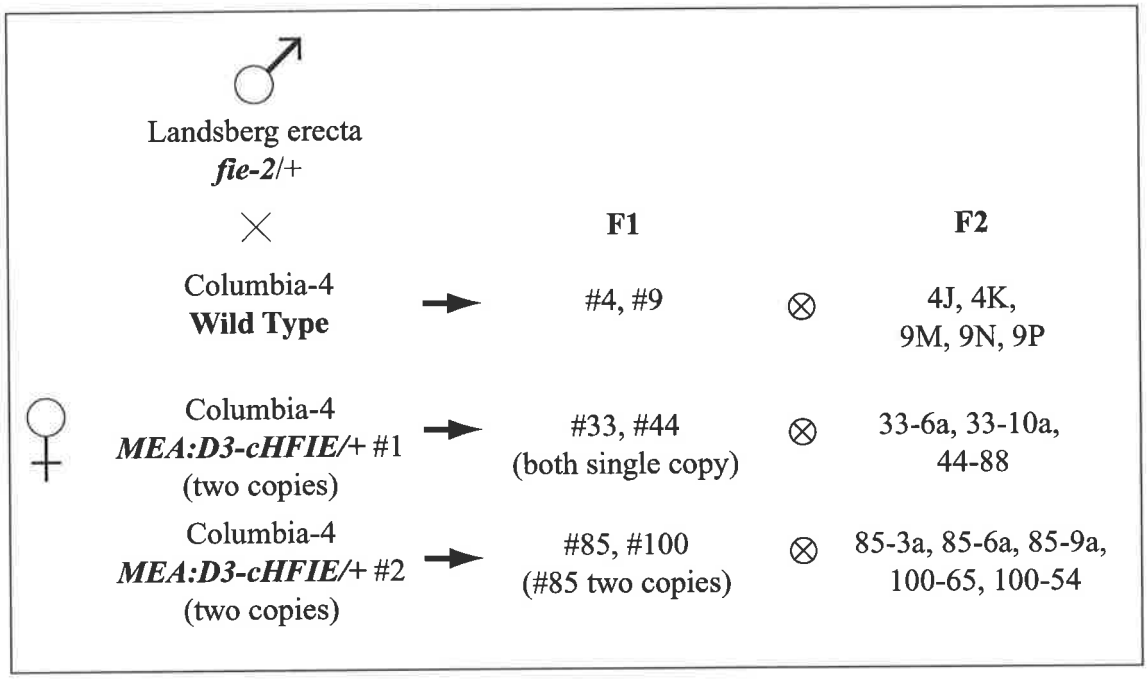

Figure 6.2 Crossing strategy for *Arabidopsis fie-2* complementation. Transgene copy number of the complementation plants is indicated.

A

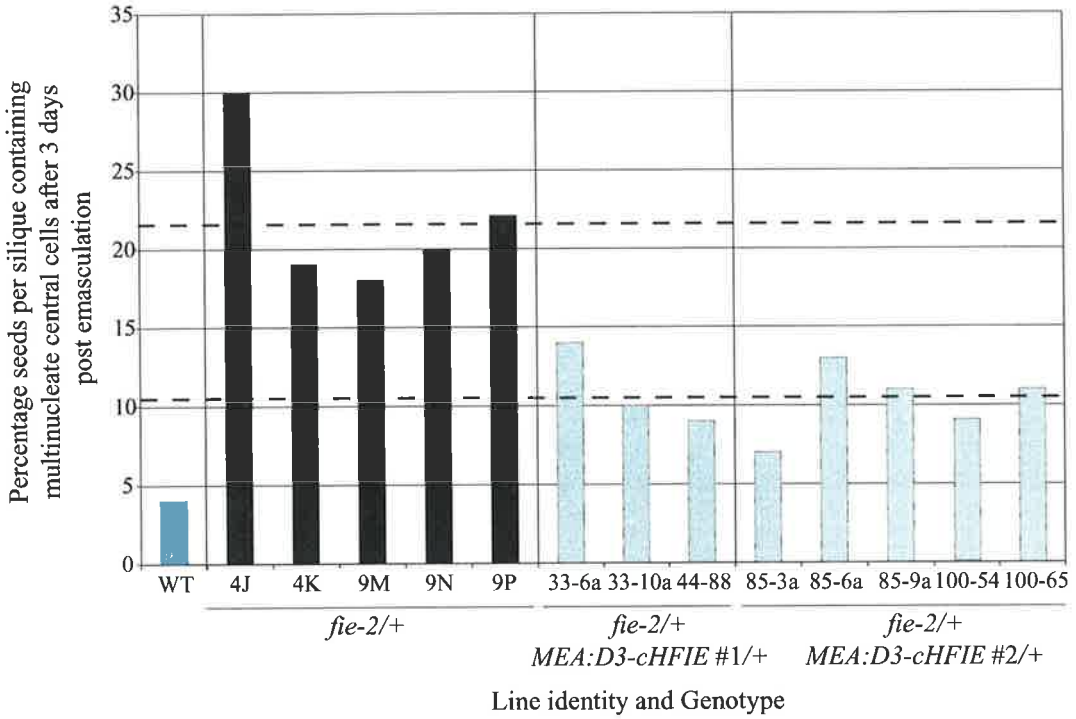

B

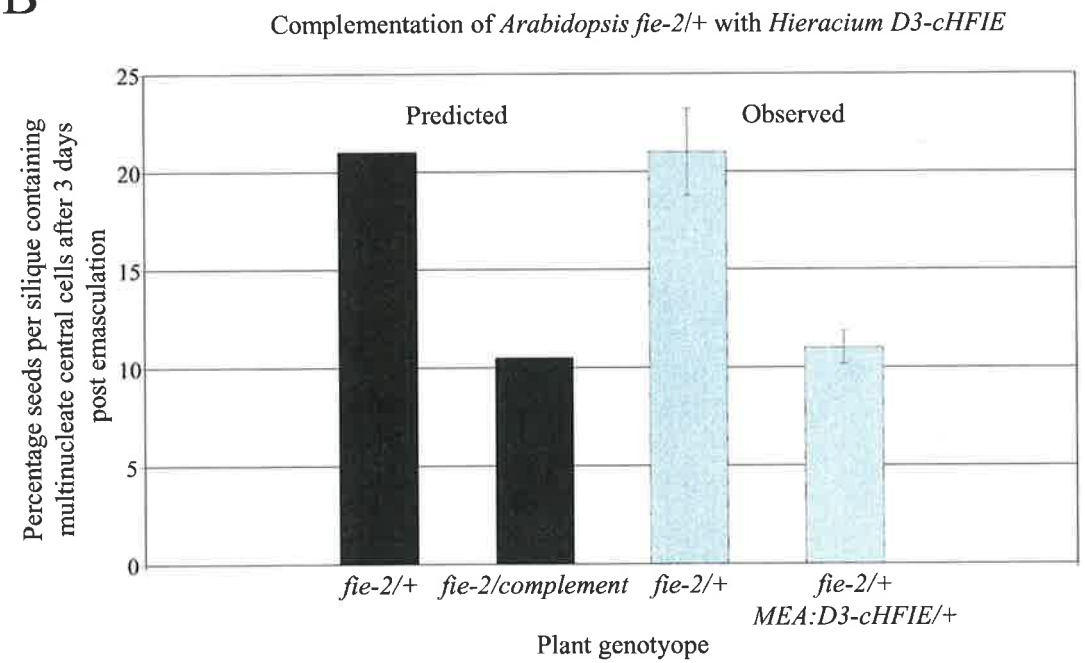

Figure 6.3 Complementation of the *Arabidopsis fie-2/+* mutant. **A** Percentage of seeds per silique displaying multinucleate central cells after 3 days emasculation in wild-type (WT), control (*fie-2/+*) and complementation (*fie-2/+ MEDEA:D3-cHFIE/+*) lines. Dashed lines indicate the average percentage of multinucleate central cells in control and complementation lines. **B** Predicted and observed levels of autonomous seed development in control and complementation lines. The predicted values were obtained from Ohad et al., (1996).

the two polar nuclei had not fused, and compared closely with the 5% figure found by Ohad et al., (1996). In L.*er* × Col-4 *fie-2*/+ control plants, 18 to 30% of the ovules from emasculated siliques (n=30) contained multinucleate cells that ranged in size from 2 to 32 nuclei (Figure 6.3A). The average number of ovules containing multinucleate central cells 3 DPE in these control plants was 21%, and this figure was the same as that determined by Ohad et al., (1996) in L. *er fie-2*/+ plants 3 days post emasculation (Table 6.1; Figure 6.3B).

The number of ovules that contained multinucleate central cells in *fie-2*/+ *MEA:D3-cHFIE* plants 3 DPE was significantly lower than that detected in *fie-2*/+ control plants that did not contain the *MEA:D3-cHFIE* gene (Table 6.1). In the complementation lines, 7 to 14% of the ovules from emasculated siliques (n=40) contained multinucleate cells that ranged in size from 2 to 32 nuclei (Figure 6.3A). The average number of ovules that contained multinucleate central cells 3 DPE in complementation plants was 11% (Table 6.1). On average, this figure represented a 52% reduction in the number of seeds containing endosperm nuclei in complementation plants, and suggested that the *MEA:D3-cHFIE* gene successfully complemented the *fie-2* mutation in ~50% of the *fie-2* seeds and ~25% of the total seeds.

Segregation data obtained from seed germination studies suggested that except for line #85, the majority of F1 lines contained only a single copy of the *MEA:D3-cHFIE* gene. Therefore, one in every four F2 plants should have been homozygous for the complementation construct. In *MEA:D3-cHFIE* homozygous *fie-2*/+ lines, complementation would be expected to restore the number of ovules containing multinucleate central cells to that of wild-type (~4%). Gene copy-analysis was not performed on seeds from the F2 plants, but the complementation percentages (Figure 6.3A) suggested that only one of the lines analysed, 85-3a, may

have been homozygous. Only 7% of the ovules analysed 3DPE from line 85-3a displayed multinucleate central cells. It is possible that this line was homozygous for the complementation construct or contained two independent copies of the *MEA:D3-cHFIE* gene resulting in a lower number of autonomous seeds. To avoid gene copy bias in determining average complementation, the data for 85-3a was not included in the graph showing the complementation averages of *Arabidopsis fie-2* (Figure 6.3B).

Expression of the *MEA:D3-cHFIE* gene did not appear to alter the embryo lethality phenotype of the *fie-2* mutation. In selfed siliques from F2 complementation plants, approximately 50% of the seeds aborted during development (Table 6.1). Fertilised seeds from F2 plants were not examined to determine whether embryo development proceeded any further than in *fie-2*/+ control plants. However, this result suggested that recovery of wild-type *FIE* endosperm in complemented plants was unable to rescue post-fertilisation embryo arrest and hence *fie* embryo lethality is not solely dependent upon an alteration in endosperm development.

Table 6.1 Characteristics of *Arabidopsis* WT, *fie-2* and complementation plants.

Genotype and Stage (Columbia-4 × Landsberg *erecta*)	**Silique length (mm)**	**Ovules containing multinucleate central cells per silique**	**Percentage aborted seeds per silique**
Wild Type (WT) anthesis pistils	2.6 ± 0.2	-	-
pollinated	11.6 ± 0.8	-	-
unpollinated	4.2 ± 0.3	1.9 ± 0.5	-
fie-2/+ 3 days post emasculation(DPE)	3.1 ± 0.4	6.5 ± 0.6	-
fie-2/+ 10 DPE	4.6 ± 0.6	-	-
fie-2/+ pollinated	12.8 ± 0.9	-	49.2 ± 1.4
fie-2/+ *MEA:D3-cHFIE*/+ 3 DPE	3.0 ± 0.4	4.0 ± 0.4	-
fie-2/+ *MEA:D3-cHFIE*/+ 10 DPE	4.7 ± 1.0	-	-
fie-2/+ *MEA:D3-cHFIE*/+ pollinated	13.4 ± 1.4	-	49.7 ± 2.2

6.3.3 Isolation of *HFIE* promoter sequences from *Hieracium* by promoter walking

The complementation data suggested that the amino acid differences in D3 HFIE did not impair its functional role in regulating fertilisation-dependent processes. However, the possibility remained that differences in the promoter sequences may alter *HFIE* function in apomictic D3 *Hieracium*.

Genomic blot analyses of sexual P4 and apomictic D3 *Hieracium* DNA suggested that only one or two closely related *HFIE* genes were likely to be present in each plant (see Chapter 5). The promoter walking technique (Siebert et al., 1995) was used to clone *HFIE* promoter sequences from sexual and apomictic *Hieracium*. This technique is less labor intensive than genomic library screening and overcomes the problems associated with the purification of phage DNA. Furthermore, the subsequent identification and sub-cloning of those regions of a genomic clone containing sequence immediately upstream of the coding genes is unnecessary.

Following three rounds of nested PCR (see Section 6.2.3), discrete products were amplified from the D3 *ScaI*, *DraI*, *EcoRV* and *PmlI* libraries, and the P4 *ScaI*, *DraI* and *EcoRV* libraries. Most reactions produced a single PCR product, except for the D3 *DraI* (3 products), *ScaI* (2 products), and P4 *EcoRV* (2 products) libraries. All of the fragments were excised from agarose gels, cloned into pGEM T-easy and sequenced.

The sequences of the cloned genomic fragments were aligned with the P4 and D3 *HFIE* cDNAs and most showed homology to the *HFIE* cDNA sequence at one end. The *HFIE* genomic DNA sequences were not identical, however, and some of the sequences contained large insertions and deletions. Schematic representations

of the promoter fragments are shown in Figure 6.4, and the nomenclature used to describe the different *HFIE* clones is shown in Table 6.2

Three *HFIE* promoter clones were identified from sexual P4 in the library screen (Figure 6.4). The 600 bp P4 *HFIE1* and 2.2 kb P4 *HFIE3* fragments encoded slightly different sequences and were identified from the P4 *EcoRV* library. The *HFIE3* sequence was also identified from the P4 *ScaI* library as a 1.3 kb fragment. The third clone, *HFIE4*, was identified as a 1.4 kb fragment from the *DraI* library, and was 97% identical to P4 *HFIE3*. The only insertion/deletion detected in the P4 *HFIE* genomic clones was a 33 bp sequence at base position -93 in *HFIE3* and *HFIE4* that was absent from *HFIE1*. The P4 *HFIE3* and P4 *HFIE4* clones also contained a TAA stop codon at position +25 within the first exon of the *HFIE* gene (Figure 6.4) and did not match the P4 *HFIE* cDNA sequence. In contrast, the P4 *HFIE1* sequence did not contain a stop codon and matched the P4 *HFIE* cDNA sequence closely.

Three different sequences were identified from the apomictic D3 promoter libraries. Overlapping clones corresponding to D3 *HFIE5* were isolated from the D3 *PmlI* and *DraI* libraries as 2.5 kb and 700 bp fragments respectively. D3 *HFIE8* was identified from the D3 *EcoRV* library as a 2.2 kb fragment and D3 *HFIE10* was identified from the *PvuII* library as an 850 bp fragment. D3 *HFIE5* and D3 *HFIE10* contained large insertions when compared to the D3 *HFIE8* sequence (Figure 6.4). However, apart from the 203 bp insertion at position -174 (Figure 6.4), the D3 *HFIE8* and D3 *HFIE10* sequences were 97% identical. Both sequences contained a 33 bp insertion at position -93 and an in-frame stop codon (TAA) at position +25 within the first exon of the *HFIE* gene (Figure 6.4). The position of the TAA stop codon was the same as that observed in the P4 *HFIE3* and *HFIE4* genes, as was the 33 bp insertion at position -93, and neither D3 *HFIE8* nor D3 *HFIE10* matched the

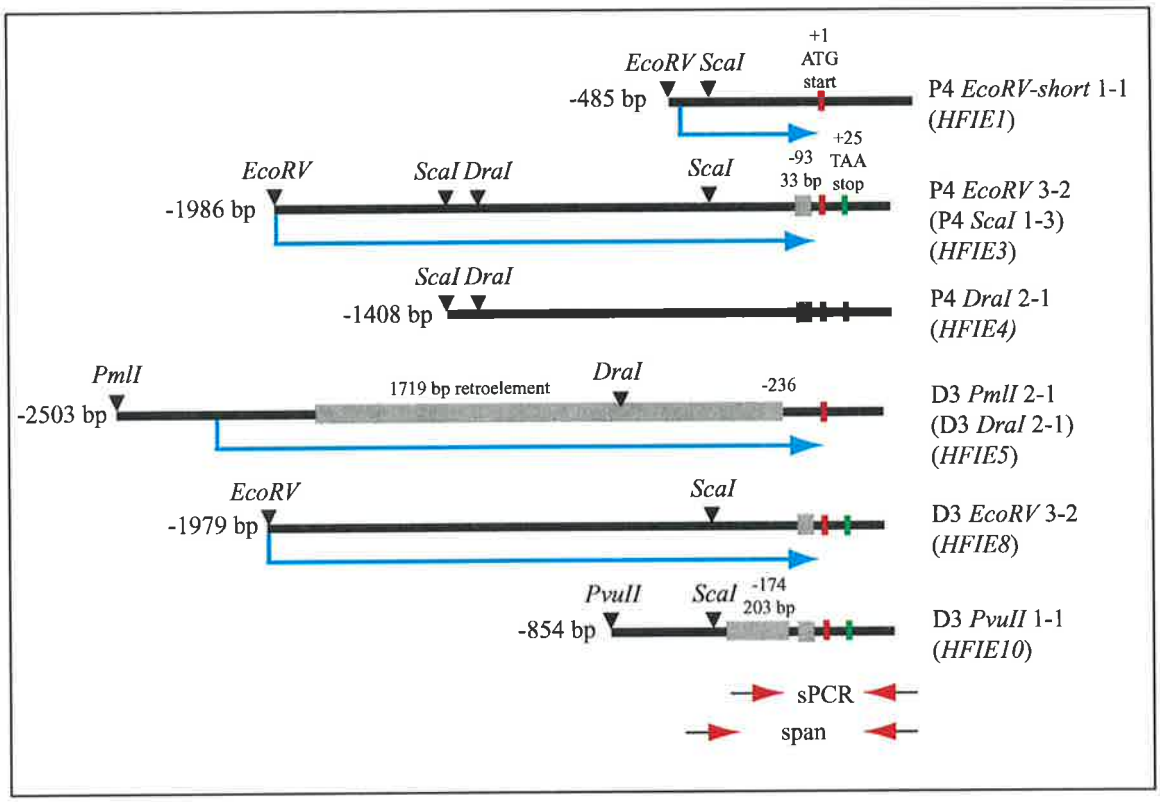

Figure 6.4 *HFIE* promoter fragments isolated from *Hieracium* genomic libraries. Green boxes indicate putative TAA stop codons, red boxes indicate putative ATG start codons, grey boxes indicate insertions and the blue arrows indicate the DNA fragments fused to GUS. The base pair positions of the various features are indicated relative to the P4 *HFIE3* sequence. The red and black arrows show the location of PCR primers designed to amplify genomic fragments spanning the ATG. The clone name and gene ID is indicated at right. See Table 6.2 for gene nomenclature.

D3 *HFIE* cDNA sequence (Figure 6.4). The D3 *HFIE5* sequence matched the D3 *HFIE* cDNA sequence, and contained a 1719 bp insertion at base position -236 bp that shared homology with a non-Long Terminal Repeat (LTR) retroelement.

Table 6.2 *HFIE* promoter clones from *Hieracium* and their specified nomenclature and similarity. The similarity between the alleles was determined by comparing the indicated DNA sequences using the BLAST 2 Sequences program.

Class	P4 clone	Gene ID	Similarity	Allele	D3 clone	Gene ID	Similarity	Allele
I	*EcoRVshort* 1-1	*HFIE1*	98% (*1* v 2)	A	*PmlI* 2-1	*HFIE5*	98% (*5* v *6*)	A
	span 1x	*HFIE2*		A'	sPCR 1-3	*HFIE6*	90% (*6* v *7*)	A'
	-	-		-	span 10x	*HFIE7*	90% (*5* v *7*)	A"
II	*EcoRV* 3-2	*HFIE3*	97% (*3* v *4*)	B	*EcoRV* 3-2	*HFIE8*	98% (*8* v *9*)	B
	DraI 2-1	*HFIE4*		B'	sPCR 1-4	*HFIE9*	98% (*9* v *10*)	B'
	-	-		-	*PvuII* 1-1	*HFIE10*	97% (*8* v *10*)	B"

6.3.4 Comparison of genomic regions in the *HFIE* promoters

The six different promoter fragments identified from the genomic libraries were divided into three regions along the length of the DNA sequence (Figure 6.5A) and then compared to each other over these regions using the BLAST 2 Sequences program (Figure 6.5B; Tatusova and Madden, 1999). Region I was ~400 bp in length and included ~70 bp of *HFIE* coding DNA, the 5'UTR and a small fragment of the promoter. This region was relatively well conserved between the sequences (87-97% identical; Figure 6.5B), apart from several small insertions and base changes (Figure 6.5A).

Region II was ~500 bp in length and coincided with the start of a variable region in P4 *HFIE1* and insertions within the D3 *HFIE5* and D3 *HFIE10* promoters

A

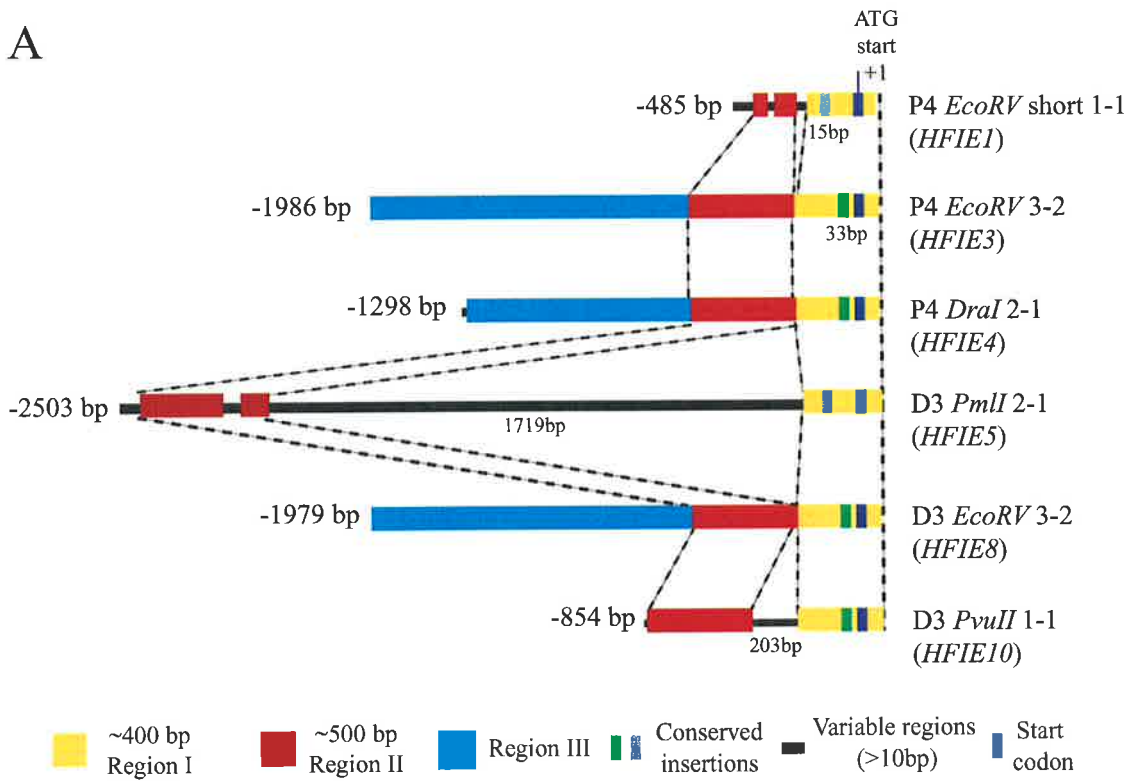

B

HFIE Promoter Library Sequences

HFIE Promoter Regions		P4 *EcoRV* short 1-1 (*HFIE1*)	P4 *EcoRV* 3-2 (*HFIE3*)	P4 *DraI* 2-1 (*HFIE4*)	D3 *PmlI* 2-1 (*HFIE5*)	D3 *EcoRV* 3-2 (*HFIE8*)	D3 *PvuII* 1-1 (*HFIE10*)
P4 *HFIE1*	region I		95%	92%	94%	93%	91%
	region II		92%	84%	94%	86%	89%
P4 *HFIE3*	whole			98%		95%	
P4 *HFIE4*	whole		98%			96%	
D3 *HFIE5*	region I	94%	90%	87%		96%	88%
	region II	94%	83%	78%		80%	79%
D3 *HFIE8*	whole		95%	96%			
D3 *HFIE10*	region I	91%	96%	96%	88%	97%	
	region II	89%	96%	93%	79%	97%	

Figure 6.5 Conservation of genomic regions in the *HFIE* library clones. **A** Regions of similarity in the six *HFIE* genomic library clones. **B** Percentage similarity of regions in the *HFIE* genomic clones as determined by the Blast 2 Sequences program (Tatusova and Madden, 1999). See Table 6.2 for gene nomenclature.

(Figure 6.5A). Region II was not complete in the P4 *HFIE1* clone and the last 60 bp showed limited homology to the other isolated *HFIE* sequences, including D3 *HFIE5*, which was its closest match (Figure 6.5B). Additional P4 *HFIE1* sequence was not obtained in the 5' direction and it was not possible to determine whether the upstream sequence was similar to that obtained for the other *HFIE* sequences. The 1719 bp partial retro-transposon insertion in D3 *HFIE5* did not cause any major deletions within the gene's promoter sequence, as region II (80% similar to D3 *HFIE8*; Figure 6.5B) was detected upstream of the insertion site (Figure 6.5A). Similarly, the 203 bp insertion in the D3 *HFIE10* clone did not appear to have altered region II, which was detected upstream and was 97% identical to the D3 *HFIE8* sequence (Figure 6.5B).

Region III was only detected in three of the promoter fragments that extended 5' of region II. This region was highly conserved in the P4 *HFIE3*, P4 *HFIE4* and D3 *HFIE8* clones and differed only by minimal base changes (Figure 6.5A and 6.5B). These four sequences were compared over the whole of their length and were 95-98% identical (Figure 6.5B).

6.3.5 Identification of *HFIE* promoter sequences by spanning PCR

It was uncertain whether the clones identified from the promoter library screens were representative of all the *HFIE* genomic sequences present in the *Hieracium* D3 and P4 genomes. To identify any other *HFIE* sequences, and to verify the presence of the TAA in-frame stop codon in the majority of *HFIE* clones, PCR primers were designed to conserved regions within the six *HFIE* genomic fragments spanning the ATG start codon. Two different primer sets were designed (sPCR and span; see

Figure 6.4) and used to amplify *HFIE* fragments from genomic DNA. The PCR products were cloned at random, ten to fifteen were sequenced for each plant and the resulting clones were aligned using PILEUP.

A further four *HFIE* sequences were identified, three from apomictic D3 and one from sexual P4, that shared varying levels of homology to the clones isolated from the promoter libraries. Clones were also identified that matched the promoter clones previously isolated from the promoter libraries. The ten different D3 and P4 *HFIE* genomic sequences were compared with the *HFIE* cDNA sequences over a 300 bp region spanning the putative ATG, and could be divided into two classes (Figure 6.6; Table 6.2).

The class I sequences from P4 and D3 were distinguished by their high similarity to *HFIE* cDNA sequences, the lack of a 33 bp insertion at position -93, and the presence of a GAA or GTA codon at base position +25 (Figure 6.6). The P4 class I clones, *HFIE1* and *HFIE2*, were 98% identical (Table 6.2) and both matched the P4 *HFIE* cDNA sequence closely. The *HFIE2* clone sequence produced an exact match for the cDNA, whereas *HFIE1* differed from the cDNA by several bases. Three class I clones were detected in apomictic D3; *HFIE5, HFIE6* and *HFIE7*. The *HFIE5* and *HFIE6* sequences were 98% identical to each other, and each differed from the D3 *HFIE* cDNA by one base pair in different positions, probably as a result of PCR artifacts. However, the D3 *HFIE5* and *HFIE6* clones clearly represented different genes, as a small two base pair deletion and several base changes distinguished them from one another (Figure 6.6). The *HFIE7* sequence was only 90% identical to *HFIE5* and *HFIE6*, because it contained a 19 bp deletion at base position +9 that resulted in a TAA stop codon at base position +44, and numerous small deletions, insertions and base substitutions (Figure 6.6).

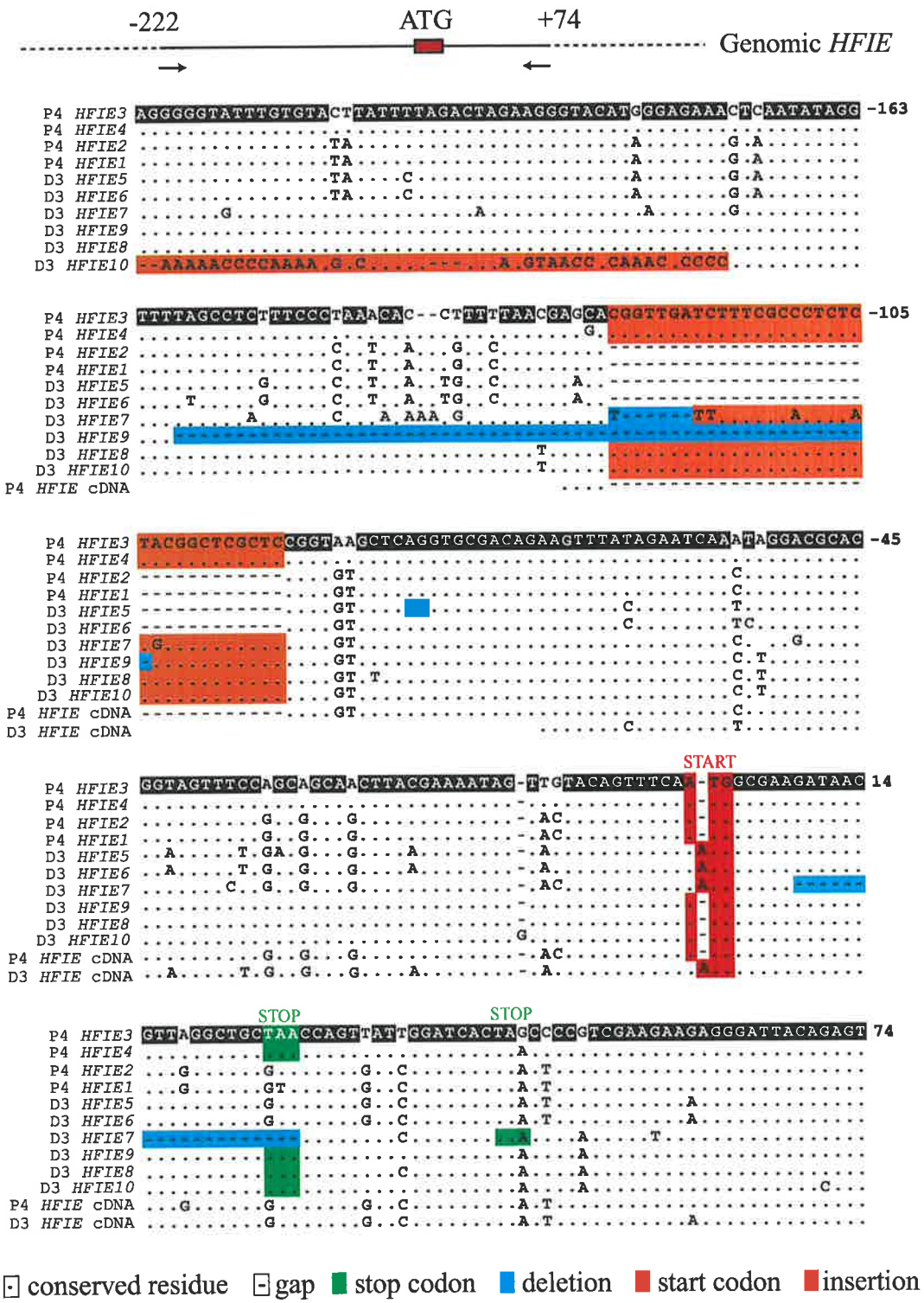

Figure 6.6 Comparison of the four P4 and six D3 genomic *HFIE* clones spanning the putative ATG start codon. The schematic diagram (top) shows the region of DNA being compared. The sequences are aligned relative to the P4 *HFIE3* clone. Black shading in the P4 *HFIE3* sequence indicates positions of high conservation in all sequences, and notable features are highlighted with coloured shading as indicated in the key at bottom.

The class II sequences from P4 and D3 were distinguished by the presence of a 33 bp insertion at position -93, and the presence of a TAA stop codon in the first *HFIE* exon at base position +25 (Figure 6.6). Two class II sequences were detected in P4, *HFIE3* and *HFIE4*, which were 97% identical to each other and differed only by base substitutions. (Figure 6.6; Table 6.2). In contrast, three class II sequences were detected in D3; *HFIE8*, *HFIE9* and *HFIE10*. D3 *HFIE8* and *HFIE9* were 98% identical to each other and differed by base substitutions and a 58 bp deletion in *HFIE9* at position -104. *HFIE10* was 97% identical to the *HFIE8* and *HFIE9* sequences, and differed by base substitutions and a 203 bp deletion at position -174. No *HFIE* cDNA sequences were identified from ovary cDNA samples that might have been derived from the class II genomic sequences.

6.3.6 Phylogenetic comparison of the D3 and P4 *HFIE* sequences

The ten fragments of *HFIE* genomic DNA that overlapped with the first exon of the *HFIE* cDNA were translated and aligned with the putative amino acid sequences of the *HFIE* cDNA clones (Figure 6.7A). In both plants, two of the class I sequences matched the putative amino acid sequence of the cDNA.

The PILEUP alignment of the ten genomic *HFIE* DNA sequences (Figure 6.6) was used to generate a phylogenetic tree showing the divergence between the sequences in the vicinity of the ATG start codon (Figure 6.7B). The putative class I *HFIE* coding genes from P4, *HFIE1* and *HFIE2*, and D3, *HFIE5* and *HFIE6* clustered in distinct groups that were closely related. Similarly, the non-coding class II P4 *HFIE3* and *HFIE4* clones and D3 *HFIE8* and *HFIE9* clones were similar, but diverged from the coding genes. Interestingly, the D3 *HFIE7* and *HFIE10* clones

A

```
     P4 HFIE1  M A K I T L G C E P V I G S L T P S K K R D Y
     P4 HFIE2  M A K I T L G C E P V I G S L T P S K K R D Y
P4 HFIE cDNA   M A K I T L G C E P V I G S L T P S K K R D Y
     D3 HFIE5  M A K I T L G C E P V I G S L T P S K K R D Y
     D3 HFIE6  M A K I T L G C E P V I G S L T P S K K R D Y
D3 HFIE cDNA   M A K I T L G C E P V I G S L T P S K K R D Y
     P4 HFIE3  M A K I T L G C * P V I G S L T P S K K R D Y
     P4 HFIE4  M A K I T L G C * P V I G S L T P S K K R D Y
     D3 HFIE8  M A K I T L G C * P V I G S L T P S K K R D Y
     D3 HFIE9  M A K I T L G C * P V I G S L T P S K K R D Y
    D3 HFIE10  M A K I T L G C * P V I G S L T P S K K R D Y
     D3 HFIE7  M A N . . . . . Q L S D H * P H R R R G I
```

B

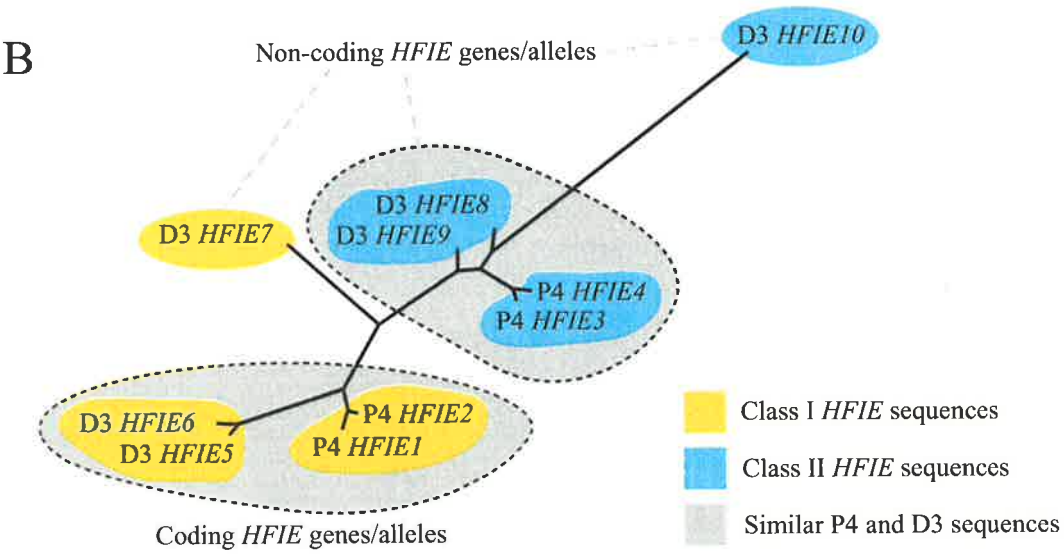

Figure 6.7 Comparison of *HFIE* sequences from sexual and apomictic *Hieracium*. **A** Putative amino acid sequence of the coding regions in the P4 and D3 *HFIE* genomic clones. **B** Unrooted phylogenetic tree showing the similarity between the P4 and D3 *HFIE* sequences. See Table 6.2 for gene nomenclature.

showed no clear counterparts in the P4 genome and were positioned some distance from the other D3 *HFIE* sequences (Figure 6.7B).

Collectively, the data obtained from the analysis of genomic *HFIE* sequences in *Hieracium* showed that four *HFIE*-like sequences were present in the genome of sexual tetraploid P4, and six *HFIE*-like sequences were present in the genome of apomictic triploid D3. These sequences could be divided into two classes based on sequence similarity, and the majority of these sequences in each plant did not appear to encode a functional *HFIE* cDNA.

6.3.7 Preliminary analysis of *HFIE:GUS* expression patterns

It seemed plausible, given the inability to clearly differentiate between the four P4 *HFIE* sequences and six D3 *HFIE* sequences on genomic blots (see Chapter 5), that some of the sequenced clones corresponded to alleles of the same gene. The D3 *HFIE* clones showed much greater variation than the P4 *HFIE* sequences, and displayed several large deletions and insertions. One of the insertions was detected in the putative D3 *HFIE5* coding promoter and represented a 1719 bp fragment of a retro-transposon. To determine whether the presence of this element in the promoter of the putative D3 coding gene could alter the spatial expression pattern of *HFIE*, promoter:GUS marker genes were generated and tested in *Arabidopsis*.

Four marker genes were generated to test the expression of the various *HFIE* promoter fragments. The *D3-* and *P4-EHFIE:GUS* constructs were generated by fusing the class II P4 *HFIE3* and D3 *HFIE7* promoter fragments to GUS respectively. Both constructs contained approximately 2 kb of DNA upstream from the ATG of the *HFIE* gene. Transgenic *Arabidopsis* No-0 and Col-4 lines

containing the *EHFIE:GUS* constructs showed no detectable GUS expression in flowers, leaves, siliques, ovules or seeds.

The *D3-cHFIE:GUS* marker gene contained approximately 2.2 kb of DNA upstream from the start codon of the class I D3 *HFIE5* gene, including the 1719 bp retroelement fragment. The *P4-cHFIE:GUS* marker gene contained approximately 500 bp of DNA upstream from the start codon of the class I P4 *HFIE1* gene, and this represented the same fragment of DNA as that in the *D3-cHFIE:GUS* gene without the retroelement insertion. *Arabidopsis* No-0 lines containing the *P4-cHFIE:GUS* gene showed GUS activity in sepals and anthers from an early stage of floral development (Figure 6.8A). GUS expression remained in the sepals during floral development (Figure 6.8B and 6.8C), and was restricted to the maturing pollen grains in the anthers after flower opening (Figure 6.8C and 6.8D). The *D3-cHFIE:GUS* gene showed a similar expression pattern in anthers (Figure 6.8E) and pollen grains (Figure 6.8F) to that observed in *P4-cHFIE:GUS* lines, but was not expressed in the sepals. GUS activity was not detected in ovules or seeds at any stage of development (Figure 6.8G).

The D3 and P4 *cHFIE:GUS* expression patterns showed that the class I P4 *HFIE1* and D3 *HFIE5* promoters contained elements capable of directing mRNA transcript to specific tissues. In contrast, the D3 and P4 *EHFIE:GUS* genes showed no detectable expression in any tissues, suggesting that the class II P4 *HFIE3* and D3 *HFIE8* promoters may be derived from non-functional genes. The retro-transposon insertion in the D3 *HFIE5* promoter appeared to alter the expression pattern of the *GUS* gene such that it was expressed at lower levels in the sepals. However, the lack of detectable *cHFIE:GUS* expression in ovules suggested that the promoter fragments were incomplete and lacking all of the required regulatory elements for expression. This made it difficult to determine if there were any spatial

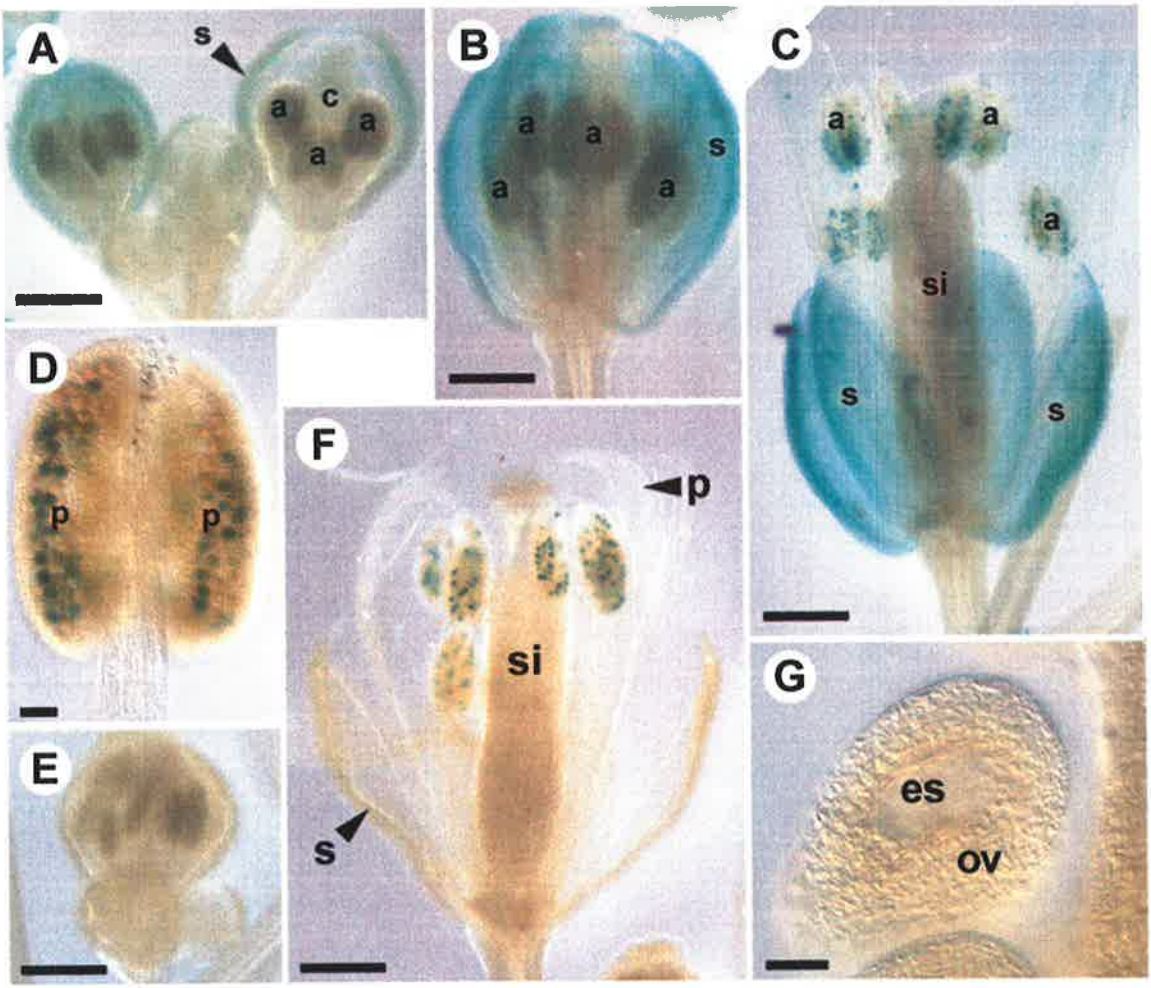

Figure 6.8 Expression of the P4 and D3 *cHFIE:GUS* genes in *Arabidopsis* No-0. Panels (**A**) to (**D**) show expression of the P4 *cHFIE:GUS* gene, and (**E**) to (**G**) show expression of the D3 *cHFIE:GUS* gene. **A** Young *Arabidopsis* flowers containing immature carpels (c) surrounded by the developing anthers (a) and sepals (s). **B** Anthesis stage flower. **C** Post-anthesis flower containing a developing silique (si) after pollination. **D** Anther containing maturing pollen (p) grains. **E** *Arabidopsis* flowers at similar stages to **A**. **F** Post-anthesis flower at a similar stage to **C**. **G** Fertilised ovule (ov) displaying no obvious GUS activity in the embryo sac (es). Bar = 1 mm in **A** to **C**, **F** and **E**, 50 μm in **D** and 30 μm in **G**.

differences in expression between the two genes that could be attributed to the retroelement insertion. Further analysis of these promoter fragments and transgenic lines is required before firm mechanistic conclusions can be drawn.

6.3.8 Further characterisation of the D3 *HFIE5* retroelement

The 1719 bp insertion in the putative D3 *HFIE5* coding promoter showed 38% putative amino acid identity and 52% similarity to a range of non-LTR retroelement reverse transcriptases from *Oryza sativa* (e.g. Ac BAA95894), *Arabidopsis* (e.g. Ac NP_680334) and *Sorghum bicolor* (e.g. Ac AAM94327). The insertion was localised within a small A-rich region of the D3 *HFIE5* promoter, and was absent from the class I P4 *HFIE* coding sequences. The insertion represented only a partial fragment of the retro-element reverse transcriptase and was at least 2.4 kb short of a full length gene (Figure 6.9A). The fragment was in complementary orientation to the D3 *HFIE5* gene and lacked any apparent promoter sequences or regulatory elements.

Genomic analysis of the *HFIE5* transposon (*2-1*) fragment identified a large number of similar sequences in the genomes of sexual P4 and apomictic D3 (Figure 6.9B), as evidenced by specific bands and a smeary pattern of background hybridisation. Some of the bands appeared to be conserved between the P4 and D3 genomes and the background hybridisation possibly corresponded to a large number of degenerate variable sequences. From the genomic analysis it was difficult to estimate whether the P4 or D3 genome contained more of the 2-1-like sequences, but a higher frequency of specific prominent bands were detected in D3 genomic DNA than in P4.

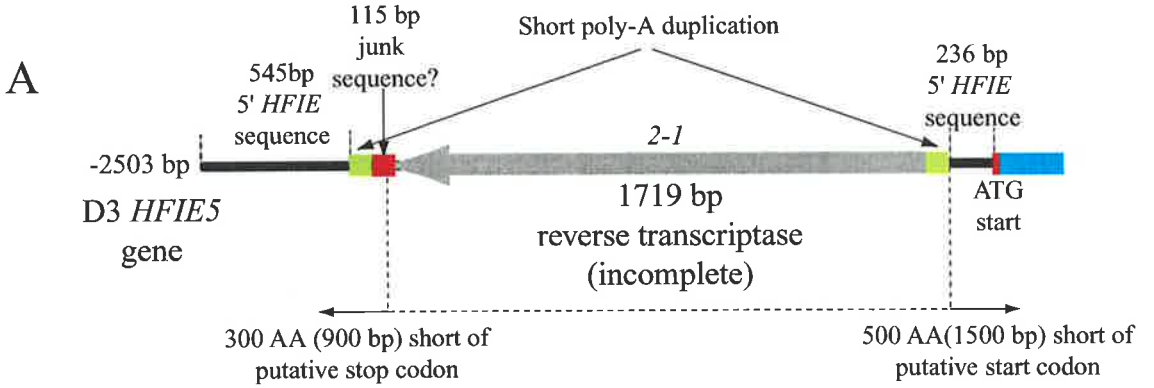

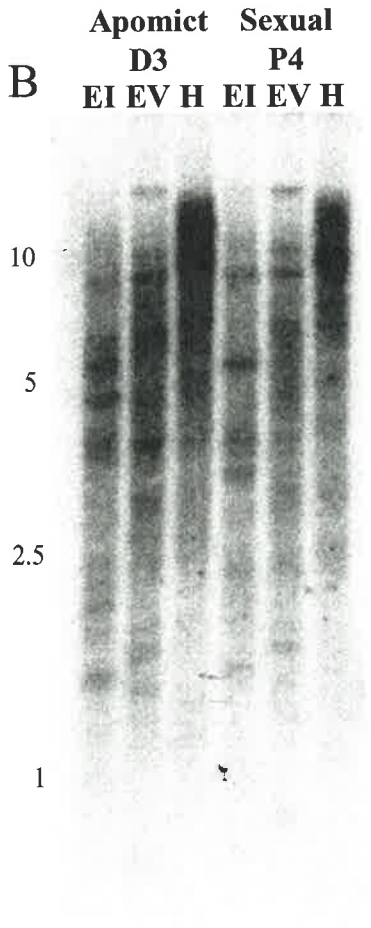

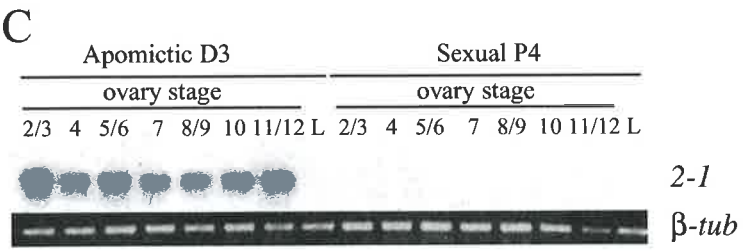

D

Transposon-like sequences from apomictic Hieracium

Clone ID	***Tissue***	***Best Match and Similarity***
2-1 (D3 *HFIE5*)	D3 ovules	*O. sativa* non-LTR retroelement reverse transcriptase; 38% ID, 52% SIM
26.07	D2 ovules	*A. thaliana* putative Enhancer/Supressor-mutator (En/Spm)-like transposon protein (class II); 43% ID, 60% SIM
27.14	D2 ovules	*A. thaliana* putative retroelement pol polyprotein; 28% ID, 44% SIM
6sp 03-02	D3 ovules	*S. bicolor* retroelement polyprotein; 60% ID, 76% SIM

Figure 6.9 Endogenous transposon sequences in *Hieracium*. **A** Schematic diagram of the D3 *HFIE5* gene showing the position of the *2-1* non-LTR retroelement. **B** Genomic blot hybridised with radioactively labelled *2-1* probe. 15 ug samples of genomic DNA were digested with *EcoRI* (EI), *EcoRV* (EV) or *HindIII* (H). The size of DNA fragments in kilobases is indicated at left. **C** RT-PCR expression of the *2-1* transposon sequence in ovaries and leaves from apomictic D3 and sexual P4. The loadings were equilibrated with a β-*tubulin* control. Numbers indicate stages of floral development (see Appendix 1). **D** Transposon sequences identified from apomictic *Hieracium*. The *2-1*, 27.14 and 6sp 03-02 sequences show homology to retroelement sequences. SIM - Similarity, ID - Identity.

RT-PCR analysis using *2-1* specific primers detected the presence of *2-1* mRNA transcript in ovaries from stage 2 to 12 in apomictic D3 (Figure 6.9C). In contrast, *2-1* mRNA was not detected in ovaries or leaves from sexual P4 or young unexpanded leaves from D3. It is unlikely that the expressed *2-1* sequence was derived from the D3 *HFIE5* promoter in apomictic D3, because transcript could not be detected by RT-PCR in *Arabidopsis* plants containing the promoter fused to GUS, and thus the origin of the expressed *2-1* sequences in apomictic D3 ovaries was uncertain.

At least four putative transposon sequences have been identified in ovule cDNA samples from apomictic *Hieracium* (Figure 6.9D). Interestingly, another retroelement clone (6sp03-02) was identified in a differential display screen targeting sequences expressed in ovaries from apomictic D3 that were absent from ovaries from sexual P4 (T. Tsuchiya and A. Koltunow, unpublished). It is uncertain whether the 26.07 and 27.14 sequences also show differential expression between the sexual and apomictic plants.

These data highlighted the presence of retroelements within the genome of apomictic D3 and sexual P4 *Hieracium*. Whether these elements represent active transposons is uncertain, but they do provide a tool for the analysis of genome evolution in apomictic and sexual plants.

6.4 Discussion

6.4.1 *D3-cHFIE* encodes a functional WD-40 *Polycomb* group (PcG) protein

The *Arabidopsis FIS* PcG genes regulate the initiation of endosperm development (Luo et al., 2000). Although numerous hypotheses have suggested that the function

of these genes might be compromised in autonomous apomictic plants, few studies have addressed this question. Recent studies have shown that *FIS*-like PcG genes are expressed during seed development in *Hieracium*, including *HFIE*, which is highly conserved in apomictic and sexual plants (see Chapter 5).

In this study, complementation data showed that the *D3-cHFIE* clone encoded a functional protein capable of restoring fertilisation-dependent endosperm development in emasculated *Arabidopsis fie-2* seeds. Interestingly, *fie*-2 embryos aborted in complementation lines despite the recovery of wild-type endosperm development, and the endosperm-specific *MEDEA* promoter may have conferred this partial complementation. The endosperm specificity of *MEA:D3-cHFIE* expression was expected based on the *AtMEA:*GUS protein fusion data that showed specific *GUS* activity in the central cell nucleus prior to fusion and during the early endosperm divisions but not in developing embryos (Luo et al., 2000).

This finding contrasts with a study that reported the embryo lethality of *fie*-1 embryos is affected by alterations in endosperm development (Kinoshita et al., 2001). Kinoshita et al., (2001) showed that a *pFIE::FIE-GFP* gene containing 1.7 kb of 5' flanking sequence fused to the full length *FIE* cDNA and *GREEN FLUORESCENT PROTEIN* (*GFP*), recovered both wild type *FIE* embryo and endosperm development in *Arabidopsis fie-1* mutants. Analysis of GFP expression suggested that the complementing *pFIE::FIE-GFP* protein was only localised to the early endosperm nuclei, and was not detectable in the embryo.

Previous spatial and temporal expression studies of the *Arabidopsis FIE* promoter have used varying lengths of 5' flanking DNA fused to *GUS* or *GFP*. Luo et al., (2000) showed that a *FIE:GUS* chimeric gene, containing 6 kb of 5' flanking sequence, the first eight exons and introns and 50 bp from exon nine of *FIE* directed *GUS* expression to both the embryo and endosperm. Similarly, two *FIE:GFP*

chimeric genes containing 1.3 kb or 4.9 kb of 5' flanking sequences from *FIE* fused to *GFP* directed expression to the early endosperm during the first four mitotic divisions of the nuclei, and then to the developing embryo and endosperm at later stages of development (Yadegari et al., 2000). It is possible that the *pFIE::FIE-GFP* construct was expressed at low levels in the embryo, below the sensitivity of detection, thus leading to complementation of *fie*-1 embryos. Alternatively, interaction of the *D3-cHFIE* protein with endogenous *Arabidopsis* factors in the endosperm may not be sufficient to restore both the wild-type endosperm phenotype and viable embryo phenotype. Embryo development in *fie-2* plants containing the *MEA:D3-cHFIE* construct was not analysed to determine whether embryo development proceeded further than in *fie-2/+* plants. It is also possible that the lack of a *HFIE* 5'UTR in the *MEA:D3-cHFIE* gene might have altered the regulation of the resulting protein.

Irrespective of the reasons why *MEA:D3-cHFIE* did not complement the embryo lethality of *fie-2*, the complementation assay showed that differences between the putative amino acid sequences of *D3-cHFIE* and *P4-cHFIE* are unlikely to alter *D3-cHFIE* function in *Hieracium* such that it cannot interact with other PcG proteins to prevent autonomous endosperm development. Alterations in the activity of one or more other members of a putative *Hieracium* PcG complex cannot be excluded. Alternatively, the entire putative FIS PcG complex may be functionally competent in apomictic *Hieracium*, and autonomous endosperm development might stem from an alteration to PcG activity by the generation of precocious "fertilisation-like" signals within the ovule.

6.4.2 Divergent *HFIE* sequences are indicative of two *HFIE* genes per genome and multiple heterogeneous alleles

Genomic blot analyses did not provide conclusive data as to the number of *HFIE* genes present within the genome of sexual P4, but estimates suggested that one or two *HFIE* genes might exist (see Chapter 5). In this study, four different genomic *HFIE* sequences were identified in tetraploid sexual P4, and these sequences clustered in two related classes after phylogenetic analysis. Class I sequences, *HFIE1* and *HFIE2*, matched the P4 *HFIE* cDNA and class II sequences, *HFIE3* and *HFIE4*, did not. Inheritance and genetic studies suggest that P4 is an autotetraploid plant derived from a doubling of a parental diploid plant (R. Bicknell, pers. comm.). Thus, barring somatic mutation, there are two sets of identical diploid genomes in each somatic cell. Combined with the sequence data, this suggests that there are two *HFIE* genes present per genome in sexual P4, each with a corresponding allele. This is somewhat similar to maize, which contains two diverged *FIE* genes (Danilevskaya et al., 2003).

Six different *HFIE* sequences were identified from triploid apomictic D3 that grouped into two classes, similar to those detected in P4. The class I *HFIE5* and *HFIE6* sequences matched the D3 *HFIE* cDNA and were closely related to *HFIE7*, whereas the class II sequences *HFIE8*, *HFIE9* and *HFIE10* did not match the cDNA. The phylogenetic origin of apomictic D3 is uncertain, but it may have arisen from (i) a cross between a tetraploid (4n) and diploid (2n) plant, (ii) self-fertilisation of an unreduced egg cell (2n) with reduced pollen (n), or (iii) self-fertilisation of a reduced egg cell (n) with unreduced pollen (2n). Irrespective of the plant's origin, the *HFIE* sequence data suggested that similar to sexual P4, two *HFIE* genes were present per genome in apomictic D3, each with two corresponding alleles.

The inability of *Hieracium* genomic blots to distinguish between the two different *HFIE* genes in D3 and P4 suggested that they might lie within a region of duplicated DNA. This could be addressed by mapping the position of the *HFIE* genes onto specific chromosomal regions. The presence of the class II non-coding genes and their conservation in both D3 and P4 raises questions about their function. It is highly likely that the class II *HFIE* genes represent pseudogenes; transcript was not detected that matched their sequence, they contained in frame stop codons and their promoter fragments failed to direct detectable GUS expression.

6.4.3 Allelic diversity and asexual reproduction

The maintenance of sexual reproduction in plants and animals is an interesting problem in evolutionary theory, because all else being equal, asexual populations have a twofold fitness advantage over their sexual counterparts and should rapidly outnumber a sexual population because every individual has the potential to reproduce (Agrawal, 2001). The absence of segregation and recombination in asexual plants also predicts reduced levels of genetic variation compared to sexual species (Diggle et al., 1998). However, studies have shown that high levels of genotypic variation can occur within and between closely related asexual species (Nybom, 1998; Waxman and Peck, 1999; Diggle et al., 1998; Storchova et al., 2002). Furthermore, sexual reproduction predominates among eukaryotes, and in general, asexual clones tend to be short-lived offshoots from sexual species.

One of the most appealing hypotheses to explain why sexual populations are not overtaken by asexual species, applicable to populations of all sizes, is that sex is

maintained as a way of efficiently purging deleterious mutations from the genome (Kondrashov, 1982; Rice, 1999). If the mutation rate is sufficiently high and deleterious mutations interact synergistically, then sexual populations can clear mutations much more efficiently and thus enjoy a higher mean fitness at mutation-selection balance than asexual populations (Charlesworth, 1990; Agrawal and Chasnov, 2001).

The analysis of allelic *HFIE* gene sequences in this study provided an insight into the genotypic variation between two closely related sexual and asexual *Hieracium* species, and tended to support the above hypothesis. The predominant differences between the P4 *HFIE* alleles were base substitutions, probably caused by environmental changes during evolution (Waxman and Peck, 1999). In contrast, the D3 *HFIE* alleles varied significantly by base pair substitutions, large deletions and insertions, one of which was caused by a retroelement. Previous studies in apomictic plants using genetic markers and isozyme analyses have also noted the highly heterozygous nature of apomictic species (Ellstrand and Roose, 1987; Krahulcova et al., 2000; Shi et al., 1996; Mes et al., 2002). However, those studies have not considered sequence changes in specific genes. Higher allelic variation in apomictic D3 may result from an inability to efficiently clear mutations from the genome by meiosis.

Chasnov (2000) showed that differences in mutation load due to recessive deleterious mutations can result in substantial advantage to sexual reproduction over asexual reproduction under some conditions. However, despite the significant levels of allelic variation in apomictic D3 and the detection of putative deleterious mutations (such as the deletion in *HFIE7*), at least one and possibly two functional *HFIE* sequences were present in the D3 genome. In terms of evolution, the presence of these coding alleles suggests that at least one or two functional D3 *HFIE* genes

are required for plant development in *Hieracium*. Presumably if *HFIE* function was not required, a full-length functional cDNA would not be produced or the promoter would be rendered incapable of directing expression. The temporal expression of the *HFIE* mRNA was similar in both sexual and apomictic *Hieracium* plants (see Chapter 5) and the putative D3 *HFIE5* coding promoter was capable of directing similar anther and pollen *GUS* expression to the putative P4 *HFIE1* coding promoter, despite the presence of the retroelement insertion. Many retrotransposon insertions in close proximity to genes affect their expression in a negative fashion by decreasing or abolishing transcription of the gene (White et al., 1994). In other cases, however, insertion of a retrotransposon sequences within or near a gene has more complex effects on gene expression, including alterations of temporal and spatial patterns of transcription, or no effect at all (Flavell et al., 1994; Kunze et al., 1997). Further studies are required to determine the spatial localisation of *HFIE* sequences during ovule development in apomictic and sexual plants.

6.4.4 Retroelements and increased chromosomal DNA levels in apomictic *Hieracium*

Retrotransposons are ubiquitous in plants and play a major role in plant gene and genome evolution (Kumar and Bennetzen, 1999). Two classes have been detected in plants including the long terminal repeat (LTR) and non-LTR retrotransposons. These elements are present in high copy numbers making them the major constituents of plant genomes (Grandbastien, 1992). Most transposable elements, commonly including retrotransposon fragments (White et al., 1994), are found within functioning genes.

Estimates suggest that around 30% of the apomictic *Hieracium* genome is comprised of retrotransposons (R. Bicknell, pers. comm.). The *2-1* retroelement identified in the *HFIE5* promoter showed homology to the reverse transcriptase protein of a non-LTR long interspersed repetitive element (LINE) from *Oryza sativa*. Retroelements were also detected in the promoters of the two *FIE* genes from maize (Danilveskaya et al., 2003), but this is not surprising given that as much as 85% of the maize genome is comprised of retrotransposons (SanMiguel et al., 1998). A large number of degenerate *2-1*-like sequences were detected in genomic DNA from apomictic D3 and sexual P4, and it is common for heterogeneous retroelements to be found in the promoters of many wild-type plant genes (White et al., 1994). The *HFIE5 2-1* LINE was incomplete, however, and was lacking the intact *gag* and *pol* regions characteristic of active LINE retroelements. This is quite common for retrotransposon insertions in plants (Wessler et al., 1995; White et al., 1994), but little is known about the mechanisms of LINE transcription or integration (Kumar and Bennetzen, 1999). Interestingly, the *2-1* LINE was not detected in either of the putative *HFIE* coding alleles from sexual P4, suggesting that its insertion in the D3 *HFIE5* promoter is a relatively recent event in terms of evolution.

Many retrotransposons show unique patterns of developmental and/or environmental regulation, and are often transcriptionally activated by various biotic and abiotic stress factors. For instance, transcripts of tobacco *Tnt1* are primarily detected in roots (Pouteau et al., 1991). DNA methylation has also been proposed as a means of containing the spread of transposable elements in host genomes (Yoder et al., 1997), and some retrotransposons can be induced in response to hypomethylation (Hirochika et al., 2000). LINE *2-1* transcript was detected during ovary development in apomictic D3 *Hieracium*, but was absent from ovaries in

sexual P4. Another *Hieracium* retroelement, 6sp 03-02, showing homology to a *Sorghum bicolor* retrotransposon was also differentially upregulated in D3 ovaries compared to sexual P4 (A. Koltunow and T. Tsuchiya, unpublished). It is uncertain why two different retrotransposon sequences are expressed at high levels in ovaries from apomictic D3 when they are expressed at low levels or undetectable in the ovaries of sexual P4. It is possible that these expression differences relate to increased abiotic stress in apomictic D3, changes in genomic methylation level or a greater number of retroelements in the D3 genome.

Retrotransposons play a major role in determining the size of plant genomes (Kumar, 1996). For example, small genomes in plants like *Arabidopsis* (1C = 130 Mbp) might be the consequence of low levels of retrotransposon insertions (Wright et al., 1996), whereas large genomes in plants like faba bean and maize might be the result of successful colonisation and amplification of retrotransposons (Pearce et al., 1996; SanMiguel et al., 1998). Flow cytometry analysis of seeds from sexual P4 and apomictic D3 highlighted that the DNA content per chromosome was higher in the apomict (see Chapter 2), and similar results have been found in apomictic *Hypericum* species (F. Matzk, pers. comm.). In apomictic plants, transposable elements may have the potential to spread rapidly in evolutionary terms (Wright and Finnegan, 2001), because they lack the means to eradicate deleterious insertions. In contrast, accumulation of retroelements in sexual species may be counteracted in three main ways; (i) after homologous chromosome pairing during meiosis, internal hemizygous insertions may loop out and be removed by repair enzymes, (ii) numerous regions of low homology (due to hemizygous insertions) may suppress meiotic pairing of homologous chromosomes and increase the frequency of univalents, and (iii) additional hemizygous copies may cause incorrect pairing and unequal cross overs that result in regional deletions (Bennetzen and Kelogg, 1997;

Fedoroff, 2000; Kidwell and Lisch, 2001; Devos et al., 2002). It is possible that the larger size of the D3 genome measured by flow cytometry may be caused by accumulation of retroelements.

Results from this study showed that it was difficult to quantify the relative numbers of retroelements in the D3 and P4 genomes by conventional analytical means. However, the detection of three different retroelement transcripts in apomictic D3, some of which are not expressed in sexual P4, provides support for the hypothesis that the D3 genome contains more inserted and active retroelements. These retroelement sequences provide a tool for the further analysis of genome size and evolution in apomictic *Hieracium*.

6.4.5 Elucidation of endogenous *HFIE* function in sexual and apomictic plants

Collectively, the data presented in this chapter suggest that despite the significant allelic diversity detected in *HFIE* sequences, at least one functional *HFIE* gene exists in the genome of apomictic D3. The protein product of this gene is capable of complementing the autonomous endosperm phenotype of the *Arabidopsis fie-2* mutant, suggesting that it can interact as part of a repressive PcG complex. Although complementation showed function of the *HFIE* sequence in *Arabidopsis*, the endogenous function of *HFIE* and other *HFIS* genes during autonomous seed development in *Hieracium* is uncertain. RNA interference (RNAi) silencing technologies targeting the down-regulation of the *HFIE* mRNA would address the function of *HFIE* in apomictic and sexual *Hieracium* plants and enable an

examination of the role of *HFIE* genes during sexual and apomictic reproduction (Chapter 7).

Chapter 7: Silencing of *FIE* genes in sexual and apomictic *Hieracium*

7.1 Introduction

In the *Arabidopsis* genome a single *FIE* gene is detected on chromosome three and appears to play a role in regulating endosperm and embryo development (Ohad et al., 1999; Kinoshita et al., 2001). In contrast, two *fie* genes are detected in maize, *ZmFIE1* and *ZmFIE2*, which are likely to have diverse functions and probably originate from two different ancestral genomes (Danilevskaya et al., 2003). In apomictic D3 and sexual P4 *Hieracium* plants, two *HFIE* genes were detected per genome (see Chapter 6). Isolation and analysis of 5' fragments from these genes highlighted an elevated degree of allelic diversity in apomictic D3 compared to sexual P4. Despite this variation, the D3 and P4 *HFIE* genes could be divided into two classes based on sequence comparisons; coding and non-coding. Only one of the *HFIE* genes in each plant appeared capable of producing a full length functional mRNA and limited genomic analyses suggested that the two genes might have arisen from an ancient duplication event (see Chapter 6).

Hypotheses have suggested that altered *FIS* gene function might lead to fertilisation-independent endosperm formation in autonomous apomictic plants (Grimanelli et al., 2001). To address the function of *HFIE* genes during seed development in sexual and apomictic *Hieracium*, RNA interference (RNAi) silencing technology was utilised to silence the *HFIE* gene (Wesley et al., 2001). RNAi, also known as hairpin RNA (hpRNA) or double stranded RNA (dsRNA), has

proved to be a successful means of silencing the mRNA expression of a gene in various plant systems including *Arabidopsis*, tobacco, cotton, wheat, maize and barley by transient or stable transformation (Wesley et al., 2001; Zentella et al., 2002; Schweizer et al., 2000). Prior to this study, RNAi technology had not been utilised in *Hieracium*. In this chapter the generation and analysis of transgenic *Hieracium* plants containing *HFIE:RNAi* genes is described. Results from this study suggest that *HFIE* function is required for plant and seed development in autonomous apomictic *Hieracium*.

7.2 Materials and Methods

7.2.1 Generation of *35S:HFIE:RNAi* and *MEA:HFIE:RNAi* silencing constructs

RNA interference (RNAi) constructs targeted against the coding *HFIE* genes from sexual and apomictic *Hieracium* were generated using a 442 bp internal fragment of the D3 *HFIE* cDNA (Figure 7.1A) and the pKANNIBAL (35S:pN6) vector (for maps and information see Wesley et al., 2001). Two primer sets were designed to amplify and clone the 442 bp *HFIE* fragment into pKANNIBAL in both sense (S) and antisense (AS) orientations, thus generating the *35S:HFIE:RNAi* gene. The S fragment was amplified using the FIESFWD-*XhoI* and FIESREV-*EcoRI* primers (see Appendix 3), digested with *XhoI* and *EcoRI* and ligated with *XhoI/EcoRI* digested pKANNIBAL, downstream of the Cauliflower Mosaic Virus (CaMV) *35S* promoter and upstream of the GUS intron spacer. The AS fragment was amplified using the FIEASFWD-*XbaI* and FIEASREV-*HindIII* primers (see Appendix 3), digested with *XbaI* and *HindIII* and ligated to *XbaI/HindIII* digested

HFIE(S):pKANNIBAL, downstream of the GUS intron. The resulting *35S:HFIE*(S/AS):pKANNIBAL plasmid was digested with *NotI* to release the 4.6 kb silencing cassette, and this was ligated to *NotI*-digested pART27 binary vector (Gleave, 1992), to generate the *35S:HFIE:RNAi* gene (Figure 7.1B).

To target the silencing construct specifically to the embryo sac, the CaMV *35S* promoter was excised with *SacI* and *XhoI*, and replaced with 2004 bp of DNA upstream from the ATG of the *Arabidopsis MEDEA* gene. This promoter fragment was amplified from the *AtMEA:GUS* construct (see Section 3.2.2) using FIS1FWD2 and FIS1REV1' primers (see Appendix 3), and cloned into the *SacI-XhoI* site of the *HFIE*(S/AS):pKANNIBAL vector. The resulting *MEA:HFIE*(S/AS):pKANNIBAL was digested with *SacI* and *NheI* to release the silencing cassette, and this was cloned into *SacI/XbaI* digested pBINplus binary vector to generate the *MEA:HFIE:RNAi* gene (Figure 7.1C).

7.2.2 Transformation of *Hieracium* plants

Both genes were mobilised in *Agrobacterium* strain LBA4404 and transformed into D3 and P4 *Hieracium* as per Section 3.2.2. Transgenic plants were identified by PCR analysis using the FIESFWD and FIESREV primers, which amplify a 450 bp construct band in positive transformants, along with a 2 kb endogenous genomic band in all D3 plants, or a 1 kb endogenous genomic band in all P4 plants. A total of nine D3 and nine P4 transgenic plants containing the *35S:HFIE:RNAi* gene and three D3 transgenic plants containing the *MEA:HFIE:RNAi* gene were obtained.

7.2.3 Tissue collection and total RNA extraction

Young unexpanded leaves (1.4 - 3.0 cm) were collected from D3 and P4 wild type (WT) and *35S:HFIE:RNAi* plants. Stage 4, 6, 7, 8 and 10 floral buds (see Appendix 1) were collected from D3 *35S:HFIE:RNAi* plants #2, #5 and #7 and D3 *MEA:HFIE:RNAi* plants #5, #6 and #7 and dissected to harvest the ovaries. Receptacle tissue from stage 4 and 6 floral buds was also collected from D3 WT and *35S:HFIE:RNAi* plants #2, #5 and #7 by removing the sepals, florets and stem tissues. All tissues were collected in 1.5 mL eppendorf tubes, frozen immediately upon dissection in liquid nitrogen and stored at -80°C. Total RNA samples were extracted as per Section 5.2.1.

7.2.4 RT-PCR analysis of HFIE expression

RNA samples were quantified using a spectrophotometer (Shimadzu) and RT-PCR analysis was performed as per Section 5.2.7.

7.2.5 Haematoxylin stains of D3 *35S:HFIE:RNAi* and *MEA:HFIE:RNAi* seeds

Ovaries were dissected from stage 7, 8, 9 and 10/11 florets from D3 WT, *35S:HFIE:RNAi* lines #2, #5 and #7 and stained with haematoxylin as per Section 2.2.2. At least 274 ovaries (eight capitula) were examined for each line.

7.2.6 Fixation, embedding and sectioning of *Hieracium* seeds

Ovaries were collected from stage 2, 3, 4, 7 and 10 florets from *35S:HFIE:RNAi* plants for fixation and sectioning. Ovary samples were dissected from the other floral organs prior to fixation, and carefully slit along the outer ovary wall with a sharp blade to allow penetration of fixatives and resins. Tissues were fixed in 3% glutaraldehyde, 0.1M sodium cacodylate buffer, pH 7.0 overnight, or longer, and then rinsed three times in 0.1M sodium cacodylate buffer, pH 7.0 prior to embedding.

The fixed, washed tissue was dehydrated through a graded acetone series to 100% and then embedded in Spurr's resin (Spurr, 1969). Blocks were trimmed, serially sectioned at 2 μm using a Reichart Jung microtome, and the sections stained in 0.1% toluidine blue in 0.02% sodium carbonate and photographed using a Spot Digital Camera (Diagnostic instruments) under brightfield optics on a Zeiss Axioplan microscope. Sectioning and embedding were performed by Susan Johnson and Ana Claudia Araujo (CSIRO, Adelaide).

7.3 Results

7.3.1 Generation of *35S:HFIE:RNAi* and *MEA:HFIE:RNAi* transgenic lines

Genes inserted into the KANNIBAL intron-hairpin RNA (ihpRNA) RNAi vector have been successfully used to down-regulate mRNA expression of marker genes and endogenous regulators in tobacco, *Arabidopsis*, cotton and rice, with silencing observed in 90% of the plants generated (Wesley et al., 2001). To determine the function of *HFIE* during plant and seed development in *Hieracium*, a fragment of

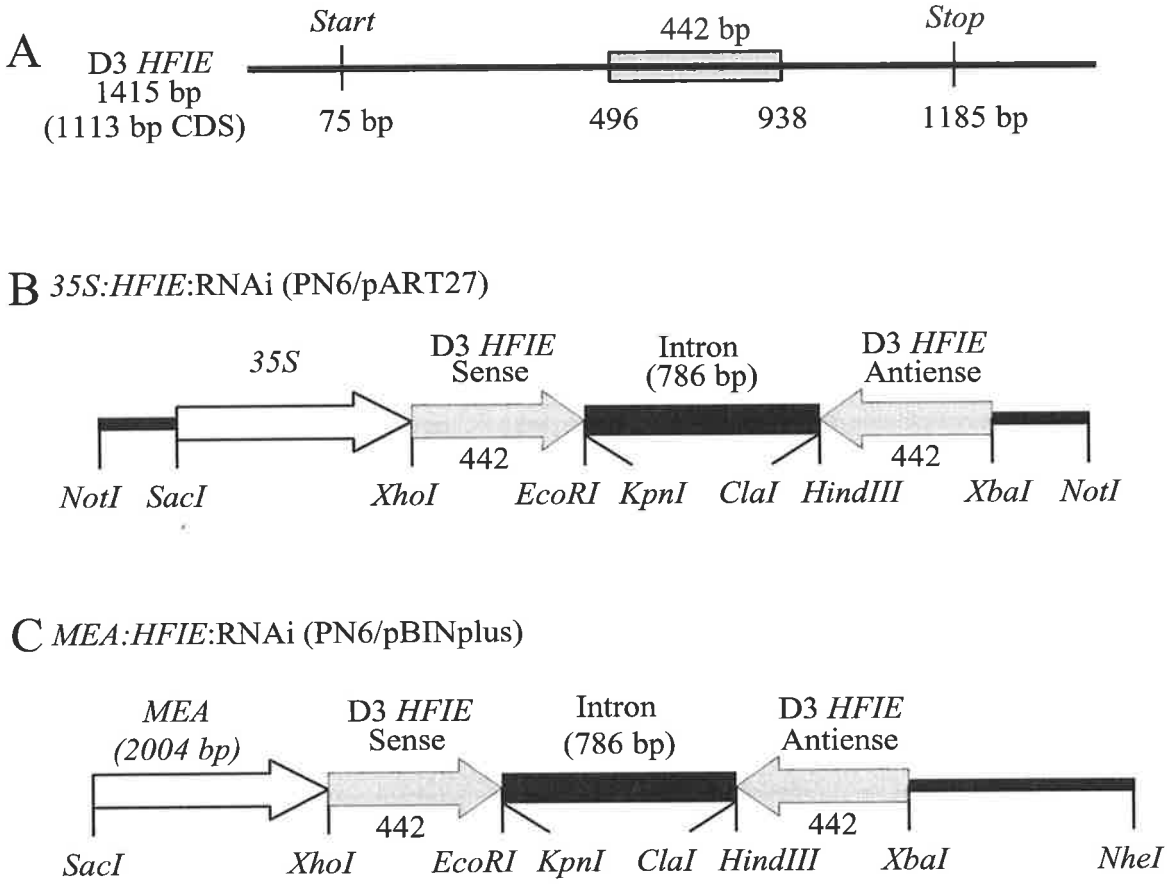

Figure 7.1 *HFIE:RNAi* genes in the KANNIBAL vector. **A** Schematic diagram of the D3 *HFIE* cDNA showing the region of mRNA targeted for silencing in the RNAi genes. **B** Schematic representation of the *35S:HFIE:RNAi* gene. **C** Schematic representation of the *MEA:HFIE:RNAi* gene.

HFIE cDNA was inserted into the KANNIBAL vector (Figure 7.1) and introduced into sexual and apomictic *Hieracium*. In total, nine D3 and nine P4 transgenic plant lines containing the *35S:HFIE:RNAi* gene, and three D3 lines containing the *MEA:HFIE:RNAi* gene were identified.

7.3.2 General morphology of *35S:HFIE:RNAi* plants and *MEA:HFIE:RNAi* plants

When compared to wild-type plants, the *HFIE:RNAi* genes had no obvious effect on seed, flower or plant morphology in the nine sexual P4 transgenic lines or in 10 of the twelve D3 transgenic lines. Only two D3 lines, #5 and #7, which contained the *35S:HFIE:RNAi* gene showed an obvious phenotype. Whereas wild type D3 plants usually attained a primary floral meristem height of 60 ±5 cm (n=25), line #5 attained a maximum height of 35 ±4 cm and line #7 attained a maximum height of 40 ±5 cm (Figure 7.2A). The number of capitula per floral raceme in these lines did not differ to wild type and consequently, #5 and #7 appeared bushier in growth habit because of shorter inflorescence and stem internodes.

Seed development was also altered in *35S:HFIE:RNAi* lines #5 and #7, and the number of fat black (FB) fertile seeds was significantly reduced compared to wild type D3 plants (Figure 7.2B). Seeds were collected from D3 WT, *AtFIS2:GUS, 35S:HFIE:RNAi* and *MEA:HFIE:RNAi* lines and divided into FB and skinny black/brown (B) classes (Figure 7.2C) as described in Section 2.2.3. D3 WT and *AtFIS2:GUS* transgenic plants flowering under the same conditions as *HFIE:RNAi* plants produced between 70% and 85% FB seeds per capitulum (75% on average; Figure 7.3A and 7.2C), and the remainder were skinny or brown in appearance

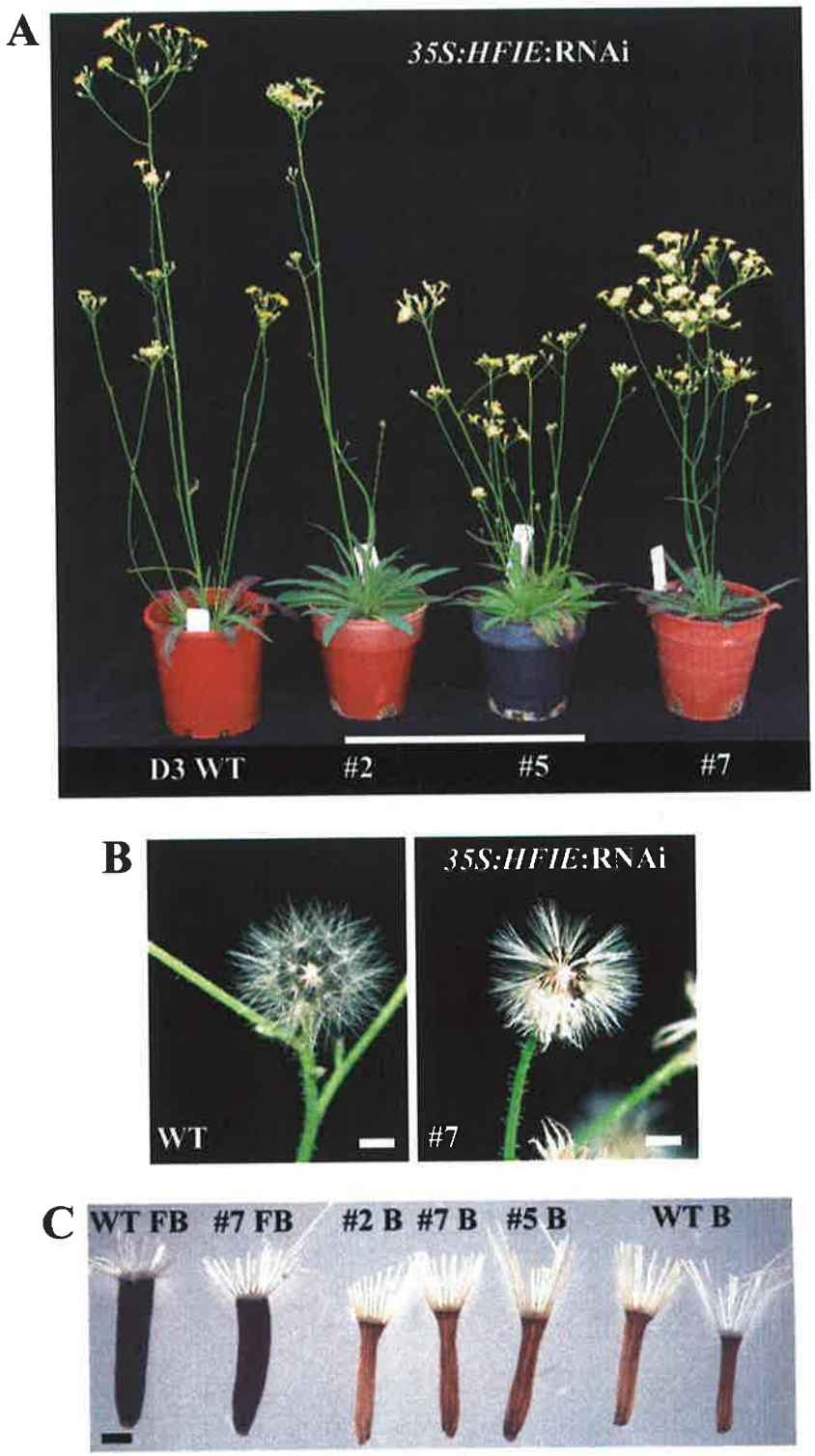

Figure 7.2 General morphology of apomictic *Hieracium* D3 *35S:HFIE:RNAi* plants compared to wild type (WT). **A** Growth habit of a D3 WT plant and *35S:HFIE:RNAi* lines #2, #5 and #7. **B** Seed heads from D3 WT and *35S:HFIE:RNAi* line #7. **C** Fat black (FB) and skinny brown (B) seeds from D3 WT plants and *35S:HFIE:RNAi* lines #2, #5 and #7. Bar = 21.5 cm in **A**, 3 mm in **B** and 1 mm in **C**.

(Figure 7.3A and 7.2C). Skinny black and brown seeds are sterile in the majority of cases (see Section 2.3.6). Of the total seeds produced per capitulum in the D3 *35S:HFIE:RNAi* lines, 54% were FB in appearance in line #5 and only 5% were FB in line #7 (Figure 7.3A). The remaining seeds were shrivelled and brown, and resembled sterile seeds from wild type D3 plants (Figure 7.2C). A slight reduction in the percentage of FB seeds was also observed in D3 *35S:HFIE:RNAi* line #2 and D3 *MEA:HFIE:RNAi* lines #5 and #6 (Figure 7.3A). No change in seed set was affected by cross-pollinating flowers from D3 *35S:HFIE:RNAi* line's #5 and #7 with pollen from WT D3, P4 or A3.4 plants.

Black seeds were collected from WT and *HFIE:RNAi* lines and germinated on 1% MS media to test their viability. On control plates, 72% of the D3 WT FB seeds (n=100) germinated after 25 days in culture and 10% of the seedlings were abnormal in appearance (Figure 7.3B). Abnormal seedlings accumulated high levels of anthocyanin in the developing root or cotyledons, displayed more than two cotyledons or displayed deformed cotyledons, hypocotyls, young leaves or roots. Most of the transgenic lines displayed similar FB seed germination frequencies to WT samples after 25 days (n=64 to 141; Figure 7.3B). However, *35S:HFIE:RNAi* lines #5 (n=92) and #7 (n=104) both displayed decreased levels of FB seed germination frequency after 25 days (57% and 53% respectively) and a higher proportion of abnormal seedlings (20% and 27% respectively) compared to WT (Figure 7.3B).

Further analysis of the germination data showed that approximately 54% of the total seeds per capitulum from D3 WT plants germinated after 25 days in culture (Figure 7.3C). Similar levels were obtained for most of the lines except *35S:HFIE:RNAi* lines #5 and #7 that displayed significantly reduced levels of seed germination (31% and 3% respectively; Figure 7.3C). Collectively, these data

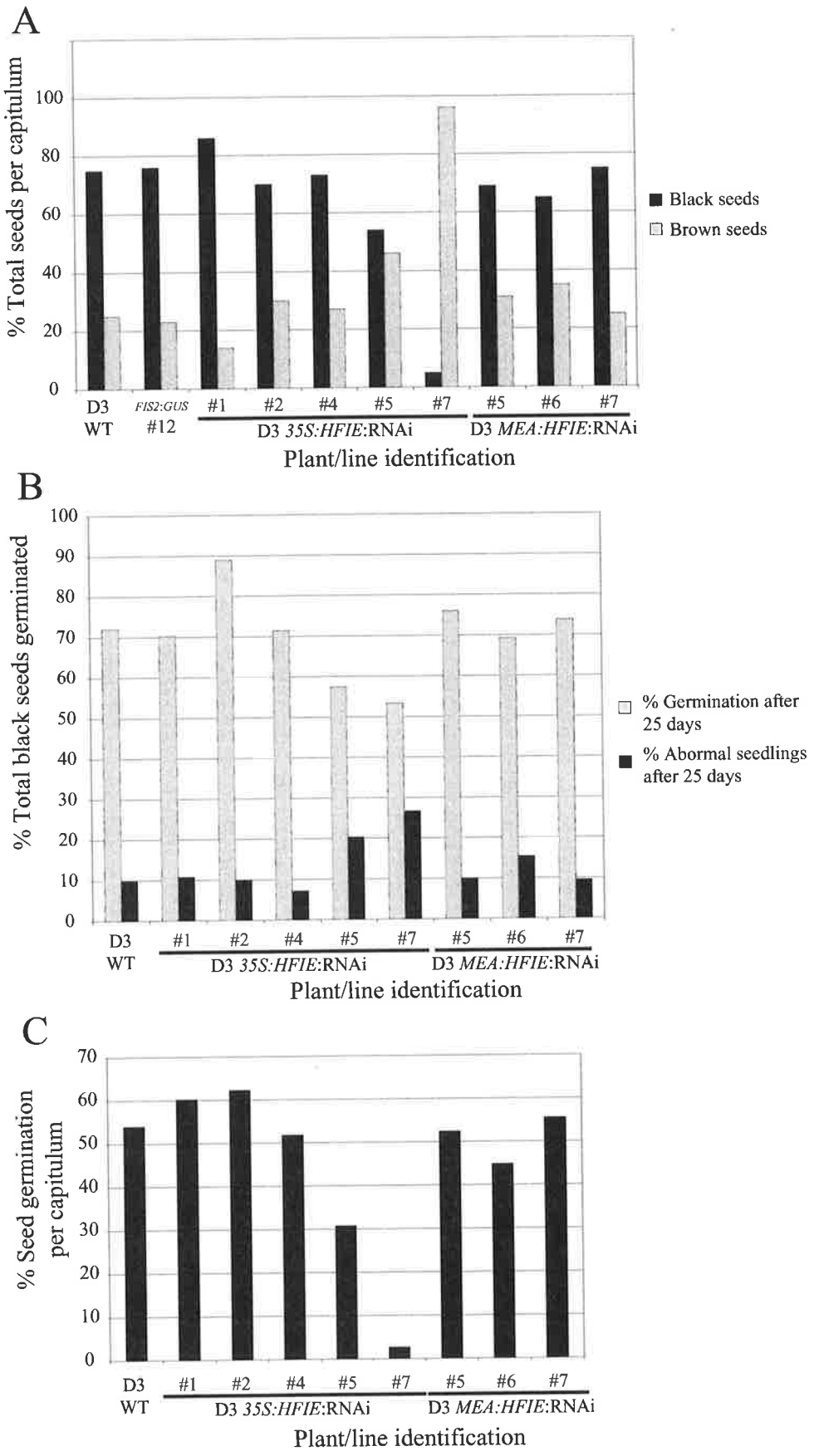

Figure 7.3 Seed morphologies and germination frequency of *Hieracium* D3 wild type (WT), *35S:HFIE:RNAi* and *MEA:HFIE:RNAi* plants. **A** Percentage of black and brown seeds per capitulum. **B** Percentage of fat black seeds and abnormal seedlings germinated after 25 days. **C** Percentage total seed germination per capitulum.

suggested that aspects of seed development were altered in D3 *35S:HFIE:RNAi* lines #5 and #7 thus preventing the formation of viable embryos.

7.3.3 Expression of *HFIE* mRNA in leaves, ovaries and receptacles of RNAi lines

To determine whether levels of *HFIE* mRNA were decreased in D3 and P4 lines containing the *HFIE:RNAi* genes, a semi-quantitative RT-PCR method was utilised. PCR primers were designed external to the *HFIE* region targeted for silencing, thus avoiding detection of construct-derived RNA. In WT *Hieracium* D3 and P4 plants, *HFIE* was expressed in all tissues examined including young leaves, roots, ovaries and flowers (see Section 5.3.4.3). Similarly, the *35S* promoter directs linked GUS expression to most *Hieracium* tissues during plant development (Koltunow et al., 2000). However, *35S:GUS* activity is absent during several stages of embryo sac and ovule development in both *Hieracium* (Koltunow et al., 2000) and *Arabidopsis* (G. Drews, pers. comm.). Consequently, it was expected that *HFIE* activity might be reduced by the *35S:HFIE:RNAi* gene in vegetative tissues but not in ovary tissues at all stages of development.

The levels of *HFIE* mRNA were quantified in young leaves of *35S:HFIE:RNAi* plants (Figure 7.4). D3 *35S:HFIE:RNAi* lines #2, #5 and #7 and P4 *35S:HFIE:RNAi* line #4 showed significantly lower levels of *HFIE* mRNA in young leaves when compared to WT plants (Figure 7.5A), although *HFIE* mRNA was not completely absent. This was the first indication to suggest that RNAi technology could be utilized in *Hieracium* to down-regulate mRNA levels. It also verified that the abnormal phenotypes in D3 *35S:HFIE:RNAi* lines #5 and #7 correlated with

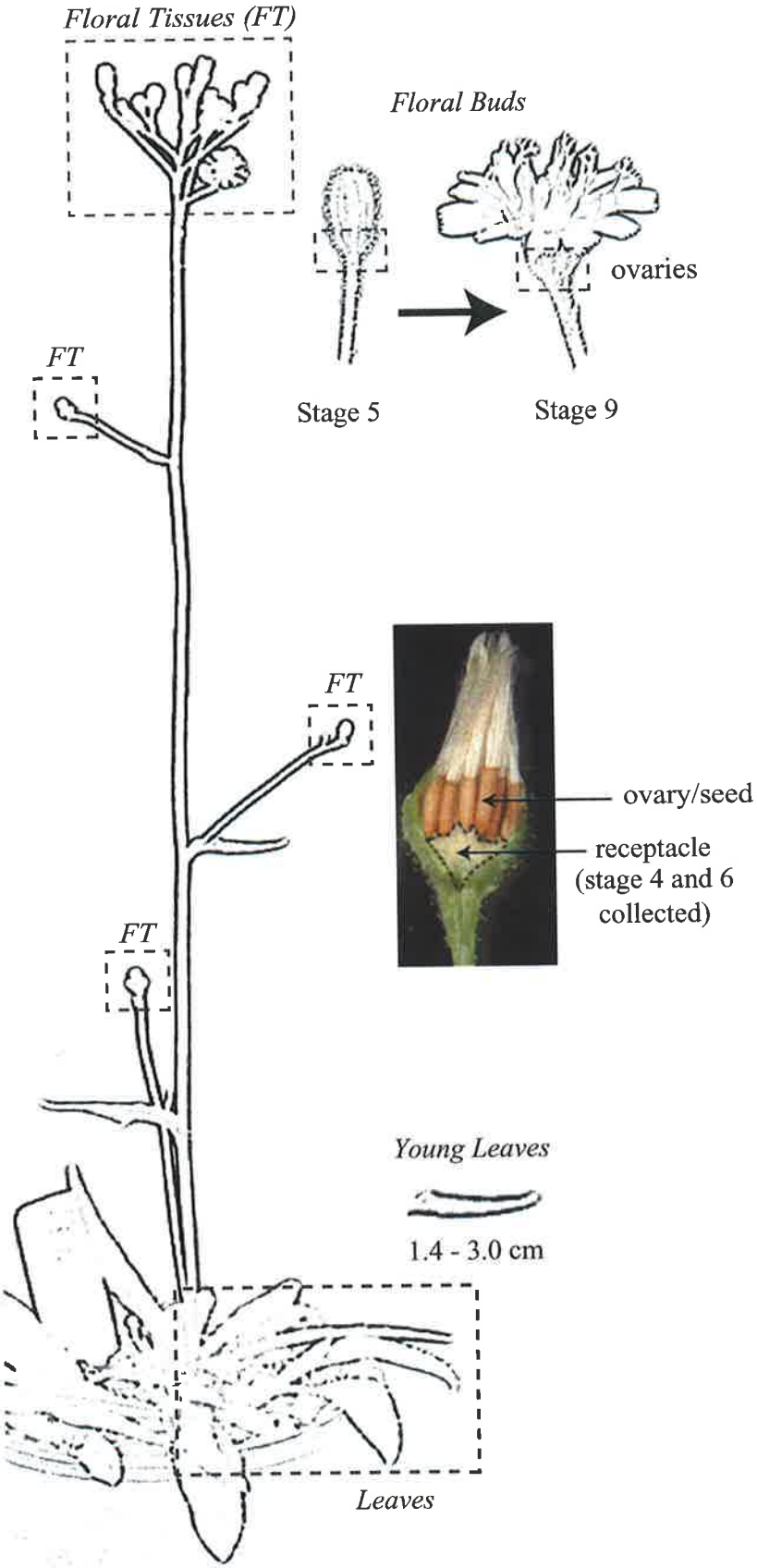

Figure 7.4 Schematic diagram of a D3 *Hieracium* plant showing the floral tissues and leaves investigated for *HFIE* silencing. The position of the seeds and receptacle are indicated in a stage 10 floral bud. See Appendix 1 for floral stages.

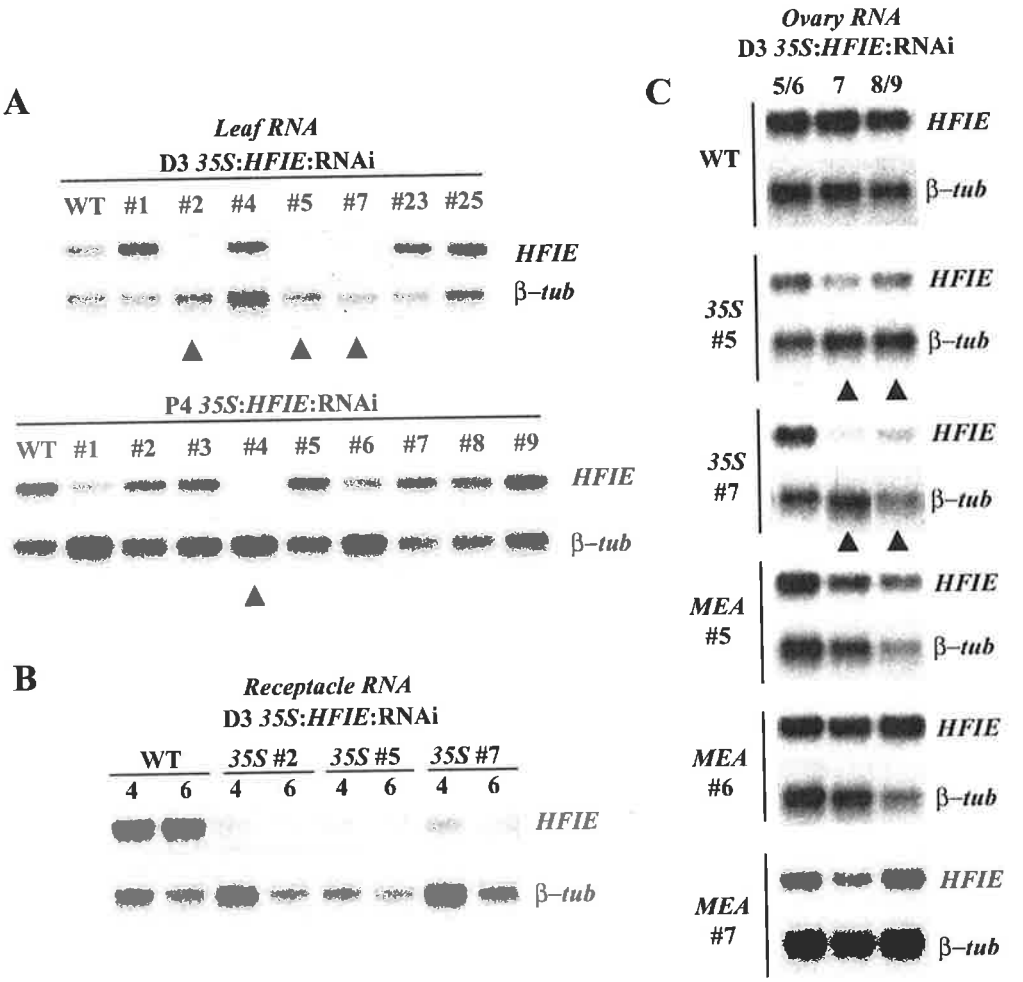

Figure 7.5 RT-PCR expression analysis of *HFIE* in D3 and P4 *HFIE:RNAi* plants. **A** *HFIE* expression in young leaves from *Hieracium* D3 and P4 WT and *35S:HFIE:RNAi* plants. **B** *HFIE* expression in receptacles from D3 WT and *35S:HFIE:RNAi* plants. **C** *HFIE* expression in ovaries from stage 5/6, 7 and 8/9 florets from D3 WT, *35S:HFIE:RNAi* and *MEA:HFIE:RNAi* plants. Loadings were equilibrated with a *Hieracium* β-*tubulin* (β-*tub*) control.

decreased levels of *HFIE* expression, and suggested that *HFIE* regulates aspects of vegetative development in apomictic *Hieracium*.

To verify that *HFIE* expression was down-regulated in other tissues of the D3 *35S:HFIE:RNAi* lines, *HFIE* RT-PCR analysis was performed on RNA extracted from receptacle tissues. The receptacle forms the base of the floral capitulum (Figure 7.4) and shows high levels of *35S:GUS* expression in transgenic plants. Similar to the expression in leaves, *HFIE* mRNA levels were decreased in receptacles from stage 4 and 6 floral buds of *35S:HFIE:RNAi* lines #2, #5 and #7.

To determine whether the seed phenotype in D3 *35S:HFIE:RNAi* lines #5 and #7 correlated with altered *HFIE* expression in ovaries, RT-PCR analysis was performed on ovary RNA samples (Figure 7.5C). Ovaries were also collected from the three D3 *MEA:HFIE:RNAi* lines, which were generated to specifically silence *HFIE* expression within the ovule, to determine the level of ovary *HFIE* expression relative to WT. No obvious changes in *HFIE* mRNA levels were detected during ovary development from floral stages 5 to 9 in the D3 *MEA:HFIE:RNAi* lines, but based on comparative levels of β-*tubulin* expression, lower levels of *HFIE* mRNA were detected in ovaries from D3 *35S:HFIE:RNAi* lines #5 and #7 at stages 7 and 8/9.

The reduction of *HFIE* expression in ovaries from D3 *35S:HFIE:RNAi* lines #5 and #7 was only observed during the early stages of seed development (floral stages 7 and 8/9), and RT-PCR analysis suggested that during most stages of early ovary development and late seed development *HFIE* mRNA levels were similar to those observed in WT plants. This suggested that the seed abortion phenotypes observed in D3 *35S:HFIE:RNAi* lines #5 and #7 may have been caused directly by a reduction in the expression of *HFIE* in seeds at stage 7 and 8/9, and indirectly by a reduction in the expression of *HFIE* in vegetative tissues.

7.3.4 Abnormalities during early ovule development in D3 *35S:HFIE:RNAi* line #7

Null mutations in the *Arabidopsis FIE* gene result in two distinct phenotypes in the seed; nuclear endosperm development in the absence of fertilisation, and embryo abortion at heart stage after fertilisation. In both cases, viable *fie* seeds do not develop. *FIE* has also been postulated to play a role in flowering in *Arabidopsis*, but has not been associated with any clear role in vegetative development (Kinoshita et al., 2001). In apomictic D3 *35S:HFIE:RNAi* lines #5 and #7, *HFIE* expression was down-regulated in leaves, receptacles and early seeds, and a high frequency of seeds aborted prior to maturity. To determine if down-regulation of *HFIE* in D3 *35S:HFIE:RNAi* lines #5 and #7 related to *fie*-like phenotypes in the seed, ovule development was characterised from initiation to maturity.

In WT D3 florets, megaspore mother cells (MMCs) were observed in ovules at stage 2/3 of development, and by stage 3/4 meiosis was complete and one or two aposporous initials (AIs) were observed in each ovule (Figure 7.6A). MMC initiation was normal in most ovules from lines #2, #5 and #7 (Figure 7.6B) and occurred at stages 2 to 3. By stage 3/4, most ovules from lines #2 and #5 contained four megaspores (Figure 7.6C), three of which were degenerating (Figure 7.6D), and one or two enlarging aposporous initial cells (Figure 7.6E). In contrast, normal tetrads were infrequently observed in ovules from line #7 (10%; Figure 7.6F), and most ovules displayed reproductive abnormalities. Some stage 3/4 ovules contained what appeared to be an aborted meiotic dyad (Figure 7.6G), or an over-enlarged aborting MMC with a nearby large aposporous initial cell (Figure 7.6H). Other

Figure 7.6 Early ovule development in D3 *35S:HFIE*:RNAi lines. All panels show 2 μm sections of ovules stained with toluidine blue. Structures shaded in yellow indicate sexual structures and structures shaded in red show putative aposporous structures. The numbers at bottom right of each panel indicate the line identity and the floral stage. All panels are in chalazal (top) to micropylar (bottom) orientation. Bar = 20 μm in all panels. **A** WT ovule showing a megaspore mother cell (mmc) and aposporous initial (ai). **B** Line #7 ovule containing a megaspore mother cell. **C** Line #2 ovule containing a megaspore tetrad (mt). **D** Line #5 ovule showing an aposporous initial cell, a selected spore (ss) and the position of the degenerating megaspores (dm). **E** Line #5 ovule showing an expanding aposporous initial (ai) cell with a prominent nucleus chalazal to a functional megaspore (fm) above the degenerating megaspores (dm). **F** Line #7 ovule containing an aposporous initial cell chalazal to a megaspore tetrad. **G** Line #7 ovule containing a distorted megaspore dyad (dy). **H** Line #7 ovule containing an aborted megaspore mother cell and an aposporous initial cell. **I** Line #7 ovule containing two megaspore tetrads (mt). **J** Serial sections of a line #7 ovule showing a megaspore tetrad with four abnormal megaspores of similar appearance. **K** Line #7 ovule containing degenerating megaspores and two expanding aposporous initial cells. Cells surrounding the nucellar lobe show signs of degeneration (cd). **L** Line #7 ovule showing cell degeneration in and around the vicinity of the megaspores. **M** Line #7 ovule containing an elongated aposporous initial (ai) cell. **N** Line #7 ovule containing multiple aposporous initial cells in and above the nucellar lobe. **O** Line #5 ovule containing an expanding aposporous initial cell. **P** Line #5 ovule containing and aposporous initial cell and an embryo sac structure (es). **Q** Line #5 ovule containing a micropylar embryo sac with an egg cell (ec) and polar nucleus (pn) and a chalazal aposporous embryo sac (aes).

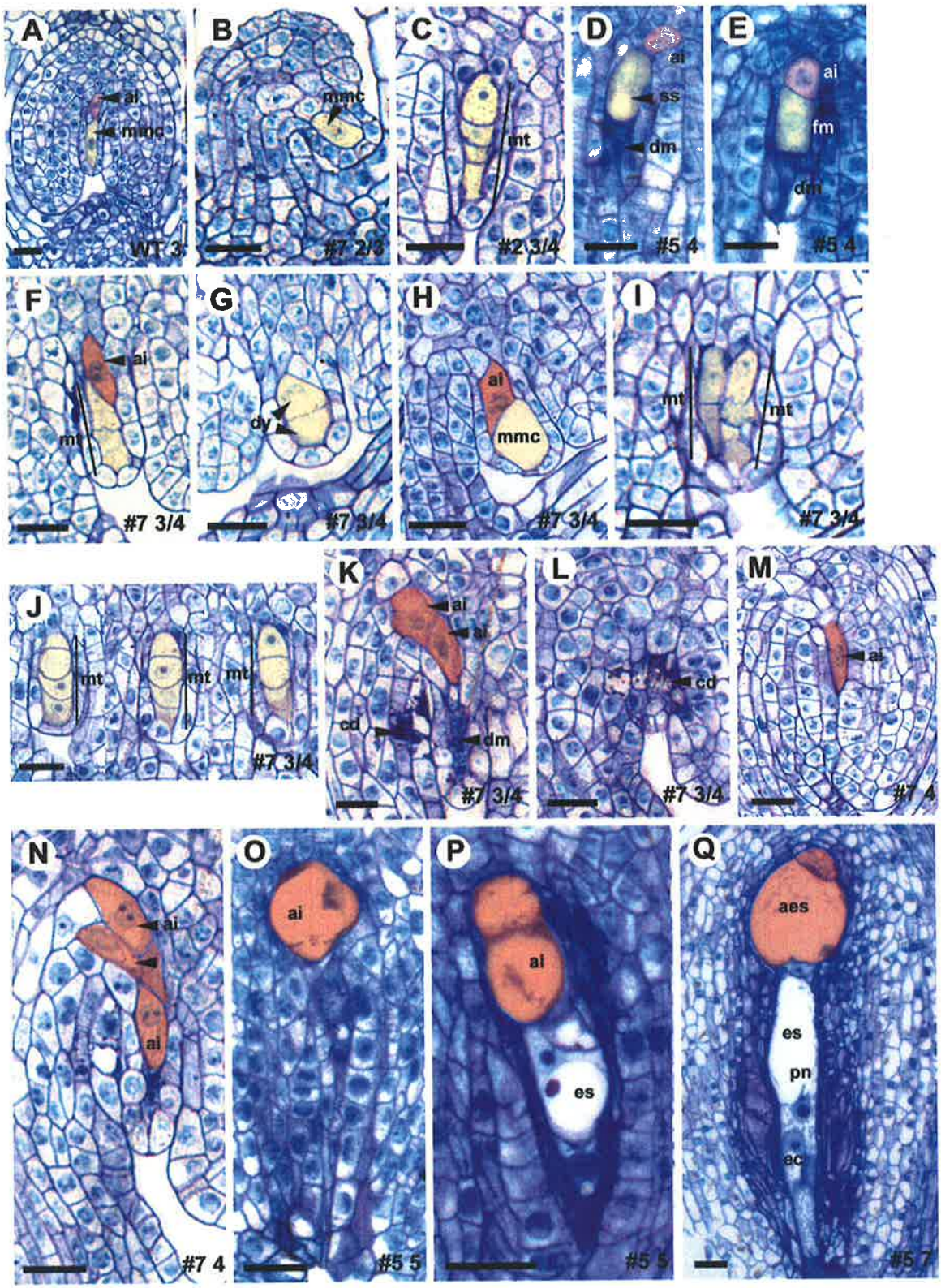
A
ai
mmc
WT 3
B
mmc
#7 2/3
C
mt
#2 3/4
D
ai
ss
dm
#5 4
E
ai
fm
dm
#5 4
F
ai
mt
#7 3/4
G
dy
#7 3/4
H
ai
mmc
#7 3/4
I
mt
mt
#7 3/4
J
mt
mt
mt
#7 3/4
K
ai
ai
cd
dm
#7 3/4
L
cd
#7 3/4
M
ai
#7 4
N
ai
ai
#7 4
O
ai
#5 5
P
ai
es
#5 5
Q
aes
es
pn
ec
#5 7

ovules from line #7 contained two meiotic tetrads (Figure 7.6I) or four abnormal megaspores of similar rounded appearance (Figure 7.6J). Some cells within and around the nucellar lobe showed signs of nuclear fragmentation and dark toluidine blue staining characteristic of cell death (Figure 7.6K and 7.6L). Most (70%) of the ovules from stage 3/4 florets in line #7 contained cells that showed characteristic morphology of aposporous initials (Figure 7.6F, 7.6K, 7.6M, 7.6N), but these rarely initiated mitosis. The reproductive abnormalities observed in line #7 did not correlate directly with a decrease in *HFIE* expression within the ovary, suggesting that decreased *HFIE* expression in tissues surrounding the ovary, such as the receptacle, might have influenced the alterations.

In contrast to line #7, early developmental abnormalities were rarely observed in ovules from line #5, and development resembled that observed in ovules from WT D3 florets. In lines #2 and #5, similar to WT, ovules from stage 4/5 florets contained dividing aposporous structures (Figure 7.6O and 7.6P), and by stage 6/7 contained mature embryo sacs (Figure 7.6Q). In contrast, most embryo sacs had failed to develop to maturity at the same stage in line #7, probably as a result of the early alterations in reproduction.

7.3.5 Embryo sacs and embryos abort in *35S:HFIE:RNAi* lines #5 and #7

Embryo sac development in *35S:HFIE:RNAi* line #2 was similar to that observed in D3 WT plants. At stage 7 of floral development the majority of seeds contained a mature embryo sac structure that enclosed an egg-like cell, two un-fused polar nuclei and often two synergids (Figure 7.7A), and/or multiple endosperm nuclei (Figure 7.7B). By contrast, open embryo sac structures in D3 *35S:HFIE:RNAi* lines

Figure 7.7 Embryo sac development in D3 *35S:HFIE*:RNAi lines. *Panels* **A** to **E** and **G** to **I** show wholemount haematoxylin stained ovaries. *Panel* **F** shows a 2 μm section stained with toluidine blue. The numbers at bottom right in each panel indicate the line identity and the floral stage. All panels are in chalazal (top) to micropylar (bottom) orientation. Bar = 20 μm in all panels. **A** Embryo sac (es) in chalazal (ch) to micropylar (mp) orientation containing an egg cell (ec), unfused polar nuclei (ufpn) and two synergids. **B** Embryo sac containing an egg cell and single polar nucleus micropylar to dividing nuclear endosperm (en). **C** Embryo sac containing a distorted egg-like cell and two displaced polar nuclei. **D** Embryo sac containing a distorted egg-like cell and two displaced polar nuclei. **E** Collapsed embryo sac (ces). **F** Collapsed embryo sac containing endosperm nuclei. **G** Embryo sac containing a small globular embryo (em) and dividing endosperm. **H** Embryo sac containing an abnormal embryo structure (em) and endosperm. **I** Embryo sac containing dividing endosperm and a chalazal embryo.

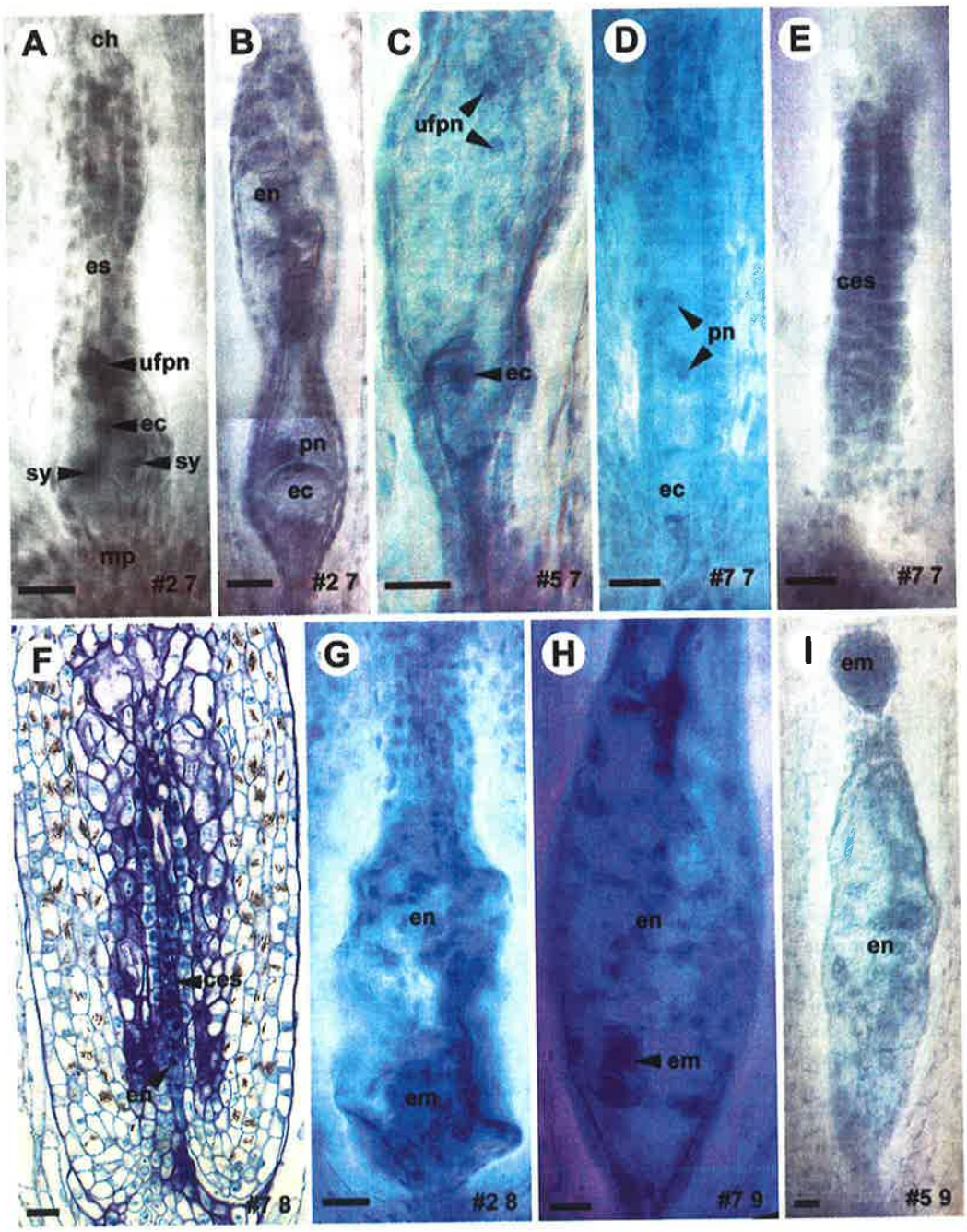
A
ch
es
ufpn
ec
sy
sy
mp
#2 7
B
en
pn
ec
#2 7
C
ufpn
ec
#5 7
D
pn
ec
#7 7
E
ces
#7 7
F
ces
en
#7 8
G
en
em
#2 8
H
en
em
#7 9
I
em
en
#5 9

#5 and #7 were abnormal, and contained distorted egg cells and displaced polar nuclei (Figure 7.7C and 7.7D). The polar nuclei were not positioned close to the egg cell, as observed in wild-type plants, but were arranged in various positions throughout the embryo sac (Figure 7.7C and 7.7D). The altered morphology of embryo sac structures in stage 7 florets from lines #5 and #7 correlated with a decrease in the expression of *HFIE* mRNA within ovaries at these stages.

In ovaries from stage 8 D3 WT florets, 16% of the embryo sacs had collapsed (see Chapter 2). In contrast, 30% and 60% of the embryo sacs had aborted in stage 8 florets from D3 *35S:HFIE:RNAi* lines #5 and #7 respectively (Figure 7.7E). The high frequency of embryo sac abortion in line #7 was possibly caused by early reproductive abnormalities during ovule development. However, sections revealed that some of these collapsed embryo sacs structures contained endosperm like nuclei (Figure 7.7F), indicating that they had aborted after the initiation of endosperm divisions.

At stage 9 of floral development in D3 WT and *35S:HFIE:RNAi* #2 plants, ~80% of the seeds displayed open embryo sacs. These contained embryo sac nuclei (~27.5%), globular to heart stage embryos and many endosperm nuclei (~36.5%; Figure 7.7G), or dividing endosperm and no embryos (~17.5%). By contrast, only 35% of the ovaries from D3 *35S:HFIE:RNAi* line #7 stage 9 florets contained open embryo sacs and less than half of these contained dividing endosperm and embryo-like structures. Most of the embryo-like structures were abnormal (Figure 7.7H). A higher frequency of ovules contained open embryo sacs in D3 *35S:HFIE:RNAi* line #5 (65%) compared to line #7, and some contained apparently viable embryos in various positions (Figure 7.7I).

During later seed development, the majority (56%) of seeds from stage 10/11 florets in D3 *35S:HFIE:RNAi* line #2 contained globular (Figure 7.8A) and/or

Figure 7.8 Late seed development in D3 *35S:HFIE*:RNAi lines. *Panels* **A**, **B**, **D** to **F** and **H** show wholemount haematoxylin stained ovaries. *Panel* **C** shows an unstained ovary cleared in methyl salicylate. *Panel* **G** shows a 2 μm ovary section stained with toluidine blue. The numbers at bottom right in each panel indicate the line identity and the floral stage. All panels are in chalazal (top) to micropylar (bottom) orientation. Bar = 20 μm in all panels except **C**, where bar = 125 μm. **A** Late globular stage embryo (em) surrounded by cellular endosperm. **B** Early heart stage embryo. **C** Brown seed containing a collapsed embryo sac (ces) within the ovule and seed coat (sc). **D** Embryo sac containing two unfused polar nuclei (pn) above an egg cell (ec) and two synergids (sy). **E** Embryo sac containing a single nucleus (n). **F** Late globular embryo and degenerating endosperm nuclei (en). **G** Misshapen embryo and cellular endosperm (cen). **H** Misshapen globular stage embryo (em) and dividing endosperm (en).

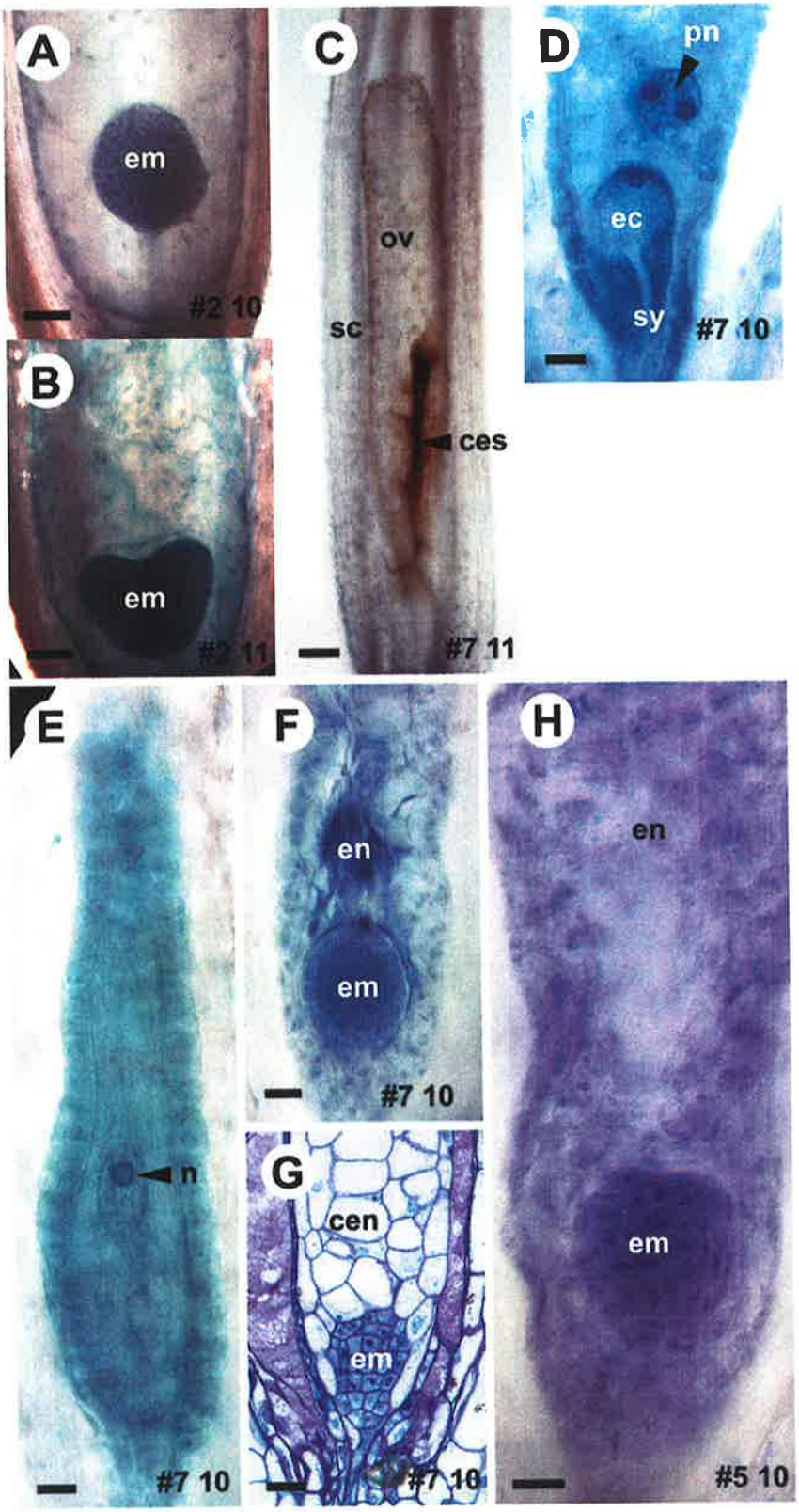
A
em
#2 10
B
em
#2 11
C
ov
sc
ces
#7 11
D
pn
ec
sy
#7 10
E
n
#7 10
F
en
em
#7 10
G
cen
em
#7 10
H
en
em
#5 10

heart stage embryos (Figure 7.8B), similar to wild-type D3 seeds. In contrast, 64% of the analysed seeds from D3 *35S:HFIE:RNAi* line #7 had collapsed and contained aborted embryo sacs within aborted ovules (Figure 7.8C). The remaining open embryo sacs contained an egg cell and polar nuclei (Figure 7.8D), one or two distorted nuclei (Figure 7.8E), a few dividing endosperm nuclei, or a misshapen embryo surrounded by degenerating (Figure 7.8F) or cellular endosperm (Figure 7.8G). Only 10% of the seeds from stage 10/11 florets in line #7 contained embryos (Figure 7.9). The phenotype in D3 *35S:HFIE:RNAi* line #5 was less extreme, because only 24% of the seeds contained aborted embryo sacs and 42% of the seeds contained embryos (Figure 7.9). However, many of the observed globular embryos were misshapen (Figure 7.8H) and 11% had aborted at the globular stage.

Collectively, the haematoxylin and sectioning analyses showed that seed development was altered in two of the three D3 lines where *HFIE* expression was down-regulated relative to wild-type D3 plants. The data also showed that reproductive development was altered at different times during development in the independent lines (Figure 7.9). Most ovules from line #7 displayed reproductive abnormalities during early megaspore meiosis and embryo sac mitosis, and these may have been indirectly caused by the alteration of HFIE activity in tissues other than the ovary. Reproductive development was altered at embryo sac maturity in both line #7 and #5 leading to embryo and embryo sac abortion (Figure 7.9), and this correlated with a decrease in *HFIE* expression in stage 7 and 8/9 ovaries. These data showed that the affect of the *35S:HFIE:RNAi* gene was not specific to the events of endosperm development, and suggested that *HFIE* has a more general role in plant and seed development compared to the *FIE* gene from *Arabidopsis*.

The inability to generate *MEA:HFIE:RNAi* lines during the timeframe of the thesis complicated attempts to characterise the specific role of *HFIE* during

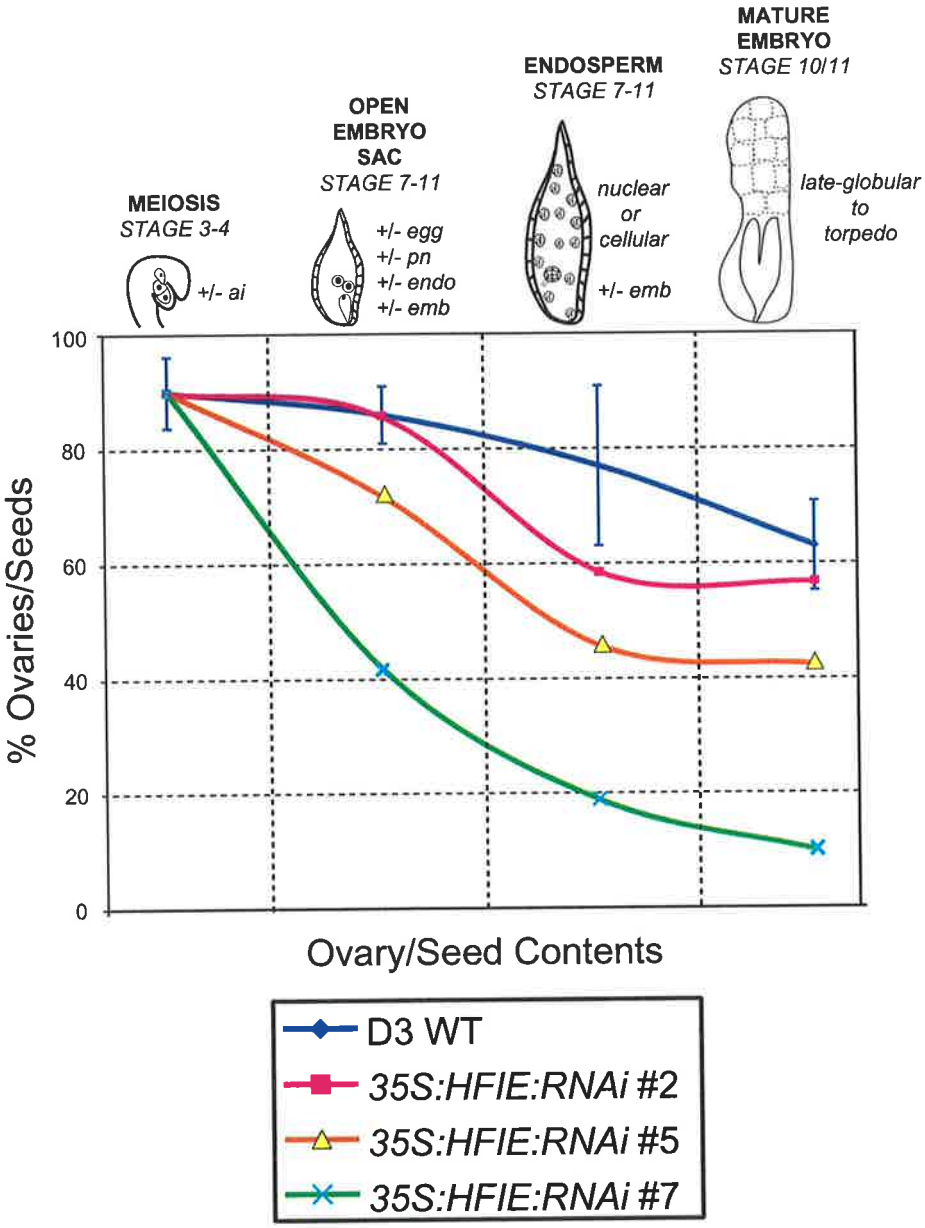

Figure 7.9 Embryo sac contents in *Hieracium* D3 WT and *35S:HFIE:RNAi* lines at key stages of floral development. The graph compares the percentage of ovaries/seeds with particular contents (meiotic structures, open embryo sacs, endosperm and late embryos; see diagrams above graphs) between D3 WT and the three down-regulated *HFIE* lines. ai - aposporous initial, egg - egg cell, pn - polar nuclei, endo - endosperm, emb - embryo.

aposporous embryo sac development, and more lines need to be obtained and analysed. To further address the role of *HFIE* during endosperm initiation in *Hieracium*, aspects of seed development were examined in down-regulated P4 *35S:HFIE:RNAi* line #4.

7.3.6 P4 *35S:HFIE:RNAi* line #4 does not develop endosperm without fertilisation

Preliminary analysis of sexual P4 lines containing the *35S:HFIE:RNAi* gene revealed that *HFIE* expression was down-regulated in young leaves from line #4. Sexual *Hieracium* P4 is a conditional self-incompatible plant. The precise mechanisms regulating self-incompatibility are unknown, but possibly relate to variations in temperature or humidity. Under self-incompatible conditions, seed development in sexual P4 does not progress past embryo sac maturity in the absence of fertilisation, and seed heads comprise entirely of skinny brown unfertilised ovaries. However, under high temperature conditions where self-incompatibility fails (R. Bicknell, pers. comm.), seed heads display fat black seeds that contain mature embryos. During the analysis of P4 *35S:HFIE:RNAi* lines, self incompatibility had failed in wild-type and transgenic plants. Therefore it was unclear by visual analysis if seeds were developing autonomously in *HFIE* down-regulated line #4.

To overcome this problem and address the question of autonomous seed development, floral buds from three of the nine P4 *35S:HFIE:RNAi* lines #1, #4 and #9 were decapitated prior to anthesis. Decapitation removed the male tissues from the flower and prevented fertilisation of the developing ovaries (Koltunow et al.,

1995a). Seeds were left to develop for 7 days without fertilisation and then collected, fixed and stained with haematoxylin.

After seven days post decapitation (DPD), 60% of the seeds (n=122) collected from decapitated D3 WT floral buds contained endosperm and/or embryos. At least 85% of the seeds (n=150) from P4 WT plants collected 7 DPD contained embryo sacs with fused central nuclei and quiescent egg cells. The remainder contained either collapsed embryo sacs or small unidentified embryo sac nuclei. Similarly, seeds (n=>100 for each line) from *35S:HFIE:RNAi* lines #1, #4 and #9 collected 7 DPD displayed mature embryo sacs with fused polar nuclei and a large egg cell after 7 DPD. Fertilisation-independent endosperm development was not observed in any seeds from the P4 *35S:HFIE:RNAi* lines. This suggested that either the *35S:HFIE:RNAi* construct was not down-regulating *HFIE* expression in ovules from line #4 or that the *HFIE* gene was not functioning to repress endosperm development in the absence of fertilisation in sexual *Hieracium*. However, more P4 lines containing the *35S:HFIE:RNAi* and *MEA:HFIE:RNAi* genes need to be generated and analysed for *HFIE* down-regulation before the role of *HFIE* in sexual P4 *Hieracium* can be ascertained.

7.4 Discussion

7.4.1 RNAi constructs silence gene expression in *Hieracium*

RNAi silencing is considered a defensive mechanism adapted by plants to prevent the infection and motility of viruses and transposable elements (Waterhouse et al., 2001). Utilisation of RNAi technology provides a useful tool for the elucidation of gene function in plant and animal systems (Waterhouse and Helliwell, 2003).

Although the precise mechanisms of RNAi are unknown, and the fact that some genes are not silenced by RNAi (Fraser et al., 2000; Gonczy et al., 2000), studies have shown that the hairpin structure formed during RNAi silencing is highly efficient at targeting the degradation of transcripts derived from transgenes, viruses and endogenous plant genes (Smith et al., 2000; Waterhouse et al., 2001). Smith et al., (2000) showed that post-transcriptional gene silencing of the *Fad2* gene in *Arabidopsis* and the potato virus Y *Niaprotease* gene in *Nicotiania tabacum* occurred in 90-100% of the plants containing introduced engineered RNAi genes.

RNAi technology was successfully utilised in this study to down-regulate the expression of a putative plant *Polycomb* group (PcG) gene, *HFIE*, in apomictic and sexual *Hieracium* plants. This finding verifies that key regulatory genes expressed at low levels in polyploid *Hieracium* can potentially be silenced using this technology. However, the results also showed that (i) a minority of *Hieracium* plants (4/21) containing a *HFIE:RNAi* gene displayed lower levels of *HFIE* mRNA compared to wild-type and (ii) only half (2/4) of the plants down-regulated for *HFIE* showed an obvious phenotype including stunted growth and seed abortion. Although these results contrast somewhat with the findings of Smith et al., (2000), similar results have been observed in gene silencing studies carried out in other plant and animal species. Chuang and Meyerowitz (2000) showed that a decrease in the expression of the *Arabidopsis PERIANTHIA* (*PAN*) by 30-90% compared to wild type did not result in the extra organ phenotypes that are observed in null *pan-1* and *pan-2* mutants. They suggested that a small portion of *PAN* activity was sufficient for its wild-type function in wild-type plants. Similarly, targeting of RNAi constructs to the *Arabidopsis AGAMOUS*, *CLAVATA* and *APETALA* genes resulted in weak, intermediate and strong phenotypes in different transgenic lines (Chuang and Meyerowitz, 2000). Expression of the *HFIE* mRNA was not completely absent

in the tissues analysed from down-regulated D3 and P4 *35S:HFIE:RNAi* lines, and it is possible that a low level of *HFIE* activity may enable the gene to function during plant development.

7.4.2 Down-regulation of *HFIE* in apomictic *Hieracium* alters plant development

A significant reduction in *HFIE* expression resulted in obvious phenotypes in apomictic D3 *35S:HFIE:RNAi* lines #5 and #7. Plant growth was stunted and seed development was altered from megasporogenesis to maturity in line #7 and during megagametogenesis and embryo development in line #5. In *Arabidopsis* the *FIE* gene is expressed in most plant tissues, but its function appears to be restricted to the events of seed development (see Chapter 6) where it is required to repress the initiation of endosperm development prior to fertilisation, to ensure the endosperm forms correctly along the anterior-posterior axis, and to repress the expression of flowering genes such as *LEAFY*, *AGAMOUS* and *APETALA3* in the embryo (Ohad et al., 1999; Kinoshita et al., 2001). No obvious phenotypes were observed in the vegetative tissues of heterozygous *Arabidopsis fie* plants. (Chaudhury et al., 1997; Ohad et al., 1996). Plants homozygous for the *fie-2* mutation have yet to be recovered, but *fie-1/fie-1 pFIE::FIE::GFP* "pseudo-homozygotes" display severe abnormalities in vegetative and floral growth due to the premature induction of flowering genes (Kinoshita et al., 2001).

The stunted vegetative growth of D3 *35S:HFIE:RNAi* lines #5 and #7 suggested that *HFIE* function is required during general plant growth in *Hieracium*, perhaps in the regulation of genes required for cell division. In contrast with

Arabidopsis fie-1/fie-1 pFIE::FIE::GFP plants, premature flowering was not observed in seedlings or mature *Hieracium 35S:HFIE:RNAi* plants to suggest that repression of putative flowering genes was altered during post-embryonic development. Further studies are required to determine the role of *HFIE* during vegetative development in *Hieracium*.

7.4.3 Promoter limitations may effect the penetrance of phenotypes in *Hieracium 35S:HFIE:RNAi* lines

Varying results in terms of RNAi silencing have been obtained from different systems using promoters with constitutive or specific expression patterns. Studies in tobacco showed that the induction of a *35S* driven RNAi response to silence expression of a viral mRNA was systemic, and could be transported from cell to cell at long distances through the plant, probably via vascular tissues (Fagard and Vaucheret, 2000). In contrast, studies in *Arabidopsis* and cotton used non-constitutive seed specific promoters to target the silencing of oil biosynthetic genes specifically within the seed, thus preventing deleterious down-regulation effects in the rest of the plant (Stoutjesdijk et al., 2002; Liu et al., 2000). The results from this study suggested that the down-regulation of *HFIE* in *Hieracium* was not systemic, despite the use of the *35S* promoter, because *HFIE* expression was not altered during ovary development in D3 *35S:HFIE:RNAi* line #2, where expression was essentially absent in leaves and receptacles, and was only altered in a few stages of seed development in lines #5 and #7.

7.4.4 Down-regulation of *HFIE* in vegetative tissues alters early seed development in apomictic *Hieracium*

The abortion of seed development at different stages in D3 *35S:HFIE:RNAi* lines #5 and #7 possibly related to a down-regulation of HFIE activity in vegetative and/or ovary tissues. The early abnormalities in ovule development observed in line #7 correlated with a change in *HFIE* expression within the receptacle, but not within the ovary. Previous studies in apomictic *Hieracium* have shown that the ablation of some cells in the funiculus and integument following introduction of a *GluB1:Rnase* gene results in abnormalities during meiotic and aposporous development (Koltunow, 2000) similar to those observed in *35S:HFIE:RNAi* line #7. Combined, these results suggest that sporophytic factors may influence megaspore development and gametogenesis, and this is supported by studies in *Arabidopsis* that highlight clear genetic interactions between the gametophyte and surrounding sporophyte (Schneitz et al., 1995). It is possible that a decrease in *HFIE* activity within the *Hieracium* receptacle alters communication with the ovary by changing gene expression or nutrient flow and results in reproductive abortion. Further lines containing the *35S:HFIE:RNAi* gene that display reduced levels of *HFIE* mRNA are required to verify these data.

7.4.5 Down-regulation of *HFIE* in developing seeds alters late seed development in apomictic *Hieracium*

The secondary seed effect of *HFIE* down-regulation was observed in both *35S:HFIE:RNAi* lines #5 and #7, which displayed abnormalities during late

megagametogenesis and early embryo and endosperm development that correlated with decreased levels of *HFIE* mRNA in the ovary. Embryo sac and embryo abortion occurred at higher frequencies in D3 *35S:HFIE:RNAi* lines #5 and #7 compared to D3 WT plants. These data suggest that *HFIE* activity is required for seed maturation in apomictic *Hieracium*, similar to *FIE* during seed development in sexual *Arabidopsis*. Consequently, if an alteration to *HFIE* activity is linked to the formation of autonomous endosperm in *Hieracium*, then it must be only a subtle alteration, because a complete lack of *HFIE* activity results in seed abortion. The analysis of lines containing the *HFIE:RNAi* gene under the control of strong ovule or embryo sac promoters such as *AtMEA*, *AtFIS2* or *AtSERK* will enable further clarification of the role of *HFIE* during endosperm initiation.

7.4.6 *MES*-6, The *C. elegans* homolog of *EXTRA SEX COMBS* (*Esc*) and *FIE*, is required for RNAi silencing

It is uncertain why such a large proportion of the *Hieracium* plants containing a *HFIE:RNAi* gene showed no obvious silencing of *HFIE* mRNA. It is possible that in some cases the gene was non-functional due to rearrangements, the level of transcription was insufficient to generate a RNAi response, or the tissues examined were partially resistant to RNAi as observed in some other species (Fire, 1999). However, an alternate hypothesis relates to a tentative link between HFIE activity and RNAi maintenance. In plants and fungi, RNAi has been proposed to additionally involve chromatin, because RNAi-like phenomena require proteins predicted to interact with chromatin - a SWI/SNF2 component, a DNA methyltransferase and a DNA helicase-like protein (Fagard et al., 2000; Morel et al.,

2000; Wu-Scharf et al., 2000; Dalmay et al., 2001) - as well as proteins predicted to interact with RNA (Mourrain et al., 2000). Studies in *Caenorhabditis elegans* show that the *maternal effect sterile* (*mes*) PcG genes *mes-3*, *mes-4* and *mes-6* are required for RNAi, because lethal dsRNAs (RNAi) do not function in worms where these genes are mutated (Dudley et al., 2002). The MES-6 WD-40 protein shares homology with Esc from *Drosophila* and FIE from *Arabidopsis*, and functions in a protein complex that is essential for the specification and survival of larval germ cells (Xu et al., 2001). To date, no studies have shown that FIE plays a role during RNAi within plant systems, and it is possible that the role of the MES PcG complex in *C. elegans* is fundamentally different to FIE PcG complex in plants, because unlike plants, where methylation induces silencing at the locus targeted by RNAi (Mette et al., 2000; Vaucheret and Fagard, 2001), little or no methylation can be detected in *C. elegans* (Simpson et al., 1986). However, if FIE function is required for RNAi in plants, then RNAi targeted silencing of FIE might be expected to produce variable results. Silencing may occur while the FIE protein is present, but once the *FIE* mRNA is degraded, silencing might be expected to cease, dependent upon the mechanisms required for maintenance of RNAi. In *C. elegans*, disabling the function of RNAi can induce the activation of endogenous transposons (Tabara et al., 1999), and this could possibly be assayed in down-regulated *HFIE* lines. A role for FIE during RNAi is difficult to test, because *fie* homozygotes cannot be generated in *Arabidopsis* to examine the functionality of RNAi constructs. However, if such a scenario exists and is conserved in *Hieracium*, then this may explain the high proportion of *Hieracium* lines that showed no obvious effects of the *35S:HFIE:RNAi* and *MEA:HFIE:RNAi* genes.

7.4.7 Functional models for the *HFIS* PcG complex

The results from this study show that *HFIE* expression is required for plant and seed development in apomictic *Hieracium*. Once again, this highlights the close molecular relationship between sexual and apomictic seed development proposed in Chapter 3. A role for a *FIE* homologue during vegetative growth has not been shown previously, and the mechanisms of this requirement are unknown. In terms of seed development in apomictic *Hieracium*, *HFIE* appears to be required during two different stages, including (i) meiosis where it may indirectly regulate aspects of the interaction between vegetative tissues and the ovule and (ii) embryo sac and embryo development where it appears to be required for seed viability, similar to that observed in *Arabidopsis*. These roles for *HFIE* in seed development are particularly interesting, because they support the functional data obtained for D3-cHFIE in Chapter 6, and suggest that there is unlikely to be a mutational lesion within *HFIE* that results in the formation of autonomous endosperm. Unfortunately it was difficult to directly assess the role of *HFIE* during the formation of autonomous endosperm in *Hieracium,* because down-regulation of the gene appeared to halt embryo sac development rather than promote the proliferation of endosperm nuclei. However, an insufficient number of P4 *35S:HFIE:RNAi* and *MEA:HFIE:RNAi* lines were identified to determine whether silencing of *HFIE* in sexual *Hieracium* resulted in the formation of fertilisation-independent endosperm. Further studies should focus on the generation of RNAi genes containing strong seed-specific promoters.

A requirement for *HFIE* during autonomous seed development in *Hieracium* has interesting ramifications for models describing the genetic control of autonomous apomixis. The disruption of *HFIE* activity in seeds from apomictic D3

Hieracium is likely to disrupt the function of a PcG protein complex that includes HMEA and HFIS2, and results in seed abortion. Hence, it follows that the *HFIS* PcG complex is required for correct seed development in autonomous apomictic *Hieracium*. If alterations to this complex are linked to the initiation of autonomous endosperm, then these alterations must be subtle and are unlikely to relate to a complete absence of *HFIS* gene activity. It seems more likely that these changes relate to either (i) the presence of a fertilisation-like signal within the ovule that de-represses the *HFIS* complex at endosperm initiation or (ii) epigenetic changes in the regulation of *HFIS* products that result in altered spatial localisation or activity of the proteins during endosperm initiation such that the PcG complex cannot repress endosperm development. Both of these scenarios are supported by the finding that autonomous endosperm development in apomictic *Hieracium* is stochastic in that not all seeds initiate endosperm development and initiation occurs at different times relative to the described stages of floral development (see Chapter 2). Further studies analysing the spatial localisation of *HFIE* products, as well as the isolation of *HMEA* and *HFIS2* homologues, will aid the elucidation of *HFIS* PcG function during endosperm initiation in *Hieracium*.

Chapter 8: Summary and Concluding Discussion

Apomixis is a reproductive process in plants whereby embryos can form in seeds without fertilisation, therefore maintaining the genotype of the maternal plant. Plants from around 40 families can reproduce by apomixis, but the process is largely absent from agriculturally important crops. An understanding of apomixis in model plants may facilitate its transfer to sexual agricultural crops and aid maintenance of desirable characteristics such as disease resistance and hybrid vigour. The *Hieracium* genus is comprised of closely related apomictic and sexual species that display short generation times, are genetically transformable, and are amenable to molecular and cytological studies of apomixis. Various studies in *Hieracium* have noted that the apomictic process initiates with apospory and incorporates autonomous embryo and endosperm development (Rosenberg, 1907; Schnarf, 1919; Skalinska, 1967; Koltunow et al., 1998).

Little is known at the molecular level of the relationship between apomictic and sexual pathways, or the cues that regulate the initiation of apomixis. However, the characterisation of apomictic components has been aided by recent mutagenesis studies in sexual *Arabidopsis* that suggest the three *FERTILISATION INDEPENDENT SEED* (*FIS*) genes *MEA*, *FIS2* and *FIE* regulate the initiation of endosperm development in plants. The products of these genes are likely to interact in a large regulatory PcG protein complex, and it has been postulated that the formation of autonomous endosperm in apomictic plants may relate to altered regulation of the *MEA*, *FIS2* and *FIE* gene products or the PcG complex. Aspects of this hypothesis and apomictic seed development were investigated in this study by

(i) cytologically characterising endosperm development, (ii) examining the molecular relationships between apomictic and sexual processes and (iii) examining the role of an endogenous *Hieracium FIE* gene in apomictic and sexual *Hieracium* plants.

Analyses of fertilisation-dependent endosperm development in sexual *Hieracium* P4 showed that the early mitotic endosperm divisions resulted in a nuclear syncytium containing nuclei positioned evenly along the anterior-posterior axis and around the periphery of the embryo sac. In contrast, early autonomous divisions of the nuclear endosperm in apomictic D3 were less ordered, and nuclei tended to cluster together and were randomly positioned in embryo sac structures (Chapter 2). The alterations during early endosperm development in apomictic D3 appeared similar to those observed in the *fis* mutants that bypass the requirement for fertilisation (Sorenson et al., 2001). It is possible that cell specification events along the anterior-posterior axis, or aspects of the microtubular cytoskeleton are altered during autonomous endosperm divisions in apomictic D3 *Hieracium*. This could be further investigated using specific endosperm cell-type marker genes, or antibodies to study the distribution of spindle-specific proteins during endosperm development (Smirnova and Bajer, 1998).

Despite the differences in early fertilisation-dependent and independent endosperm development, a cellular endosperm product was required in apomictic D3 for embryo development to maturity, and the morphology of the endosperm nuclei during nuclear divisions and cell wall formation was similar in sexual and apomictic plants (Chapter 2). The expression patterns of *AtMEA:GUS*, *AtFIS2:GUS* and *AtFIE:GUS* genes during embryo sac development in sexual and apomictic *Hieracium* plants were also strikingly similar (Chapter 3). Fertilisation-dependent and independent divisions of the endosperm nuclei were both marked by the

AtFIS2:GUS and *AtMEA:GUS* genes, despite differences in early nuclear migration patterns.

AtFIS2:GUS was also expressed in degenerating megaspores during megasporogenesis in *Hieracium*, in a differential pattern between sexual and apomictic plants that correlated with the presence of AI cells in apomictic D3 and A3.4 (Chapter 3). The expression data suggested that AIs might share functional identity with selected megaspores even though meiotic reduction does not occur. Notably, during megagametogenesis, expression of the *AtFIS2:GUS* gene was conserved from the first mitotic division of the functional megaspore and the aposporous initial(s) in sexual and apomictic *Hieracium* plants respectively, and similar *AtMEA:GUS, AtFIS2:GUS* and *AtFIE:GUS* expression patterns were also maintained during the subsequent events of seed development (Chapter 3). Central cell nuclei in mature embryo sacs from sexual P4 and apomictic D3 were similarly marked by intense *AtMEA:GUS* and *AtFIS2:GUS* activity prior to endosperm initiation, suggesting that endosperm divisions initiated from the polar nuclei irrespective of whether ovules were fertilised. Collectively, these studies highlighted the interrelatedness of sexual and apomictic processes in *Hieracium*.

Flow cytometric analysis of DNA content in mature seeds highlighted the different reproductive routes by which embryos and endosperm could be derived in the facultative apomictic D3. This further emphasised the overlaps between sexual and apomictic processes in *Hieracium* (Chapter 2). Seeds from the same D3 capitulum could be derived through either apomictic or sexual processes, or a combination of both. Although the majority of embryos (82-89%) detected in mature D3 seeds were derived from parthenogenesis and were unreduced and maternal in origin, a small percentage of embryos displayed lower ploidy levels indicating that they were likely to be derived via parthenogenetic development of a

reduced egg. Sexual seeds (B_{II} hybrids) were also detected in apomictic D3 capitula as were seeds derived from the fertilisation of an unreduced egg (B_{III} hybrids). Interestingly, the apomict D3 exhibited a higher DNA content per chromosome than sexual P4, and this may relate to the accumulation of retrotransposons and similar mobile elements (Chapters 2 and 6).

These results and the findings of the flow cytometry study suggest that apomixis in *Hieracium* is a developmental process closely related to sexuality, and that the two pathways utilise essentially the same molecular mechanisms to produce a seed. This supports theories that suggest apomixis occurs as a result of changes to the function of gene(s) normally required for sexual reproduction (Peacock et al., 1995; Carman, 1997; Spillane et al., 2001).

Molecular aspects of autonomous endosperm initiation were investigated by targeting *Hieracium FIS*-gene homologues and potential *FIS Polycomb* group interactors for isolation and characterisation (Chapters 5, 6 and 7). *Hieracium* sequences showing homology to the *Arabidopsis MET*, *HDAC*, *FIS2* and *FIE* genes were identified. Further characterisation of the *HMET* and *HHDAC* genes is required before their role in *Hieracium* can be clarified, and it is tempting to speculate that they function to epigenetically regulate gene expression during seed development. Three *Hieracium* cDNA sequences sharing homology with *Arabidopsis FIS2* showed greater homology to *Arabidopsis EMF2*, a regulator of post-embryonic flowering time (Chapter 5), and silencing or complementation studies are required to determine their functional identity.

HFIE sequences were investigated in greater detail in both sexual and apomictic *Hieracium* plants. Two *HFIE* genes were identified per genome in sexual P4 and apomictic D3, and in both cases only one gene appeared to be functional and capable of producing a full-length mRNA (Chapter 6). A single full-length *HFIE*

cDNA was identified from both apomictic D3 and sexual P4 *Hieracium*, and the two *HFIE* putative amino acid sequences differed by only three amino acid residues (Chapter 5). Function of the D3 HFIE protein, and orthology to *Arabidopsis* FIE, was confirmed by complementation of fertilisation-independent endosperm development in the *Arabidopsis fie-2* mutant (Chapter 6). *In vivo* function of *HFIE* in apomictic D3 *Hieracium* was also verified by silencing the gene, which led to abnormal plant growth and seed abortion through defects in female meiosis, embryo sac formation and embryo development (Chapter 7). Combined, these findings suggest that the D3 *HFIE* gene is orthologous to *Arabidopsis FIE* and is likely to be involved in a regulatory complex required for seed development in apomictic *Hieracium*.

Autonomous endosperm development in apomictic *Hieracium* is not related to a mutation in the D3 *HFIE* coding region. However, further studies are required to characterise the function of the *HMEA* and *HFIS2* genes, because even in the absence of direct mutation it is possible that spatial alterations in *HMEA*, *HFIS2* or *HFIE* expression, combined with altered epigenetic regulation of other maternal genes, might induce the development of autonomous endosperm.

Collectively, the data from this study support the concept that apomixis is manifested from the molecular framework regulating sexual reproduction, and is not a unique reproductive pathway in *Hieracium*. While the underlying molecular cause of apomixis remains unknown, its major developmental hallmark appears to be a deregulation of the sexual process in time and space. It is likely that at key checkpoints during seed development in apomictic *Hieracium*, such as megasporogenesis and endosperm initiation, the expression of regulatory genes is altered to allow continuation of subsequent downstream events. Whether the program of events enabling alterations at these key stages is put in place during AI

cell differentiation remains uncertain. It is possible that the checkpoint alterations occur independently of one another or are linked by modifications in a common regulator. Further analysis of *AtFIS2:GUS* marker gene regulation during megasporogenesis and aposporous initial cell differentiation in apomictic *Hieracium* (Chapter 3) should provide clues as to the molecular factors altered at the time of AI cell differentiation.

On a broader scale, the conclusions from this study suggest that attempts to engineer apomixis into sexual crop species might have the potential to succeed. If the expression of key genes controlling checkpoints in sexual reproduction can be modified appropriately to avoid meiosis and fertilisation, then a background of sexual regulators can facilitate the interim steps of development to produce viable seeds. However, the key is to determine the combination of "checkpoint" control genes that must be de-regulated, and how to effectively link them without perturbing downstream events. The dissection of the genetic components involved in ovule, embryo sac and seed development currently underway in sexual plant systems needs to be combined with analysis of the genetic and molecular processes regulating reproduction in functional apomicts. Not only will this provide the new tools to understand the molecular mechanisms underlying sexual and apomictic reproduction, it will also provide information to control seed production in agriculture with much greater flexibility.

Appendix 1: Stages of floral development in *Hieracium*

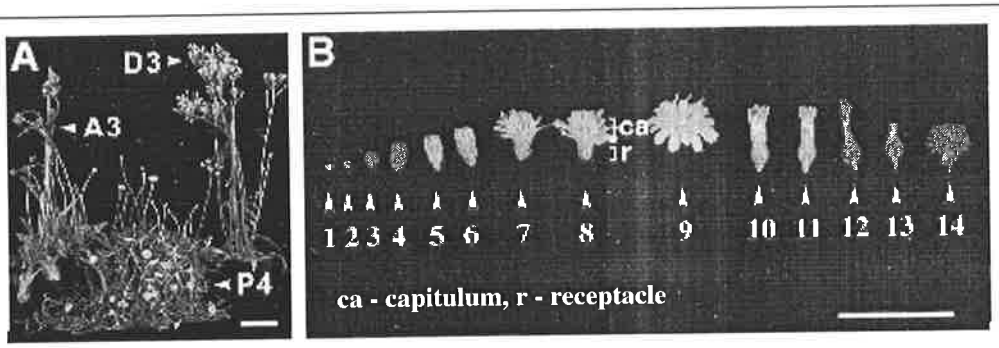

Stage	Description	*H. pilosella* P4	*H. piloselloides* D3
1	Capitulum Length (CL) (P4 2.85 mm, D3 1.0 mm)	Floret primordia initiated	Floret primordia initiated
2	CL (4.5, 1.5)	MMC differentiated	Ovules still undifferentiated
3	CL (5.5, 2.4)	MMC undergoing meiosis, endothelium forming	MMC differentiated and undergoing meiosis, endothelium forming
4	CL (6.8, 4.0)	Meiosis / Megaspore selection	Meiosis / Megaspore selection / differentiation of 1-4 aposporous initial cells
5	Capitulum length (8.0, 5.6)	Four-nucleate embryo sac (megagametogenesis)	Predominantly single elongated embryo sacs undergoing megagametogenesis
6	Bracts open at apex, forming hole; petals coloured	Mature embryo sac, intact antipodals	Embryo and endosperm initiation
7	Outer whorl of florets open	Florets cross-pollinated	Early-globular embryos and nuclear endosperm development
8	Half of florets open	Embryo and endosperm initiation	Globular embryos
9	All florets open	Early-globular embryos and nuclear endosperm development	Globular embryos
10	Florets senescing, petals and bracts closing	Heart stage embryos	Globular-heart embryos
11	Petals coloured, soft, crushed, forming "paint brush", bracts constricted	Early torpedo embryos, aleurone initiation	Globular-torpedo embryos, aleurone initiation, sometimes polyembryonic
12	Petals browning, dry and fall off on touch, bracts closed	Elongated torpedo embryo, endosperm almost utilised	Globular-full torpedo embryos, sometimes polyembryonic
13	Five days post petal fall	Near full length torpedo embryo, aleurone formed	Large globular-torpedo embryos, sometimes polyembryonic, proliferating aleurone
14	Bracts fully opened, exposed mature seed head	Mature seed with two cotyledons and two-celled aleurone layer adjacent to seed coat	Mature seed containing one or more embryos with varying cotyledon numbers, and two celled aleurone layer

Appendix 2: Contents of haematoxylin stained seeds

Wild Type D3 Seeds

Seed Contents	Floral Stage													
	5 - 6		6 - 7		7		8		9		10		11		12	
	n	%	n	%	n	%	n	%	n	%	n	%	n	%	n	%
collapsed embryo sac	8	9	24	31	22	17	18	16	15	20	18	16	4	6	8	12
egg cell, unfused polar nuclei (+/- synergids)	62	67	10	13	30	23	9	8	11	15	23	20	2	3	4	6
4-8 unidentified nuclei	16	17	8	10	1	1	0	0	2	3	0	0	0	0	0	0
4-16 large endosperm nuclei with egg cell*	0	0	22	29	17	13	10	9	5	7	0	0	0	0	0	0
8-16 large endosperm nuclei with no embryo	0	0	0	0	25	19	0	0	0	0	0	0	0	0	0	0
>16 small endosperm nuclei, no embryo	0	0	0	0	5	4	16	14	10	13	11	10	4	6	2	3
cellular endosperm and no embryo	0	0	0	0	0	0	0	0	0	0	9	8	10	16	7	11
4-8 large endosperm nuclei with small embryo	6	7	4	5	0	0	0	0	0	0	0	0	0	0	0	0
8-16 endosperm nuclei with small globular embryo	0	0	9	12	23	17	18	16	4	5	0	0	0	0	0	0
>16 small endosperm nuclei with globular embryo	0	0	0	0	10	8	35	30	24	32	12	11	5	8	0	0
cellularising endosperm with globular embryo**	0	0	0	0	0	0	10	9	2	3	6	5	9	15	0	0
cellular endosperm and globular embryo**	0	0	0	0	0	0	0	0	0	0	11	10	6	10	10	15
cellular endosperm and heart embryo**	0	0	0	0	0	0	0	0	2	3	22	19	20	32	8	12
cellular endosperm and torpedo embryo**	0	0	0	0	0	0	0	0	0	0	2	2	2	3	7	11
consumed endosperm and late torpedo embryo**	0	0	0	0	0	0	0	0	0	0	0	0	0	0	20	30
TOTAL	92		77		133		116		75		114		62		66	

Seed Contents	Floral Stage													
	5 - 6		6 - 7		7		8		9		10		11		12	
multiple embryos	0	0	0	0	0	0	0	0	0	0	14	12	7	11	10	15
multiple embryo sacs	0	0	8	10	11	8	12	10	7	9	9	8	5	8	4	6

* the egg cell was sometimes dividing

** these seeds sometimes contained multiple embryos

35S:HFIE:RNAi and MEA:HFIE:RNAi D3 Seeds

Seed Contents	Stage 7						Stage 8					
	35S #2		35S #5		35S #7		35S #2		35S #5		35S #7	
	n	%	n	%	n	%	n	%	n	%	n	%
collapsed embryo sac	9	15	13	24	30	45	9	14	17	30	30	60
collapsed embryo sac and ovule	0	0	0	0	0	0	0	0	0	0	0	0
unidentified nuclei	7	12	8	15	11	16	2	3	4	7	6	12
polar nucleus and egg cell	19	32	13	24	14	21	10	15	11	19	7	14
nuclear endosperm and no embryo	21	36	18	33	12	18	18	28	14	25	3	6
cellular endosperm and no embryo	0	0	0	0	0	0	4	6	0	0	1	2
nuclear endosperm and globular embryo	3	5	2	4	0	0	22	34	11	19	3	6
cellular endosperm and globular embryo	0	0	0	0	0	0	0	0	0	0	0	0
cellular endosperm and heart embryo	0	0	0	0	0	0	0	0	0	0	0	0
strange embryo and/or strange endosperm	0	0	0	0	0	0	0	0	0	0	0	0
aborted embryo	0	0	0	0	0	0	0	0	0	0	0	0
TOTAL	59		54		67		65		57		50	

Seed Contents	Stage 9						Stage 10/11					
	35S #2		35S #5		35S #7		35S #2		35S #5		35S #7	
	n	%	n	%	n	%	n	%	n	%	n	%
collapsed embryo sac	12	18	21	35	27	47	13	10	25	24	0	0
collapsed embryo sac and ovule	0	0	0	0	10	18	0	0	0	0	64	64
unidentified nuclei	9	13	6	10	4	7	0	0	0	0	3	3
polar nucleus and egg cell	11	16	6	10	5	9	28	21	9	9	9	9
nuclear endosperm and no embryo	10	15	6	10	5	9	5	4	15	14	11	11
cellular endosperm and no embryo	5	7	3	5	1	2	9	7	0	0	3	3
nuclear endosperm and globular embryo	18	26	10	17	4	7	6	4	14	13	5	5
cellular endosperm and globular embryo	2	3	2	3	1	2	14	10	22	21	5	5
cellular endosperm and heart embryo	1	1	1	2	0	0	51	38	8	8	0	0
strange embryo and/or strange endosperm	0	0	5	8	0	0	5	4	0	0	0	0
aborted embryo	0	0	0	0	0	0	4	3	11	11	0	0
TOTAL	68		60		57		135		104		100	
Seed Contents	35S #2		35S #5		35S #7		35S #2		35S #5		35S #7	
	n	%	n	%	n	%	n	%	n	%	n	%
polyembryony	1	0	0	0	0	0	9	7	2	2	0	0

Appendix 3: Primers and PCR Conditions

A. PCR reagents

Taq Polymerase

RedTaq	-	Sigma
Standard Taq Polymerase	-	Invitrogen
Platinum High Fidelity Taq Polymerase	-	Invitrogen

B. Conditions

Standard PCR*sprint* or PCR*express* machines (Hybaid) were used for the incubation of PCR reactions.

A typical PCR protocol was designed as follows, unless specified otherwise in the text:

94°C 3 minutes
then 18 to 35 cycles of

94°C denaturation for 30 seconds to 1 minute
X°C annealing for 30 seconds to 1 minute (X = annealing temperature of primer, usually 42-75°C)
72°C elongation for Y minutes (where 1 kb = 1 minute of elongation)

and a final elongation of

72°C for 7 minutes
4°C soak

Primer annealing temperatures were calculated for a $[Na^+] = 0.1$ M using the formula:-

$Tm = 81.5 + (16.6 \times \log[Na^+]) + 0.41 \times \%GC - (675/length)$

Typical PCR reactions contained

0.5 μM of each primer
0.2 mM of each dNTP
0.5 to 1 unit of Taq polymerase
2 mM $MgCl_2$
0.1 volumes of PCR Buffer

C. *Arabidopsis* promoter primers

MEDEA/FIS1 primers

FIS1FWD2	5'-CACGACGATTATCCATCTGC-3'
FIS1REV1'	5'-TTAACCACTCGCCTCTTCTTT-3'

Enhancer Trap primers

1391zREV1	5'-GTGAGCGCAACGCAATTAATGT-3'
1041AvrIIFWD	5'-AAGAGTCCTAGGCAACGGTTGACT-3'
1041AvrIIREV	5'-CGTGGTCTTCCTAGGTTTCAAAACTT-3'
1811SalIFWD	5'-ACGCGTCGACCTATTGTTGTTATGTTA-3'

1811NcoIREV	5'-GAACCCATGGCTGATTTTCAA-3'
2567Fwd	5'-AAACTGCAGACGAAGCTGAAG-3'
2567NcoIRev	5'-TGTGGTAGTAGAGTCCATGGTATGAGAA-3'
2209.1FwdBam	5'-CGGGATCCCGTCTTCACAGCCAAAAACCT-3'
2209.1RevNco	5'-TTCTCTTCTTTGCCATGGCGGAATTGGCGGTTT-3'
2209.2FwdBam	5'-CGGGATCCCGATTGGCGGTTTTAATGGTT-3'
2209.2RevNco	5'-TGTGGAGAACCATGGTCTTCACAGCCAAA-3'
3536Fwd	3'-TTTGAGATGAGTTTTATCGTTTG-5'
3536NcoIRev	3'-GTAGTCTCCATGGCTATTACGAT-5'

D. General primers

β-glucoronidase (GUS) gene primers

GUSFWD	5'-CTGTAGAAACCCCAACCCGTG-3'
GUSREV	5'-CATTACGCTGCGATGGATCCC-3'

Hygromycin phosphotransferase gene primers

HygroFWD	5'-GTGCTTTCAGCTTCGATGTAGGA-3'
HygroREV	5'-TCACGCCATGTAGTGTATTGACC-3'

E. Gene isolation primers

B26 and B25 primers

B26	5'-GACTCGAGTCGACATCGATTTTTTTTTTTTTTTT-3'
B25	5'- GACTCGAGTCGACATCG-3'

Degenerate FIS3/FIE primers

FIS3F433	5'-GATGARGATAAGG-3'
FIS3R656	5'-CATYCCACARICKAAC-3'
FIS3F459	5'-ACACDSTRAGTTGGGC-3'
FIS3R636	5'-GATTSATYYTTGTTDGCAG-3'

MET Primers

MF3204	5'-TGGGCDATYGARTAYGAAG-3'
MR3848	5'-ACATGCATHGGYTCWGG-3'
MF3280	5'-AAYTGYAATGTGAT-3'
MR3754	5'-ACCTGRTAWCCCAT-3'
MF3407	5'-ATGGAKAARTGTGGRGAT-3'

HDAC primers

HDF287	5'-AARAARTTYAAYYTICC-3'
HDR418	5'-TAYTCRTCRTCIC-3'
HDF297	5'-GGIGGIGGIGGITAYAC-3'
HDR416	5'-TCRTCICKYTCYTTRTC-3'

FIS2 primers

fis2fwd1630	5'-CARTTYTAYCAYTC-3'
fis2fwd1828	5'-GCIGAYGGICAYGTICCITGG-3'
fis2fwd1837	5'-CAYGTICCITGGGCITGYGA-3'

F. RT-PCR primers

B-tubulin

BtubRTfwd	5'-GGGTGCTGGAAACAATTGGGCTAA-3'
BtubRTrev	5'-ACTGCTCACTCACGCGCCTAA-3'

HFIE

RTHFIEF3	5'-CCGTGTCATTGATGCTGGCAAT-3'
RTHFIER2	5'-GCAGCTGCATTGTAGTGGAAATCA-3'

FIS2/EMF2

RTFIS2likeF1	5'-CTGTGCAGTCAGTCCCTGAA-3'
RTFIS2likeR1	5'-CCAACACCACAGAAGTGACG-3'

HDAC

HDSFWD	5'-CCGCTCGAGCGGGGTGGAGGGTATACAAAAGAAAA-3'
HDSREV	5'-GGAATTCCCATTTCGCTCATCTGGGTTT-3'

G. CAPS PCR primers

fie-2

fie-2Fwd	5'- TGTTCTATGTATCCTAGCAAATGCTTC-3'
fie-2Rev	5'- TCCTTATTCAATTAAAACGTAACAGC-3'

H. *Hieracium* promoter primers

Library adapter primers

AP1	5'-GGATCCCTAATACGACTCACTATAGGG-3'
AP2	5'-AATAGGGCTCGAGCGGC-3'

Nested HFIE primers

PrFIE3	5'-ACCGCCGACAGTGGCGAAGACATT-3'
PrFIE2	5'-AATTGGGCGCTTGCCTTCCTGTAG-3'
PrFIE1	5'-CCTTCCTGTAGCCTGTTGGTGACT-3'

HFIE 5'UTR spanning primers

D3PrF-232	5'-AAGASAAATCAGGGGGTATTTGTGT-3'
P4PrF-228	5'-GAAATCAGGGGGTATTTGTGTA-3'

D3 and P4 EHFIE:GUS primers

PrFIEFwd	5'-CCCGGGCAGGTATCACATACATTA-3'
PrFIERev	5'-AACGTTATCTTCG**CCATGG**AAACTGT-3'

D3 and P4 cHFIE:GUS primers

P4codeFwd	5'-GCAGGTACCCTTTCCCTCCTG-3'
P4**NcoI**Rev	5'-CGTTATCTTCG**CCATGG**AAACTGTAGT-3'

D3code2-1Fwd	5'-TTCATTACTTTTGCTCGATTGCTTG-3'
D3NcoIRev	5'-ATCTTCG**CCATGG**GAAACTGTACT-3'

I. *Hieracium* RNAi primers

FIESFWD-***XhoI***	5'-***CCGCTCGAGCGG***-CTTCTCTTGTGCTTTCTGCAAGT-3'
FIESREV-***EcoRI***	5'-***GGAATTCC***-GGTACGGGATATTTCCGCAGTAT-3'
FIEASFWD-***XbaI***	5'-***GCTCTAGAGC***-CTTCTCTTGTGCTTTCTGCAAGT-3'
FIEASREV-***HindIII***	5'-***CCCAAGCTT***-GGGGGTACGGGATATTTCCGCAGTAT-3'

Bibliography

Agrawal A.F. (2001). Sexual selection and the maintenance of sexual reproduction. Nature **411**, 692-695.

Agrawal A.F. & Chasnov J.R. (2001). Recessive mutations and the maintenance of sex in structured populations. Genetics **158**, 913-917.

Altschul S.F., Gish W., Miller W., Myers E.W. & Lipman D.J. (1990). Basic local alignment search tool. J. Mol. Biol. **215**, 403-410.

Araujo A.C.G., Mukhambetzhanov S., Pozzobon M.T., Santana E.F. & Carneiro V.T.C. (2000). Female gametophyte development in apomictic and sexual *Brachiaria brizantha* (Poaceae). Revue de Cytologie et Biologie vegetales-Le Botaniste **23**, 13-26.

Asker S.E. & Jerling L. (1992) *Apomixis in plants*. CRC Press, Boca Raton.

Barcaccia G., Mazzucato A., Albertini E., Zethof J., Gerats A., Pezzotti M. & Falcinelli M. (1998). Inheritance of parthenogenesis in *Poa pratensis* L.: auxin test and AFLP linkage analyses support monogenic control. Theor. Appl. Genet. **97**, 74-82.

Batchelor A.H., Piper D.E., de la Brousse F.C., McKnight S.L. & Wolberger C. (1998). The structure of GABP alpha/beta: An ETS domain ankyrin repeat heterodimer bound to DNA. Science **279**, 1037-1041.

Battaglia E. (1989). The evolution of the female gametophyte in angiosperms: An interpretative key. Annali de Botanica (Roma) **47**, 7-144.

Becraft P.W. & Asuncion-Crabb Y. (2000). Positional cues specify and maintain aleurone cell fate in maize endosperm development. Development **127**, 4039-4048.

Becraft P.W., Stinard P.S. & McCarty D.R. (1996). CRINKLY4: A TNFR-like receptor kinase involved in maize epidermal differentiation. Science **273**, 1406-1409.

Belitsky B.R. & Sonenshein A.L. (1999). An enhancer element located downstream of the major *glutamate dehydrogenase* gene of *Bacillus subtilis*. Proc. Natl. Acad. Sci. USA. **96**, 10290-10295.

Bellen H.J., O'Kane C.J., Wilson C., Grossniklaus U., Pearson R.K. & Oehring W.J. (1989). P-element-mediated enhancer detection: a versatile method to study development in *Drosophila*. Gen. & Dev. **3**, 1288-1300.

Bennetzen J.L. & Kellogg E.A. (1997). Do plants have a one-way ticket to genomic obesity? Plant Cell **9**, 1509-1514.

Berger F. (2003). Endosperm: the crossroad of seed development. Curr. Opin. Plant Biol. **6**, 42-50.

Bicknell R.A. (1994). Micropropagation of *Hieracium aurantiacum*. Plant Cell Tiss. Org. Cult. **37**, 197-199.

Bicknell R.A. (1997). Isolation of a diploid, apomictic plant of *Hieracium aurantiacum*. Sex. Plant Reprod. **10**, 168-172.

Bicknell R.A. & Borst N.K. (1994). Agrobacterium-Mediated Transformation of *Hieracium aurantiacum*. Int. J. Plant Sci. **155**, 467-470.

Bicknell R.A., Borst N.K. & Koltunow A.M. (2000). Monogenic inheritance of apomixis in two *Hieracium* species with distinct developmental mechanisms. Heredity **84**, 228-237.

Bier E., Vaessin H., Sheperd S., Lee K., McCall K., Barbel S., Ackerman L., Caretto R., Uemura T., Grell E., Jan L.Y. & Jan Y.N. (1989). Searching for pattern and mutation in the *Drosophila* genome with P-lacZ vector. Gen. & Dev. **3**, 1273-1287.

Birve A., Sengupta A.K., Beuchle D., Larsson J., Kennison J.A., Rasmuson-Lestander A. & Muller J. (2001). *Su(z)12*, a novel *Drosophila Polycomb* group gene that is conserved in vertebrates and plants. Development **128**, 3371-3379.

Bouman F. (1984) The ovule. In: *Embryology of Angiosperms* (ed B.M. Johri), pp. 123-157. Springer-Verlag, Berlin Heidelberg.

Boutilier K., Offringa R., Sharma V.K., Kieft H., Ouellet T., Zhang L.M., Hattori J., Liu C.M., van Lammeren A.A.M., Miki B.L.A., Custers J.B.M. & Campagne M.M.V. (2002). Ectopic expression of *BABY BOOM* triggers a conversion from vegetative to embryonic growth. Plant Cell **14**, 1737-1749.

Brink R.A. & Cooper D.C. (1947). The endosperm in seed development. Bot. Rev. **13**, 423-541.

Brown R.C., Lemmon B.E., Nguyen H. & Olsen O.A. (1999). Development of endosperm in *Arabidopsis thaliana*. Sex. Plant Reprod. **12**, 32-42.

Brown R.C., Lemmon B.E. & Olsen O.A. (1996). Polarization predicts the pattern of cellularization in cereal endosperm. Protoplasma. **192**, 168-177.

Bruck D.K. & Walker D.B. (1985). Cell determination during embryogenesis in *Citrus jarmbhiri*. L. Ontogeny of the epidermis. Bot. Gaz. **146**, 188-195.

Brutovska R., Cellarova E. & Dolezel J. (1998). Cytogenetic variability of in vitro regenerated *Hypericum perforatum* L plants and their seed progenies. Plant Sci. **133**, 221-229.

Buttrose M. (1963). Ultrastructure of the developing aleurone cells of wheat grain. Aust. J. Biol. Sci. **16**, 768-774.

Campisi L., Yang Y.Z., Yi Y., Heilig E., Herman B., Cassista A.J., Allen D.W., Xiang H.J. & Jack T. (1999). Generation of enhancer trap lines in *Arabidopsis* and characterization of expression patterns in the inflorescence. Plant J. **17**, 699-707.

Canales C., Bhatt A.M., Scott R. & Dickinson H. (2002). *EXS*, a putative LRR receptor kinase, regulates male germline cell number and tapetal identity and promotes seed development in *Arabidopsis*. Curr. Biol. **12**, 1718-1727.

Cao R., Wang L.J., Wang H.B., Xia L., Erdjument-Bromage H., Tempst P., Jones R.S. & Zhang Y. (2002). Role of histone H3 lysine 27 methylation in *Polycomb* group silencing. Science **298**, 1039-1043.

Carman J.G. (1997). Asynchronous expression of duplicate genes in angiosperms may cause apomixis, bispory, tetraspory, and polyembryony. Biol. J. Linn. Soc. **61**, 51-94.

Carman J.G. (2001) The gene effect: genome collisions and apomixis. In: *The Flowering of Apomixis: From Mechanisms to Genetic Engineering*. (eds Y. Savidan, J.G. Carman, & T. Dresselhaus), pp. 95-110. CIMMYT, IRS, Eur. Comm. DG VI, Mexico.

Chandler J., Wilson A. & Dean C. (1996). *Arabidopsis* mutants showing an altered response to vernalization. Plant J. **10**, 637-644.

Chapman G.P. & Darlington C.D. (1992) Apomixis and evolution. In: *Grass evolution and domestication* (ed G.P. Chapman), pp. 138-155. Cambridge Uni Press, Cambridge.

Charlesworth B. (1990). Mutation-selection balance and the evolutionary advantage of sex and recombination. Genet. Res. **55**, 199-221.

Chasnov J.R. (2000). Mutation selection balance, dominance and the maintenance of sex. Genetics **156**, 1419-1425.

Chaudhury A.M., Koltunow A., Payne T., Luo M., Tucker M.R., Dennis E.S. & Peacock W.J. (2001). Control of early seed development. Ann. Rev. Cell Dev. Biol. **17**, 677-699.

Chaudhury A.M., Ming L., Miller C., Craig S., Dennis E.S. & Peacock W.J. (1997). Fertilization-independent seed development in *Arabidopsis thaliana*. Proc. Natl. Acad. Sci. USA. **94**, 4223-4228.

Chevalier D., Sieber P. & Schneitz K. (2002) The genetic and molecular control of ovule development. In: *Plant Reproduction* (ed S.D. O'Neil & J.A. Roberts), pp. 61-85. Sheffield Academic Press, Sheffield, UK.

Chimielewski J.G. (1994). The *Antennaria frieseana* (Asteraceae: Inuleae) polyploid complex: morphological variation in sexual and agamasporous taxa. Can. J. Bot. **72**, 1018-1026.

Choi Y.H., Gehring M., Johnson L., Hannon M., Harada J.J., Goldberg R.B., Jacobsen S.E. & Fischer R.L. (2002). DEMETER, a DNA glycosylase domain protein, is required for endosperm gene imprinting and seed viability in *Arabidopsis*. Cell **110**, 33-42.

Christensen C.A., Gorsich S.W., Brown R.H., Jones L.G., Brown J., Shaw J.M. & Drews G.N. (2002). Mitochondrial *GFA2* is required for synergid cell death in *Arabidopsis*. Plant Cell **14**, 2215-2232.

Christensen C.A., King E.J., Jordan J.R. & Drews G.N. (1997). Megagametogenesis in *Arabidopsis* wild type and the *Gf* mutant. Sex. Plant Reprod. **10**, 49-64.

Chuang C.F. & Meyerowitz E.M. (2000). Specific and heritable genetic interference by double-stranded RNA in *Arabidopsis thaliana*. Proc. Natl. Acad. Sci. USA. **97**, 4985-4990.

Clough S.J. & Bent A.F. (1998). Floral dip: a simplified method for *Agrobacterium*-mediated transformation of *Arabidopsis thaliana*. Plant J. **16**, 735-743.

Colombo L., Franken J., VanderKrol A.R., Wittich P.E., Dons H.J.M. & Angenent G.C. (1997). Downregulation of ovule-specific MADS box genes from petunia results in maternally controlled defects in seed development. Plant Cell **9**, 703-715.

Cooper D.C. & Brink R.A. (1949). The endosperm-embryo relationship in an autonomous apomict, *Taraxacum officianale*. Bot. Gaz. **111**, 139-152.

Costas-Lippmann M. (1979). Embryogeny of *Cortaderia selloana* and *C. jubata* (Gramineae). Bot. Gaz. **140**, 393-397.

Dalmay T., Horsefield R., Braunstein T.H. & Baulcombe D.C. (2001). SDE3 encodes an RNA helicase required for posttranscriptional gene silencing in *Arabidopsis*. Embo J. **20**, 2069-2077.

Danilevskaya O.N., Hermon P., Hantke S., Muszynski M.G., Kollipara K. & Ananiev E.V. (2003). Duplicated *fie* genes in Maize: Expression pattern and imprinting suggest distinct functions. Plant Cell **14**, 1-14.

Davis G.L. (1968). Apomixis and abnormal anther development in *Calotis lappulaceae* Benth. (Compositae). Aust. J. Bot. **16**, 1-17.

DeLille J.M., Sehnke P.C. & Ferl R.J. (2001). The *Arabidopsis* 14-3-3 family of signalling regulators. Plant Phys. **126**, 35-38.

Denisenko O., Shnyreva M., Suzuki H. & Bomsztyk K. (1998). Point mutations in the WD40 domain of Eed block its interaction with Ezh2. Mol. Cell. Biol. **18**, 5634-5642.

Devos K.M., Brown J.K.M. & Bennetzen J.L. (2002). Genome size reduction through illegitimate recombination counteracts genome expansion in *Arabidopsis*. Gen. Res. **12**, 1075-1079.

DeYoung B.J. & Clark S.E. (2001). Signaling through the CLAVATA1 receptor complex. Plant Mol. Biol. **46**, 505-513.

Diggle P.K., Lower S. & Ranker T.A. (1998). Clonal diversity in alpine populations of *Polygonum viviparum* (polygonaceae). Int. J. Plant Sci. **159**, 606-615.

Doyle J.J. (1991) DNA protocols for plants. In: *Molecular techniques in taxonomy* (eds G.M. Hewitt, A.W.B. Johnston, & J.P.W. Young), pp. 283-293. Springer, Berlin Heidelberg New York.

Drews G.N. & Yadegari R. (2002). Development and function of the angiosperm female gametophyte. Ann. Rev. Gene. **36**, 99-124.

Dudley N.R., Labbe J.C. & Goldstein B. (2002). Using RNA interference to identify genes required for RNA interference. Proc. Natl. Acad. Sci. USA. **99**, 4191-4196.

Duwayri M., Tran D.V. & Nguyen V.N. (2000) Reflections on yield gaps in rice production: how to narrow the gaps. In: *Bridging the Rice Yield Gap in the Asia-Pacific Region* (eds M.K. Papademetriou, J. Frank, & E.M. Herath). FAO, Bangkok, Thailand.

Egnell K. (1989). Embryology of barley: time course and analysis of controlled fertilisation and early embryo formation after fertilisation of the egg cell. Nord. J. Bot. **9**, 265-280.

Ellstrand N.C. & Roose M.L. (1987). Patterns of genotypic diversity in clonal plant species. Am. J. of Bot. **74**, 123-131.

Ernst A. (1918) *Die Bastardierung als Ursache der Apogamie im Pflanzenre.* Fischer, Jena, Germany.

Ernst A. & Bernard C.H. (1912). Entwicklungsgeschichte des embryosackes, des Embryos und des Endosperms von *Burmannia coelestis* Don. Ann Jard Bot Buitenzorg II. **11**, 234-257.

Eshed Y., Baum S.F. & Bowman J.L. (1999). Distinct mechanisms promote polarity establishment in carpels of *Arabidopsis*. Cell **99**, 199-209.

Estrada-Luna A.A., Huanca-Mamani W., Acosta-Garcia G., Leon-Martinez G., Becerra-Flora A., Perez-Ruiz R. & Vielle-Calzada J.P. (2002). Beyond promiscuity: From sexuality to apomixis in flowering plants. In Vitro Cell. Dev. Biol. Plant. **38**, 146-151.

Fagard M. & Vaucheret H. (2000). Systemic silencing signal(s). Plant Mol. Biol. **43**, 285-293.

FAO (Food and Agricultural Organisation of the United Nations) (1996) *Role of research in global food security and agricultural development. In: Report of the World Food Summit.* Paper presented at the World Food Summit, Rome, Italy.

Faure J.E., Rotman N., Fortune P. & Dumas C. (2002). Fertilization in *Arabidopsis thaliana* wild type: Developmental stages and time course. Plant J. **30**, 481-488.

Fedoroff N. (2000). Transposons and genome evolution in plants. Proc. Natl. Acad. Sci. USA. **97**, 7002-7007.

Felker F.C., Peterson D.M. & Nelson O.E. (1985). Anatomy of immature grains of eight maternal effect *shrunken* endosperm barley mutants. Am. J. Bot. **72**, 248-256.

Ferl R.J., Chung H.J. & Sehnke P.C. (1999). The 14-3-3 proteins: cellular regulators of plant metabolism (vol 4, pg 367, 1999). Trends Plant Sci. **4**, 463-463.

Finnegan E.J. (2001). Is plant gene expression regulated globally? Trends Genet. **17**, 361-365.

Finnegan E.J. & Kovac K.A. (2000). Plant DNA methyltransferases. Plant Mol. Biol. **43**, 189-201.

Finnegan E.J., Peacock W.J. & Dennis E.S. (1996). Reduced DNA methylation in *Arabidopsis thaliana* results in abnormal plant development. Proc. Natl. Acad. Sci. USA. **93**, 8449-8454.

Finnegan E.J., Peacock W.J. & Dennis E.S. (2000). DNA methylation, a key regulator of plant development and other processes. Curr. Opin. Genet. Dev. **10**, 217-223.

Flavell A.J., Pearce S.R. & Kumar A. (1994). Plant transposable elements and the genome. Curr. Opin. Genet. Dev. **4**, 838-844.

Focke W.O. (1881) Die Pflanzenmischlinge. Verlag von Gebruder Borntraeger, Berlin.

Fraser A.G., Kamath R.S., Zipperlen P., Martinez-Campos M., Sohrmann M. & Ahringer J. (2000). Functional genomic analysis of *C-elegans* chromosome I by systematic RNA interference. Nature **408**, 325-330.

Friedman W.E. (1994). The Evolution of Embryogeny in Seed Plants and the Developmental Origin and Early History of Endosperm. Am. J. Bot. **81**, 1468-1486.

Gasser C.S., Broadhvest J. & Hauser B.A. (1998). Genetic analysis of ovule development. Ann. Rev. Plant Phys. Plant Mol. Biol. **49**, 1-24.

Gendall A.R., Levy Y.Y., Wilson A. & Dean C. (2001). The *VERNALIZATION 2* gene mediates the epigenetic regulation of vernalization in *Arabidopsis*. Cell **107**, 525-535.

Genger R.K., Kovac K.A., Dennis E.S., Peacock W.J. & Finnegan E.J. (1999). Multiple DNA methyltransferase genes in *Arabidopsis thaliana*. Plant Mol. Biol. **41**, 269-278.

Gomez E., Royo J., Guo Y., Thompson R. & Hueros G. (2002). Establishment of cereal endosperm expression domains: Identification and properties of a maize transfer cell-specific transcription factor, *ZmMRP-1*. Plant Cell **14**, 599-610.

Gonczy P., Echeverri C., Oegema K., Coulson A., Jones S.J.M., Copley R.R., Duperon J., Oegema J., Brehm M., Cassin E., Hannak E., Kirkham M., Pichler S., Flohrs K., Goessen A., Leidel S., Alleaume A.M., Martin C., Ozlu N., Bork P. & Hyman A.A. (2000). Functional genomic analysis of cell division in C-elegans using RNAi of genes on chromosome III. Nature **408**, 331-336.

Gorina S. & Pavletich N.P. (1996). Structure of the p53 tumour suppressor bound to the ankyrin and SH3 domains of 53BP2. Science **274**, 1001-1005.

Grandbastien M.-A. (1992). Retroelements in higher plants. Trends Genet. **8**, 103-108.

Grimanelli D., Hernandez M., Perotti E. & Savidan Y. (1997). Dosage effects in the endosperm of diplosporous apomictic *Tripsacum* (Poaceae). Sex. Plant Reprod. **10**, 279-282.

Grimanelli D., Leblanc O., Espinosa E., Perotti E., De Leon D.G. & Savidan Y. (1998). Mapping diplosporous apomixis in tetraploid *Tripsacum*: one gene or several genes? Heredity **80**, 33-39.

Grimanelli D., Leblanc O., Perotti E. & Grossniklaus U. (2001). Developmental genetics of gametophytic apomixis. Trends Genet. **17**, 597-604.

Grini P.E., Jurgens G. & Hulskamp M. (2002). Embryo and endosperm development is disrupted in the female gametophytic *capulet* mutants of *Arabidopsis*. Genetics **162**, 1911-1925.

Grossniklaus U. (2001) From sexuality to apomixis: molecular and genetic approaches. In: *The Flowering of Apomixis: From Mechanisms to Genetic Engineering* (eds Y. Savidan, J.G. Carman, & T. Dresselhaus), pp. 168-211. CIMMYT, IRS, Eur. Comm. DG VI, Mexico.

Grossniklaus U., Bellen H.J., Wilson C. & Gehring W.J. (1989). P-element-mediated enhancer detection applied to the study of oogenesis in *Drosophila*. Development **107**, 189-200.

Grossniklaus U., Koltunow A. & Campagne M.V. (1998a). A bright future for apomixis. Trends Plant Sci. **3**, 415-416.

Grossniklaus U., Nogler G.A. & van Dijk P.J. (2001a). How to avoid sex: The genetic control of gametophytic apomixis. Plant Cell **13**, 1491-1497.

Grossniklaus U., Spillane C., Page D.R. & Kohler C. (2001b). Genomic imprinting and seed development: endosperm formation with and without sex. Curr. Opin. Plant Biol. **4**, 21-27.

Grossniklaus U. & Schneitz K. (1998). The molecular and genetic basis of ovule and megagametophyte development. Sem. Cell Dev. Biol. **9**, 227-238.

Grossniklaus U., Vielle-Calzada J.P., Hoeppner M.A. & Gagliano W.B. (1998b). Maternal control of embryogenesis by *medea*, a *Polycomb* group gene in *Arabidopsis*. Science **280**, 446-450.

Grossniklaus U. & Vielle-Calzada J.P. (1998) ...response: Parental conflict and infanticide during embryogenesis. Trends Plant Sci. **3**, 328.

Guerin J., Rossel J.B., Robert S., Tsuchiya T. & Koltunow A. (2000). A *DEFICIENS* homologue is down-regulated during apomictic initiation in ovules of *Hieracium*. Planta **210**, 914-920.

Hanna W.W. & Bashaw E.C. (1987). Apomixis: Its identification and use in plant breeding. Crop Sci. **27**, 1136-1139.

Hecht V., Vielle-Calzada J.P., Hartog M.V., Schmidt E.D.L., Boutilier K., Grossniklaus U. & de Vries S.C. (2001). The *Arabidopsis SOMATIC EMBRYOGENESIS RECEPTOR KINASE 1* gene is expressed in developing ovules and embryos and enhances embryogenic competence in culture. Plant Phys. **127**, 803-816.

Herr J.M. (1999). Endosperm development in *Arabidopsis thaliana* (L.) Heynh. Acta Biol. Crac. Ser. Bot. **41**, 103-109.

Hirner B., Fischer W.N., Rentsch D., Kwart M. & Frommer W.B. (1998). Developmental control of H+/amino acid permease gene expression during seed development of *Arabidopsis*. Plant J. **14**, 535-544.

Hirochika H., Okamoto H. & Kakutani T. (2000). Silencing of retrotransposons in *Arabidopsis* and reactivation by the ddm1 mutation. Plant Cell **12**, 357-368.

Hodge R., Paul W., Draper J. & Scott R. (1992). Cold-Plaque Screening - a Simple Technique For the Isolation of Low Abundance, Differentially Expressed Transcripts From Conventional cDNA Libraries. Plant J. **2**, 257-260.

Hong S.K., Kitano H., Satoh H. & Nagato Y. (1996). How is embryo size genetically regulated in rice? Development. **122**, 2051-2058.

Hoshikawa K. (1993) Anthesis, fertilisation and development of caryopsis. In: *Science of the Rice Plant I: Morphology* (eds T. Matsuo & H. Hoshikawa), pp. 339-376. Nobunkyo, Tokyo.

Huang B.Q. & Sheridan W.F. (1996). Embryo sac development in the maize *indeterminate gametophyte1* mutant: Abnormal nuclear behaviour and defective microtubule organization. Plant Cell **8**, 1391-1407.

Ingram G.C., Simon R., Carpenter R. & Coen E.S. (1998). The *Antirrhinum ERG* gene encodes a protein related to bacterial small GTPases and is required for embryonic viability. Curr. Biol. **8**, 1079-1082.

Izmailow R. (1994). Further observations in embryo sac development in *Alchemilla* L (subsection Heliodrosium Rothm). Acta Biol. Crac. Ser. Bot. **36**, 37-41.

Jacobs J.J.L. & van Lohuizen M. (1999). Cellular memory of transcriptional states by *Polycomb* group proteins. Sem Cell Dev. Biol. **10**, 227-235.

Jacobs J.J.L. & van Lohuizen M. (2002). *Polycomb* repression: from cellular memory to cellular proliferation and cancer. Bioch. Biophys. Acta - Rev. On Cancer **1602**, 151-161.

Jacobsen S.E. & Meyerowitz E.M. (1997). Hypermethylated *SUPERMAN* epigenetic alleles in *Arabidopsis*. Science **277**, 1100-1103.

Jang I.-C., Pahk Y.-M., Song S.I., Kwon H.-J., Nahm B.H. & Kim J.-K. (2003). Structure and expression of the rice class-1 type histone deacetylase genes *OsHDAC1-3*: *OsHDAC1* overexpression in transgenic plants leads to increased growth rate and altered architecture. Plant J. **33**, 531-541.

Jassem B. (1990). Apomixis in the genus *Beta*. Apomixis Newsletter. **2**, 7.

Jeddeloh J.A., Stokes T.L. & Richards E.J. (1999). Maintenance of genomic methylation requires a SW12/SNF2-like protein. Nat. Genet. **22**, 94-97.

Johnston S.A., den Nijs T.P.M., Peloquin S.K. & Hanneman R.E. (1980). The significance of genic labance to endosperm development in interspecific crosses. Theor. Appl. Genet. **57**, 5-9.

Johri B.M. & Ambegoakar K.B. (1984) Embryology: Then and now. In: *Embryology of angiosperms* (ed B.M. Johri), pp. 1-47. Springer Verlag, Berlin.

Johri B.M. & Tiagi B. (1952). Floral morphology and seed formation in *Cuscuta reflexa* Roxb. Phytomorphology **2**, 162-180.

Jones R.L. (1969). The fine structure of barley aluerone cells. Planta **85**, 359-376.

Kakutani T. (2002). Epi-alleles in plants: Inheritance of epigenetic information over generations. Plant Cell Physiol. **43**, 1106-1111.

Kakutani T., Jeddeloh J.A., Flowers S.K., Munakata K. & Richards E.J. (1996). Developmental abnormalities and epimutations associated with DNA hypomethylation mutations. Proc. Natl. Acad. Sci. USA. **93**, 12406-12411.

Kehle J., Beuchle D., Treuheit S., Christen B., Kennison J.A., Bienz M. & Muller J. (1998). dMi-2, a hunchback-interacting protein that functions in *Polycomb* repression. Science **282**, 1897-1900.

Kidwell M.G. & Lisch D.R. (2001). Perspective: Transposable elements, parasitic DNA, and genome evolution. Evolution. **55**, 1-24.

Kinoshita T., Harada J.J., Goldberg R.B. & Fischer R.L. (2001). *Polycomb* repression of flowering during early plant development. Proc. Natl. Acad. Sci. USA. **98**, 14156-14161.

Kishimoto N., Sakai H., Jackson J., Jacobsen S.E., Meyerowitz E.M., Dennis E.S. & Finnegan E.J. (2001). Site specificity of the *Arabidopsis METI* DNA methyltransferase demonstrated through hypermethylation of the superman locus. Plant Mol. Biol. **46**, 171-183.

Kojima A. & Nagato Y. (1997). Discovery of highly apomictic and highly amphimictic dihaploids in *Allium tuberosum*. Sex. Plant Reprod. **10**, 8-12.

Koltunow A.M., Vivian-Smith A., Tucker M.R. & Paech N.P. (2002) The central role of the ovule in apomixis and parthenocarpy. In: *Plant Reproduction* (eds S.D. O'neill & J.A. Roberts), pp. 221-256. Sheffield Academic Press, Sheffield, UK.

Koltunow A.M. (1993). Apomixis: embryo sacs and embryos formed without meiosis or fertilization in ovules. Plant Cell **5**, 1425-1437.

Koltunow A.M. (2000). The genetic and molecular analysis of apomixis in the model plant *Hieracium*. Acta Biol. Crac. Ser. Bot. **42**, 61-72.

Koltunow A.M., Bicknell R.A. & Chaudhury A.M. (1995a). Apomixis: molecular strategies for the generation of genetically identical seeds without fertilization. Plant Phys. **108**, 1345-1352.

Koltunow A.M. & Grossniklaus U. (2003). Apomixis: A developmental perspective. Ann. Rev. Plant. Biol. **54** (in press).

Koltunow A.M., Johnson S.D. & Bicknell R.A. (1998). Sexual and apomictic development in *Hieracium*. Sex. Plant Reprod. **11**, 213-230.

Koltunow A.M., Johnson S.D. & Bicknell R.A. (2000). Apomixis is not developmentally conserved in related, genetically characterised *Hieracium* plants of varying ploidy. Sex. Plant Reprod. **12**, 253-266.

Koltunow A.M., Johnson S.D., Lynch M., Yoshihara T. & Costantino P. (2001). Expression of *rolB* in apomictic *Hieracium piloselloides* Vill. causes ectopic meristems in planta and changes in ovule formation, where apomixis initiates at higher frequency. Planta **214**, 196-205.

Koltunow A.M., Soltys K., Nito N. & McClure S. (1995b). Anther, ovule, seed, and nucellar embryo development in *Citrus sinensis* cv. Valencia. Can. J. Bot. **73**, 1567-1582.

Koltunow A.M. & Tucker M.R. (2003) Advances in apomixis research: can we fix heterosis? In: *Plant biotechnology and beyond* (ed I.K. Vasil). pp 39-46. Kluwer, Dordrecht, The Netherlands.

Kondrashov A.S. (1982). Selection against harmful mutations in large sexual and asexual populations. Genet. res. **40**, 325-332.

Korthout H. & de Boer A.H. (1994). A Fusicoccin Binding-Protein Belongs to the Family of 14-3-3- Brain Protein Homologs. Plant Cell **6**, 1681-1692.

Koscinska-Pajak M. (1996). Embryological problems in the apomictic species *Chondrilla juncea* L (Compositae). Fol. Geo. & Phyto. **31**, 397-403.

Koscinska-Pajak M. (1998). Intraindividual variability of endosperm in autonomously apomictic *Chondrilla juncea* L. Acta Biol. Crac. Ser. Bot. **40**, 69-73.

Krahulcova A., Krahulec F. & Chapman H.M. (2000). Variation in *Hieracium* subgen. Pilosella (Asteraceae): What do we know about its sources? Folia Geobot. **35**, 319-338.

Kumar A. (1996). The adventures of the Ty1-copia group of retrotransposons in plants. Trends Genet. **12**, 41-43.

Kumar A. & Bennetzen J.L. (1999). Plant retrotransposons. Ann. Rev. Genet. **33**, 479-532.

Kunze R., Saedler H. & Lonnig W.E. (1997) Plant transposable elements. In: *Advances in Botanical Research, Vol 27*, pp. 331-470.

Kuzmichev A., Nishioka K., Erdjument-Bromage H., Tempst P. & Reinberg D. (2002). Histone methyltransferase activity associated with a human multiprotein complex containing the Enhancer of Zeste protein. Gen. & Dev. **16**, 2893-2905.

Lakshmanan K.K. & Ambegaokar K.K. (1984) Polyembryony. In: *Embryology of Angiosperms* (ed B.M. Johri), pp. 445-474. Springer-Verlag, Berlin.

Lambermon M.H.L., Fu Y., Kirk D.A.W., Dupasquier M., Filipowicz W. & Lorkovic Z.J. (2002). UBA1 and UBA2, two proteins that interact with UBP1, a multifunctional effector of pre-mRNA maturation in plants. Mol. Cell. Biol. **22**, 4346-4357.

Leblanc O., Armstead I., Pessino S., Ortiz J.P., Evans C., doValle C. & Hayward M.D. (1997). Non-radioactive mRNA fingerprinting to visualise gene expression in mature ovaries of *Brachiaria* hybrids derived from *B. brizantha*, an apomictic tropical forage. Plant Sci. **126**, 49-58.

Leblanc O., Grimanelli D., IslamFaridi N., Berthaud J. & Savidan Y. (1996). Reproductive behaviour in maize-*Tripsacum* polyhaploid plants: Implications for the transfer of apomixis into maize. J. Hered. **87**, 108-111.

Leblanc O., Peel M.D., Carman J.G. & Savidan Y. (1995). Megasporogenesis and megagametogenesis in several *Tripsacum* species. Am. J. Bot. **82**, 57-63.

Lee H.S. & Chen Z.J. (2001). Protein-coding genes are epigenetically regulated in *Arabidopsis* polyploids. Proc. Natl. Acad. Sci. USA. **98**, 6753-58.

Lin B.Y. (1984). Ploidy barrier to endosperm development in maize. Genetics **107**, 103-115.

Liu C.M. & Meinke D.W. (1998). The *titan* mutants of *Arabidopsis* are disrupted in mitosis and cell cycle control during seed development. Plant J. **16**, 21-31.

Liu Q., Singh S. & Green A. (2000). Genetic modification of cotton seed oil using inverted-repeat gene-silencing techniques. Biochem. Soc. Trans. **28**, 927-929.

Liu Y.G., Mitsukawa N., Oosumi T. & Whittier R.F. (1995). Efficient Isolation and Mapping of *Arabidopsis thaliana* T-DNA Insert Junctions By Thermal Asymmetric Interlaced PCR. Plant J. **8**, 457-463.

Lopes M.A. & Larkins B.A. (1993). Endosperm Origin, Development, and Function. Plant Cell **5**, 1383-1399.

Lord E.M. & Russell S.D. (2002). The mechanisms of pollination and fertilization in plants. Ann. Rev. Cell Dev. Biol. **18**, 81-105.

Lorkovic Z.J. & Barta A. (2002). Genome analysis: RNA recognition motif (RRM) and K homology (KH) domain RNA-binding proteins from the flowering plant *Arabidopsis thaliana*. Nucleic Acids Res. **30**, 623-635.

Lotan T., Ohto M., Yee K.M., West M.A.L., Lo R., Kwong R.W., Yamagishi K., Fischer R.L., Goldberg R.B. & Harada J.J. (1998). *Arabidopsis LEAFY COTYLEDON1* is sufficient to induce embryo development in vegetative cells. Cell **93**, 1195-1205.

Luo M., Bilodeau P., Dennis E.S., Peacock W.J. & Chaudhury A. (2000). Expression and parent-of-origin effects for *FIS2*, *MEA*, and *FIE* in the endosperm and embryo of developing *Arabidopsis* seeds. Proc. Natl. Acad. Sci. USA. **97**, 10637-10642.

Luo M., Bilodeau P., Koltunow A., Dennis E.S., Peacock W.J. & Chaudhury A.M. (1999). Genes controlling fertilization-independent seed development in *Arabidopsis thaliana*. Proc. Natl. Acad. Sci. USA. **96**, 296-301.

Mager J.C., Montgomery N.D., de Villena F.P.M. & Magnuson T. (2002). A role for a mouse *Polycomb* group gene in imprinting. Dev. Biol. **247**, 94.

Maheshwari P. (1950) *An introduction to the embryology of angiosperms*. McGraw-Hill, New York.

Malecka J. (1971). Cyto-taxanomical and embryological investigations on a natural hybrid between *Taraxacum kok-saghyz* Rodin and *T. officinale* Web. and their putative parent species. Acta Biol. Crac. Ser. Bot. **14**, 179-201.

Malecka J. (1973). Problems of the mode of reproduction in microspecies of *Taraxacum* section Palustria Dahlstedt. Acta Biol. Crac. Ser. Bot. **16**, 37-84.

Manning J.C. & van Staden J. (1987). The development and mobilisation of seed reserves in some African orchids. Aust. J. Bot. **35**, 343-353.

Mansfield S.G. & Briarty L.G. (1990). Endosperm cellularisation in *Arabidopsis thaliana* L. *Arabidopsis* Information Service. **27**, 65-72.

Mansfield S.G., Briarty L.G. & Erni S. (1991). Early Embryogenesis in *Arabidopsis thaliana* .1. the Mature Embryo Sac. Can. J. Bot. Rev. **69**, 447-460.

Marshall D.R. & Brown A.H.D. (1981). The evolution of apomixis. Heredity **47**, 1-15.

Martin M.P., Gerlach V.L. & Brow D.A. (2001). A novel upstream RNA polymerase III promoter element becomes essential when the chromatin structure of the yeast U6 RNA gene is altered. Mol. Cell. Biol. **21**, 6429-6439.

Matzk F., Meister A. & Schubert I. (2000). An efficient screen for reproductive pathways using mature seeds of monocots and dicots. Plant J. **21**, 97-108.

McMeniman S. & Lubulwa G. (1997) *Project Development Assessment: An Economic Evaluation of the Potential Benefits of Integrating Apomixis into Hybrid Rice*. pp 1-26. ACIAR, Canberra.

Mes T.H.M., Kuperus P., Kirschner J., Stepanek J., Storchova H., Oosterveld P. & Den Nijs J.C.M. (2002). Detection of genetically divergent clone mates in apomictic dandelions. Mol. Ecol. **11**, 253-265.

Mette M.F., Aufsatz W., van der Winden J., Matzke M.A. & Matzke A.J.M. (2000). Transcriptional silencing and promoter methylation triggered by double-stranded RNA. Embo J. **19**, 5194-5201.

Miller M.E. & Chourey P.S. (1992). The Maize Invertase-Deficient *miniature-1* Seed Mutation Is Associated With Aberrant Pedicel and Endosperm Development. Plant Cell **4**, 297-305.

Mogie M. (1992) *The Evolution of Asexual Reproduction in Plants*. Chapman & Hall, London.

Moore J.M., Calzada J.P.V., Gagliano W. & Grossniklaus U. (1997). Genetic characterization of *hadad*, a mutant disrupting female gametogenesis in *Arabidopsis thaliana*. Cold Spring Harbor Symposia On Quantitative Biology **62**, 35-47.

Morel J.B., Mourrain P., Beclin C. & Vaucheret H. (2000). DNA methylation and chromatin structure affect transcriptional and post-transcriptional transgene silencing in *Arabidopsis*. Curr. Biol. **10**, 1591-1594.

Mourrain P., Beclin C., Elmayan T., Feuerbach F., Godon C., Morel J.B., Jouette D., Lacombe A.M., Nikic S., Picault N., Remoue K., Sanial M., Vo T.A. & Vaucheret H. (2000). *Arabidopsis SGS2* and *SGS3* genes are required for posttranscriptional gene silencing and natural virus resistance. Cell **101**, 533-542.

Muller J., Hart C.M., Francis N.J., Vargas M.L., Sengupta A., Wild B., Miller E.L., O'Connor M.B., Kingston R.E. & Simon J.A. (2002). Histone methyltransferase activity of a *Drosophila Polycomb* group repressor complex. Cell **111**, 197-208.

Murbeck S. (1904). Parthenogenese bei den Gattungen *Taraxacum* und *Hieracium*. Bot. Not. **6**, 285-296.

Nagashima T. (1989). Embryogenesis, seed formation and immature seed germination in vitro in *Ponerorchis graminifolia* Reichb. f. Jap. Soc. Hort. Sci. **58**, 187-194.

Naumova T.N. (1993) *Apomixis in angiosperms. Nucellar and integumentary embryony*. CRC Press, Boca Raton, Fla.

Naumova T.N. & Willemse M.T.M. (1995). Ultrastructural characterization of apospory in *Panicum maximum*. Sex. Plant Reprod. **8**, 197-204.

Neer E.J., Schmidt C.J., Nambudripad R. & Smith T.F. (1994). The Ancient Regulatory-Protein Family of WD-Repeat Proteins. Nature **371**, 297-300.

Nogler G. (1984) Gametophytic apomixis. In: *Embryology of Angiosperms* (ed B.M. Johri), pp. 475-518. Springer-Verlag, Berlin Heidelberg.

Nogler G.A. (1982). How to obtain diploid apomictic *Ranunculus auricomus* plants not found in the wild state. Bot. Helv. **91**, 13-22.

Nogler G.A. (1995). Genetics of Apomixis in *Ranunculus auricomus*. 6. Epilogue. Bot. Helv. **105**, 111-115.

Noyes R.D. & Rieseberg L.H. (2000). Two independent loci control agamospermy (apomixis) in the triploid flowering plant *Erigeron annuus*. Genetics **155**, 379-390.

Nybom H. (1998). Biometry and DNA fingerprinting detect limited genetic differentiation among populations of the apomictic blackberry *Rubus nessensis* (Rosaceae). Nord. J. Bot. **18**, 323-333.

Nygren A. (1946). The genesis of some Scandinavian species of *Calamagrostis*. Hereditas **32**, 131-262.

Ogas J., Cheng J.C., Sung Z.R. & Somerville C. (1997). Cellular differentiation regulated by gibberellin in the *Arabidopsis thaliana pickle* mutant. Science **277**, 91-94.

Ogas J., Kaufmann S., Henderson J. & Somerville C. (1999). PICKLE is a CHD3 chromatin-remodelling factor that regulates the transition from embryonic to vegetative development in *Arabidopsis*. Proc. Natl. Acad. Sci. USA. **96**, 13839-13844.

Ohad N., Margossian L., Hsu Y.C., Williams C., Repetti P. & Fischer R.L. (1996). A mutation that allows endosperm development without fertilization. Proc. Natl. Acad. Sci. USA. **93**, 5319-5324.

Ohad N., Yadegari R., Margossian L., Hannon M., Michaeli D., Harada J.J., Goldberg R.B. & Fischer R.L. (1999). Mutations in *FIE*, a WD *Polycomb* group gene, allow endosperm development without fertilization. Plant Cell **11**, 407-415.

Olsen O.A. (1998). Endosperm developments. Plant Cell **10**, 485-488.

Olsen O.A. (2001). Endosperm development: Cellularization and cell fate specification. Ann. Rev. Plant Phys. Plant Mol. Biol. **52**, 233-267.

Olsen O.A., Brown R.C. & Lemmon B.E. (1995). Pattern and Process of Wall Formation in Developing Endosperm. Bioessays **17**, 803-812.

Olsen O.A., Linnestad C. & Nichols S.E. (1999). Developmental biology of the cereal endosperm. Trends Plant Sci. **4**, 253-257.

Opsahl-Ferstad H.G., LeDeunff E., Dumas C. & Rogowsky P.M. (1997). *ZmEsr*, a novel endosperm-specific gene expressed in a restricted region around the maize embryo. Plant J. **12**, 235-246.

Ostenfeld C.H. & Raunkiaer C. (1903). Kasteringsforsog med *Hieracium* og andre Cichorieae. Bot Tidsskr. **25**, 409-413.

Otegui M.S., Capp R. & Staehelin L.A. (2002). Developing seeds of *Arabidopsis* store different minerals in two types of vacuoles and in the endoplasmic reticulum. Plant Cell **14**, 1311-1327.

Ozias-Akins P., Roche D. & Hanna W.W. (1998). Tight clustering and hemizygosity of apomixis-linked molecular markers in *Pennisetum squamulatum* genetic control of apospory by a divergent locus that may have no allelic form in sexual genotypes. Proc. Natl. Acad. Sci. USA. **95**, 5127-5132.

Page R.D.M. (1996). Treeview: an application to display phylogenetic trees on personal computers. Comput Applic Biosci. **12**, 357-358.

Pandey R., Muller A., Napoli C.A., Selinger D.A., Pikaard C.S., Richards E.J., Bender J., Mount D.W. & Jorgensen R.A. (2002). Analysis of histone acetyltransferase and histone deacetylase families of *Arabidopsis* thaliana suggests functional diversification of chromatin modification among multicellular eukaryotes. Nucleic Acids Res. **30**, 5036-5055.

Papademetriou M.K. (2000) Rice production in the Asia-Pacific region: issues and perspectives. In: *Bridging the Rice Yield Gap in the Asia-Pacific Region* (eds M.K. Papademetriou, J. Frank, & E.M. Herath). FAO, Bangkok, Thailand.

Peacock J.W. (1992) Genetic engineering and mutagenesis for apomixis in rice. In: *Proceedings of the International Workshop on Apomixis in Rice, Changsha, China* (ed K.J. Wilson), pp. 11-21. The Rockefeller Foundation, New York.

Peacock W.J., Luo M., Craig S., Dennis E. & Chaudhury A. (1995) A mutagenesis programme for apomixis genes in *Arabidopsis*. In: *Induced Mutations and molecular techniques for crop improvement*, pp. 117-125. FAO/IAEA, Vienna, Austria.

Pearce S.R., Harrison G., Li D.T., Heslop-Harrison J.S., Kumar A. & Flavell A.J. (1996). The Ty1-copia group retrotransposons in *Vicia* species: Copy number, sequence heterogeneity and chromosomal localisation. Mol. Gen. Genet.. **250**, 305-315.

Philipson M.N. (1978). Apomixis in *Cortaderia jubata* (Gramineae). NZ J. Bot. **16**, 45-59.

Pouteau S., Spielmann A., Meyer C., Grandbastien M.A. & Caboche M. (1991). Effects of Tnt1 Tobacco Retrotransposon Insertion On Target Gene-Transcription. Mol. Gen. Genet. **228**, 233-239.

Quarin C.L. (1999). Effect of pollen source and pollen ploidy on endosperm formation and seed set in pseudogamous apomictic *Paspalum notatum*. Sex. Plant Reprod. **11**, 331-335.

Quarin C.L., Espinoza F., Martinez E.J., Pessino S.C. & Bovo O.A. (2001). A rise of ploidy level induces the expression of apomixis in *Paspalum notatum*. Sex. Plant Reprod. **13**, 243-249.

Quarin C.L. & Hanna W.W. (1980). Effect of three ploidy levels on meiosis and mode of reproduction in *Paspalum hexastachyum*. Crop Sci. **20**, 69-75.

Ramachandran S. & Sundaresan V. (2001). Transposons as tools for functional genomics. Plant Phys. Biochem. **39**, 243-252.

Reiser L. & Fischer R.L. (1993). The Ovule and the Embryo Sac. Plant Cell **5**, 1291-1301.

Reitzer L.J. & Magasanik B. (1986). Transcription of Glna in *Escherichia coli* Is Stimulated By Activator Bound to Sites Far From the Promoter. Cell. **45**, 785-792.

Reyes J.C., Hennig L. & Gruissem W. (2002). Chromatin-remodelling and memory factors. New regulators of plant development. Plant Phys. **130**, 1090-1101.

Rice P. (1994) *Genetics computer group EGCG program manual*. The Sanger Centre, Cambridge.

Rice W.R. (1999). Genetic polarization: unifying theories for the adaptive significance of recombination - Commentary. J. Evol. Biol. **12**, 1047-1049.

Robinson-Beers K., Pruitt R.E. & Gasser C.S. (1992). Ovule development in wild-type *Arabidopsis* and two female-sterile mutants. Plant Cell **4**, 1237-1249.

Roche D., Cong P.S., Chen Z.B., Hanna W.W., Gustine D.L., Sherwood R.T. & Ozias-Akins P. (1999). An apospory-specific genomic region is conserved between Buffelgrass (*Cenchrus ciliaris* L.) and *Pennisetum squamulatum* Fresen. Plant J. **19**, 203-208.

Roche D., Hanna W.W. & Ozias-Akins P. (2001). Is supernumerary chromatin involved in gametophytic apomixis of polyploid plants? Sex. Plant Reprod. **13**, 343-349.

Rosenberg O. (1907). Cytological studies on the apogamy in *Hieracium*. Bot. Tidskr. **28**, 143-170.

Rosenquist M., Alsterfjord M., Larsson C. & Sommarin M. (2001). Data mining the *Arabidopsis* genome reveals fifteen 14-3-3 genes. Expression is demonstrated for two out of five novel genes. Plant Phys. **127**, 142-149.

Roy B.A. (1995). The breeding systems of six species of *Arabis* (Brassicaceae). Am. J. Bot. **82**, 869-877.

Rutishauser A. (1948). Pseudogamie un d Polymorphie in der Gattung *Potentilla*. Arch Julius Klaus-Stift Vererbungsforsch. **23**, 267-424.

SanMiguel P., Gaut B.S., Tikhonov A., Nakajima Y. & Bennetzen J.L. (1998). The paleontology of intergene retrotransposons of maize. Nat. Genet. **20**, 43-45.

Satijn D.P.E., Gunster M.J., vanderVlag J., Hamer K.M., Schul W., Alkema M.J., Saurin A.J., Freemont P.S., vanDriel R. & Otte A.P. (1997). RING1 is associated with the *Polycomb* group protein complex and acts as a transcriptional repressor. Mol. Cell. Biol. **17**, 4105-4113.

Savidan Y. (1982). Nature and inheritance of apomixis in *Panicum maximum* Jacq. [Nature et heredite de l'apomixie chez Panicum maximum Jacq.]. Travaux et Documents de l'ORSTOM. **153**, 1-159.

Savidan Y. (1990). The genetic control of apomixis. Apomixis newsletter. **2**, 24.

Savidan Y. (2000). Apomixis, the way of cloning seeds. Biofutur. **2000**, 38-43.

Savidan Y.H. (2001) Transfer of apomixis through wide crosses. In: *The Flowering of Apomixis: From Mechanisms to Genetic Engineering* (eds Y. Savidan, J.G. Carman, & T. Dresselhaus), pp. 153-67. CIMMYT, IRS, Eur. Comm. DG VI, Mexico.

Schiefthaler U., Balasubramanian S., Sieber P., Chevalier D., Wisman E. & Schneitz K. (1999). Molecular analysis of *NOZZLE*, a gene involved in pattern formation and early sporogenesis during sex organ development in *Arabidopsis thaliana*. Proc. Natl. Acad. Sci. USA. **96**, 11664-11669.

Schnarf K. (1919). Beobachtungen uber die Endospermtwicklung von *Hieracium aurantiacum*. Sitzber Akad der Wiss math natur Wien Kl I. **128**, 1-17.

Schneitz K. (1999). The molecular and genetic control of ovule development. Curr. Opin. Plant Biol. **2**, 13-17.

Schneitz K., Hulskamp M., Kopczak S.D. & Pruitt R.E. (1997). Dissection of sexual organ ontogenesis: A genetic analysis of ovule development in *Arabidopsis thaliana*. Development. **124**, 1367-1376.

Schneitz K., Hulskamp M. & Pruitt R.E. (1995). Wild-Type Ovule Development in *Arabidopsis thaliana* - a Light- Microscope Study of Cleared Whole-Mount Tissue. Plant J. **7**, 731-749.

Schumacher A., Faust C. & Magnuson T. (1996). Positional cloning of a global regulator of anterior-posterior patterning in mice. Nature **383**, 250-253.

Schweizer P., Pokorny J., Schulze-Lefert P. & Dudler R. (2000). Double-stranded RNA interferes with gene function at the single-cell level in cereals. Plant Journal **24**, 895-903.

Scott R.J., Spielman M., Bailey J. & Dickinson H.G. (1998). Parent-of-origin effects on seed development in *Arabidopsis thaliana*. Development **125**, 3329-3341.

Sehnke P.C., Chung H.J., Wu K. & Ferl R.J. (2001). Regulation of starch accumulation by granule-associated plant 14-3-3 proteins. Proc. Natl. Acad. Sci. USA. **98**, 765-770.

Sheldon C.C., Conn A.B., Dennis E.S. & Peacock W.J. (2002). Different regulatory regions are required for the vernalization-induced repression of *FLOWERING LOCUS C* and for the epigenetic maintenance of repression. Plant Cell **14**, 2527-2537.

Sheridan W.F., Avalkina N.A., Shamrov, II, Batygina T.B. & Golubovskaya I.N. (1996). The mac1 gene: Controlling the commitment to the meiotic pathway in maize. Genetics **142**, 1009-1020.

Shi Y., Gornall R.J., Draper J. & Stace C.A. (1996). Intraspecific molecular variation in *Hieracium* sect Alpina (Asteraceae), an apomictic group. Folia Geobot. & Phyto. **31**, 305-313.

Shiu S.H. & Bleecker A.B. (2001). Receptor-like kinases from *Arabidopsis* form a monophyletic gene family related to animal receptor kinases. Proc. Natl. Acad. Sci. USA. **98**, 10763-10768.

Siebert P.D., Chenchik A., Kellogg D.E., Lukyanov K.A. & Lukyanov S.A. (1995). An improved PCR method for walking in uncloned genomic DNA. Nucleic Acids Res. **23**, 1087-8.

Simpson V.J., Johnson T.E. & Hammen R.F. (1986). *Caenorhabditis elegans* DNA does not contain 5-methylcytosine at any time during development or aging. Nucleic Acids Res. **14**, 6711-6719.

Sindhe A.N.R., Swamy B.G.L. & Govindappa D.A. (1980). Synergid embryo in *Pennisetum squamulatum*. Curr. Sci. (Bangalore) **49**, 914-915.

Skalinska M. (1967). Cytological analysis of some *Hieracium* species, subgenus *Pilosella*, from mountains of southern Poland. Acta Biol. Crac. Ser. Bot. **10**, 127-141.

Skalinska M. (1971). Experimental and embryological studies in *Hieracium aurantiacum* L. Acta Biol. Crac. Ser. Bot. **14**, 139-155.

Skalinska M. (1973). Further studies in facultative apomixis of *Hieracium aurantiacum* L. Acta Biol. Crac. Ser. Bot. **16**, 121-137.

Skalinska M. (1976). Cytological diversity in the progeny of octaploid facultative apomicts of *Hieracium aurantiacum*. Acta Biol. Crac. Ser. Bot. **19**, 39-47.

Smith N.A., Singh S.P., Wang M.B., Stoutjesdijk P.A., Green A.G. & Waterhouse P.M. (2000). Gene expression - Total silencing by intron-spliced hairpin RNAs. Nature **407**, 319-320.

Smith T.F., Gaitatzes C., Saxena K. & Neer E.J. (1999). The WD repeat: a common architecture for diverse functions. Trends Biochem. Sci. **24**, 181-185.

Soppe W.J.J., Jacobsen S.E., Alonso-Blanco C., Jackson J.P., Kakutani T., Koornneef M. & Peeters A.J.M. (2000). The late flowering phenotype of *fwa* mutants is caused by gain- of-function epigenetic alleles of a homeodomain gene. Mol.Cell. **6**, 791-802.

Sorensen M.B., Chaudhury A.M., Robert H., Bancharel E. & Berger F. (2001). *Polycomb* group genes control pattern formation in plant seed. Curr. Biol. **11**, 277-281.

Spillane C., MacDougall C., Stock C., Kohler C., Vielle-Calzada J.P., Nunes S.M., Grossniklaus U. & Goodrich J. (2000). Interaction of the *Arabidopsis Polycomb* group proteins FIE and MEA mediates their common phenotypes. Curr. Biol. **10**, 1535-1538.

Spillane C., Steimer A. & Grossniklaus U. (2001). Apomixis in agriculture: the quest for clonal seeds. Sex. Plant Reprod. **14**, 179-187.

Springer N.M., Danilevskaya O.N., Hermon P., Helentjaris T.G., Phillips R.L., Kaeppler H.F. & Kaeppler S.M. (2002). Sequence relationships, conserved domains and expression patterns for maize homologs of the *Polycomb* group genes *E(z)*, *esc*, and *E(Pc)*. Plant Phys. **128**, 1332-1345.

Springer P.S. (2000). Gene traps: Tools for plant development and genomics. Plant Cell. **12**, 1007-1020.

Springer P.S., Holding D.R., Groover A., Yordan C. & Martienssen R.A. (2000). The essential Mcm7 protein PROLIFERA is localized to the nucleus of dividing cells during the G(1) phase and is required maternally for early *Arabidopsis* development. Development. **127**, 1815-1822.

Springer P.S., McCombie W.R., Sundaresan V. & Martienssen R.A. (1995). Gene Trap Tagging of *Prolifera*, an Essential Mcm2-3-5-Like Gene in *Arabidopsis*. Science. **268**, 877-880.

Stam M., Belele C., Dorweiler J.E. & Chandler V.L. (2002). Differential chromatin structure within a tandem array 100 kb upstream of the maize b1 locus is associated with paramutation. Gen. & Dev. **16**, 1906-1918.

Stangeland B., Salehian Z., Aalen R., Mandal A. & Olsen O.A. (2003). Isolation of GUS marker lines for genes expressed in *Arabidopsis* endosperm, embryo and maternal tissues. J. Exp. Bot. **54**, 279-290.

Stebbins G.L. & Jenkins J.A. (1939). Aposporic development in the North American species of *Crepis*. Genetica. **21**, 191-224.

Steimer A., Amedeo P., Afsar K., Fransz P., Scheid O.M. & Paszkowski J. (2000). Endogenous targets of transcriptional gene silencing in *Arabidopsis*. Plant Cell. **12**, 1165-1178.

Stelly D.M., Peloquin S.J., Palmer R.G. & Crane C.F. (1984). Mayer's hemalum-methyl salicylate: a stain clearing technique for observations within whole ovules. Stain Tech. **59**, 155-161.

Stone S.L., Kwong L.W., Yee K.M., Pelletier J., Lepiniec L., Fischer R.L., Goldberg R.B. & Harada J.J. (2001). LEAFY COTYLEDON2 encodes a B3 domain transcription factor that induces embryo development. Proc. Natl. Acad. Sci. USA. **98**, 11806-11811.

Storchova H., Chrtek J., Bartish I.V., Tetera M., Kirschner J. & Stepanek J. (2002). Genetic variation in agamospermous taxa of *Hieracium* sect. Alpina (Compositae) in the Tatry Mts. (Slovakia). Plant Syst. Evol. **235**, 1-17.

Stoutjesdijk P.A., Singh S.P., Liu Q., Hurlstone C.J., Waterhouse P.A. & Green A.G. (2002). hpRNA-mediated targeting of the *Arabidopsis FAD2* gene gives highly efficient and stable silencing. Plant Phys. **129**, 1723-1731.

Sundaresan V., Springer P., Volpe T., Haward S., Jones J.D.G., Dean C., Ma H. & Martienssen R. (1995). Patterns of Gene-Action in Plant Development Revealed By Enhancer Trap and Gene Trap Transposable Elements. Gen. & Dev. **9**, 1797-1810.

Swamy B.G.L. & Parameswaran N. (1963). The helobial endosperm. Biol. Rev. **38**, 1-50.

Tabara H., Sarkissian M., Kelly W.G., Fleenor J., Grishok A., Timmons L., Fire A. & Mello C.C. (1999). The rde-1 gene, RNA interference, and transposon silencing in *C-elegans*. Cell **99**, 123-132.

Tatusova T.A. & Madden T.L. (1999). BLAST 2 SEQUENCES, a new tool for comparing protein and nucleotide sequences. Fems Micro. Lett. **174**, 247-250.

Tian L. & Chen Z.J. (2001). Blocking histone deacetylation in *Arabidopsis* induces pleiotropic effects on plant gene regulation and development. Proc. Natl. Acad. Sci. USA. **98**, 200-205.

Tie F., Furuyama T., Prasad-Sinha J., Jane E. & Harte P.J. (2001). The *Drosophila Polycomb* Group proteins Esc and E(z) are present in a complex containing the histone-binding protein p55 and the histone deacetylase RPD3. Development **128**, 275-286.

Torki M., Mandaron P., Mache R. & Falconet D. (2000). Characterization of a ubiquitous expressed gene family encoding polygalacturonase in *Arabidopsis thaliana*. Gene **242**, 427-436.

Tucker M.R., Paech N.A., Willemse M.T.M. & Koltunow A.M.G. (2001). Dynamics of callose deposition and beta-1,3-glucanase expression during reproductive events in sexual and apomictic *Hieracium*. Planta **212**, 487-498.

Tutin T.G., Heywood V.H., Burgess N.A., Moore D.M., Valentine D.H., Walters S.M. & Webb D.A. (1976) *Flora Europea. Volume 4. Plantaginaceae to Compositae (and Rubiaceae).* Cambridge University Press, Cambridge, UK.

van Baarlen P., Verduijn M. & van Dijk P.J. (1999). What can we learn from natural apomicts? Trends Plant Sci. **4**, 43-44.

van Baarlen P., de Jong J.H. & van Dijk P.J. (2002). Comparative cyto-embryological investigations of sexual and apomictic dandelions (*Taraxacum*) and their apomictic hybrids. Sex. Plant Reprod. **15**, 31-38.

van der Vlag J. & Otte A.P. (1999). Transcriptional repression mediated by the human *Polycomb* group protein EED involves histone deacetylation. Nat. Genet. **23**, 474-478.

van Dijk P.J., Tas I.C.Q., Falque M. & Bakx-Schotman T. (1999). Crosses between sexual and apomictic dandelions (*Taraxacum*). II. The breakdown of apomixis. Heredity **83**, 715-721.

van Hengel A.J., Guzzo F., van Kammen A. & de Vries S.C. (1998). Expression pattern of the carrot EP3 endochitinase genes in suspension cultures and in developing seeds. Plant Phys. **117**, 43-53.

van Lohuizen M. (1999). The trithorax-group and *Polycomb* group chromatin modifiers: implications for disease. Curr. Opin. Genet. Dev. **9**, 355-361.

Vaucheret H. & Fagard M. (2001). Transcriptional gene silencing in plants: targets, inducers and regulators. Trends Gen. **17**, 29-35.

Vielle-Calzada J.P., Baskar R. & Grossniklaus U. (2000). Delayed activation of the paternal genome during seed development. Nature. **404**, 91-94.

Vielle-Calzada J.P., Nuccio M.L., Budiman M.A., Thomas T.L., Burson B.L., Hussey M.A. & Wing R.A. (1996). Comparative gene expression in sexual and apomictic ovaries of *Pennisetum ciliare* (L) Link. Plant Mol. Biol. **32**, 1085-1092.

Vielle-Calzada J.P., Thomas J., Spillane C., Coluccio A., Hoeppner M.A. & Grossniklaus U. (1999). Maintenance of genomic imprinting at the *Arabidopsis medea* locus requires zygotic *DDM1* activity. Gen.& Dev. **13**, 2971-2982.

Vinkenoog R. & Scott R.J. (2001). Autonomous endosperm development in flowering plants: how to overcome the imprinting problem? Sex. Plant Reprod. **14**, 189-194.

Vinkenoog R., Spielman M., Adams S., Fischer R.L., Dickinson H.G. & Scott R.J. (2000). Hypomethylation promotes autonomous endosperm development and rescues postfertilization lethality in *fie* mutants. Plant Cell **12**, 2271-2282.

Visser N.C. & Spies J.J. (1994). Cytogenetic studies in the genus *Tribolium* (Poaceae, Danthonieae). 2. A report on embryo sac development with special reference to the occurrence of apomixis in diploid specimen. S. Afr. J. Bot. **60**, 22-26.

Vivian-Smith A., Luo M., Chaudhury A. & Koltunow A. (2001). Fruit development is actively restricted in the absence of fertilization in *Arabidopsis*. Development. **128**, 2321-2331.

Vongs A., Kakutani T., Martienssen R.A. & Richards E.J. (1993). *Arabidopsis thaliana* Dna Methylation Mutants. Science **260**, 1926-1928.

Wakana A. & Uemoto S. (1988). Adventive Embryogenesis in Citrus (Rutaceae). 2. Postfertilization Development. Am. J. Bot. **75**, 1033-1047.

Waterhouse P.M. & Helliwell C.A. (2003). Exploring plant genomes by RNA-induced gene silencing. Nat. Rev. Genet. **4**, 29-38.

Waterhouse P.M., Wang M.B. & Finnegan E.J. (2001). Role of short RNAs in gene silencing. Trends Plant Sci. **6**, 297-301.

Waxman D. & Peck J.R. (1999). Sex and adaptation in a changing environment. Genetics **153**, 1041-1053.

Webb M.C. & Gunning B.E.S. (1991). The microtubular cytoskeleton during development of the zygote, proembryo and free-nuclear endosperm in *Arabidopsis thaliana* (L.) Heynh. Planta **184**, 187-195.

Wen X.S., Ye X.L., Li Y.Q., Chen Z.L. & Xu S.X. (1998). Embryological studies on apomixis in *Pennisetum squamulatum*. Acta Bot. Sin. **40**, 598-604.

Wesley S.V., Helliwell C.A., Smith N.A., Wang M.B., Rouse D.T., Liu Q., Gooding P.S., Singh S.P., Abbott D., Stoutjesdijk P.A., Robinson S.P., Gleave A.P., Green A.G. & Waterhouse P.M. (2001). Construct design for efficient, effective and high-throughput gene silencing in plants. Plant J. **27**, 581-590.

Wessler S.R., Bureau T.E. & White S.E. (1995). LTR-Retrotransposons and Mites - Important Players in the Evolution of Plant Genomes. Curr. Opin. Genet. Dev. **5**, 814-821.

White S.E., Habera L.F. & Wessler S.R. (1994). Retrotransposons in the Flanking Regions of Normal Plant Genes - a Role For Copia-Like Elements in the Evolution of Gene Structure and Expression. Proc. Natl. Acad. Sci. USA. **91**, 11792-11796.

Willemse M.T.M. & van Went J.L. (1984) The female gametophyte. In: *Embryology of Angiosperms* (ed B.M. Johri), pp. 159-191. Springer-Verlag, Berlin Heidelberg.

Wilms H.J., van Went J.L., Cresti M. & Ciampolini F. (1983). Adventive embryogenesis in Citrus. Caryologia **36**, 65-78.

Wright D.A., Ke N., Smalle J., Hauge B.M., Goodman H.M. & Voytas D.F. (1996). Multiple non-LTR retrotransposons in the genome of *Arabidopsis thaliana*. Genet. **142**, 569-578.

Wright S. & Finnegan D. (2001). Genome evolution: Sex and the transposable element. Curr. Biol. **11**, R296-R299.

Wu H.M. & Cheung A.Y. (2000). Programmed cell death in plant reproduction. Plant Mol. Biol. **44**, 267-281.

Wu K., Rooney M.F. & Ferl R.J. (1997). The *Arabidopsis* 14-3-3 multigene family. Plant Phys. **114**, 1421-1431.

Wu K.Q., Malik K., Tian L.N., Brown D. & Miki B. (2000a). Functional analysis of a RPD3 histone deacetylase homologue in *Arabidopsis thaliana*. Plant Mol. Biol. **44**, 167-176.

Wu K.Q., Tian L.N., Malik K., Brown D. & Miki B. (2000b). Functional analysis of HD2 histone deacetylase homologues in *Arabidopsis thaliana*. Plant J. **22**, 19-27.

Wu-Scharf D., Jeong B.R., Zhang C.M. & Cerutti H. (2000). Transgene and transposon silencing in *Chlamydomonas reinhardtii* by a DEAH-Box RNA helicase. Science **290**, 1159-1162.

Xu L., Fong Y.Y. & Strome S. (2001). The Caenorhabditis elegans maternal-effect sterile proteins, MES-2, MES-3, and MES-6, are associated in a complex in embryos. Proc. Natl. Acad. Sci. USA. **98**, 5061-5066.

Yadegari R., Kinoshita T., Lotan O., Cohen G., Katz A., Choi Y., Nakashima K., Harada J.J., Goldberg R.B., Fischer R.L. & Ohad N. (2000). Mutations in the *FIE* and *MEA* genes that encode interacting polycomb proteins cause parent-of-origin effects on seed development by distinct mechanisms. Plant Cell **12**, 2367-2381.

Yang C.H., Chen L.J. & Sung Z.R. (1995). Genetic-Regulation of Shoot Development in *Arabidopsis* - Role of the *Emf* Genes. Dev. Biol. **169**, 421-435.

Yang W.C. & Sundaresan V. (2000). Genetics of gametophyte biogenesis in *Arabidopsis*. Curr. Opin. Plant Biol. **3**, 53-57.

Yang W.C., Ye D., Xu J. & Sundaresan V. (1999). The *SPOROCYTELESS* gene of *Arabidopsis* is required for initiation of sporogenesis and encodes a novel nuclear protein. Gen. & Dev. **13**, 2108-2117.

Ye X.L. & Guo J.Y. (1995). Female gametophyte development and embryogeny in *Cymbidium sinense* (Andr.) Willd. J. Trop. Subtrop. Bot. **3**, 54-58.

Yeung E.C. & Peterson R.L. (1971). Studies on the rosette plant *Hieracium floribundum*. I. Observations related to flowering and axillary bud development. Can. J. Bot. **50**, 73-78.

Yoshida N., Yanai Y., Chen L.J., Kato Y., Hiratsuka J., Miwa T., Sung Z.R. & Takahashi S. (2001). EMBRYONIC FLOWER2, a novel *Polycomb* group protein homolog, mediates shoot development and flowering in *Arabidopsis*. Plant Cell **13**, 2471-2481.

Young B.A., Sherwood R.T. & Bashaw E.C. (1979). Cleared pistil and thick sectioning techniques for detecting aposporous apomixis in grasses. Can. J. Bot. **57**, 1668-1672.

Yuh F.Y., Archer S.J., Domaille P.J., Smith B.O., Owen D., Brotherton D.H., Raine A.R.C., Xu X., Brizuela L., Brenner S.L. & Laue E.D. (1997). Structure of the cyclin-dependent kinase inhibitor p19(Ink4d). Nature **389**, 999-1003.

Zentella R., Yamauchi D. & Ho T.H.D. (2002). Molecular dissection of the gibberellin/abscisic acid signalling pathways by transiently expressed RNA interference in barley aleurone cells. Plant Cell **14**, 2289-2301.

Zuo J., Niu Q.W., Frugis G. & Chua N.H. (2002) The *WUSCHEL* gene promotes vegetative-to-embryonic transition in Arabidopsis. Plant J. **30**, 349-59.